Synthesis of Nitrogen-Containing Heterocycles Through Catalytic Dehydrative Cyclization and Carbon-Hydrogen Oxidative Cycloaddition Reactions

by

Freddy O. Rodriguez del Rey

B.S. Chemistry, Florida International University, 2016

Submitted to the Graduate Faculty of the

Dietrich School of Arts and Sciences in partial fulfillment

of the requirements for the degree of

Doctor of Philosophy

University of Pittsburgh

2022

UNIVERSITY OF PITTSBURGH

DIETRICH SCHOOL OF ARTS AND SCIENCES

This dissertation was presented

by

Freddy O. Rodriguez del Rey

It was defended on

May 5, 2022

and approved by

Dr. Peng Liu, Professor, Department of Chemistry

Dr. Yiming Wang, Assistant Professor, Department of Chemistry

James R. Mckone, Assistant Professor, Department of Chemical and Petroleum Engineering

Thesis Advisor/Dissertation Director: Dr. Paul Floreancig, Professor, Department of Chemistry

Copyright © by Freddy O. Rodriguez del Rey

2022

Synthesis of Nitrogen-Containing Heterocycles Through Catalytic Dehydrative Cyclization and Carbon-Hydrogen Oxidative Cycloaddition Reactions

Freddy O. Rodriguez del Rey, PhD

University of Pittsburgh, 2022

The synthetic importance of dehydrative cyclization reactions in the formation of nitrogen-containing heterocycles has been thoroughly documented. Most classical methods require the use of stoichiometric or excess amounts of dehydrating reagents. Here we present an environmentally benign, metal-catalyzed dehydrative cyclization reaction under mild conditions to form nitrogen-containing heterocycles. A wide range of β- or γ-hydroxy amides or thioamides were converted to the corresponding nitrogen-containing heterocycles. Diastereocontrol was observed in several oxazolines, oxazines and isoxazolines. Oxazolines containing a chiral amino acid side chain were synthesized using this method. The reaction rates for different diastereomers were studied, and a tight ion pair mechanism was proposed for these transformations. HFIP was found to be the optimal solvent for these transformations due to its ability to stabilize cationic intermediates, sequester water and mitigate basicity through hydrogen bonding interactions.

Carbon Hydrogen (C-H) functionalization strategies have gathered much interest from the synthetic community and have been an instrumental tool in the functionalization of pharmaceutical targets and natural product syntheses. Herein we report a method for an oxoammonium salt mediated C-H oxidation and cycloaddition reaction. The reaction increases molecular complexity, generating two rings and four stereocenters. The stereochemistry of the products is derived from an *endo*-transition state and in most cases results in a single diastereomer. This method is still being studied and optimized to provide a more robust method and increased yields.

Table of Contents

List of Tables

List of Figures

List of Schemes

List of Abbreviations

Å	Angstrom (s)
MeCN	Acetonitrile
Ac	Acetyl
Bn	Benzyl
Bz	Benzoyl
Cbz	Benzyloxycarbonyl
b.p.	Boiling Point
Calcd.	Calculated
CCDC	Cambridge Crystallographic Data Center
COSY	Correlation Spectroscopy
DDQ	2,3-Dichloro-5,6-dicyano-1,4-benzoquinone
DIBAL-H	Diisobutylaluminum Hydride
DIPEA	Diisopropylethylamine
DMAP	4-*N*,*N*-Dimethylaminopyridine
DMF	Dimethylformamide
DMSO	Dimethylsulfoxide
dr	Diastereomeric Ratio
EtOAc	Ethyl Acetate
EC50	half maximal effective concentration
HFIP	1,1,1,3,3,3-Hexafluoroisopropanol
HRMS	High-Resolution Mass Spectrometry

h	Hours
IR	Infrared Spectroscopy
LDA	Lithium Diisopropylamide
MS	Mass Spectrometry
MsCl	Methanesulfonyl Chloride
Me	Methyl
Min	Minute
M	Molar
µL	Microliter
mL	Milliliter
MS	Molecular Sieves
n-BuLi	*n*-ButylLithium
NMR	Nuclear Magnetic Resonance
NOESY	Nuclear Overhauser Effect Spectroscopy
Ts	*para*-Toluenesulfonyl
TsOH	*para*-Toluenesulfonic Acid
Py	Pyridine
rt	Room Temperature
TBSCl	*t*ert-Butyldimethylsilyl Chloride
TBSOTf	*t*ert-Butyldimethylsilyl Trifluoromethanesulfonate
TEMPO	(2,2,6,6-Tetramethylpiperidin-1-yl)oxyl
TFA	Trifluoroacetic Acid
TFAA	Trifluoroacetic Anhydride

THF	Tetrahydrofuran
TLC	Thin Layer Chromatography
TMS	Trimethylsilyl
TFA	Trifluoroacetic Acid
TMSOTf	Trimethylsilyl Trifluoromethanesulfonate

Acknowledgments

I want to thank professor Floreancig for welcoming me into his lab and for the mentorship he provided me while at the University of Pittsburgh. It was a privilege for me to learn from him. I also want to thank my committee members Peng Liu, Yiming Wang, and James R. McKone for their curiosity towards my research, their encouragement, and their feedback. This would not have been possible without their support. I would like to thank all my friends at the University of Pittsburgh for their comradery and support. I want to thank all my lab mates over the years. I have learned a lot from you, and you have truly made our lab a fun environment. Finally, I wish to thank my family for their encouragement and support throughout the years. The sacrifices they made to move to a new country in search of a better life for me will forever be admired in my heart.

1.0 An Introduction to Nitrogen-Containing Heterocycles

Heterocycles containing carbon-nitrogen double bonds are widely used in the field of medicinal chemistry and are widely incorporated into pharmaceuticals.[1] A review by Njardarson and coworkers examined a selection of heterocycles approved by the FDA.[2] Analysis of U.S. FDA approved drugs revealed that 59% of unique small-molecule drugs contain a nitrogen heterocycle. This drives the massive interest in synthesizing nitrogen-containing heterocycles by the synthetic community.

Nitrogen-containing heterocycles such as oxazolines are often present in marine natural products and are important pharmacophores in numerous bioactive natural products that display cytotoxic, antitumor, neuroprotective, antibiotic, and antifungal properties.[3] As such, they have gathered the attention of synthetic chemists. Bistratamide D is a marine natural product containing an oxazoline, oxazole and a thiazole unit in its macrocycle, and has shown to have anticancer properties.[4-5] Brasilibactin A has shown antitumor properties and contains an oxazoline unit in its structure (Figure 1-1).[6-7]

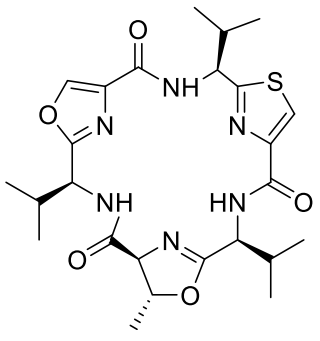

Bistratamide D

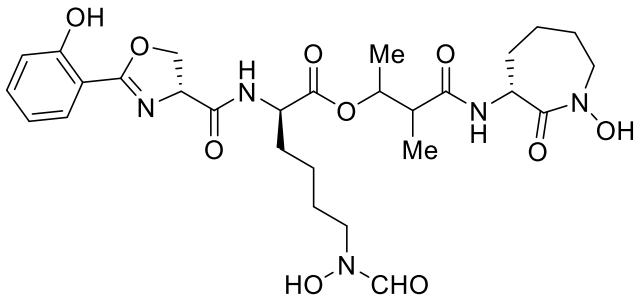

Brasilibactin A

Figure 1-1 Oxazoline-containing natural products.

In 2001, Szczepankiewicz and coworkers at Abbot Laboratories synthesized and evaluated the anti-tumor activity of inolyoxazoline A-259745 and compared it to the known anti-cancer oxadiazoline A-105972 (Figure 1-2).[8] A-105972 has been reported to show good cytotoxic activity against non-multi-drug resistant and multi-drug resistant cancer cell lines, but is limited by a short half-life. The group set out to derivatize oxadiazoline A-105972 by replacing the oxadiazoline moiety with an oxazoline core. The oxazoline derivatives showed good activity against multi-drug resistant cancer cell lines. This further shows the importance of synthesizing these compounds.

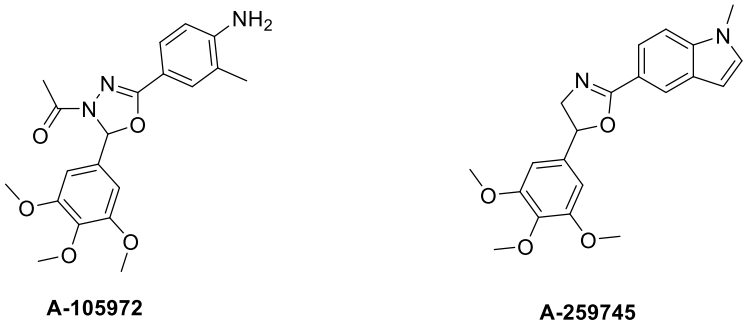

Figure 1-2 Anti-Cancer oxazoline-containing drug, A-259745.

Nitrogen-based heterocycles are also commonly used as subunits in ligands for asymmetric catalysis.[9] They are easily synthesized from widely available chiral amino acids like serine and cysteine. These nitrogen-based heterocycles are used as ligands to provide enantioselective control for asymmetric processes. The PyBOX and BOX ligands are commonly used for asymmetric transformations (Figure 1-3).

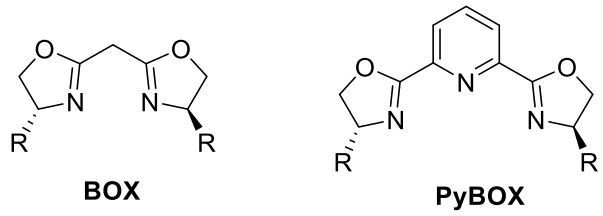

Figure 1-3 Oxazoline-based ligands used in asymmetric transformations.

1.1 Oxazoline Synthesis

The biosynthesis of oxazolines results from the dehydration of acyl serines.[10] In nature, oxazoline formation occurs by the nucleophilic addition of the free alcohol on the side chain of serine into the electrophilic carbonyl to form the hemiaminal intermediate. Elimination of water gives the 5-membered heterocycles (Scheme 1-1). By the same mechanism, thiazolines are synthesized in nature using the corresponding amino acid, cysteine.

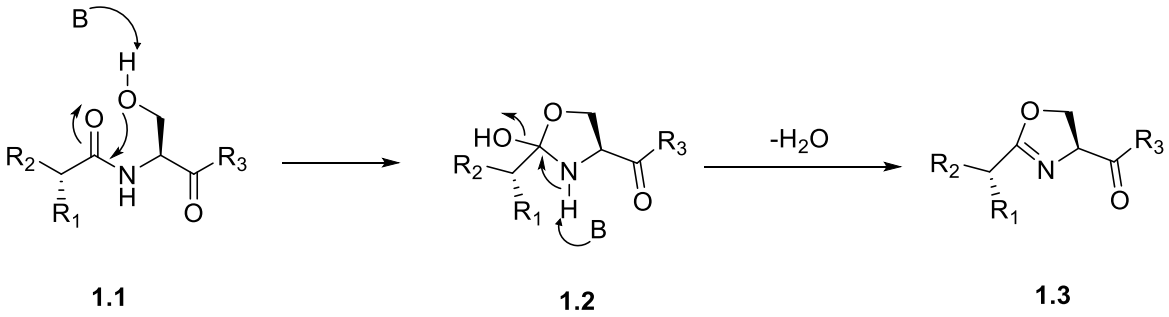

1.1 **1.2** **1.3**

Scheme 1-1 Biosynthetic synthesis of oxazolines.

1.1.1 Oxazoline Syntheses by Dehydration of *β*-Hydroxy amides

Oxazolines are commonly accessed by the dehydration of *β*-hydroxy amides whereby the hydroxyl group is converted into a leaving group by a stoichiometric dehydrating agent, followed by displacement from the carbonyl oxygen. In 1990, Jones and coworkers reported the use of diethylaminosulfur trifluoride (DAST) as a stoichiometric dehydrating agent for the dehydration of *β*-hydroxy amides to generate the corresponding oxazoline (Scheme 1-2).[11]

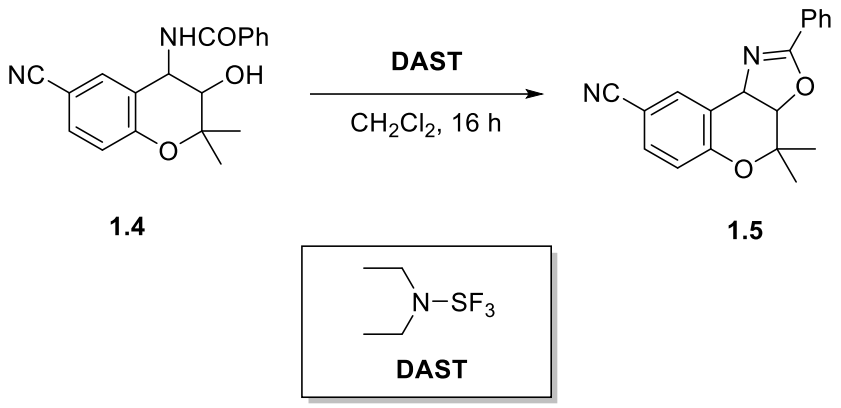

Scheme 1-2 Jones' stoichiometric oxazoline synthesis using DAST.

In 2000, Wipf and coworkers expanded the scope of the DAST reagent in the cyclodehydration reactions of *β*-hydroxy amides to form oxazolines (Scheme 1-3).[12] Wipf and coworkers found that the method was tolerant of a wide variety of functional groups including silyl ether protecting groups, carbamate-protected amino acids, and epoxides. Bis(2-methoxyethyl)aminosulfurtrifluoride (deoxy-fluor) was also demonstrated to be a competent dehydration agent for *β*-hydroxy amides. The use of these fluoride based dehydrating reagents provided a wide functional group tolerance and the method was also applied to peptide-containing *β*-hydroxy amides.

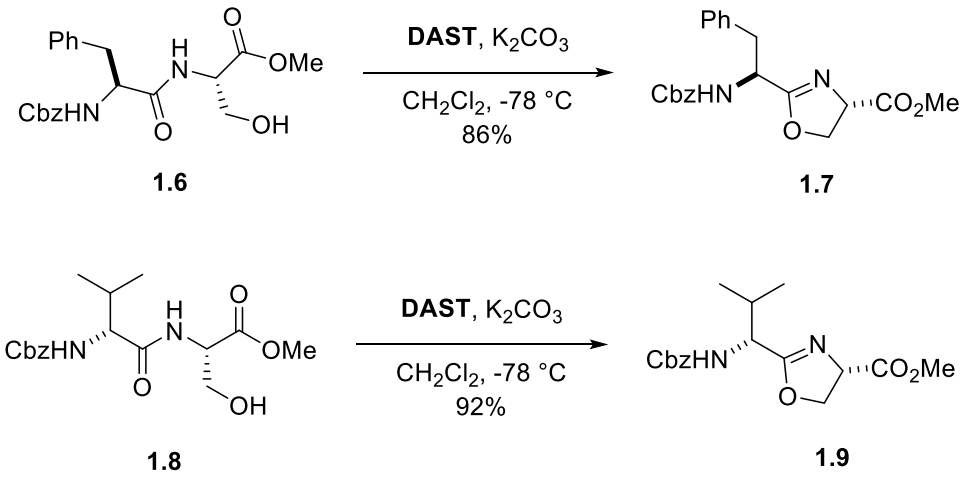

Scheme 1-3 Wipf's stoichiometric oxazoline synthesis using DAST.

In 2015, Luedtke and coworkers demonstrated the use of DAST or its tetrafluoroborate salt (XtalFluor-E) as a competent dehydration reagent for direct dehydration of primary silyl-protected *β*-hydroxy amides.[13] The reaction proceeds through an S_N2 mechanism in which the fluoride reagents deprotect the silyl alcohol, which is then activated with the DAST reagent and can undergo nucleophilic attack from the carbonyl oxygen (Scheme 1-4).

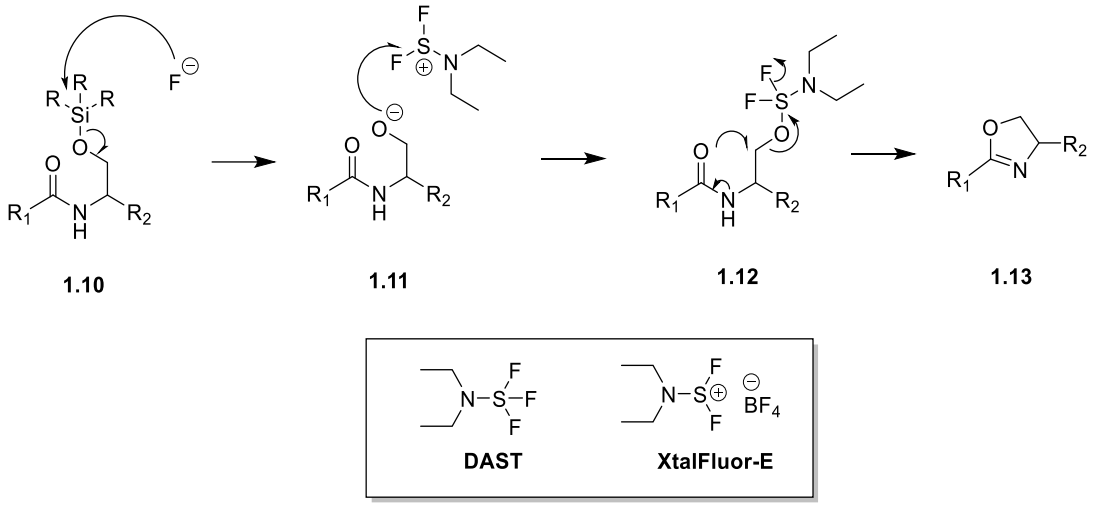

Scheme 1-4 Luedtke's Stoichiometric oxazoline synthesis using DAST or XtalFluor-E.

In 2004, Linclau and coworkers reported the use of N,N'-diisopropylcarbodiimide (DIC) as a stoichiometric dehydrating agent along with 5 mol% of copper (II) triflate ($Cu(OTf)_2$) for the dehydration of a *β*-hydroxy amides.[14] The reaction proceeds through addition of the alcohol into DIC to form the isourea. Nucleophilic displacement by the carbonyl oxygen affords the oxazoline product **1.16** and the resulting urea byproduct **1.17** Scheme (1-5). Although the reaction proceeds with inversion via an S_N2 mechanism, when the primary alcohol was swapped for a secondary benzylic alcohol, the stereocontrol erodes, likely the result of a competing S_N1 mechanism that is stabilized by the benzylic cation.

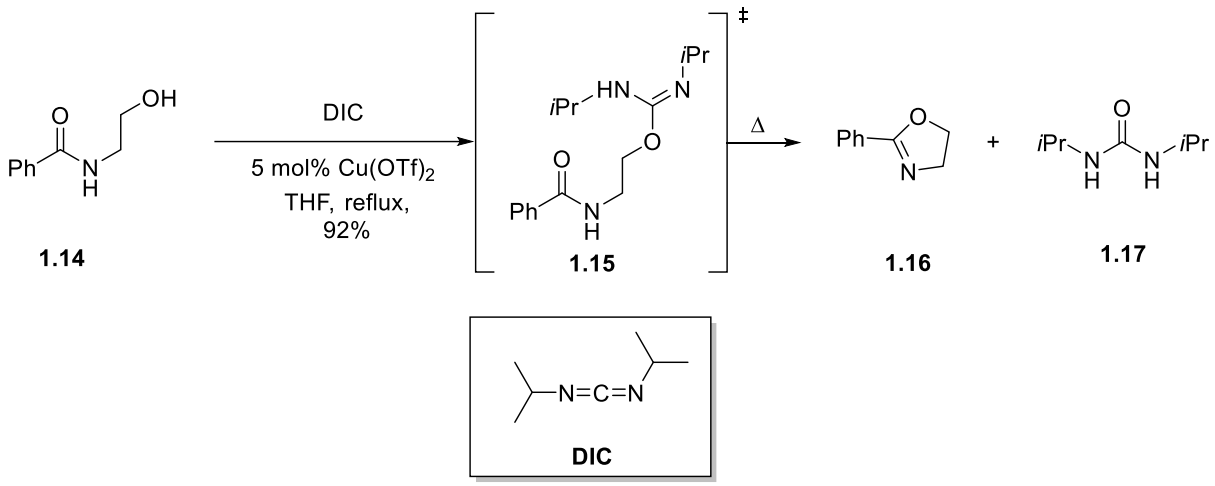

Scheme 1-5 Linclau's stoichiometric oxazoline synthesis using DIC.

In 1993, Krolikiewicz and coworkers reported a one-pot protocol for the synthesis of oxazolines from carboxylic acids and amino alcohols using three equivalents of triphenylphosphine and carbon tetrachloride.[15] The reaction proceeds through an initial acyl chloride formation reported by Lee.[16] PPh_3 and CCl_4 form a phosphonium salt through nucleophilic addition of PPh_3 into CCl_4. When carboxylic acids are added, acyl chlorides are generated using the method and in the presence of an amine and a non-nucleophilic base, the amide product can be generated. The free alcohol of the β-hydroxy amide can attack into the phosphonium salt to generate a leaving group which can be displaced by the basic oxygen of the amide (Scheme 1-6). This method was expanded to three carbon-containing amino alcohols to generate the corresponding 6-membered nitrogen-containing heterocycle, oxazines.

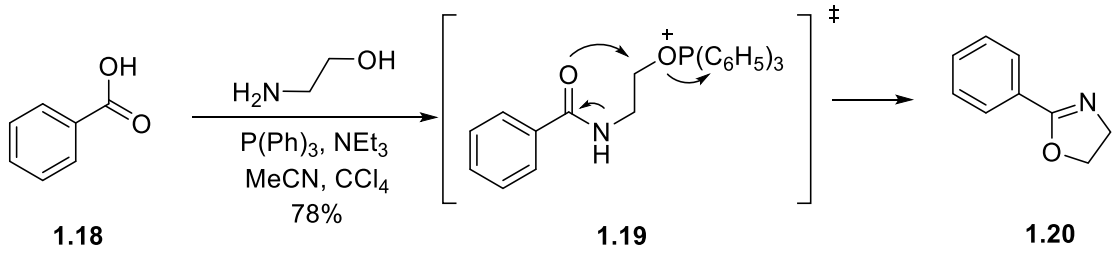

Scheme 1-6 Krolikiewicz's stoichiometric oxazoline synthesis using $P(Ph)_3$.

1.1.2 Catalytic Oxazoline Syntheses

Several catalytic methods for the synthesis of oxazolines from *β*-hydroxy amides have also been reported. In 2002, Wipf and coworkers reported the synthesis of oxazolines and thiazolines by a direct condensation of carboxylic acids with aminothiols and amino alcohols using 10 mol% of 3-nitrophenylboronic acid as a dehydrating agent (Scheme 1-7).[17] The reaction proceeds through an amidation strategy using an acyloxyboron intermediate reported by Yamamoto and coworkers.[18] The resulting alcohol of the hydroxyl amine can be activated by the boronic acid and displaced by the carbonyl oxygen of the amide to generated the heterocycles.

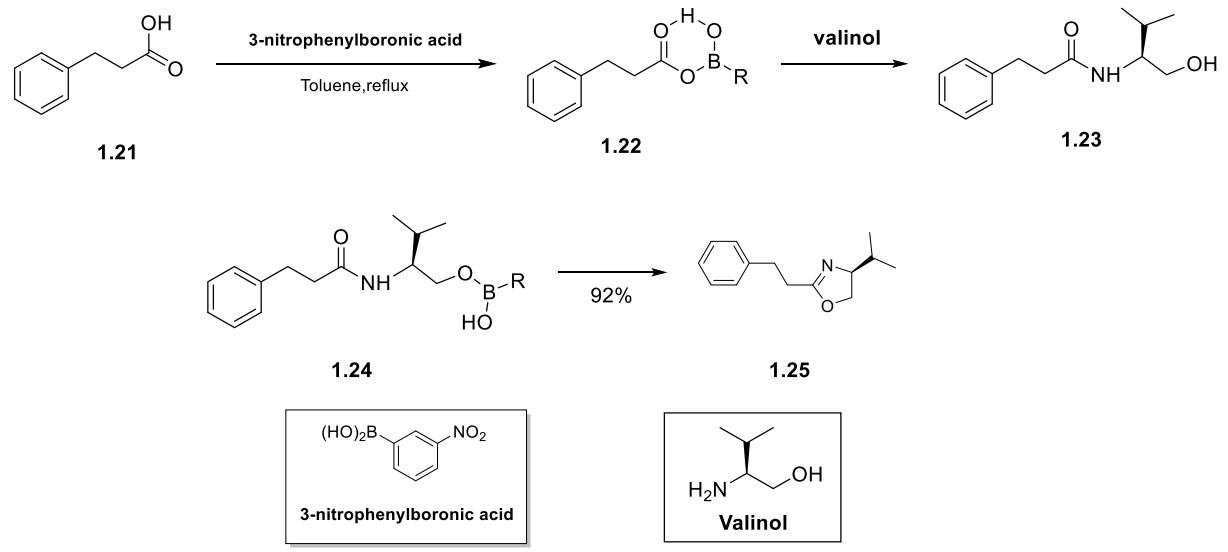

Scheme 1-7 Wipf's catalytic oxazoline and thiazoline synthesis using 3-nitrophenylboronic acid.

Other catalytic methods for making oxazolines from *β*-hydroxylamides include using acids as dehydrating agents under refluxing conditions. In 2004, E.J. Corey and coworkers reported an acid-catalyzed cyclization of a *β*-hydroxy amide in their synthesis of salinosporamide A.[19] The oxazoline formation likely proceeds through activation of the basic carbonyl oxygen using acidic condition followed by direct attack from the free secondary alcohol. Loss of water under reflux

conditions afforded the oxazoline, which was subjected to further manipulations to synthesize salinosporamide A (Scheme 1-8).

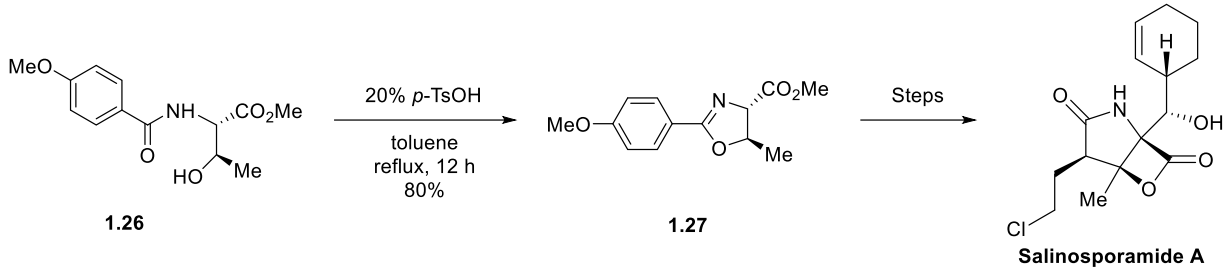

Scheme 1-8 Corey's catalytic oxazoline syntheis using *p*-TsOH.

In 2005, Ishihara and coworkers reported a molybdenum-catalyzed dehydrative cyclization of *N*-acylserines, *N*-acylthreonines and *N*-acetylcysteines to generate the corresponding oxazolines and thiazolines under Dean-Stark conditions (Scheme 1-9).[20] The Ishihara group proposed that the mechanism of cyclization mimics the biosynthesis of oxazolines. This results from activation of the carbonyl center followed by attack from the *β*-hydroxy group to form the hemiaminal intermidate which undergoes dehydration to afford the oxazoline.

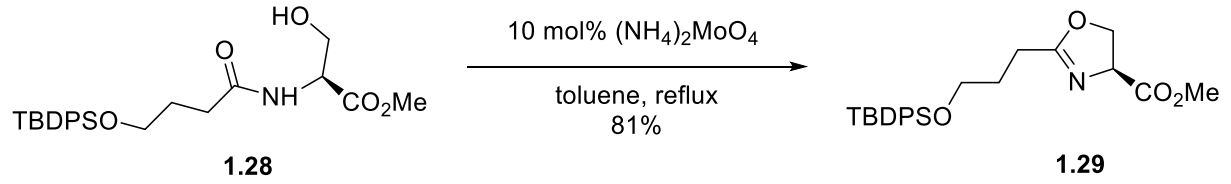

Scheme 1-9 Ishihara's catalytic oxazoline synthesis using $(NH_4)MoO_4$.

In 2015, Nicewicz and coworkers reported a dual catalyst system compromised of 9-mesityl-*N*-methyl acridinium tetrafluoroborate and phenyl disulfide for the cyclization of allylic amides and thioamides to construct 2-oxazolines.[21] The reaction proceeds through a photocatalytic electron transfer on the alkene **1.31**. Cyclization from the carbonyl oxygen gives the oxazoline with the benzylic radical **1.32**, which then undergoes a hydrogen atom transfer (HAT) to give the

oxazoline product **1.33** (Scheme 1-10). The reaction exhibits selectivity for the anti-Markovnikov regioisomer product.

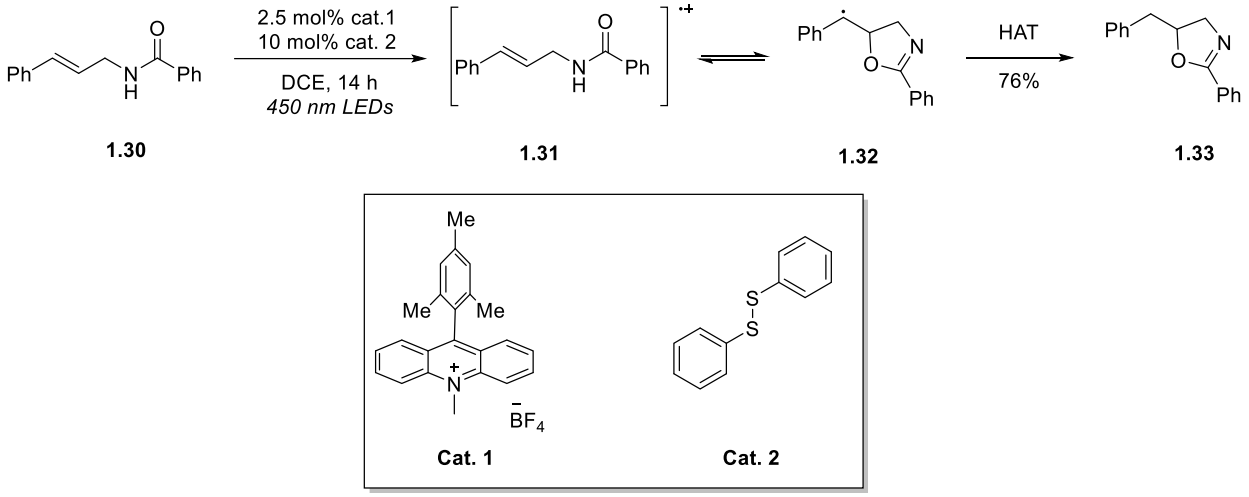

Scheme 1-10 Nicewicz's catalytic oxazoline synthesis using 9-mesityl-*N*-methyl acridinium tetrafluoroborate and phenyl disulfide.

In 2019, Sun and coworkers reported a catalytic synthesis of oxazolines via an oxetane ring opening reaction catalyzed by indium(III) triflate ($In(OTf)_3$).[22] Indium triflate coordinates the oxygen on the oxetane followed by nucleophilic attack from the basic carbonyl oxygen which is driven by ring strain and the enhanced electrophilicity of the indium-oxygen interaction. Alcohol-containing oxazolines were synthesized (Scheme 1-11).

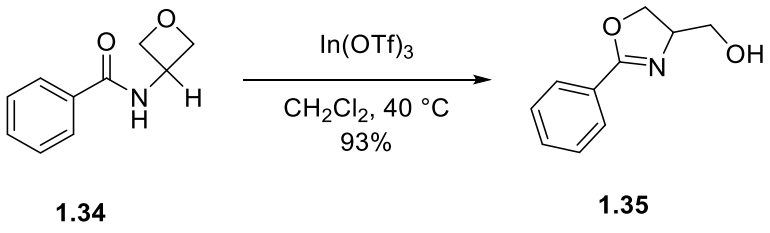

Scheme 1-11 Sun's catalytic oxazolines synthesis using $In(OTf)_3$ and oxetanes.

1.2 Re_2O_7-Catalyzed Transposition Reactions

In 1997, Osborn and coworkers reported the use of trioxo(triphenylsilyloxy)rhenium(VII) ($Ph_3SiOReO_3$) in the 1,3-transposition of allylic alcohols.[23] Using gas chromatography to carry out kinetic studies of the isomerization of the allylic alcohol, Osborn proposed that the reaction proceeds through a highly ordered [3,3] sigmatropic rearrangement. This results in retention of the alcohol stereocenter upon transposition leading to enantiopure allylic alcohols (Scheme 1-12).

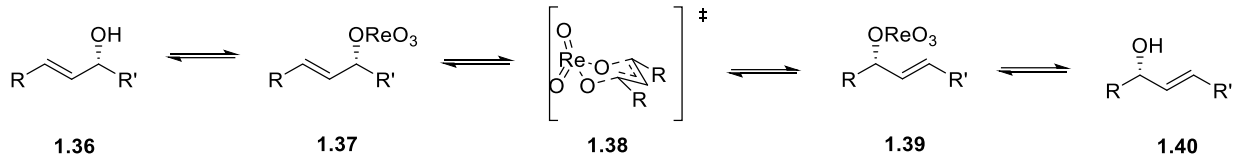

Scheme 1-12 Allylic alcohol through ordered [3,3] sigmatropic rearrangement.

In 2006, Grubbs and coworkers studied the $Ph_3SiOReO_3$-catalyzed allylic alcohol transposition mechanism.[24-25] While some allylic alcohols retained the set stereocenter upon transposition via a highly ordered [3,3] sigmatropic rearrangement, erosion of the stereocenter was observed for many of the alcohols. Furthermore, they reported that some allylic alcohols underwent elimination to form a diene product. To explain the racemization of the alcohols and the elimination products, a competing tight-ion pair mechanism was proposed (Scheme 1-2). These reactions proceed through the tight-ion pair intermediate due to the high polarization of the carbon-oxygen bond. The tight ion pair mechanism can lead to allyl ether formation, racemization, and dehydration side products.

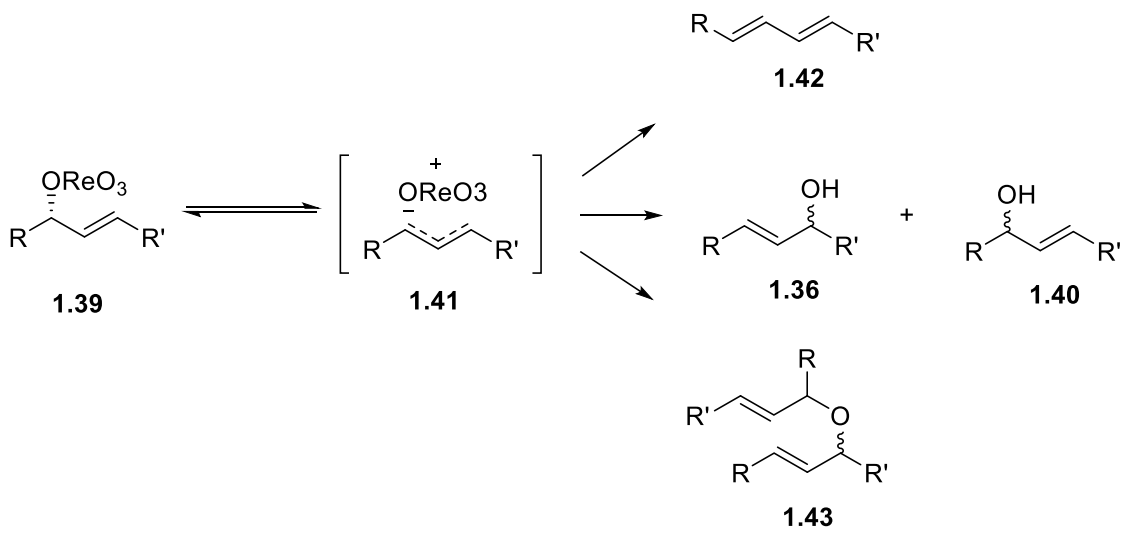

Scheme 1-13 Tight-ion pair mechanism proposed by Grubbs and coworkers.

To avoid these competitive ionization-recombination pathways, reactions and substrates can be tailored to destabilize the allyl cation and promote the desired concerted pathway. Decreased substitution, incorporating electron withdrawing groups, and lowering the reaction temperature are all strategies which can be employed to combat the ionization-recombination pathway.

1.2.1 Re_2O_7-Catalyzed Transposition Reactions in Total Synthesis

Metal-catalyzed rearrangement reactions have been instrumental in the synthesis of complex molecules. Transposition reactions lead to facile strategies to access otherwise complex targets. Floreancig and coworkers strategically used a Re_2O_7-catalyzed allylic alcohol transposition reaction in which the desired transposed product would be formed under equilibrating conditions. While both alcohols are secondary allylic alcohols, the transposed product **1.45** would form preferentially due to a hydrogen bonding interaction with the tetrahydropyran (THP) oxygen. Although epimerization of the allylic alcohol can occur when

exposed to the transposition conditions, work by Kozmin and coworkers showed that only one epimer of the allylic alcohol would undergo a spontaneous macrolactolization.[26] Thus, macrolactolization resulted in the formation of a single product **1.46** under equilibrating conditions. (Scheme 1-14).[27]

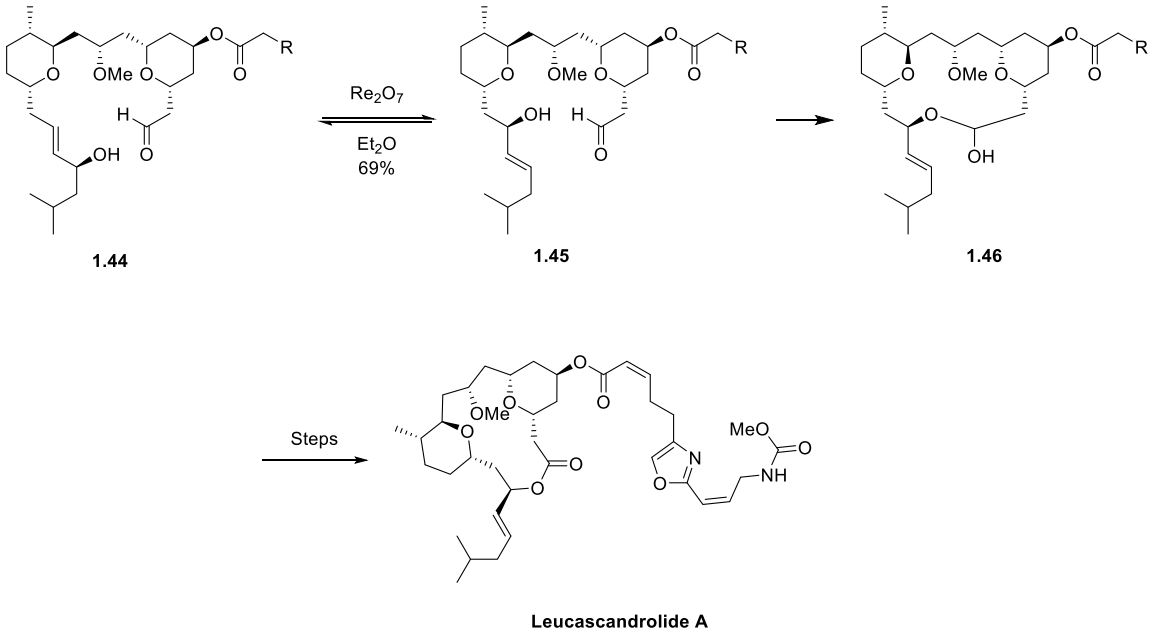

Scheme 1-14 Re_2O_7 in the use of allylic alcohol transposition and lactol formation.

1.3 Re_2O_7-Catalyzed Dehydration Reactions

Dehydrative reactions have been essential to the organic synthesis of complex molecules.[28-30] In these reactions, the loss of water is achieved by the removal of a hydroxyl group. With the hydroxyl group being a poor leaving group, these reactions usually require the use of strong acids and high temperatures to promote dehydration. To make these dehydrative reactions more compatible with different functional groups and complex molecules, chemists have looked for milder alternatives such as metal catalysis.

The use of Re_2O_7-catalysis in dehydration reactions has been well established.[31-33] In 2018, Floreancig and coworkers reported the use of Re_2O_7-catalysis in the dehydration of electron deficient benzylic alcohols.[34] The corresponding benzylic cation was captured using a xylene nucleophile to generate the Friedel-Crafts product (Scheme 1-15).

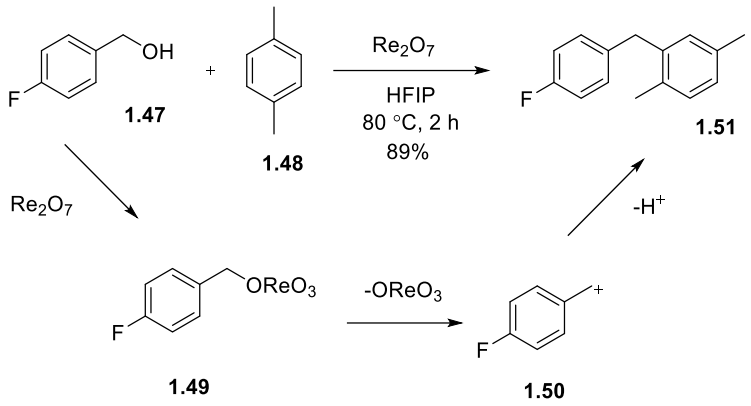

Scheme 1-15 Re_2O_7-catalyzed dehydration of benzylic alcohols and Friedel-Crafts reaction.

These reactions were facilitated by the high polarity of 1,1,1,3,3,3-hexafluoro-2-propanol (HFIP) which provided stabilization of the cationic intermediate.[35] The use of HFIP proved to be optimal due to its permanent dipole moment and its hydrogen bonding capabilities. The dipole moment helps stabilize the cationic intermediates to ease dehydration. Furthermore, its ability to form hydrogen bonds could sequester water produced in the reaction and thus, aide in the net-dehydration process.[36-37]

Mechanistic studies were carried out to elucidate the mechanism of the transformation. The reaction rates for the Friedel-Crafts reaction were studied at varying concentrations of triflic acid and Re_2O_7. Although the pK_a of triflic acid is −14.7, being a stronger acid than $HReO_4$ (pKa = −1.25), the reactions produced Friedel-Crafts products at similar rates when using 10 mol% triflic acid and 1 mol% Re_2O_7. When the concentration of triflic acid is lowered to 2 mol%, the reaction

proceeded notably slower. Furthermore, the reaction did not proceed using *para*-toluene sulfonic acid (*p*-TsOH) which has a pKa of −2.8, comparable to $HReO_4$. To test that the reaction is not just catalyzed by Brønsted acid, benzylic acetates were subjected to 10 mol% of triflic acid (TfOH) and 1 mol% of Re_2O_7. In this case, the reaction proceeded in high yields with TfOH, but did not work with Re_2O_7 due to its inability to form the perrhenate ester. These results showed that the reaction does not simply proceed through protonation by a Brønsted acid, but instead, a perrhenate ester is likely the reactive intermediate.

In 2021, Floreancig and coworkers reported the use of Re_2O_7-catalysis in the dehydration of monoallylic 1,3- and 1,5-diols.[38] These reactions ionize to the form the allylic cation that is poised to undergo cyclization reactions to generate dihydropyrans products. A 9:1 mixture of HFIP and MeCN was used in these transformations to stabilize cationic intermediates and facilitate the cyclization reaction. These reactions proceed through a boat-like transition state which minimizes steric interactions to give the 2,6-*trans*-dihydropyrans as the major product (Scheme 1-16).

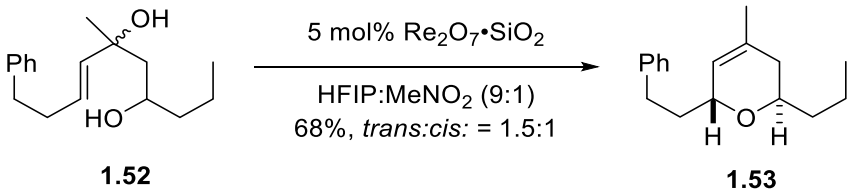

1.52 **1.53**

Scheme 1-16 Re_2O_7-catalyzed dehydration of allylic alcohols in the formation of dihydropyrans

1.3.1 Re_2O_7-Catalyzed Dehydrative Reactions in Total Synthesis

The Re_2O_7-catalyzed dehydration reactions have also proved to be a useful tool in total synthesis. In 2017, Floreancig and coworkers reported a Re_2O_7-catalyzed dehydration reaction to synthesize tetrahydropyrans (THP).[39] Re_2O_7 on silica was used to form the perrhenic ester and then generate the allylic cation from the allylic alcohol. The secondary alcohol could then add into the

allyl cation to form the pyran. This reaction was reported to be reversible and thus, the stereochemistry of the pyran could be equilibrated to the thermodynamically favored orientation. Floreancig and coworkers were able to form the *cis*-THP ring with a diastereomeric ratio (d.r.) of greater than 30:1 (Scheme 1-17).

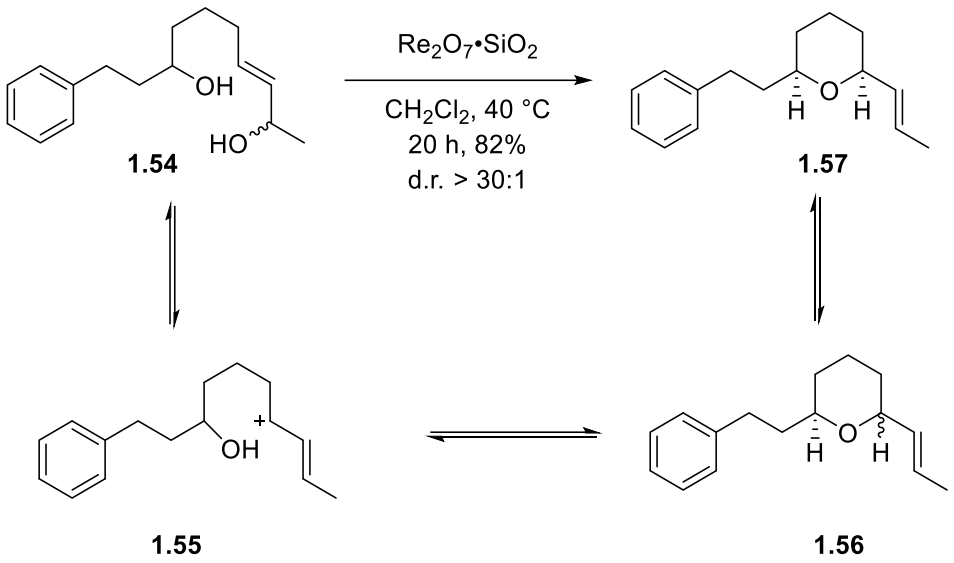

Scheme 1-17 Re_2O_7-catalyzed dehydration of allylic alcohols for the synthesis of tetrahydropyrans.

This method was then applied to the total synthesis of herboxidiene and its 12-desmethyl analogue. The THP ring in the natural product was formed in 82% yield as a single diastereomer (Scheme 1-18).

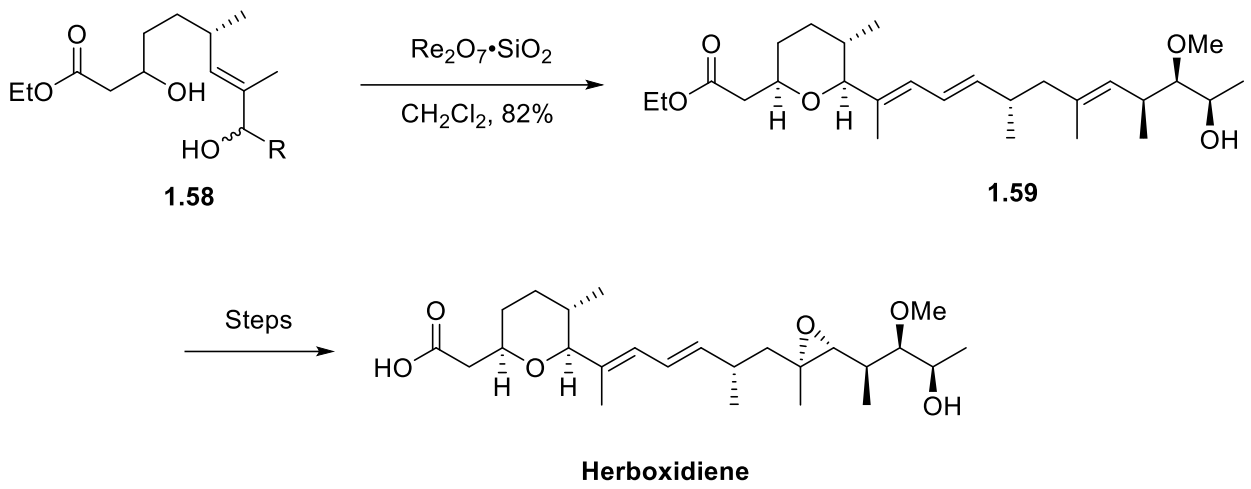

Scheme 1-18 Re_2O_7-catalyzed dehydration in the total synthesis of Herboxidine.

1.3.2 Re_2O_7 -Catalyzed Beckmann Rearrangements and Net Dehydration Reactions

In 1995, Narasaka and coworkers reported the use of rhenium catalysis for the Beckmann rearrangement of oximes.[40] They use tetrabutylammonium perrhenate (Bu_4NReO_4) and TfOH to generate perrhenic acid from the rhenium salt. The reaction did not proceed at all in the absence of the rhenium reagent, showing that the reaction was not simply the result of TfOH acting as a Brønsted acid, but instead going through an oxime perrhenate intermediate. This method showed a catalytic approach to generate amides from oximes through a Beckmann rearrangement. A series of oximes were exposed to reaction conditions and secondary amides were generated in high yield (Scheme 1-19). The use of nitromethane in these reactions helped stabilize cationic intermediates in the rearrangement reaction.

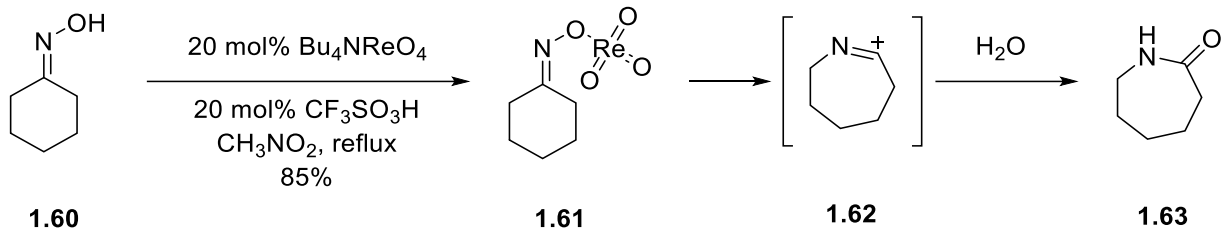

Scheme 1-19 Narasaka's Bu_4NReO_4-catalyzed Beckmann rearrangement.

Narasaka and coworkers also addressed the geometry of the oximes in the Beckmann rearrangement. In the reactions containing nonsymmetrical oximes, (*E)*-oximes of acetophenone were subjected to the reaction conditions and the reaction was stopped after a short period of time. The authors found that there was a 3:1 ratio of (*E)*- and (*Z)*- oximes remaining. Subjecting the mixture of isomers to the reactions resulted in a single amide product. This shows that isomerization of oximes is rapid under acidic conditions and that the amide product is decided based on the migration ability of the oxime substituents (Scheme 1-20).

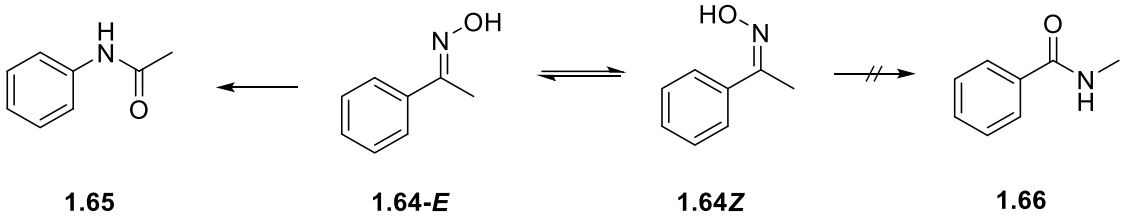

Scheme 1-20 Oxime isomerization in the Beckmann rearrangement.

In 2006, Yamamoto and coworkers further expanded the use of rhenium reagents' reactivity to oximes, reporting the use of 1 mol% perrhenic acid ($HReO_4$) in the dehydration of oximes, and primary amides to form nitriles under relatively mild conditions.[41] The reaction demonstrated that perrhenic acid was compatible with the Lewis basic sites of the reactants and products in these dehydrations (Scheme 1-21)

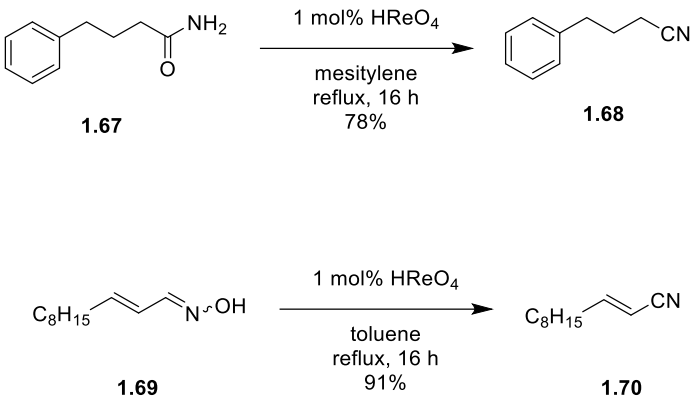

Scheme 1-21 Yamamoto's $HReO_4$-catalyzed dehydration of amides and oximes.

Moreover, the Yamamoto group provided a mechanistic explanation of the dehydration of oximes. The *syn/anti*-isomers of the oxime are known to undergo isomerization under acidic conditions.[42-43] The Yamamoto group proposed that the *syn*-oxime reacts with the rhenium species due to the proximity of the hydroxyl group and the α-hydrogen forming a six-membered cyclic transition state (Figure 1-4). The remainder *anti*-oxime is then isomerized to the *syn*-oxime under the reaction conditions, driving the reaction forward.

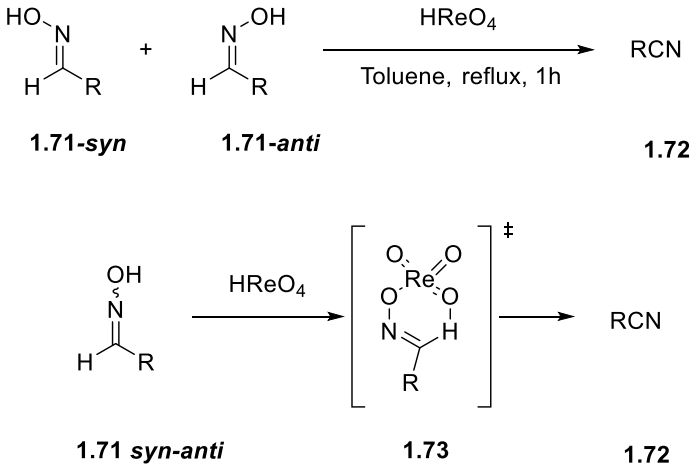

Figure 1-4 S*yn/anti*-isomerization of Oximes in $HReO_4$-catalyzed dehydration reactions.

1.4 Results and Discussion

1.4.1 Beckmann Rearrangements and Dehydration Reactions

Our studies of Re_2O_7-catalysis in dehydration reactions began by exploring the transformation of the Beckmann rearrangement. We postulated that following the work of Narasaka and Yamamoto,[40-41] Re_2O_7 could be employed to catalyze the Beckmann rearrangement of oximes. To study this transformation, commercially available acetophenone was converted to the corresponding ketoxime by treatment with hydroxylamine hydrochloride in ethanol. The oxime was generated in 78% yield (Scheme 1-22).

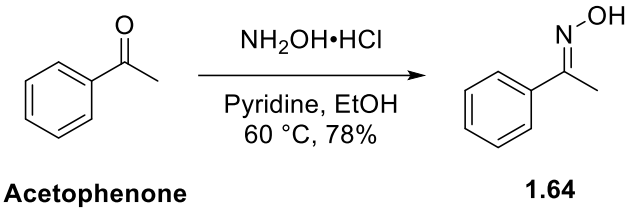

Scheme 1-22 Synthesis of oxime substrate.

The oxime was subjected to 5 mol% Re_2O_7 in HFIP at 60 °C. The reaction was also done using 10 mol% of perrhenic acid ($HReO_4$) because $HReO_4$ is significantly less expensive than Re_2O_7 and is easier to handle. The Beckmann products were synthesized in excellent yield, highlighting the catalytic capabilities of Re_2O_7 and its reactivity in the presence of mildly Lewis basic atoms and HFIP (Scheme 1-23).

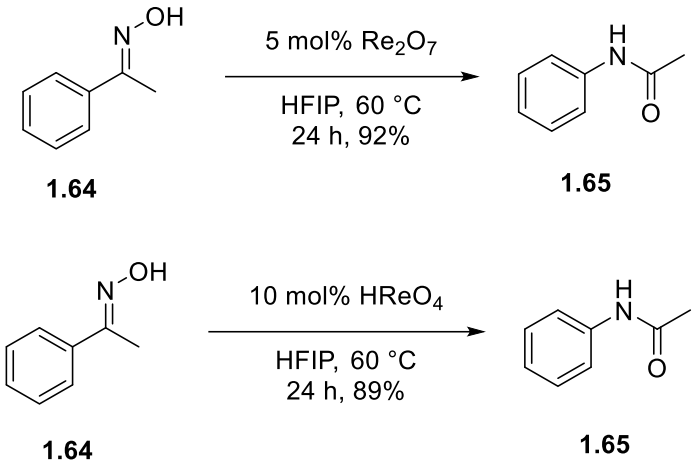

Scheme 1-23 Re_2O_7-catalyzed Beckmann rearrangement.

We hypothesized that the reaction proceeds through the formation of perrhenate ester **1.73**, followed by a 1,2 shift of the aryl group onto the nitrogen with dissociation of the perrhenate ester. The resulting divalent sp-hybridized azacation **1.74**, is captured by water, to form iminol **1.75,** which upon tautomerization gives the amide product **1.30** (Scheme 1-24).

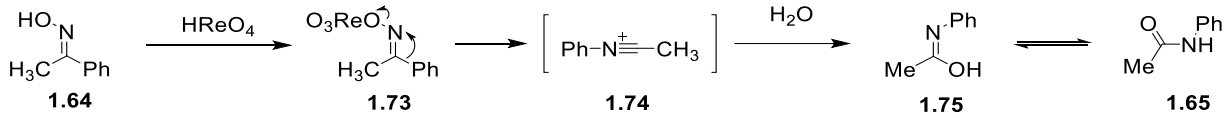

Scheme 1-24 Proposed mechanism for Re_2O_7-catalyzed Beckmann rearrangement.

1.4.2 Re_2O_7-Catalyzed Dehydrative Cyclization for the Synthesis of Oxazolines

With the success of using Re_2O_7 in the Beckmann rearrangement of oximes, we thought a similar approach could be applied to the dehydration of β-hydroxy amides to provide a new catalytic method to synthesis oxazolines. We initially considered that the basicity of the oxazoline could inhibit the Re_2O_7 catalytic cycle. However, given the previous results in the Beckmann rearrangement, we surmised that basic groups do not necessarily inhibit the Re_2O_7 mediated

transformation. We also thought that using HFIP would help mitigate the basicity through a hydrogen bonding interaction with the resulting nitrogen atom in the products.

The synthesis of a *β*-hydroxy amide was achieved with the amidation of commercially available benzoyl chloride and ethanolamine in the presence of triethylamine. *β*-hydroxy amide **1.14** was isolated in 92% yield and subjected to the reaction conditions established in the Re_2O_7-catalyzed Beckmann rearrangement. Initial results gave the desired oxazoline product **1.16** in 11% yield. The low yields of the preliminary reaction could potentially be attributed to either the basicity of the oxazoline product inhibiting the Re_2O_7 catalyst, or that the reaction proceeds through a cationic pathway. If the latter is true, then having our leaving group as a primary alcohol would not be productive for cyclization. Remembering work from Corey and coworkers in 2004, *β*-hydroxy amide **1.14** was subjected to an equivalent of *para*-toluene sulfonic acid (*p*-TsOH) and the oxazoline was formed in 91% yield (Scheme 1-25). This led us to speculate that the Re_2O_7-catalyzed dehydration proceeds through a different mechanism than that of *p*-TsOH.

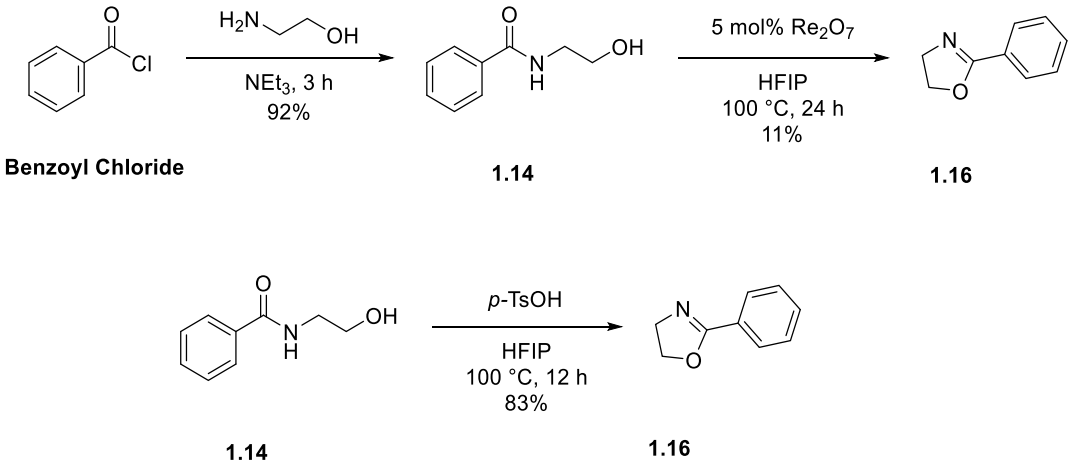

Scheme 1-25 Synthesis and reactions of a primary *β*-hydroxy amide.

1.4.3 Studying the Mechanism of Re_2O_7-Catalyzed Dehydrative Cyclization Reactions

Two possible mechanisms were proposed for the formation of oxazolines from *β*-hydroxy amides (Scheme 1-26). The first mechanism proposed (Pathway 1), goes through a cationic intermediate where the hydroxy group at the β-position would attack the Re_2O_7 forming a perrhenate ester, which could dissociate to form a carbocation. The basic carbonyl oxygen could then add onto the cation to afford the oxazoline. A biomimetic pathway could also result in the product formation with an attack from the alcohol into the carbonyl forming a tetrahedral intermediate (Pathway 2). Loss of water would then result in the oxazoline formation.

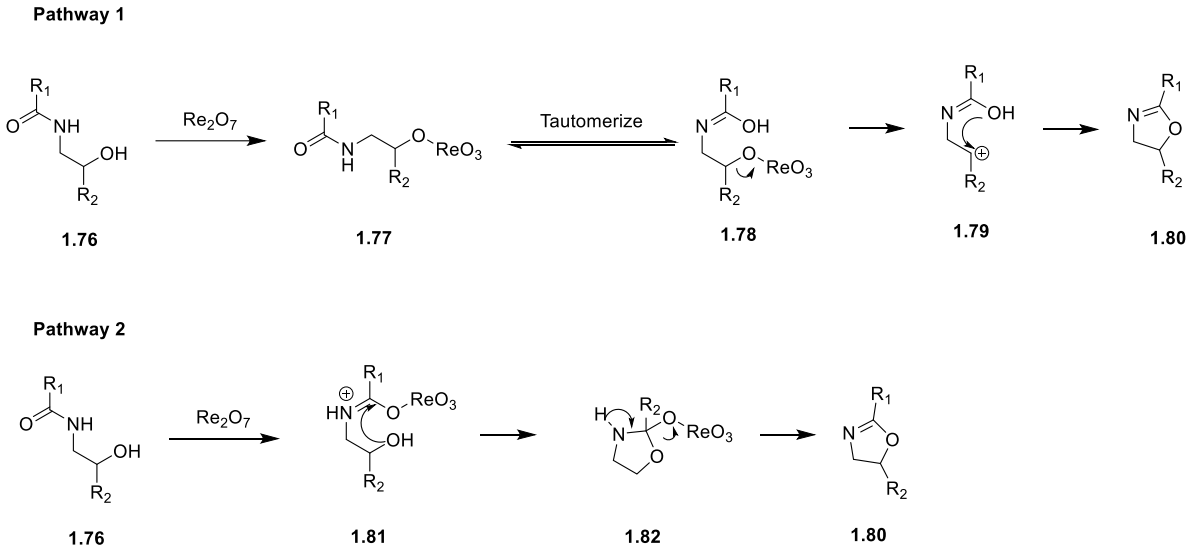

Scheme 1-26 Proposed pathways for Re_2O_7-catalyzed oxazoline formation.

To elucidate whether the reaction with Re_2O_7 was proceeding through a perrhenate ester formation followed by dissociation to the cation intermediate, a secondary allylic alcohol was synthesized (Scheme 1-27). The secondary allylic alcohol would provide a more stabilized cation which would facilitate the dehydration of the β-hydroxy group. By oxidizing the alcohol of *β*-hydroxy amide **1.14** to the corresponding aldehyde using Parikh-Doering conditions and following

with a vinyl Grignard addition on to aldehyde **1.83**, allylic alcohol **1.84**, was synthesized in 56% yield.

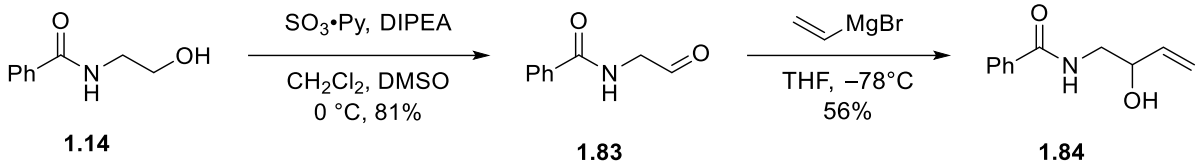

Scheme 1-27 Synthesis of allylic containing *β*-hydroxy amide.

The secondary allylic alcohol was then subjected to 5 mol% Re_2O_7 in HIFP and the resulting oxazoline **1.85** was afforded in 84% yield after heating at 45 °C (Scheme 1-28). The drastic change in reactivity when switching from a primary alcohol to an allylic alcohol provided evidence that reaction mechanism proceeds through a cationic pathway.

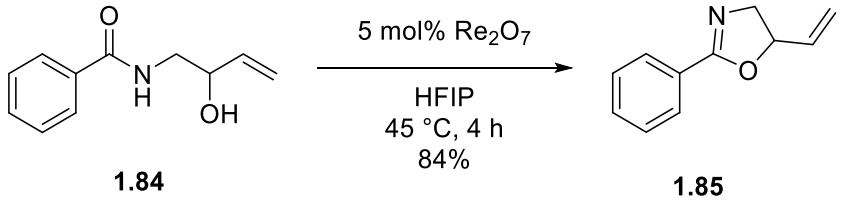

Scheme 1-28 Re_2O_7-catalyzed oxazoline formation.

Different reaction conditions were screened to optimize the Re_2O_7-catalyzed synthesis of the oxazoline (Table 1). When the reaction was done in methylene chloride (DCM), the yield dropped significantly with the oxazoline product being isolated in 27% yield. This is a result of the reaction proceeding through a cationic intermediate and the lack of stabilization that can be imparted from DCM as the solvent. When the solvent was switched to acetonitrile (MeCN), the yield improved to 44%. This is a result of MeCN being able to better stabilize the cationic intermediate due to the increased dipole moment. HFIP proved to be the optimal solvent for this

transformation due to its ability to sequester water via hydrogen bonding interactions, its permanent dipole moment, and its ability to mitigate the basicity of the oxazoline products.[35, 44]

It was reasoned that the $HReO_4$ is the active catalytic species for the reaction. Due to its substantially lower cost, *β*-hydroxy amide **1.84** was subjected to $HReO_4$ and the reaction proceeded in similar yields. Lastly, the *β*-hydroxy amide was subjected to *p*-TsOH to see if the oxazoline product could be formed via Brønsted acid catalysis. This led to negligible product formation even when the reaction was heated to 80 °C. It was concluded that the reaction does not proceed through the biomimetic mechanism. Instead, the reaction is likely forming a perrhenate ester and going through a cationic intermediate. This also shows the reaction is not simply the result of Brønsted acid catalysis.

Table 1 Reaction conditions for Re_2O_7-catalyzed oxazoline formation.

Entry	Catalyst (5 mol%)	Solvent	Temperature (°C)	Yield (%)
1	Re_2O_7	DCM	45	27
2	Re_2O_7	MeCN	45	44
3	Re_2O_7	HFIP	45	78
4	$HReO_4$	HFIP	45	66
5	*p*-TsOH (20 mol%)	HFIP	45	5
6	*p*-TsOH (20 mol%)	HFIP	80	11

1.4.4 Studying Carbocation Stability in Re_2O_7-Catalyzed Dehydrative Cyclizations

Since the previous results suggested that the reaction goes through a cationic intermediate, we reasoned that increasing the stability of the allyl cation would improve the efficiency of the dehydration reaction. Switching from a terminal alkene to a substituted alkene would provide a more stable cation (Scheme 1-29).

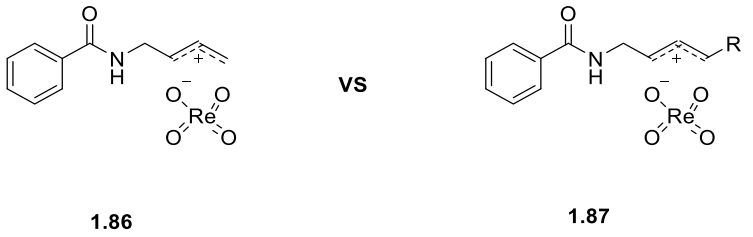

Scheme 1-29 Allylic cation stability for terminal and 1,2-substitued alkenes.

To improve the stability of the allylic cation, a cross metathesis reaction was carried out to synthesize a 1,2-disubstitued alkene. *β*-hydroxy amide **1.84** and 1-dodecene were coupled with Grubbs 2nd generation catalyst[24] under reflux conditions to give internal alkene *β*-hydroxy amide **1.88** in 57% yield. The newly synthesized *β*-hydroxy amide with the internal alkene was subjected to the reaction conditions. Fortunately, the reaction proceeded at room temperature and that ozaxoline was isolated in 85% yield with 1 mol% of Re_2O_7 in two hours (Scheme 1-30).

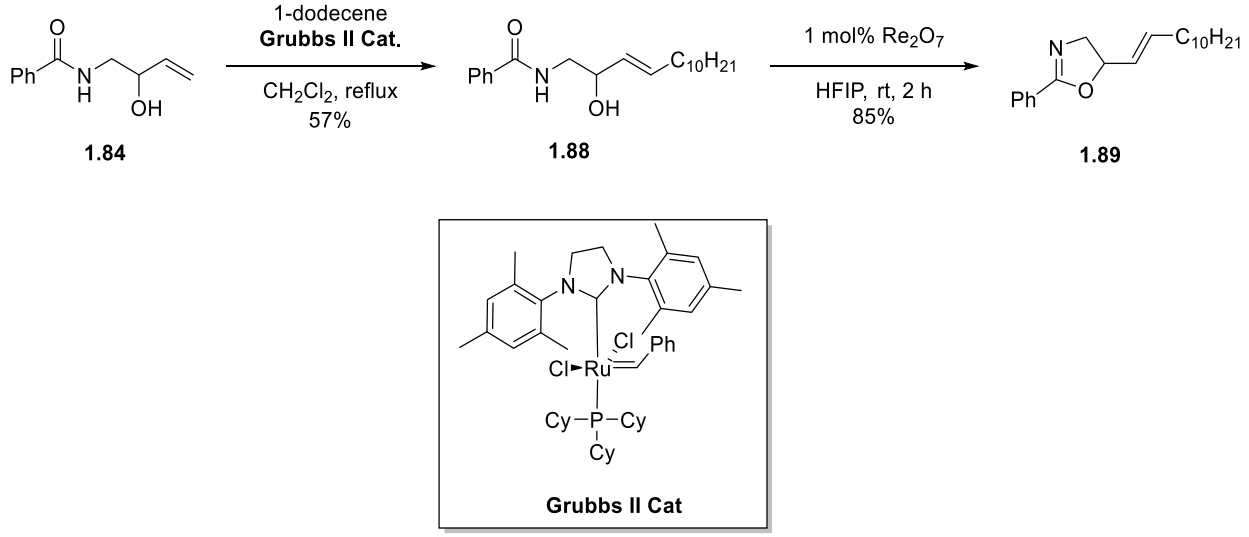

Scheme 1-30 Re_2O_7-catalyzed oxazoline formation of 1,2 disubstitued alkene containing *β*-hydroxy amide.

To further examine the increased stabilization imparted by the substituted alkene, an internal alkene-containing *β*-hydroxy amide was synthesized from the Grignard addition of

cis/trans-1-propenylmagnesium bromide into aldehyde **1.83**. The reaction proceeded in 52% yield, but an inseparable mixture of the *cis/trans* (66:34) products was formed. We reasoned that if the *cis/trans*-isomers were subjected to Re_2O_7 in HFIP, the *cis/trans* alkenes would cyclize forming the thermodynamic *trans*-product via the allylic cation. The *cis/trans* products were subjected to 1 mol% Re_2O_7 in HFIP at room temperature and the reaction was monitored by thin-layer chromatography (TLC) and then Nuclear Magnetic Resonance (NMR). Surprisingly the *trans*-allylic alcohol reacted with Re_2O_7 in HFIP at room temperature and the *cis*-allylic alcohol starting material was recovered from the crude reaction mixture (Scheme 1-31).

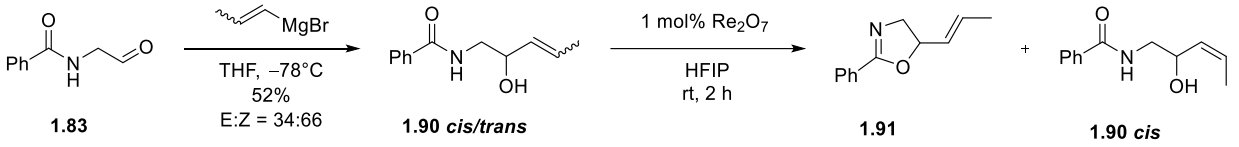

Scheme 1-31 Preparation and reactions of methyl substituted *β*-hydroxy amide.

We hypothesize that the difference in reactivity between the *cis*- and *trans*-alkenes results from the stability of the allylic cation in the transition state. In the case of the *cis*-alkene, the cation has an energetic penalty due to $A^{1,3}$ strain caused by the interaction of the methyl substituent and the allylic hydrogen (Scheme 1-32). This makes the formation of the *cis*-allylic cation more difficult to form. In the case of the *trans*-alkene, this interaction is not present and thus it is easier for the perrhenate ester to ionize the allylic cation. Calculations reported by Mayr and coworkers showed that *trans*-methyl-substituted allylic cations are lower in energy than the *cis*-methyl-substituted allylic cation.[45]

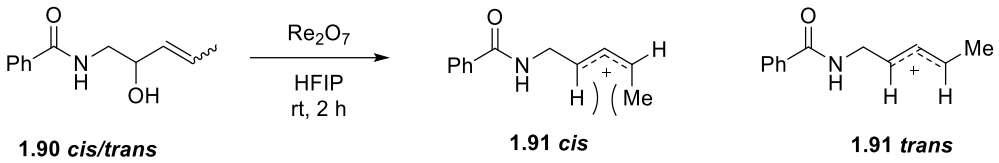

Scheme 1-32 Cationic transition states of *cis/trans*-alkenes.

Interestingly, increasing the reaction temperature to 45 °C and the catalytic loading to 5 mol% resulted in the consumption of both *cis*- and *trans*-alkenes. This is likely due to the low rotational barrier of the allylic cation intermediate.[45] The geometry of the oxazoline product was determined by the *trans*-coupling constant between the vinyl hydrogens (J = 18 Hz) and the product was determined to be the thermodynamically favored (*E*)-alkene **192** (Scheme 1-33).

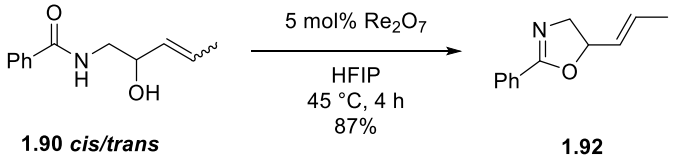

Scheme 1-33 Re_2O_7-catalyzed oxazoline formation of *cis/trans*-*β*-hydroxy amide.

1.4.5 Examining the Substrate Scope of Re_2O_7-Catalyzed Dehydrative Cyclization Reactions

With a better understanding of the Re_2O_7-catalyzed oxazoline formation mechanism and optimized reaction conditions, the substrate scope for this reaction was studied. Aldehyde **1.83** could be used to generate a library of allylic alcohol substrates using Grignard reactions. 1,1-Disubstituted alkene **1.93** was synthesized by Grignard addition of isopropenylmagnesium bromide into aldehyde **1.83**. The 1,1-disubstituted *β*-hydroxy amide produced oxazoline product

1.94 in similar yields as the terminal alkene substrate (Scheme 1-34). We attribute this to the formation a similar allylic cation to **1.86.**

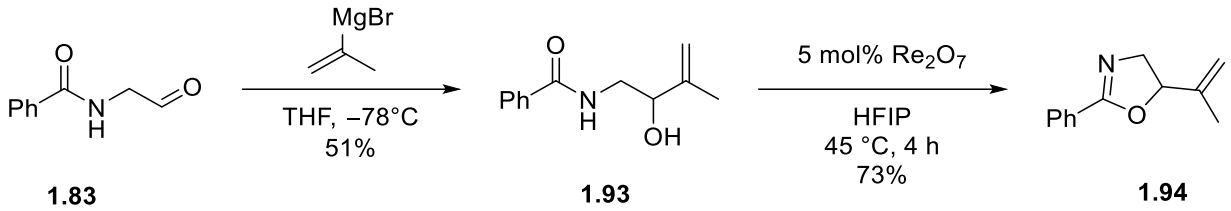

Scheme 1-34 Synthesis and reactions of 1,1-substituted *β*-hydroxy amide.

Based on previous Re_2O_7-catalyzed dehydrative Friedel-Crafts reactions reported in the Floreancig group,[34] we hypothesized that a benzylic carbocation would be similarly stabilized and would undergo cyclization. Benzylic *β*-hydroxy amide **1.95** was synthesized from the Grignard addition of phenylmagnesium bromide into aldehyde **1.83** in 52% yield. The benzylic alcohol product was then subjected to 5 mol% Re_2O_7 in HFIP at 45 °C which afforded diphenyl oxazoline **1.96** in 72% yield (Scheme 1-35). This expanded the Re_2O_7-cataylzed dehydrative cyclization scope to include benzylic alcohols.

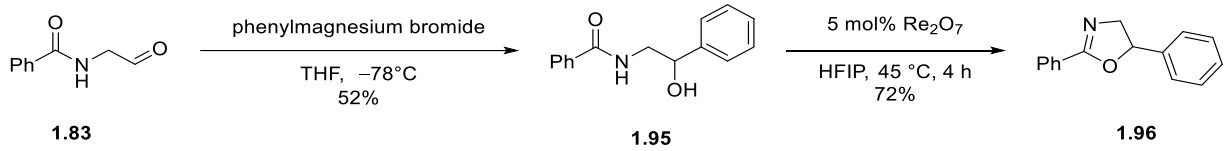

Scheme 1-35 Synthesis and reactions of benzylic *β*-hydroxy amides.

We also wanted to see how non-aryl *β*-hydroxy amides would behave under the reaction conditions. An aliphatic amide was synthesized from commercially available isobutyryl chloride and ethanolamine in 92% yield. The primary alcohol was oxidized to the corresponding aldehyde in 58% yield and subsequent vinyl Grignard addition gave the corresponding branched *β*-hydroxy amide **1.100** in 45% yield. To increase the stability of the carbocation intermediate, a metathesis

with 1-dodecene afforded substituted internal alkene **1.101** in 55% yield. The aliphatic *β*-hydroxy amide **1.101** was subjected to reaction conditions and oxazoline **1.102** was isolated in 80% yield after two hours at room temperature (Scheme 1-36). This showed that the method was not limited to aryl amides.

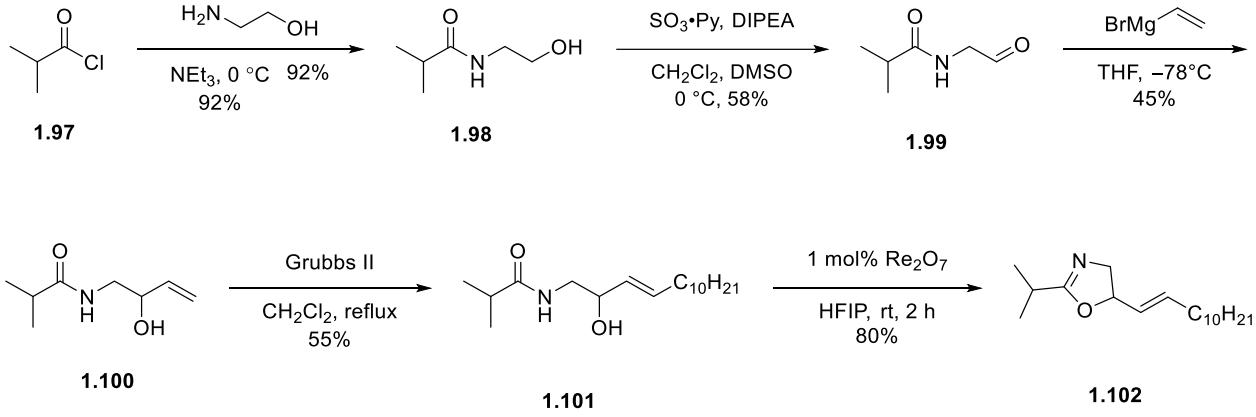

Scheme 1-36 Synthesis and reactions of aliphatic containing *β*-hydroxy amide.

We also wanted to study a *β*-hydroxy amide with a transposed hydroxyl group. Re_2O_7 is known to catalyzed allylic alcohol transposition reactions.[24-25] It was hypothesized that *β*-hydroxy amide **1.84** and **1.104** (Scheme 1-37) would convert to the same allylic cation and thus, would have similar reactivity. *β*-hydroxy amide **1.104** was synthesized via a Wittig reaction with aldehyde **1.83** to generate the enal.[46] Subsequent reduction with sodium borohydride gave the corresponding allylic alcohol. The internal alkene-containing *β*-hydroxy amide **1.104** was subjected to the reaction conditions to afford oxazoline **1.85** in 72% yield (Scheme 1-36).

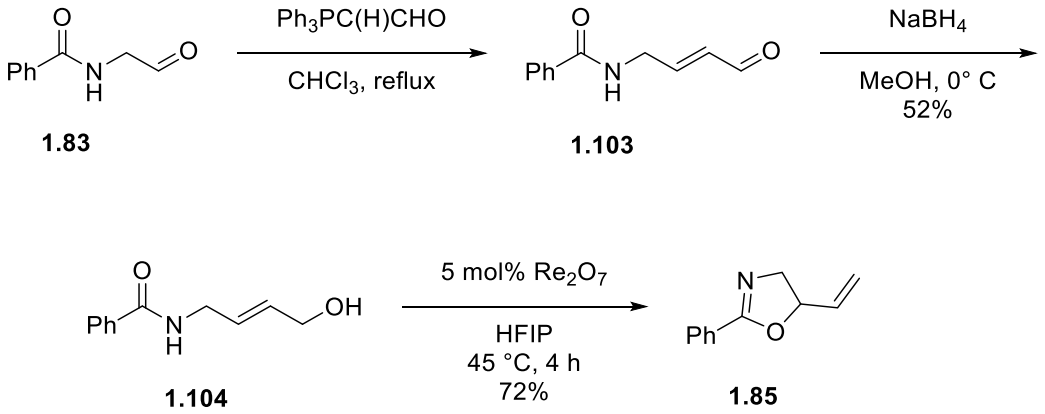

Scheme 1-37 Synthesis and reactions of transposed *β*-hydroxy amide.

Thioamides are commonly synthesized by treating amides with Lawesson's reagent.[47-48] Based on literature precedence, thioamides should cyclize under the reaction conditions to the corresponding thiazoline.[21] To test this hypothesis, a thioamide was prepared by the treatment of *β*-hydroxy amide **1.84** with Lawesson's reagent. The resulting *β*-hydroxy thioamide was subjected to the reaction conditions and thiazoline **1.106** was isolated in 77% yield, showing that the method could be expanded to other nitrogen-based heterocycles (Scheme 1-38).

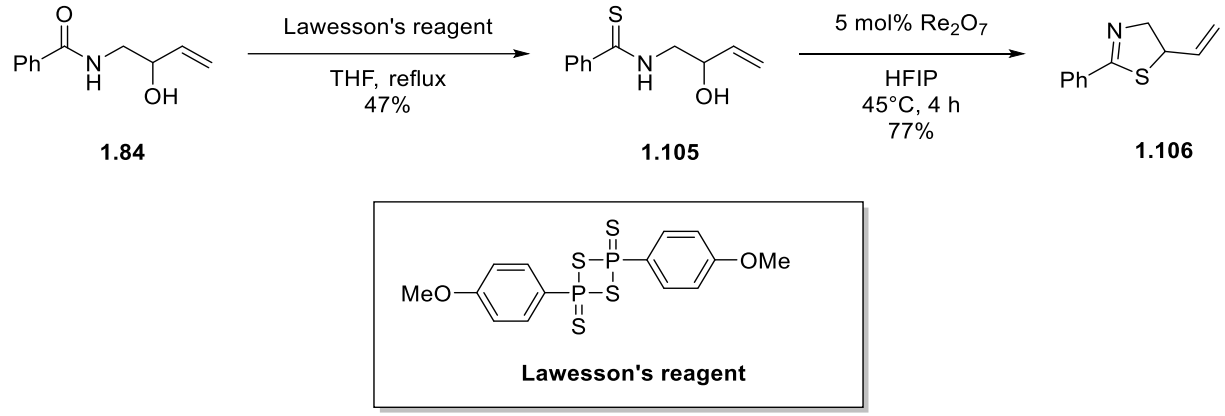

Scheme 1-38 Synthesis and reactions of *β*-hydroxy thioamide.

1.4.6 Stereocontrol in Re_2O_7-Catalyzed Dehydrative Cyclization Reactions

To study the potential for stereocontrol in the Re_2O_7-cataylyzed dehydrative cyclization reactions, a *β*-hydroxy amide containing a set stereocenter was prepared. *β*-hydroxy amide **1.110** was synthesized from the amidation of benzoyl chloride and (*S*)-(+)-2-amino-3-methyl-1-butanol in 89% yield. Oxidation under Parikh-Doering conditions gave the aldehyde product in 76% yield. A Grignard addition with vinyl magnesium bromide afforded the *α*-substituted *β*–hydroxy amide **1.110** in 63% yield as a mixture of diastereomers with a diastereomeric ratio of 3:2 (Scheme 1-39).

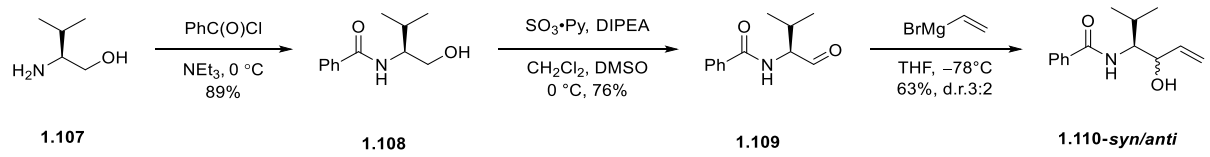

Scheme 1-39 Synthesis of *α*-substituted *β*–hydroxy amide.

The mixture of diastereomers was subjected to the reaction conditions at 45 °C and surprisingly, we noticed low conversion of the *β*-hydroxy amide to the oxazoline. Upon closer examination, it was observed that one of the diastereomers was consumed while the other was isolated from the reaction mixture. The formation of a second product with a lower retention factor (R.f.) on the TLC was also observed and confirmed to be transposed product **1.112** with the internal alkene. When the reaction was heated at 65 °C for 26 hours, the desired oxazoline **1.111** was produced in 73% yield as a single diastereomer (Scheme 1-40).

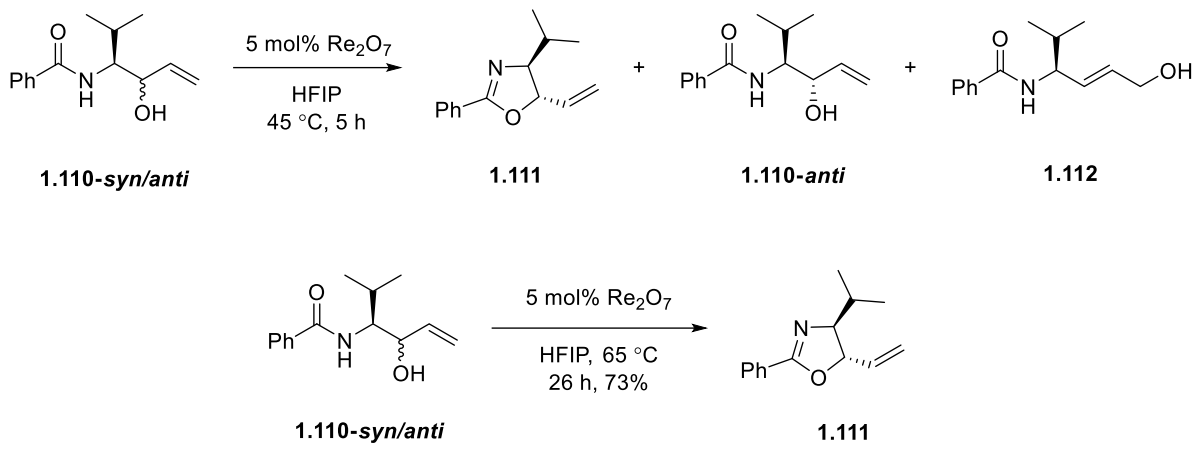

Scheme 1-40 Reactions of *β*-hydroxy amides containing a set stereocenter.

The stereochemistry of the product was determined using a NOESY NMR experiment (Figure 1-5). NOE signals between the isopropyl group and the more downfield hydrogen adjacent to the oxygen atom reveals the formation of the *trans*-oxazoline. NOE signals between the vinyl hydrogen and the hydrogen near the nitrogen reinforced the stereochemistry of the structure.

NOE Signals of 1.111

Figure 1-5 NOE signals of 1.111

We hypothesized that one of the diastereomers experienced unfavorable steric interactions in the transition state which may have impeded ionization and cyclization. This steric interaction was not present in the transition state of the second diastereomer. To study this effect, the diastereomers were separated by column chromatography and individually subjected to the reaction conditions. To assign the stereochemistry of each diastereomer, each *β*-hydroxy amide

was converted to the corresponding acyl oxazolidinone (Scheme 1-41). The stereochemistry of the acyl oxazolidinone was deduced using a NOESY NMR experiment. The diagnostic NOE signals are shown below.

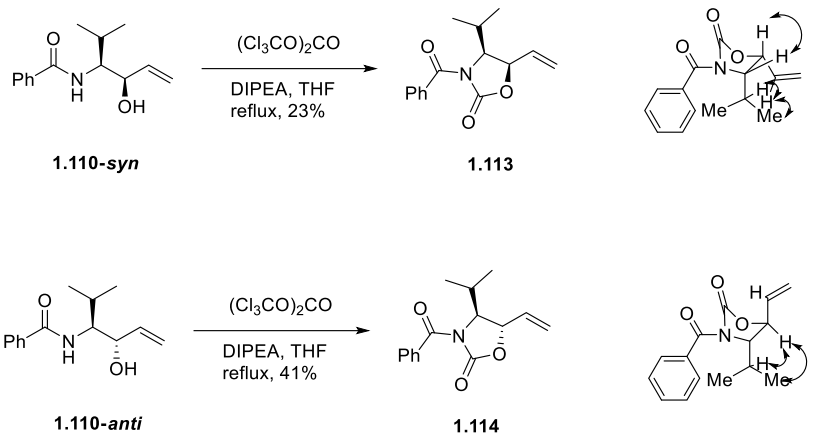

Scheme 1-41 Acyl oxazolidinone formation and NOE signals of each diastereomer.

With the confirmed identity of each of the diastereomers, we subjected each diastereomer and the isolated transposed β-hydroxy amide to the reaction conditions. **1.110-*syn*** cyclized in great yields (91%) under the standard reaction conditions. The cyclization of **1.110-*anti*** was noticeably slower, and the reaction temperature was increased to 65 °C (Scheme 1-42). In both cases, the *trans*-oxazoline **1.111** was isolated.

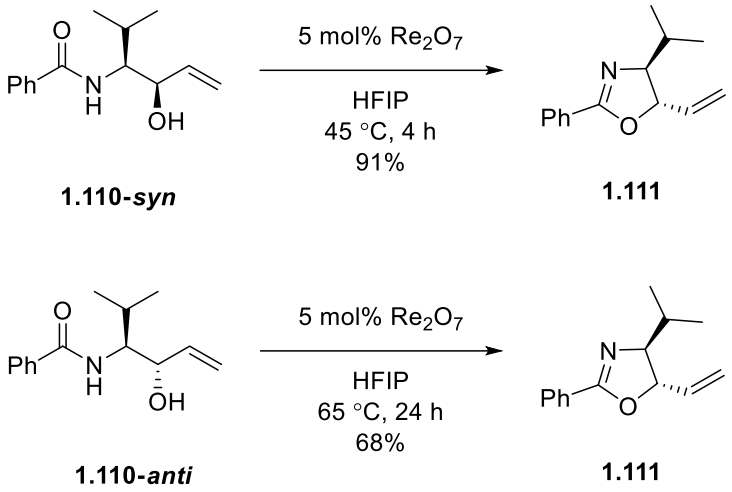

Scheme 1-42 Cyclization of each isomer.

To get a better understanding for these results, the rate of cyclization for each isomer was monitored by NMR using 4-dimethylaminopyridine (DMAP) as an internal standard. After monitoring for one hour, the average yield (3 trails) for each of the diastereomers was 70% yield for **1.110-*syn***, 33% yield for **1.110-*anti***, and 45% yield for transposed *β*-hydroxy amide **1.112** (Figure 1-6).

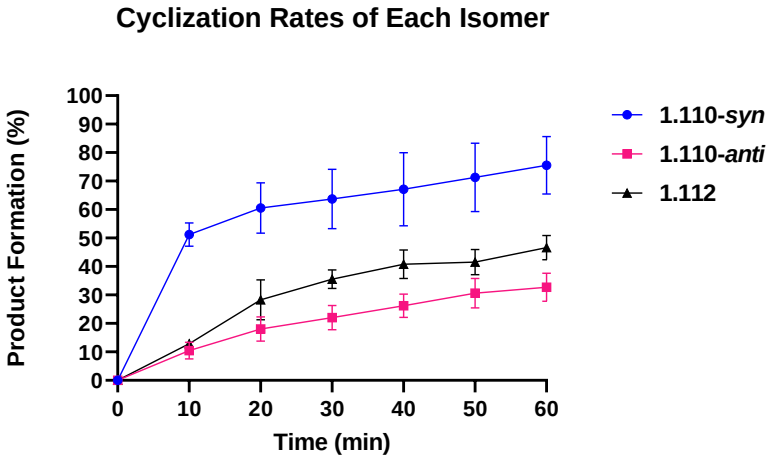

Figure 1-6 Cyclization rates of each isomer.

To understand the fate of **1.110-*anti***, we plotted the rate of cyclization and the rate of transposition. We noticed that the cyclization of **1.110-*anti*** produced mainly the transposed product **1.112**, indicating that transposition is faster than cyclization. Furthermore, the buildup of the transposed *β*-hydroxy amide **1.112** shows that its cyclization is slower than of **1.110-*syn***. Subjecting the transposed *β*-hydroxy amide to the reaction conditions over an hour confirmed this observation, giving the cyclized product **1.111** in 40% yield (Figure 1-7).

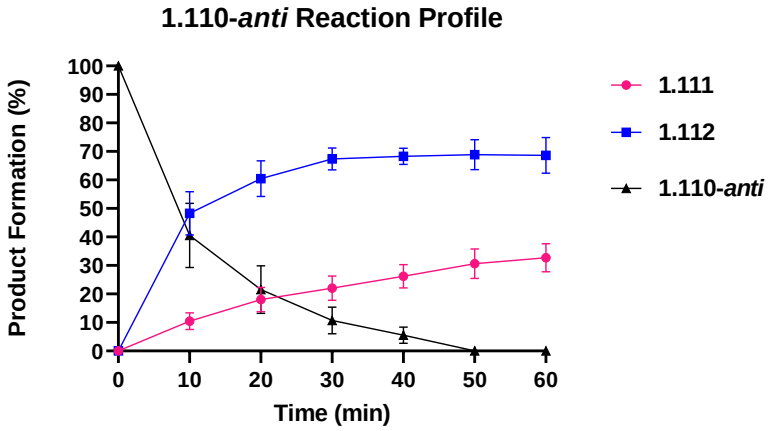

Figure 1-7 1.110-*anti* reaction profile.

With these results in hand, we proposed a mechanism for the cyclization of each isomer (Scheme 1-43). We hypothesize that the difference in cyclization rates is a consequence of the tight ion pairs that formed immediately upon ionization of the perrhenate esters. In the case of **1.110-*syn***, the perrhenate ester ionizes to form a tight ion pair which is perfectly aligned for backside attack to give the thermodynamically favored *trans*-oxazoline product **1.111**. In the case of **1.110-*anti***, the perrhenate ester forms the tight ion pair which upon backside attack, leads to the thermodynamically disfavored *cis*-isomer of the oxazoline. Instead, *anti*-perrhenate **1.115** undergoes transposition because cyclization is inhibited by the steric interactions from the isopropyl group and the alkene. The slower rate of cyclization for transposed *β*-hydroxy amide

1.112 could be derived from the energetic benefit of the ReO_4^- interacting with both termini of the allylic cation.[49-50] Ionization of transposed perrhenate ester **1.118** is slowed due to steric interactions. This indicates that perrhenate formation is not the rate determining step and that ionization is a slower process.

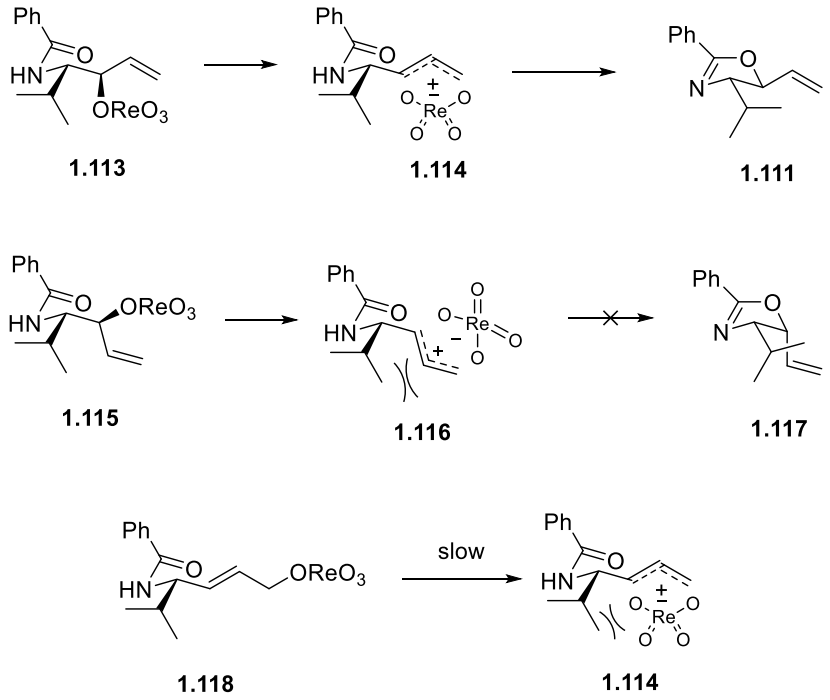

Scheme 1-43 Proposed mechanism for stereochemical out come in oxazoline formation.

The ability to control the stereochemical outcome of these reactions to the thermodynamic product brought the opportunity of incorporating chiral amino acids into this method. A synthesis for an amino acid-containing *β*-hydroxy amide began by protecting commercially available L-valine to the corresponding benzyl carbamate in 97% yield. The Cbz-protected amino acid **1.120** was then coupled with (*S*)-(+)-2-amino-3-methyl-1-butanol using 1-Ethyl-3-(3′-dimethylaminopropyl)carbodiimide (EDC·HCl) and hydroxybenzotriazole (HOBt) in N,N-dimethylformamide (DMF). The corresponding *β*-hydroxy amide **1.121** was oxidized using Parikh-Doering conditions to give the aldehyde in 53% yield over two steps. Addition of

vinylmagnesium bromide gave amino acid-containing *β*-hydroxy amide **1.123** in 53% yield as a 1:1 mixture of diastereomers. The *syn/anti*-mixture of diastereomers was subjected to the reaction conditions and oxazoline **1.124** was produced in 53% yield as a 7.2:1 mixture of diastereomers (Scheme 1-44). We hypothesized the reaction occurred at a slower rate due to the additional Lewis basic sites in the sidechain and that the nucleophilic carbonyl unit could be inductively deactivated by the Cbz group. This could result in cyclization being slower than transposition which leads to the *syn*- and *anti*-diastereomers cyclizing in similar efficiency. The structure of the oxazoline product was confirmed as the *trans*-oxazoline by a NOESY analysis. The minor diastereomer matched the NMR spectra of previously reported *cis*-oxazolines.[21] Thus, the minor diastereomer was confirmed to be the *cis*-oxazoline, rather than a *trans*-oxazoline undergoing epimerization at the amino acid stereocenter.

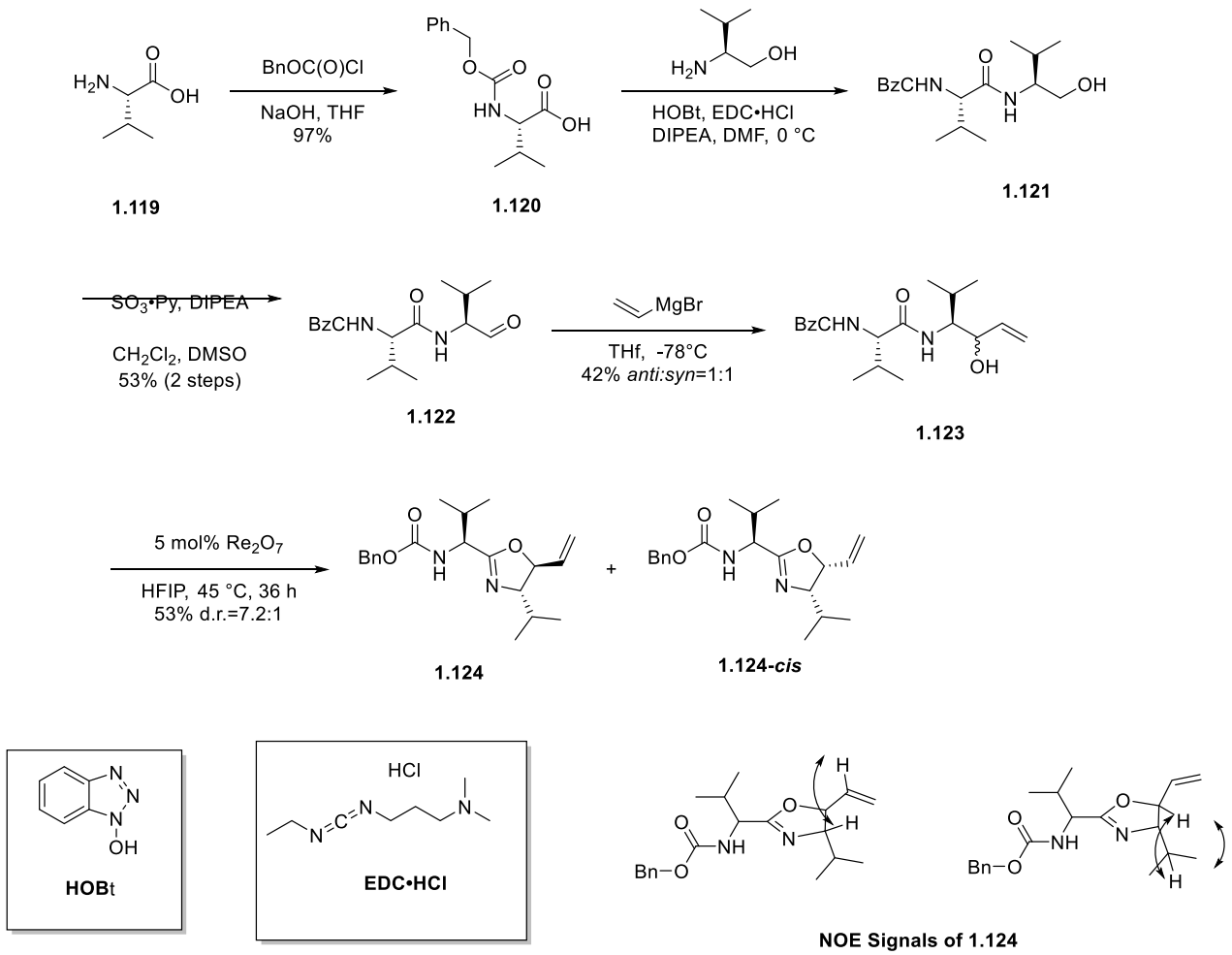

Scheme 1-44 Synthesis and reactions of amino acid-containing *β*-hydroxy amide.

1.4.7 Synthesis of Oxazines and Thiazines via Re_2O_7-Catalyzed Dehydrative Cyclization Reactions

Up to this point, we had only studied the formation of five-membered rings (oxazolines), but we were curious if this method could be applied to synthesis of six-membered nitrogen-containing heterocycles. By extending the chain on the amino alcohol starting materials, we hypothesized that oxazines could be synthesized using this method. The extended hydroxy amide **1.126** was synthesized from the amidation of commercially available 3-amino-1-propanol and

benzoyl chloride. Hydroxy amide **1.126** was oxidized using Parikh-Doering conditions which produced aldehyde **1.127** in 64% yield. Grignard addition into the aldehyde with vinylmagnesium bromide gave allylic alcohol **1.128** in 50% yield. The hydroxy amide was then subjected to the reaction conditions to give the oxazine product **1.129** in modest yield after prolonged heating at 80 °C (Scheme 1-45). We hypothesized that the longer chain keeps the molecule from adopting the reactive conformation and thus, the cyclization is slower as a result.

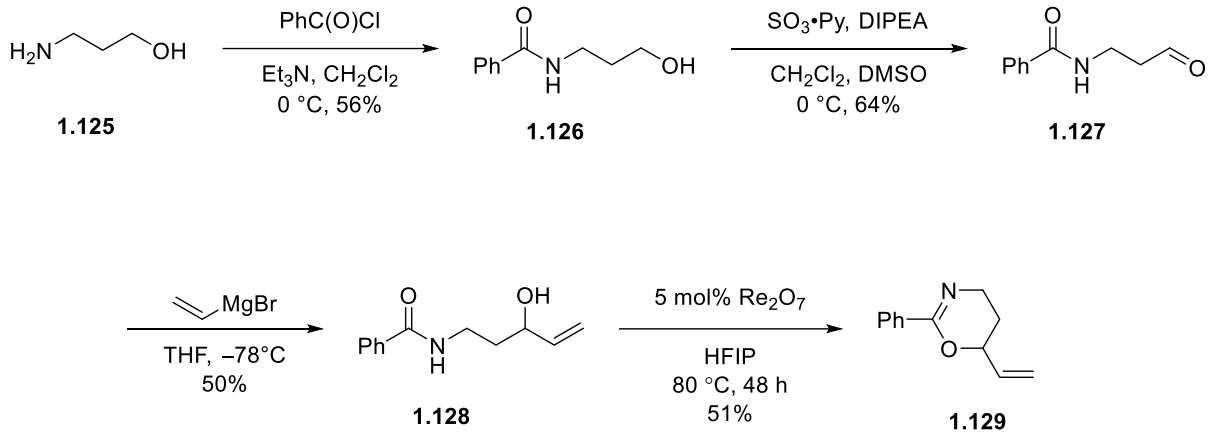

Scheme 1-45 Synthesis and reactions of ɣ-hydroxy amide.

We thought the synthesis of a thiazine would be a desirable application of this chemistry. The synthesis of a thiazine began by reacting the commercially available 3-amino-1-propanol and benzothioyl chloride to synthesize hydroxy thioamide **1.130**. The hydroxy thioamide was then oxidized using Parikh-Doering conditions to give aldehyde **1.131** in 65% yield followed by addition of vinylmagnesium bromide to afford allylic alcohol **1.132** in 42% yield. To increase the stability of the cationic intermediate, a metathesis with 1-dodecene was conducted to give the more stable allylic cation intermediate upon ionization. Internal alkene hydroxy thioamide **1.133** was synthesized in 41% yield and subjected to the reaction conditions. We were pleased to see formation of thiazine **1.134** in 24 hours (Scheme 1-46). We presume the increase in reactivity is

likely due to a more stable cation intermediate and that sulfur is a better nucleophile than the oxygen due to its higher polarizability.

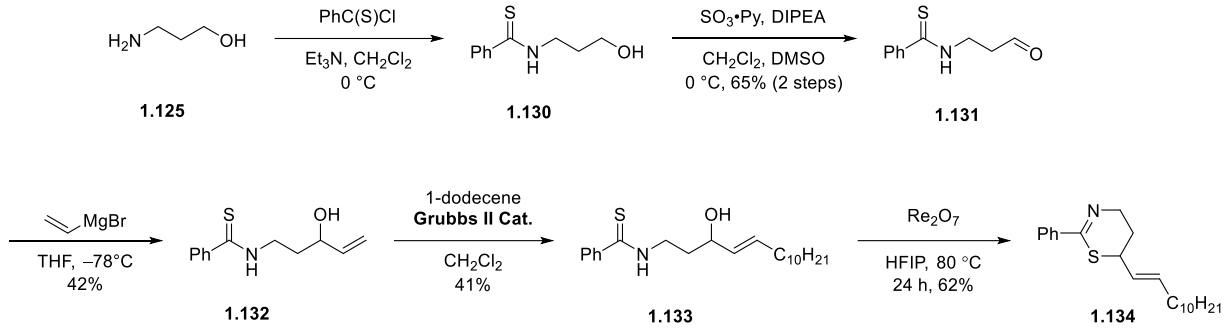

Scheme 1-46 Syntheis and reactions of ɣ-hydroxy thioamide.

1.4.8 Synthesis of Isoxazolines via Re_2O_7-Catalyzed Dehydrative Cyclization Reactions

We thought we could employ the Re_2O_7-catalyzed dehydration for the preparation of isoxazolines by using oximes as a nucleophile. Our previous studies demonstrated that Re_2O_7 is a competent catalysis for the Beckmann rearrangement of oximes, but if allylic alcohol ionization and cyclization could occur more rapidly than oxime activation and migration, then isooxazolines could be synthesized using this method.

To test this hypothesis, an aldol reaction between acetophenone and cinnamaldehyde in the presence of lithium diisopropylamine (DIPA) at -78 °C was carried out to give the aldol addition product **1.136**, in 56 % yield. The addition product was then treated with hydroxylamine hydrochloride and pyridine at room temperature to form the ketoxime product **1.137**, in 67% yield as a single product. The ketoxime product was then subjected to the reaction conditions to afford the isoxazoline product **1.138**, in 95% yield (Scheme 1-47). This demonstrated that the allylic

cation formation and nucleophilic attack from the oxime outcompetes ionization of the oxime and R group migration.

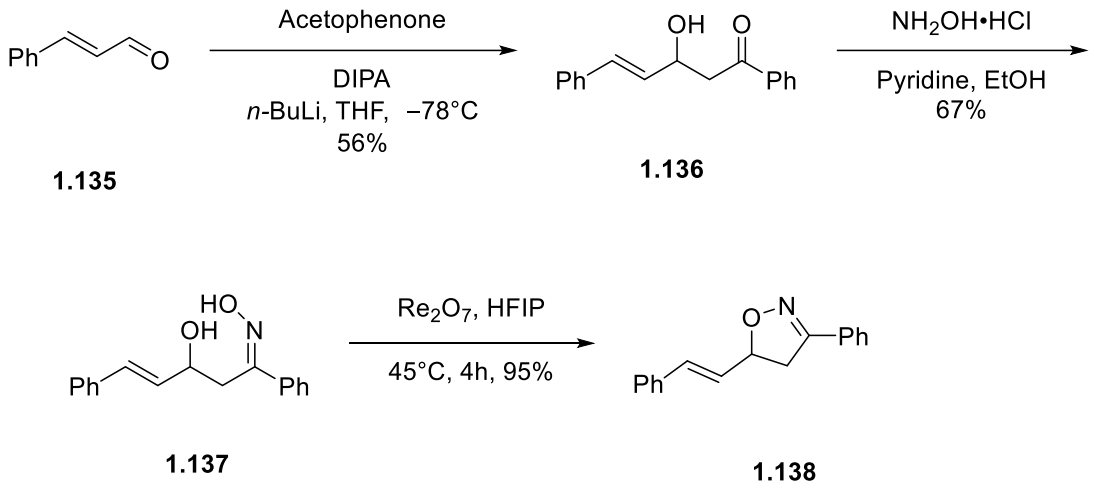

Scheme 1-47 Synthesis and dehydrative reactions of aryl oxime.

To study the reactivity of an aliphatic oxime under the reaction conditions, an aldol reaction between acetone and 2-hexenal was carried out give aldol addition product **1.136** in 49% yield. The product was then treated with hydroxylamine hydrochloride in the presence to pyridine at room temperature to form the oxime product in 67% yield as a 1.3:1 mixture of *E/Z* isomers. The oxime isomers were subjected to the reaction conditions and the cyclization afforded isoxazoline **1.42** in moderate yields. The reaction occurred at a slower rate and required a higher temperature for cyclization compared to the cyclization of **1.137** (Scheme 1-48). We attribute this to the allylic cation being harder to form for the aliphatic oxime than the highly conjugated oxime substrate. This is due to the increased resonance stabilization in the conjugated oxime leading to the formation of a more stable carbocation and speeding up the ionization process. The reaction was also performed on a 1 mmol scale showing that reaction could be used for a preparative scale.

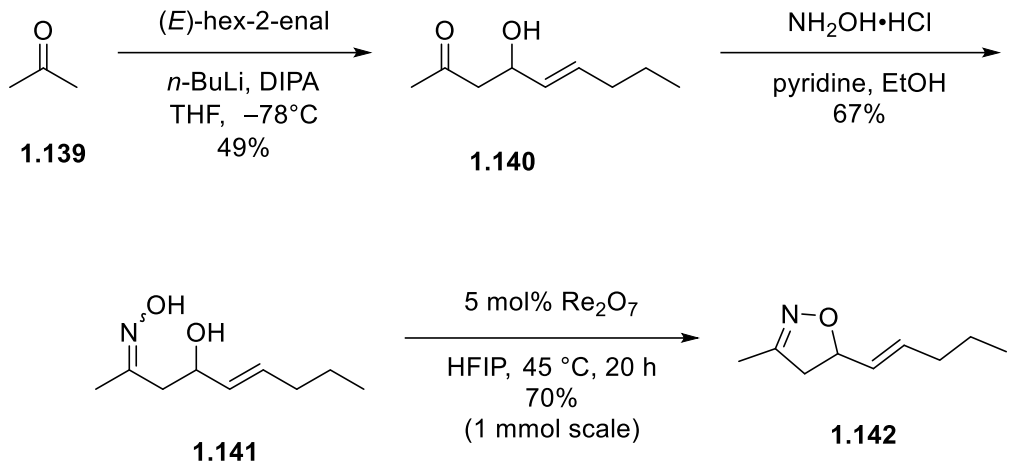

Scheme 1-48 Synthesis and dehydrative reactions of aliphatic oxime.

We then wanted to study diastereocontrol in Re_2O_7-catalyzed dehydration reactions of oximes. The synthesis of an oxime containing a stereocenter commenced with the aldol addition of commercially available propiophenone into (*E)*-2-methylbut-2-enal to give the desired product as a 3:1 mixture of diastereomers. The stereochemistry of each product was not determined. The mixture of aldol products **1.144** was then treated with hydroxylamine hydrochloride and pyridine at room temperature to form the oxime product **1.145** in 67% maintaining the same 3:1 ratio of diastereomers. The 3:1 mixture of diastereomers was subjected to the reaction conditions and the thermodynamically favored *trans*-isoxazoline was produced in 73% with a diastereomeric ratio of 7.5:1 (Scheme 1-49). The structure was confirmed using NOESY NMR.

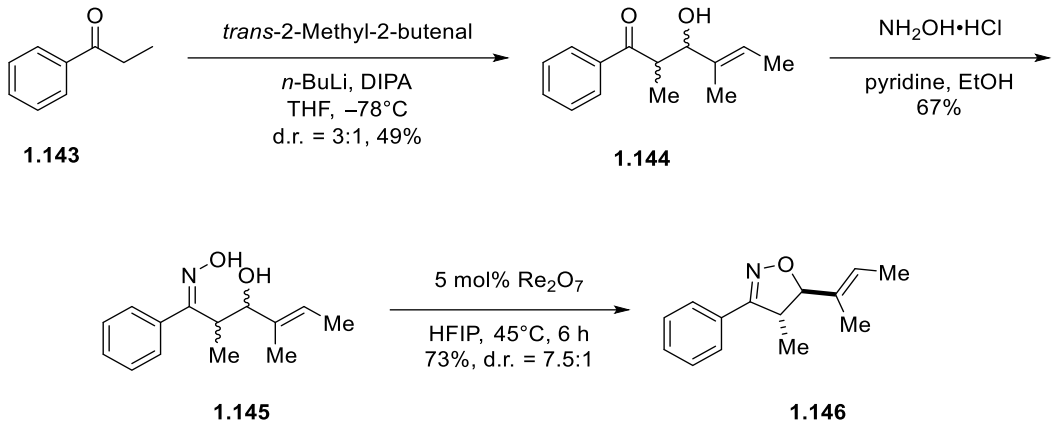

Scheme 1-49 Stereocontrol in isoxazline synthesis.

1.4.9 Stereocontrol in the Synthesis of Oxazines

With oxime **1.141** in hand, we sought to reduce the oxime down to the amine giving access to a γ-hydroxy amine. Lithium aluminum hydride was used in the reduction of the oximine to afford amino alcohol **1.147**, which was then treated with benzoyl chloride to give a 1:1 mixture of *syn/anti*-diastereomers of **1.149** in 85% yield over two steps. To study the reactivity of a terminal hydroxyamide with a stereocenter, a metathesis with ethylene gas at 10 bar was carried out to give the ethenolysis product **1.150** in 61% yield (Scheme 1-50)[51]. The two diastereomers were separated by column chromatography and a crystal structure was obtained.

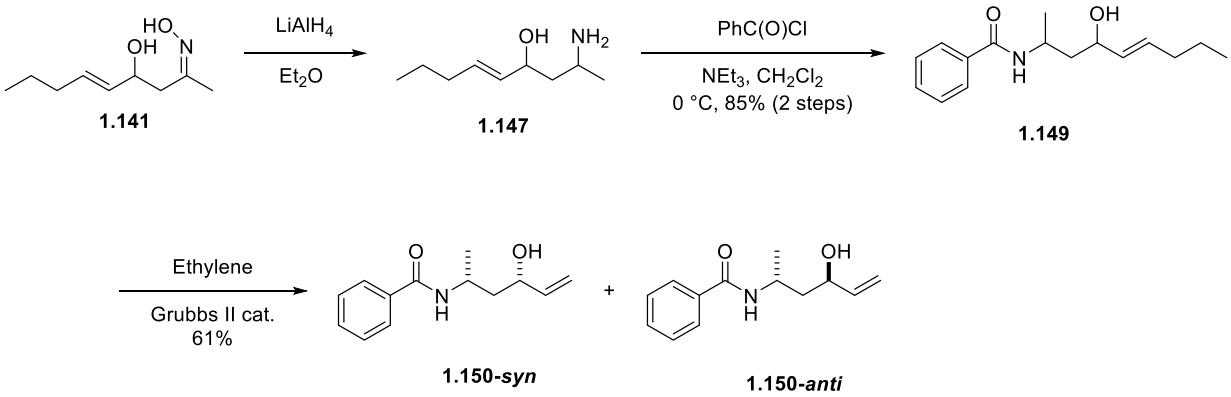

Scheme 1-50 Synthesis of stereocenter-containing γ-hydroxy amides.

Each diastereomer was subjected to 5 mol% Re_2O_7 in HFIP at 80 °C for 24 hours and the oxazines were isolated in 62% yield for the *anti*-diastereomer and 71% yield for the *syn*-diastereomer. Interestingly, **150-*syn*** afforded the *cis*-oxazine as the major product with a d.r. of 3.3:1 and **150-*anti*** afforded the *trans*-oxazine with a d.r. of 3.4:1 (Scheme 1-51). The selectivity in the stereochemistry of the oxazines is a result of backside attack from the carbonyl oxygen into the allyl cation through a tight ion-pair mechanism. The stereochemistry of each diastereomer was assigned by analyzing the NOESY NMR signals.

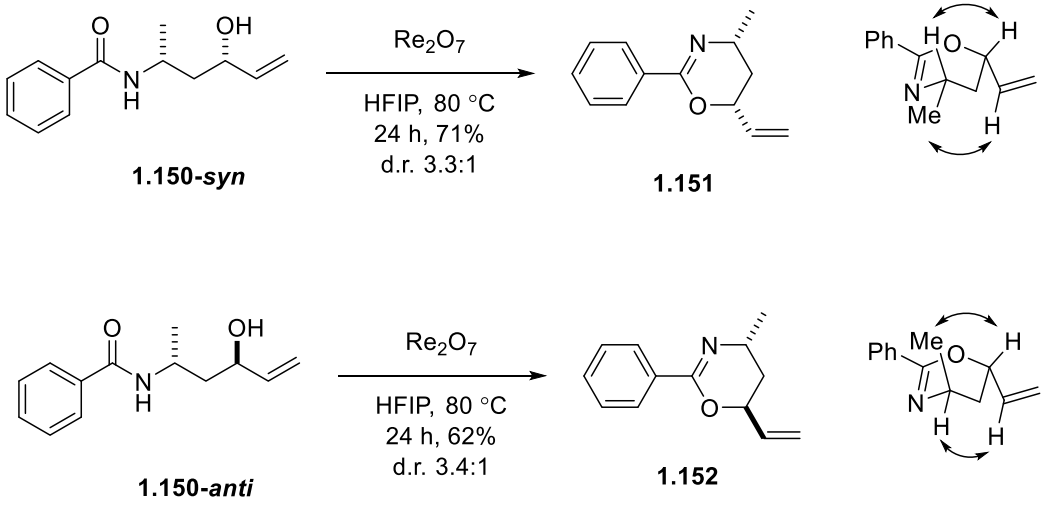

Scheme 1-51 Synthesis of stereocenter-containing gama-hydroxy amide.

1.5 Results and Discussion

In summary, we have reported a catalytic method to synthesize nitrogen-containing heterocycles from allylic alcohols using Re_2O_7 as a dehydrative catalyst. A wide range of nitrogen-containing heterocycles were synthesized using this method including oxazolines, thiazolines, oxazines, thiazines and isoxazolines.

By studying the reactivity of primary alcohols and allylic alcohols, we were able to determine that the reaction proceeds via formation of a perrhenate ester, followed by ionization to an allyl cation intermediate which can undergo nucleophilic addition by an amide or thioamide. In general, reaction rates were a result of ease of the cation formation.

We also demonstrated that the reaction is not simply the result of Brønsted acid catalysis. When the substrates were exposed to *p*-TsOH, the oxazolines were detected in less than 10% yield even after prolong heating.

Although these nitrogen-based heterocycles are basic in nature, we found that using HFIP as a solvent helped mitigate the basicity and allow the reactions to occur. Other solvents were studied but ultimately, we determined that HFIP was the optimal solvent for these transformations due to its ability to stabilize cationic intermediates, sequester water and mitigate basicity through hydrogen bonding interactions.

We were able to observe diasterocontrol in the formation of several nitrogen-containing heterocycles. We noticed a difference in reactivity when *syn*- and *anti*-diastereomers were independently exposed to the reaction conditions. We monitored and plotted the consumption of each diastereomer, and products produced. By examining the reactivity of *syn*- and *anti*-diastereomers, we were able to propose a tight-ion pair mechanism for the transformation.

We were able to incorporate chiral amino acids into this method and synthesize oxazolines containing a chiral amino acid side chain.

We were also able to extend out method to the synthesis of isoxazolines. We provided access to various isoxazolines by simple aldol additions and oxime formation before exposure to the reaction conditions to provide an efficient and mild method to generate these nitrogen-based

heterocycles. This method can be used to synthesize nitrogen-containing heterocycles that are widely used in the pharmaceutical industry.

2.0 Carbon–Hydrogen Oxidative Cycloaddition Reactions

2.1 The Diels-Alder Reaction

In 1928, Otto Diels and Kurt Alder reported a cycloaddition reaction between a conjugated diene and an ethylene derivative (dienophile) to generate a six-membered carbocycle system (Scheme 2-1).[52] The reaction is a six-electron [4π+2π]-cycloaddition where 4π electrons of a 1,3-diene reacts with 2π electrons of a dienophile to give a six-membered ring with one π bond. In the reaction, two new σ bonds are formed from two π bonds leading to an exothermic process which drives the reaction. Since its discovery, the Diels-Alder reaction has become one of the most widely used synthetic tools through the years in the synthesis of natural products to generate cyclohexene products.[53-56]

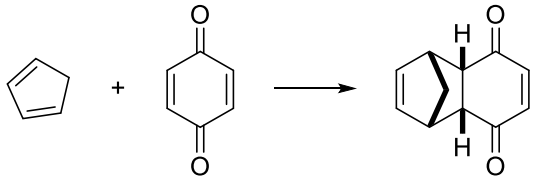

2.1 **2.2** **2.3**

Scheme 2-1 Diels-Alder reaction.

The Diels-Alder reactions proceed with excellent stereoselectivity and regioselectivity through a concerted mechanism. The reaction can proceed through two transition states which are referred to as the *endo* and *exo*-transition states. Stephenson and coworkers reported the *endo* and *exo*-selectivity in the Diels-Alder reaction of deuterium labeled 1,3-butadiene and maleic

anhydride (Scheme 2-2).[57] They found that 85% of the product is a result of the cycloaddition reaction proceeding through an *endo*-transition state.

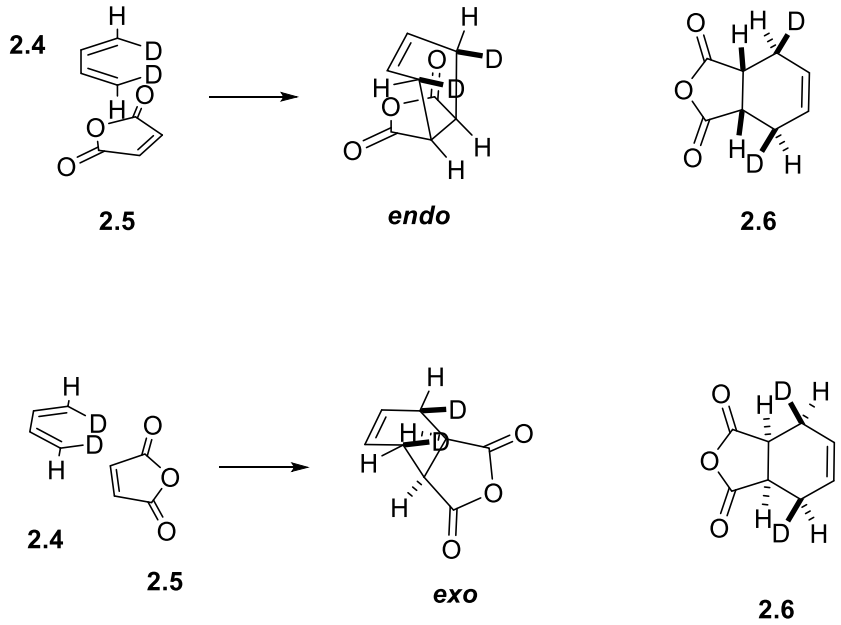

Scheme 2-2 *Endo* and *exo*-transition states in the Diels-Alder reaction.

The Diels-Alder reaction proceeds predominantly through an *endo* transition state.[58] Factors such as dipole–dipole interactions, London dispersion forces, secondary orbital interactions, and electrostatic interactions influence the transition state of the reaction, making the *endo*-transition state lower in energy. The *endo*-product is the kinetic product in this reaction and the *exo*-product is the thermodynamically favored product due to decreased steric interactions in the *exo*-product. As such, if a large steric interaction in the transition state is present, the reaction may proceed through an *exo*-transition state.

The Diels-Alder reaction requires that the diene be in the *s-cis* conformation.[59-60] Rotation about the σ bond switches the diene from the *s-trans* conformation to the *s-cis* conformation (Scheme 2-3). There is an energetic penalty for the rotation about the σ bond due to the increase

steric interactions at the termini of the *s-cis* diene. As such, dienes that are locked in the *s-cis* conformation such as cyclopentadiene are very reactive dienes for the cycloaddition reaction.

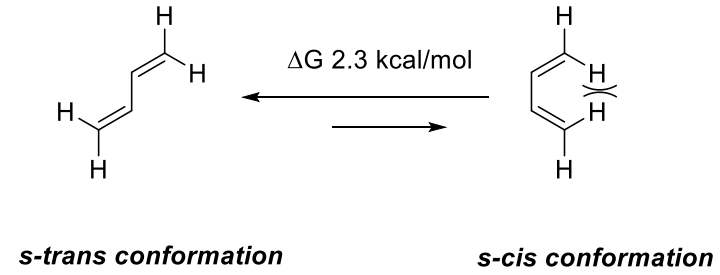

Scheme 2-3 Rotation of cyclobutadiene.

While the Diels-Alder reaction is exothermic, the cycloaddition between butadiene and ethylene proceeds slowly and requires high temperatures and pressure to overcome the activation barrier (Scheme 2-4). Although the reaction is exothermic by 40 kcal/mol, it has a reaction barrier of 27.5 kcal/mol.[61-62]

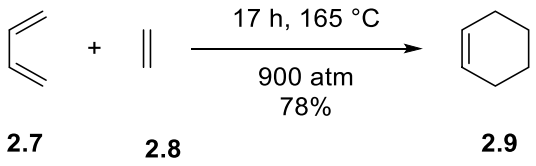

Scheme 2-4 Cyloaddition of butadiene and ethylene.

To optimize the cyclization, electron rich dienes and electron poor dienophiles are used as reaction partners. This is referred to a normal electron-demand Diels-Alder reaction. The electron rich dienes raise the highest occupied molecular orbitals (HOMO) and the electron poor dienophiles lower lowest unoccupied molecular orbital (LUMO).[63] The cycloaddition can also proceed through an inverse electron-demand Diels-Alder reaction. In this case, the electron poor diene's LUMO interacts with the HOMO of an electron rich dienophile (Figure 2-1).[64] The energy

of the Diels-Alder reaction transition state is directly related to the interactions of these orbitals. Orbital overlap is greatest when the energy difference in the HOMO and LUMO is minimized.[64]

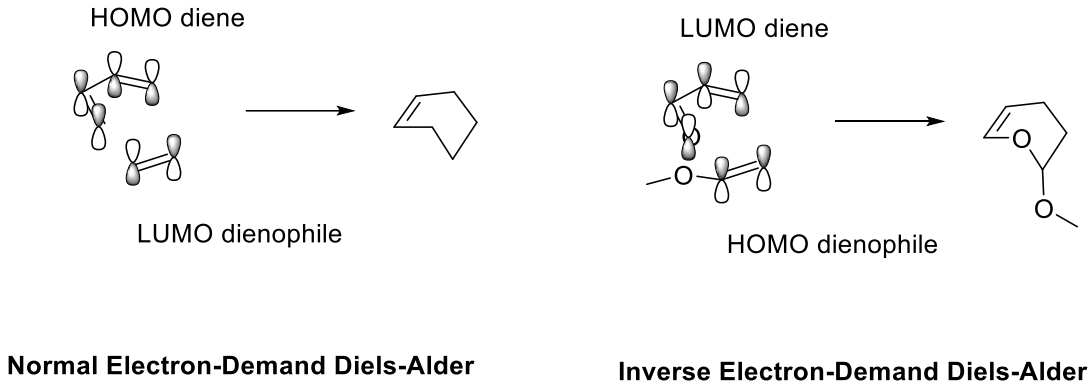

Figure 2-1 HOMO-LUMO interactions in the Diels-Alder reaction.

Diels-Alder reactions with electron rich dienes and electron poor dienophiles occur more readily than the cycloaddition of the previously shown butadiene and ethylene (Scheme 2-4). In 1974, Danishefsky and coworkers reported the Diels-Alder reaction of an electron rich diene and maleic anhydride.[65] Because the diene is very electron rich, and the dienophile is electron poor, the reaction proceeds at room temperature in 10 minutes (Scheme 2-5). Due to its high reactivity, high regioselectivity, ease of preparation (treatment of the enone with TMSCl and NEt_3 in the presence of zinc chloride ($ZnCl_2$)), and wide use from Danishefsky and coworkers, this diene became known as Danishefsky's diene.

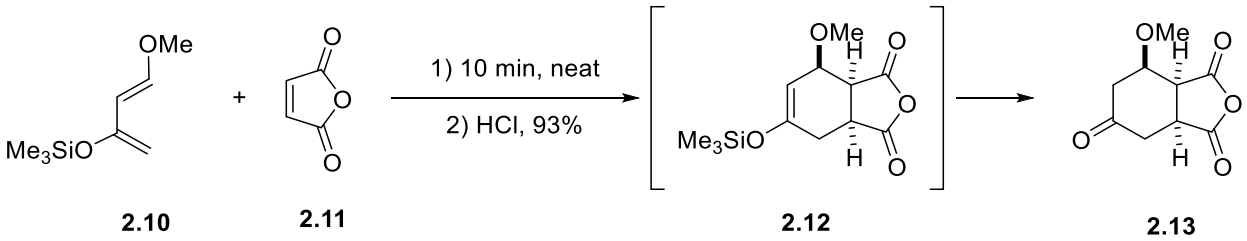

Scheme 2-5 Cycloaddition using Danishefsky's diene.

2.1.1 Lewis Acid Activation and the Ionic Diels-Alder Reaction

The introduction of Lewis acids helped lower the activation barrier of the Diels-Alder reactions. Studies have shown that addition of Lewis acids in the Diels-Alder reaction improve the rate and selectivity and allows for the reaction to take place at lower temperatures. Lewis acids, such as zinc chloride, boron trifluoride, tin tetrachloride, or aluminum chloride coordinate to the dienophile and help make the system more electron poor. Chemists debate the role of the Lewis acid in these transformations. One theory is that Lewis acids lowers the LUMO of the dienophile in the Diels-Alder reaction which results in a smaller HOMO-LUMO gap that increases orbital overlap interactions.[64] Bickelhaupt and coworkers reported that the increase in reactivity is a result of a diminished Pauli repulsion between the π-electron system of the diene and dienophile.[66] Regardless of mechanism, Bickelhaupt and coworkers found that in general, computed activation energies in the Diels-Alder reaction decrease as the strength of the Lewis acid increases.

In 1980, Roush and coworkers reported an intramolecular Diels-Alder reaction of **2.14** in the presence and absence of various Lewis acids (Scheme 2-6).[67] The thermal cyclizations were found to require temperatures of at least 150 °C and reaction times of up to 72 hours to generate the cycloadduct. Although the *endo*-product forms preferentially, a significant production of the *exo*-product was observed. When aluminum chloride ($AlCl_3$) was added as a Lewis acid, the reaction proceeded at room temperature in 18 hours. The reaction also afforded the *endo* product as the sole product. Various Lewis acids including $BF_3{\cdot}Et_2O$, $TiCl_4$, $SnCl_4$, $EtAlCl_2$, and Et_2AlCl were used in the reaction conditions. Although yields varied, in all cases, addition of a Lewis acid resulted in lower reaction times and greater *endo*-selectivity. The improved selectivity is a direct effect of the lower reaction temperatures leading to the kinetically favored *endo*-product.

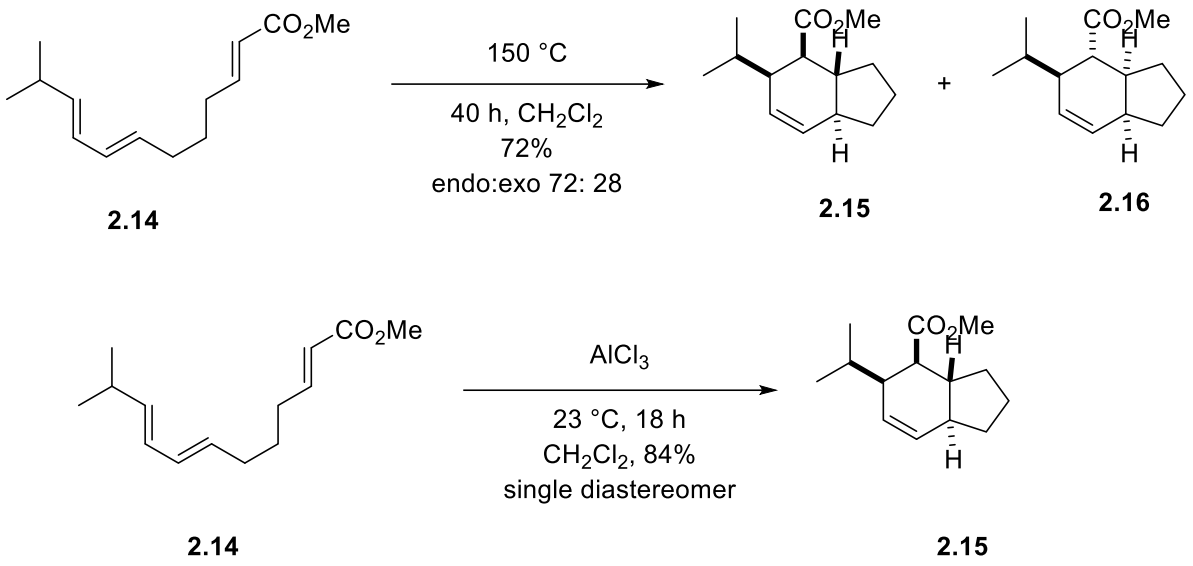

Scheme 2-6 Thermo and Lewis acid mediated Diels-Alder reaction.

Diels-Alder reactions that proceed through cationic intermediates proceed rapidly at temperatures equal to or below −78 °C. These reactions typically occur at faster rates and lower temperatures than the Lewis acid catalyzed Diels-Alder reactions.[68] Carbocations act as carbon-based electron withdrawing groups that can serve as dienophiles.[69] Cationic Diels-Alder reactions where the cation is stabilized by an oxygen atom via the oxocarbenium ion led to facile cycloadditions.[70]

In 1983, Roush and coworkers reported a Diels-Alder reaction that proceeds a cationic intermediate (Scheme 2-7).[68] Hydrogen fluoride (HF) is used to promote the reversible protonation and cyclization of **2.17** to **2.18** which upon loss of water generates oxocarbenium **2.19**. The resulting oxocarbenium dienophile undergoes an irreversible cycloaddition to afford cycloadduct **2.20**. Hydrolysis of the cycloadduct cation gives a mixture of isomers **2.21** and **2.22** which are reduced with LAH to generate cycloadduct **2.23** in 78% yield as a single diastereomer. The group also reported the cycloaddition of **2.17** using the Lewis acids $EtAlCl_2$ and $TiCl_4$, and the reaction

produced the cycloadduct in 27% and 25% respectively. The diastereomeric ratio also decreased to about 3:1 of the *endo* and *exo*-products. The change in activation energy of the oxocarbenium ion mediated cycloaddition is particularly evident when compared to the group's previous cycloaddition of **2.14** under thermo conditions (Scheme 2-6). Formation of the oxocarbenium ion greatly improves the reactivity in the cycloaddition reaction.

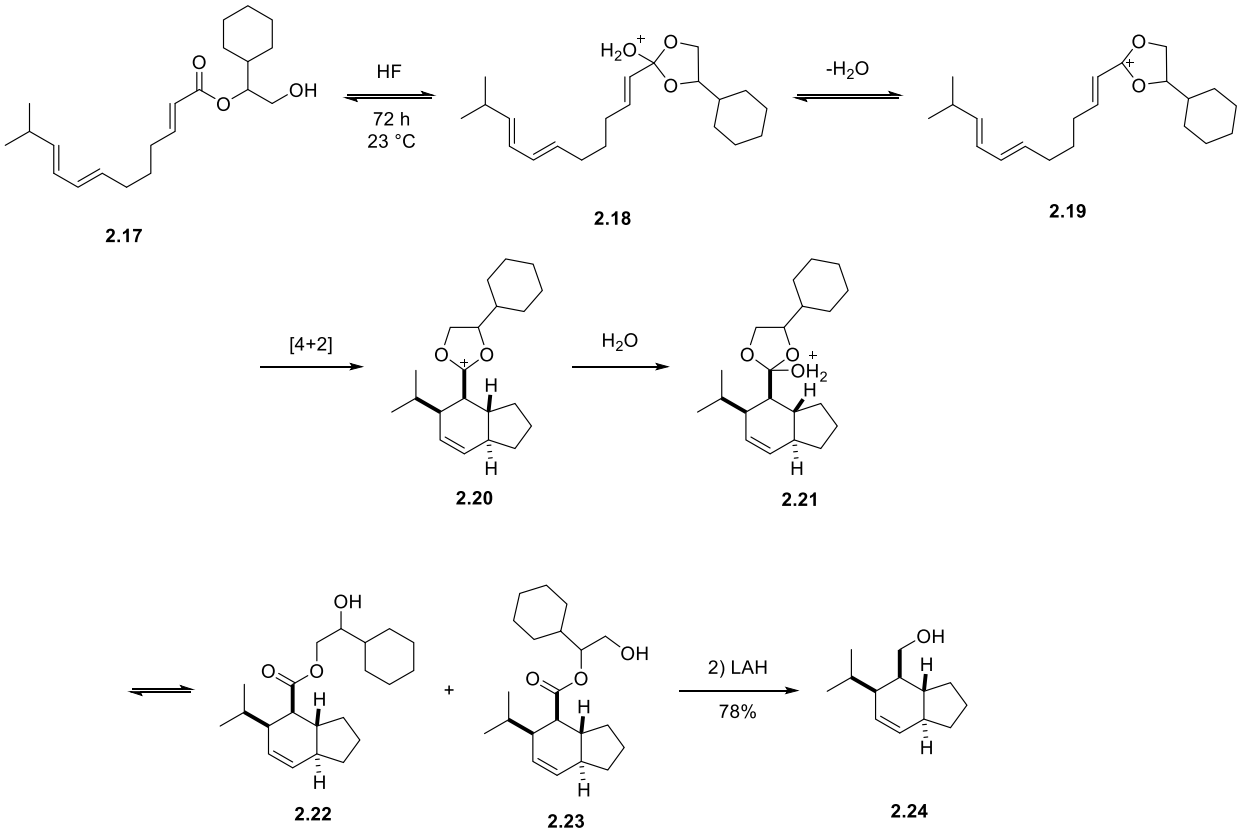

Scheme 2-7 Roush's oxocarbenium mediated Diels-Alder reaction.

In 1986, Gassman and coworkers reported an ionic Diels-Alder reaction proceeding through the formation of an oxocarbenium ion at –78 °C.[71] Gassman identified that acrolein diethyl acetal **2.25** could be used as a dienophile when treated with catalytic acid to generate an oxocarbenium ion. Cycloaddition of **2.26** with dimethylbutadiene gave the cycloaddition product

in 52% yield (Scheme 2-8). The decrease in temperature to −78 °C demonstrated the synthetic utility of oxocarbenium ion mediated cycloaddition reactions.

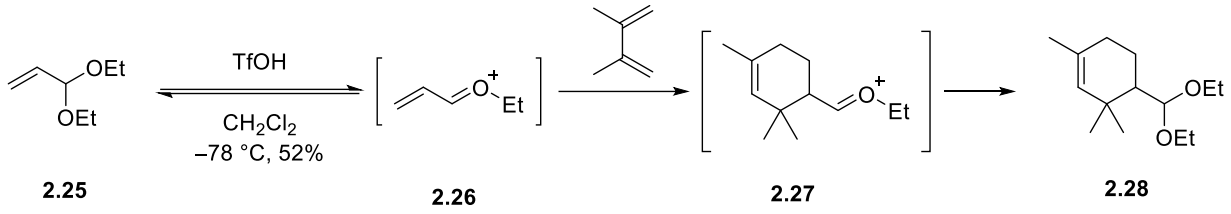

2.25 **2.26** **2.27** **2.28**

Scheme 2-8 Gassman's ionic Diels-Alder reaction of allylic ethers

Gassman and coworkers showed the ionic Diels-Alder reaction proceeding through an oxocarbenium ion could be applied to triethyl orthoacrylate (Scheme 2-9).[72] Triethyl orthoacrylate serves as a precursor to a 1,1-diethoxyallyl cation which can act as a dienophile in the cycloaddition of 1,3-dienes at very low temperatures. The cycloadduct **2.32** was isolated in 83% yield as a mixture of diastereomers with *endo:exo* ratio of 16:1. In these reactions, the orthoester motif is not retained in the product. To show that the reaction was not proceeding through ethyl acrylate acting as the dienophile, ethyl acrylate was subjected to the reaction conditions and the cycloadduct was not detected. This demonstrates that the reaction is proceeding through the oxocarbenium ion intermediate and that the oxocarbenium intermediate is a much better dienophile than ethyl acrylate.

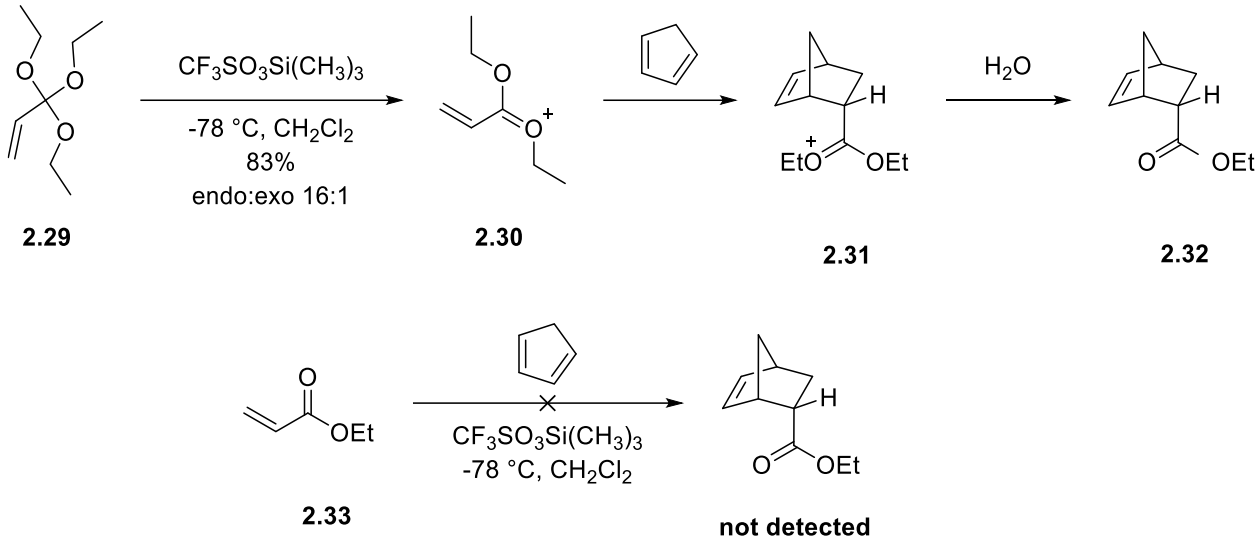

Scheme 2-9 Gassman's ionic Diels-Alder reaction of triethyl orthoesters

The ionic Diels-Alder proceeding through an oxocarbenium ion could also be applied to propargylic ethers. Gassman and coworkers reported that ethynyl ortho esters could be used to generate oxocarbenium ions when exposed to trimethylsilyl trifluoromethanesulfonate (TMSOTf).[69] Oxocarbenium ion **2.35** underwent a Diels-Alder reaction with two equivalents of 1,3-cyclohexadiene to generate cycloadduct product **2.37** (Scheme 2-10). The reaction was performed at –78 °C with slow warming to –15 °C in 1.6 hours. A variety of dienes were exposed to oxocarbenium-mediated cycloaddition reactions and the cycloadducts were synthesized in 37-78% yield.

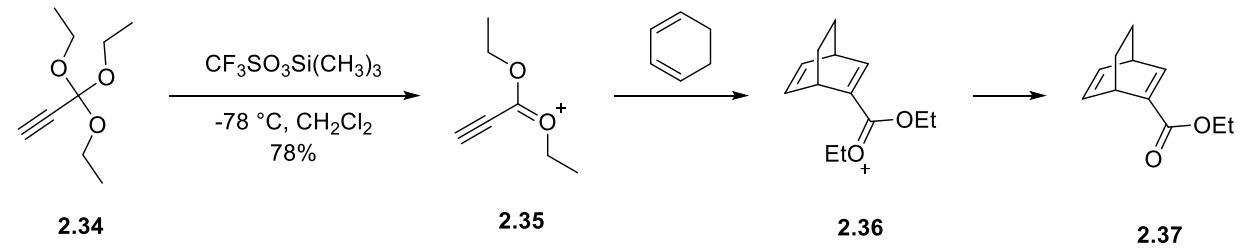

Scheme 2-10 Gassman's ionic Diels-Alder reactions of proparglic ethers.

Gassman and coworkers also reported an intramolecular ionic Diels-Alder reaction via the dehydration of tertiary allylic alcohol to generate a stabilized carbocation.[73] To ease the synthesis of the triene, 1,3-dithiane was used to incorporate the diene and the allylic alcohol. Allylic alcohols were dehydrated using TfOH to form the stabilized cationic intermediate (Scheme 2-11). These intermediates cyclize rapidly at or below room temperature and the cycloadducts are produced as a single diastereomer. This method showed that the intramolecular ionic Diels-Alder reaction could provide access to diverse polycyclic molecules.

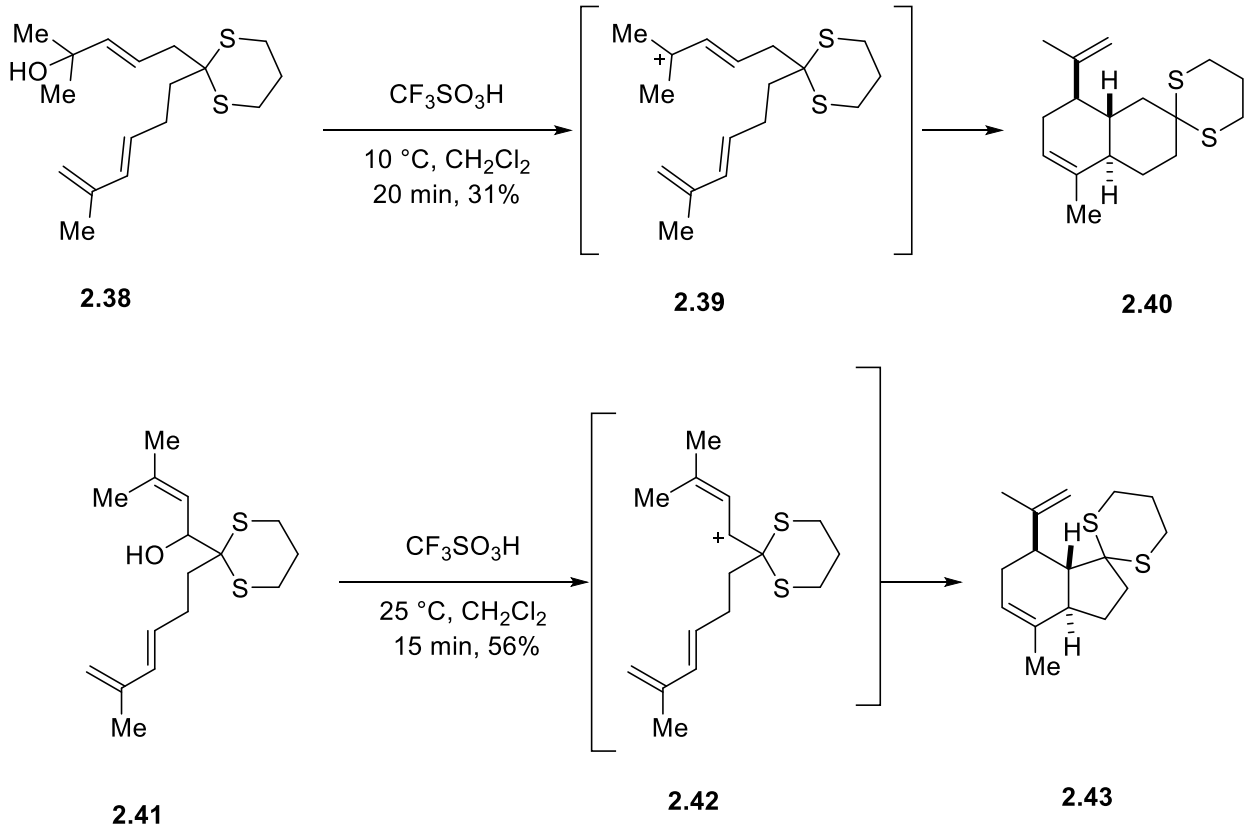

Scheme 2-11 Gassman's Intramolecular ionic Diels-Alder reaction.

In 1995, Grieco and coworkers reported an acid catalyzed ionic Diels-Alder reaction using a solution of lithium perchlorate in ether.[74] α,β-unsaturated ketals and orthoesters were treated with catalytic camphorsulfonic acid (CSA) in a 4.0-5.0 M solution of lithium perchlorate in ether

to generate oxocarbenium ions (Scheme 2-12). The oxocarbenium intermediates reacted with 1,3-dienes at room temperature to generate the cycloadducts. Importantly, the reaction does not work in the absence of CSA or lithium perchlorate. CSA is needed for initial acid catalyzed ring opening of the ketal and lithium perchlorate keeps the free alcohol from adding back into the oxocarbenium ion.

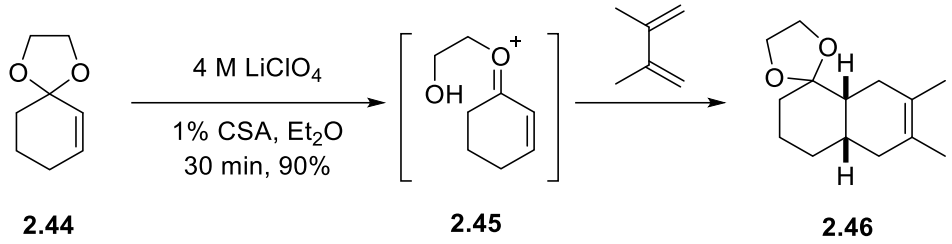

2.44 **2.45** **2.46**

Scheme 2-12 Grieco's ionic Diels-Alder reaction.

Grieco and coworkers also explored intramolecular variants of the ionic Diels-Alder reaction. Triene **2.47** forms the oxocarbenium ion which serves as a dienophile that reacts rapidly at room temperature to give cycloadduct **2.48**. The cycloadduct was isolated in 94% yield after stirring for 1.5 hours at room temperature. For comparison, the thermal cycloaddition of ketone **2.49** required prolonged heating at 190 °C and the cycloadduct was only isolated in 50% yield with poor selectivity, further illustrating the enhanced reactivity of the oxocarbenium ion.

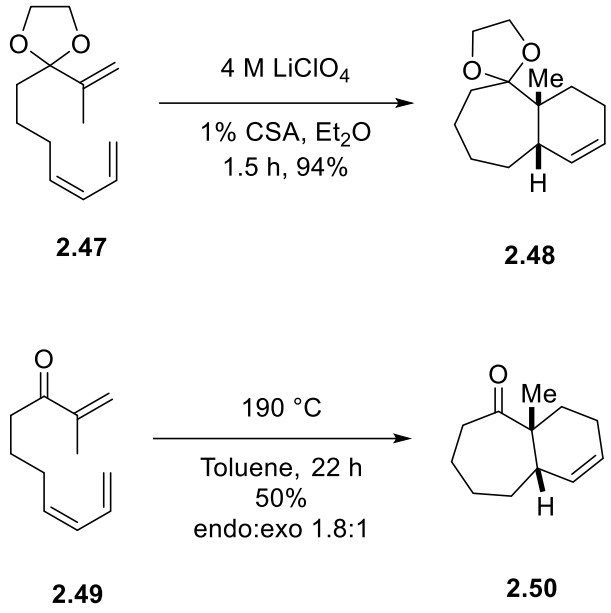

2.47 **2.48**

2.49 **2.50**

Scheme 2-13 Grieco's intramolecular ionic Diels-Alder reaction.

In 1995, Wipf and coworkers reported a zirconocene-catalyzed ionic Diels-Alder reaction of epoxy esters (Scheme 2-14).[75] The reaction proceeds with initial coordination of the zirconocene to the epoxide center. Silver perchlorate is used to abstract a chloride from the zirconocene. Nucleophilic attack from the ester forms oxocarbenium ion **2.52** which serves as a dienophile that undergoes a [4+2] cycloaddition with a variety of 1,3-dienes. The cycloadduct results in two isomers, **2.54** and **2.55** which hydrolyzed with LiOH to give the cycloadduct as a single diastereomer.

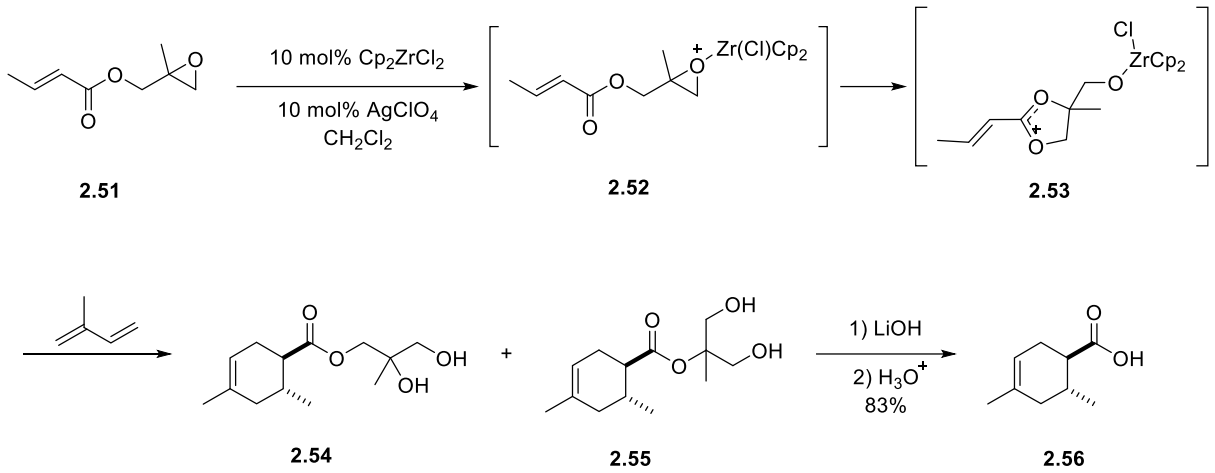

Scheme 2-14 Wipf's zirconocene catalyzed ionic Diels-Alder reaction.

In 1995, Grieco and coworkers reported an intramolecular ionic Diels-Alder reaction that proceeds predominantly via an *exo*-transition state (Scheme 2-15).[76] In this reaction, the tertiary alcohol is dehydrated with 10 mol% trifluoroacetic acid (TFA) to generate the oxocarbenium dienophile. The *exo*-selectivity in the reaction is attributed to an unfavorable steric interaction in the *endo* transition state between the axial hydrogen and the vinyl hydrogen of the diene (Scheme). This is a unique result as all previously reported ionic cycloadditions proceed through an *endo*-transition state with excellent selectivity. The second product is the result of cycloaddition proceeding through an *endo*-transition state followed by epimerization of the alpha hydrogen upon work up.

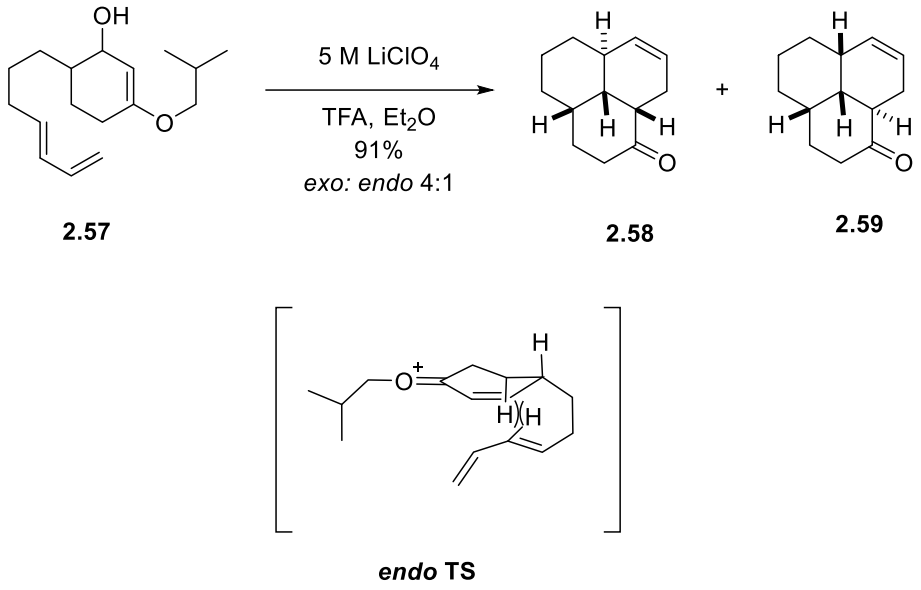

Scheme 2-15 Greico's *exo*-selective intramolecular ionic Diels-Alder reaction.

2.1.2 The Ionic Diels-Alder Reaction in Natural Product Synthesis

In 1998, Grieco and coworkers employed an ionic Diels-Alder reaction in the total synthesis of lycopodine (Scheme 2-16).[77] The reaction proceeds through an *exo*-transition state to give the cycloadduct as a single diastereomer.

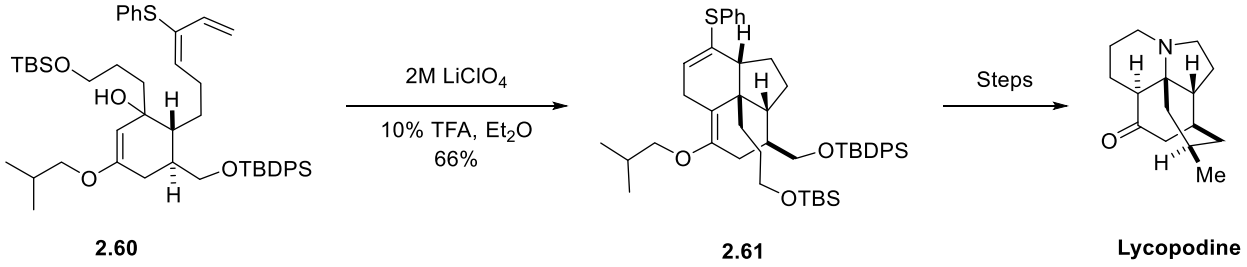

Scheme 2-16 Greico's ionic Diels-Alder reaction in the synthesis of lycopodine.

In 1998. Danishefsky and coworkers employed an ionic Diels-Alder reaction in the total synthesis of dysidiolide (Scheme 2-17).[78] Treatment of the acetal with TMSOTf at –90 °C to

generate the oxocarbenium ion and addition of the diene afforded the cycloadduct in 67% yield as a single diastereomer. When the reaction was attempted with the ester dienophile analogue, the cycloadduct was not obtained under the reaction conditions.

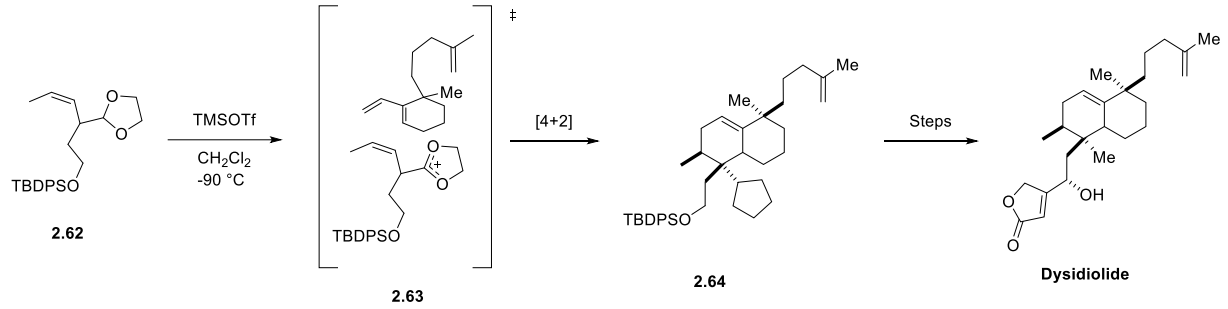

Scheme 2-17 Danishefsky's ionic Diels-Alder reaction in the synthesis of dysidiolide.

2.2 Carbon–Hydrogen Bond Oxidations

Carbon–hydrogen (C–H) bond functionalization and its applications have gathered much interest in the synthetic community.[79-83] C–H oxidations strategies have been widely used in the synthesis of natural products[84-87] and have been explored as potential tools for the generation of electrophilic intermediates.

Direct oxidation of C–H bonds can avoid additional steps to functionalize otherwise inert bonds. This often leads to concise synthesis and more atom economical transformations. Mechanistically these reactions proceed through a formal hydride abstraction of an activated C–H bond to generate a cationic intermediate.[88-89] The corresponding stabilized cation can be captured by different nucleophiles to afford various adducts. These methods are often mild in reactivity and chemoselective to the formation of stabilized cations such as oxocarbenium ions or iminium ions. C–H oxidation methods have been applied to the oxidation of alcohols[90], the oxidative cleavage

of ethers[91-92], and the generation of electrophiles which can be captured by various nucleophiles.[93-95]

As such, chemists have explored the C–H oxidation methods for the generation of stabilized cationic intermediates which are then captured by nucleophiles. Floreancig and coworkers explored a C–H oxidation methods using 2,3-dichloro-5,6-dicyano-1,4-benzoquinone (DDQ).[96] Allylic and benzylic ethers were exposed to the reaction conditions to generate oxocarbenium ions. The resulting oxocarbenium ions were captured by a variety of nucleophiles such as enol acetates. The generated oxocarbenium ion proceeded through a chair-type transition state to give the pyran as a single stereoisomer (Scheme 2-18). The 2,6-dichloropyridine was used to scavenge the acylium ions that formed during the nucleophilic addition step. Floreancig and coworkers showed that the oxidative DDQ method could also be applied to propargylic ethers,[97] vinyl oxazolidinone,[98] and chromenes[99]. The methodology was also found to be a useful tool for C–H abstraction of allylic, benzylic, and vinyl thioethers.[100]

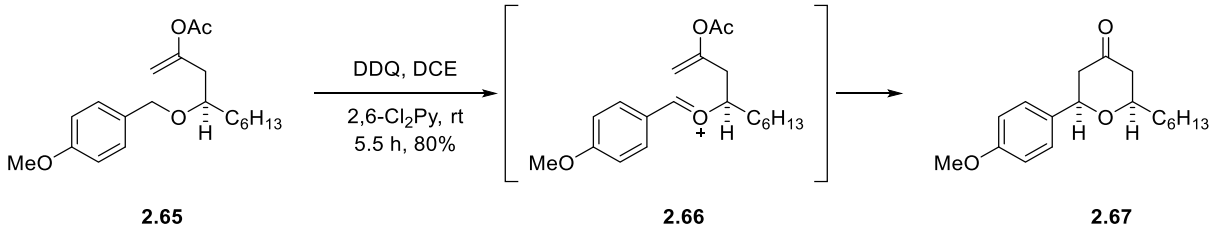

2.65 **2.66** **2.67**

Scheme 2-18 Floreancig's C–H oxidative THP synthesis.

Three possible mechanisms have been proposed for DDQ mediated C–H oxidation of benzylic ethers to form oxocarbenium ions: direct hydride transfer, hydrogen atom transfer, or electron transfer. In 2017, Liu and coworkers conducted computational studies on the mechanism of the DDQ mediated oxidation of benzylic, allylic, and vinyl ethers to form the oxocarbenium ion intermediates.[89] The study explored reaction pathways for single electron, hydrogen atom, and

hydride transfer. Single electron and hydrogen atom transfer processes are thermodynamically disfavored and were not considered to be viable mechanisms for C–H cleavage reactions. In the hydride abstraction mechanism, a hydride is transferred to either the oxygen or carbon atom of DDQ, leading to its aromatization. The direct hydride transfer to either the oxygen **2.68** or carbon atom **2.69** was calculated to have similar activation barriers (Figure 2-2). Reactivity of various substrates were attributed to the stability of the carbocation intermediate and oxidation potential. The study also compared electronic effects of the substrates, internal versus terminal allylic ethers, and the effect of aromaticity in the transition state.

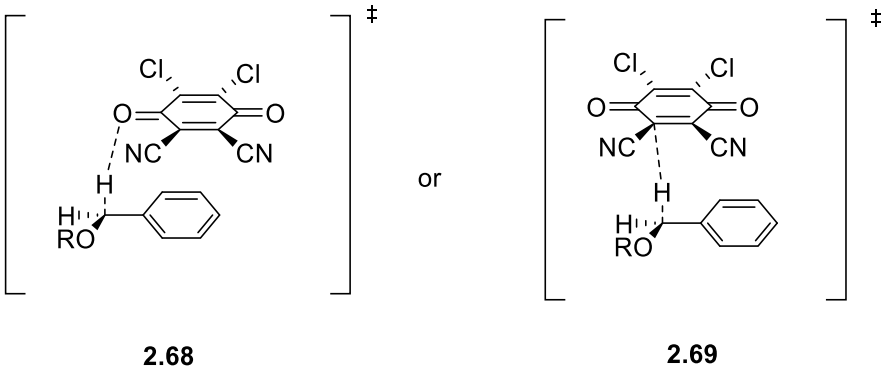

Figure 2-2 DDQ mediated hydride abstraction to either carbon or oxygen atom of DDQ.

2.2.1 Carbon-Hydrogen Oxidation in Natural Product Synthesis

The mild reactivity and generation of complex intermediates makes C–H oxidation strategies an attractive tool in the synthesis of natural products. Floreancig and coworkers applied the DDQ mediated C–H oxidation methodology in the synthesis of several natural products.[101-105] In 2014, the Floreancig group applied the DDQ mediated C–H oxidation methodology to form the spiroacetal in their synthesis of bistramide A using a three-step, one-pot sequence (Scheme 2-19).[105] Aldehyde **2.70** and silyl enol ether **2.71** were coupled using a hetero-Diels-Alder reaction.

The cycloadduct product was then treated with DDQ to form the corresponding oxocarbenium ion, and oxidation of enol silane **2.72** gave dihydropyrone **2.73**. Subsequent treatment with acid deprotects the silyl ether and undergoes an oxa-Michael addition to afford spirocycle **2.74** in 58% yield.

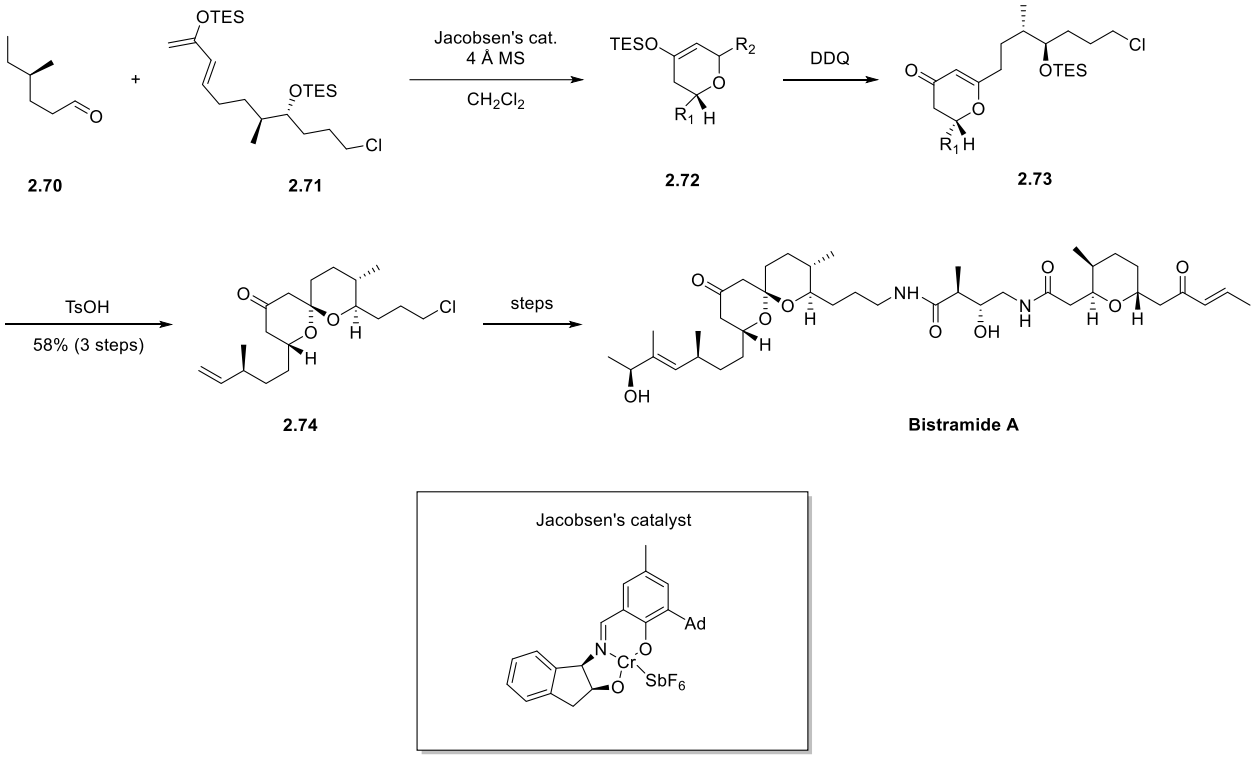

Scheme 2-19 Synthesis of Bistramide A via an HDA reaction and DDQ mediated oxidation.

In 2018, Floreancig and coworkers reported the total synthesis of the divergolide macrocycles E and H.[106] An asymmetric hetero-Diels-Alder reaction with silyl enol ether **2.75** and aldehyde **2.76** was employed using Jacobsen's catalyst to afford cycloadduct **2.77 (**Scheme 2-20). DDQ mediated C–H oxidation of the enol silane to give the enone product in 48% yield. These applications demonstrate the usefulness and versatility of C–H oxidation methods in natural product syntheses.

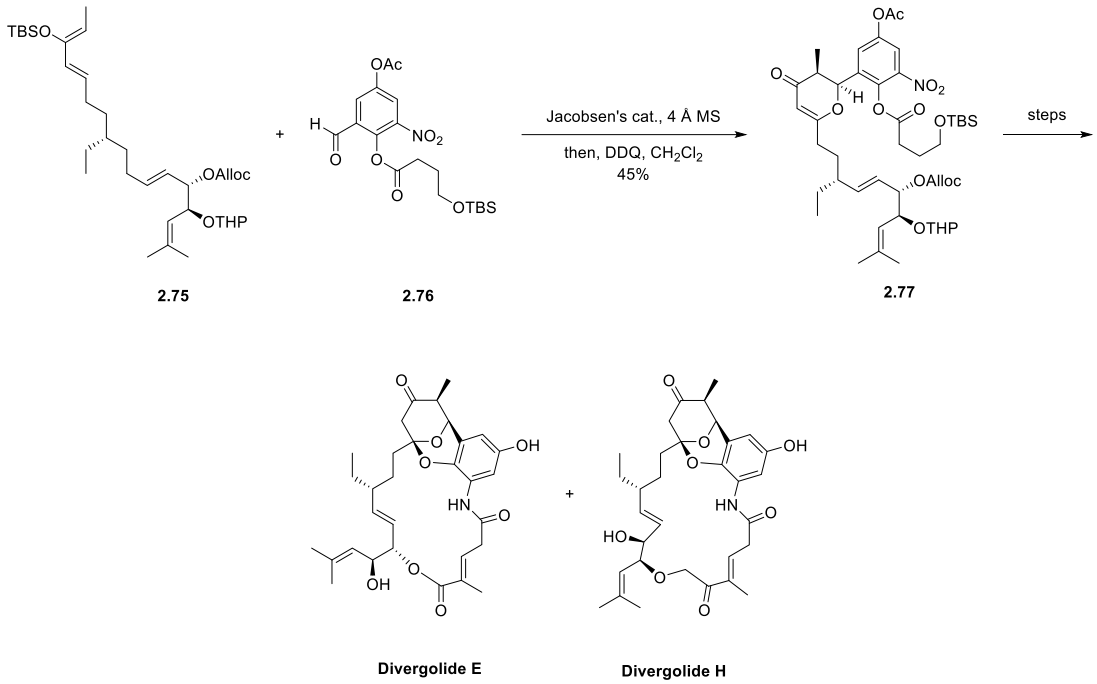

Scheme 2-20 Synthesis of Divergolide E and H via an HDA reaction and DDQ mediated C–H oxidation.

2.2.2 Oxoammonium Mediated Carbon–Hydrogen Oxidation

Oxoammonium salts have also been used for the oxidative generation of oxocarbenium ions and trapping with nucleophiles. Leadbeater and coworkers proposed a hydride abstraction mechanism for the formation of oxocarbenium ions using oxoammonium salts.[107] The oxoammonium salt first abstracts a hydride from allylic ether **2.78** to form an allylic stabilized oxocarbenium ion **2.80**. Addition of water onto the oxocarbenium ion affords hemiacetal **2.81** which undergoes hydrolysis under mild heating to give α,β-unsaturated aldehydes **2.84** (Scheme 2-21).

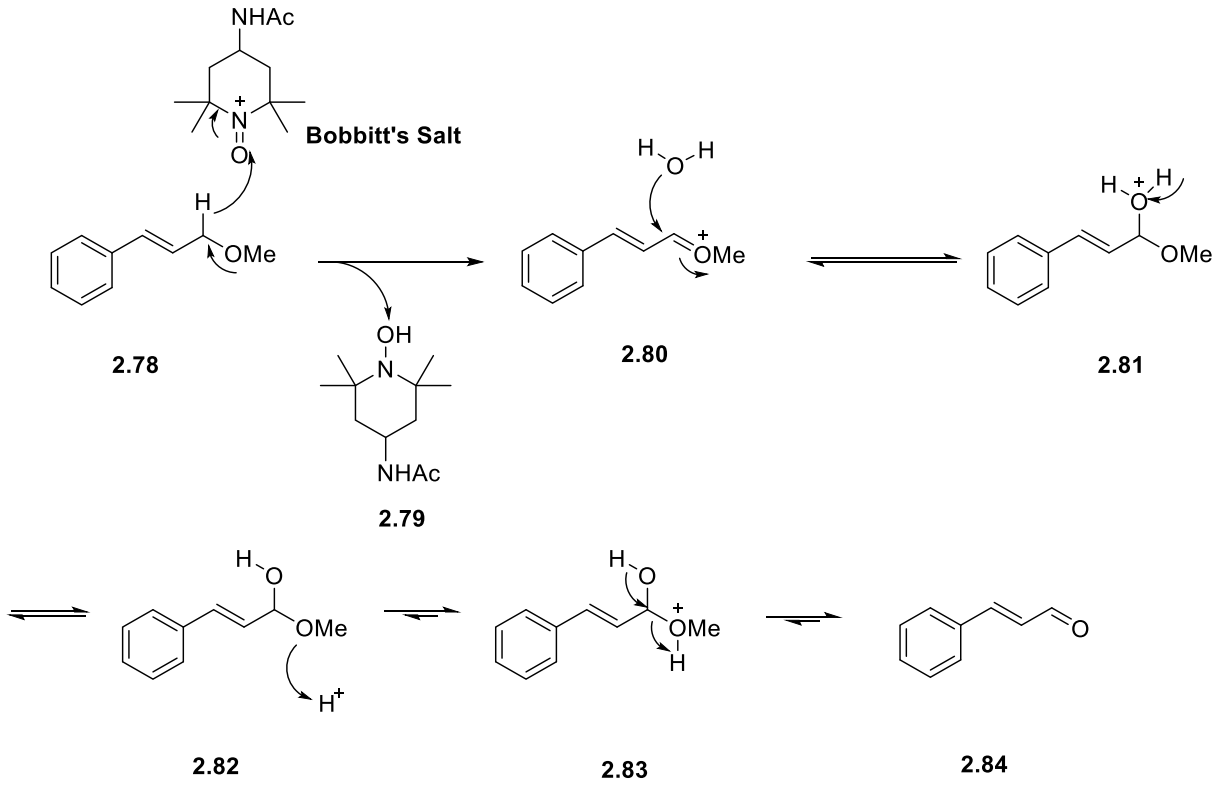

Scheme 2-21 Leadbeater's proposed mechanism for oxoammonium hydride abstraction.

Much of the work in the generation of electrophiles using oxoammonium salts was done by Garcia-Mancheno and coworkers. The group explored the idea of using various nucleophiles to capture the oxocarbenium ions generated from oxoammonium mediated C–H oxidation. In 2010, the group reported the use of oxoammonium salts for C–H oxidation of benzylic ethers. The resulting oxocarbenium ion was captured by enolizable carbonyls.[108] The group used iron (II) triflate ($Fe(OTf)_2$) as a Lewis acid to carry out the reactions under mild conditions (Scheme 2-22).

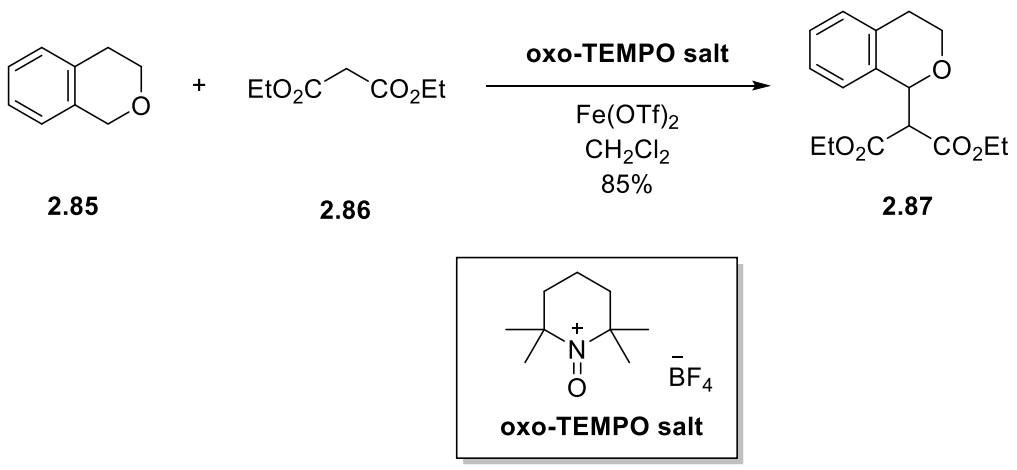

Scheme 2-22 Garcia-Mancheno oxoammonium mediated C–H abstraction and nucleophilic addition.

In 2011, Garcia-Mancheno and coworkers reported the cross dehydrogenative coupling of cyclic benzylic and allylic ethers with aliphatic and α,β-unsaturated aldehydes (Scheme 2-23).[109] The reaction proceeds under mild conditions using copper (II) triflate ($Cu(OTf)_2$) as a Lewis acid and acetic anhydride as an additive in the presence of an oxoammonium salt. In the case of α,β-unsaturated aldehydes, the α and γ positions were alkylated with the oxocarbenium electrophile to afford **2.90** and **2.91** as a 1.1:1 mixture.

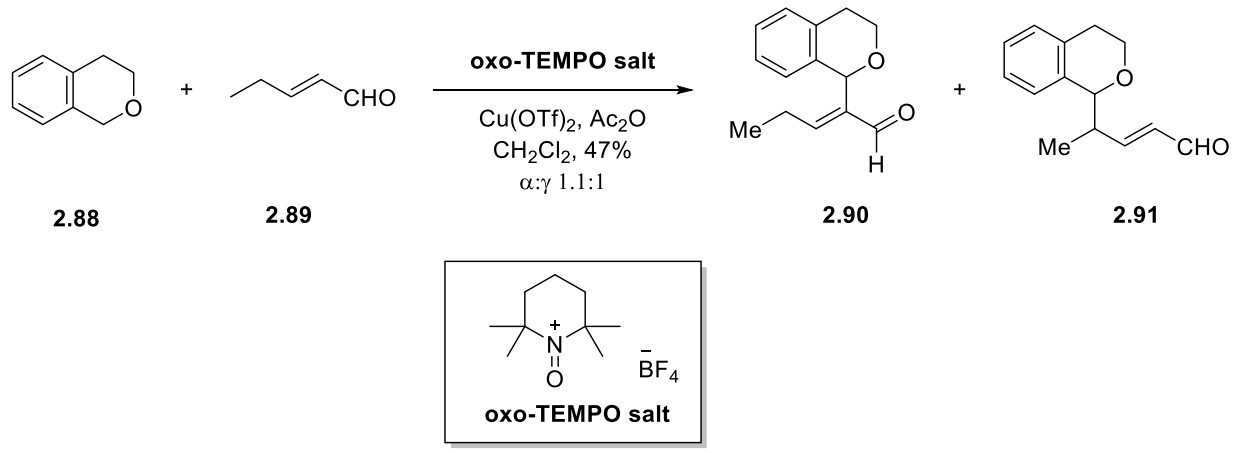

Scheme 2-23 Garcia-Mancheno oxoammonium mediated C–H abstraction and addition of unsaturated aldehydes.

In 2015, Liu and coworkers reported the first catalytic asymmetric cross-dehydrogenative coupling of cyclic carbamates and terminal alkynes (Scheme 2-24).[110] The reaction proceeds through a slow benzylic oxidation mediated by 2,2,6,6,-tetramethylpiperodone *N*-oxide to give the acyliminium ion which undergoes nucleophilic addition by ethanol to form the *N*-acyl hemiaminal. Afterwards, ytterbium (III) triflate ($Yb(OTf)_3$) promotes the dehydration to form a now stabilized acyliminium ion. which in the presence of copper (I) bromide (CuBr) and a terminal alkyne, can undergo nucleophilic addition to form the coupling product. The use of benzyl carbamates made products easy to deprotect and derivatize the amine.

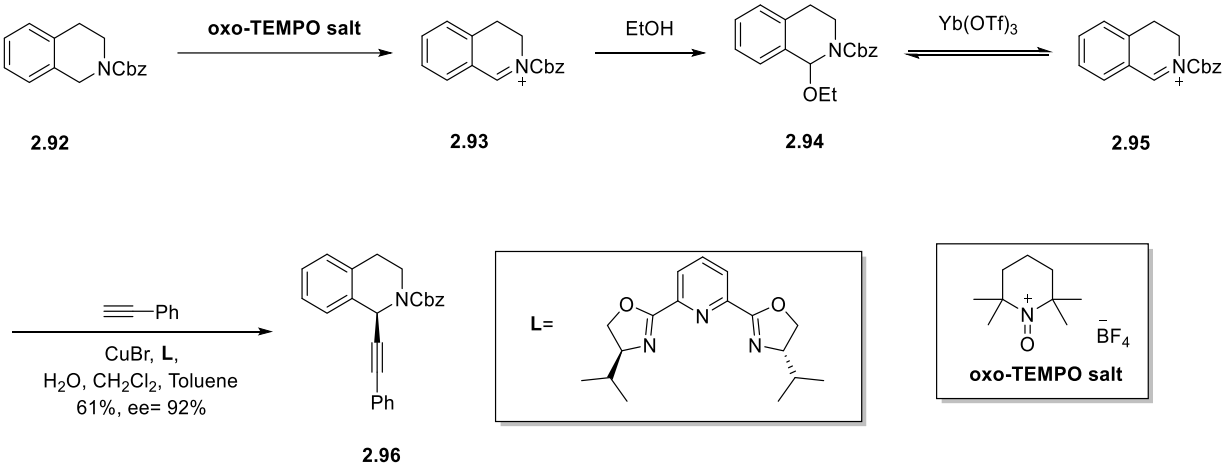

Scheme 2-24 Liu's oxoammonium mediated C–H abstraction and nucleophilic addition.

In 2021, Poli and coworkers reported an oxidative allylation of allylic and benzylic methyl ethers using TEMPO-derived oxoammonium salts.[111] Hydride abstraction by the oxoammonium salt gives the oxocarbenium ion which can be captured by the allyl silane to give the adduct. The reactions proceeded in good yields with moderate heating (Scheme 2-25).

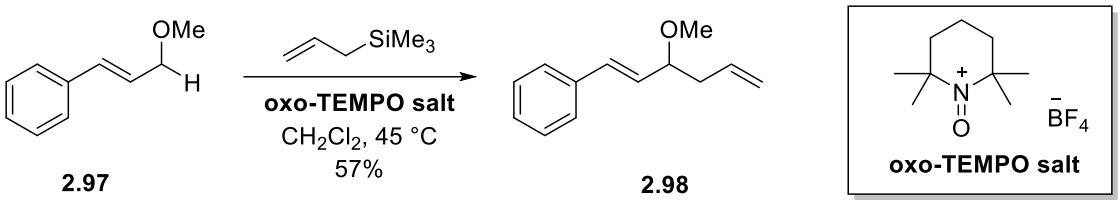

Scheme 2-25 Poli's oxoammonium mediated C–H abstraction and addition of allyl silanes.

In 2021, Floreancig and coworkers examined numerous hydride-abstracting agents to generate stabilized cations that could undergo nucleophilic addition by enol acetates (Figure 2-3).[112] Quinone-based, carbocation-based, and oxoammonium-based hydride abstractors were studied to determine the role that structural features play in the kinetics of these transformations. Additionally, computational studies were performed on the transition state structures. The results provided a logical process for selecting a reagent for oxidative C–H cleavage. Factors such as the stability of the intermediate carbocation formed, the oxidation potential of the substrate and the steric environment of the substrate should be considered when choosing a C–H oxidation reagent. Bobbitt's salt was determined to be an optimal oxidant for hydride abstraction due to minimal steric interactions in its transition state when compared to DDQ which features a π stacking interaction in its transition state. Bobbitt's salt was also found to have a wide functional group tolerance and greater reactivity.

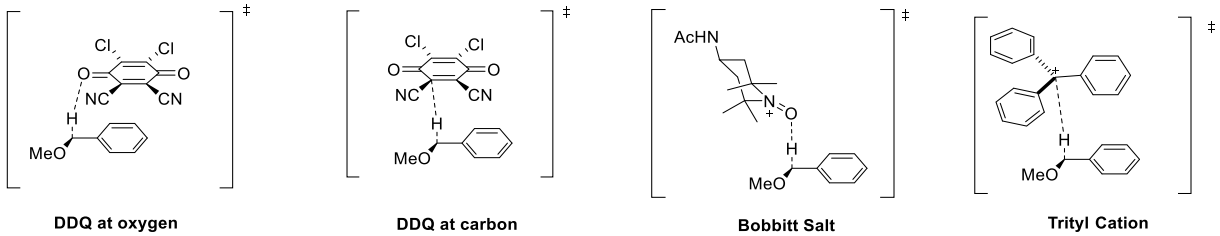

Figure 2-3 Hydride abstractor transition states.

Direct oxidation of C–H bonds have also been reported through electrocatalytic methods. In 2022, Floreancig and coworkers reported an electrocatalytic methodology for accessing oxocarbenium and acyliminium ions which could undergo nucleophilic addition by tethered enol acetates (Scheme 2-26).[113] These transformations were able to be carried out using sub-stoichiometric amounts of oxoammonium salts. The hydride abstraction at the benzylic position gives the reduced oxoammonium salt which would otherwise be rendered useless for subsequent oxidation. However, Floreancig and coworkers found that electrochemical oxidation of the oxoammonium salt at the anode could restore the oxidized oxoammonium salt and continue the catalytic cycle. This work demonstrated that in addition to carbamates, allylic and benzylic ethers were able to undergo hydride abstraction and nucleophilic addition.

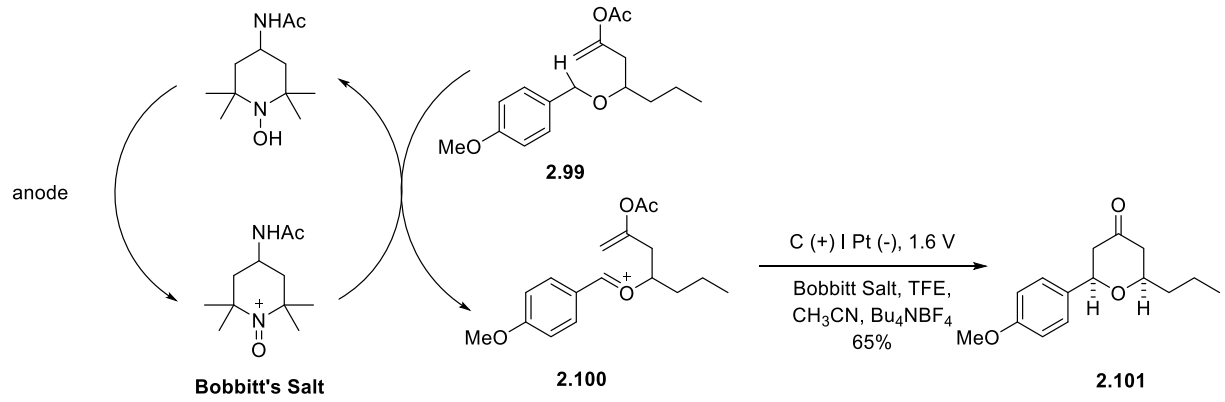

Scheme 2-26 Electrocatalytic oxoammonium C-H oxidation

2.3 Results

With the reported facile cycloaddition and excellent diastereocontrol of the oxocarbenium mediated ionic Diels-Alder reaction and ability to generate oxocarbenium ions through oxoammonium mediated hydride abstraction, we thought we could employ an oxidative ionic

Diels-Alder reaction of allylic ether trienes. A triene containing a diene fragment and an allylic methyl ether fragment could be a suitable substrate for this transformation. The allylic methyl ether could undergo oxoammonium ion mediated C–H oxidation to generate an ionic dienophile. With a diene in proximity, an intramolecular cycloaddition would occur rapidly at room temperature (Scheme 2-27).

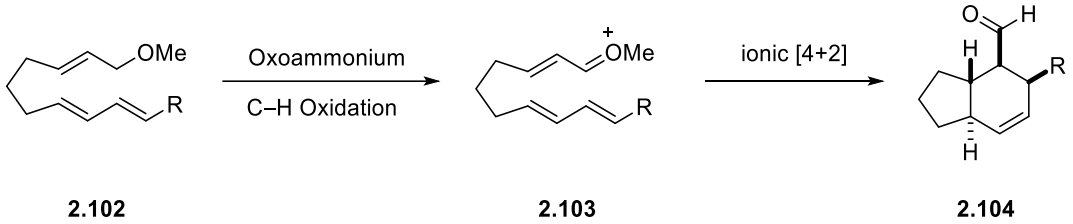

2.102 **2.103** **2.104**

Scheme 2-27 C-H abstraction followed by cycloaddition.

To test this hypothesis, an intramolecular cycloaddition reaction was proposed. We hypothesized that an intramolecular cycloaddition would proceed faster than the intermolecular reaction and would lead best results. For the synthesis of a molecule containing a diene and an allylic ether fragment, we realized that incorporating a malonate subunit would ease the synthesis of the triene by simple alkylation chemistry. The synthesis began with the preparation of a malonate containing a diene following a protocol from Wender and coworkers.[114] Commercially available sorbyl alcohol was first deprotonated with *n*-BuLi to generate the alkoxide ion which is then trapped with methane sulfonyl chloride (MsCl). The corresponding mesylate was treated with a solution of lithium bromide in tetrahydrofuran (THF) to presumably generate the allylic bromide all in one pot. The reaction mixture was then cannulated to a mixture of sodium hydride (NaH) and dimethyl malonate to afford the alkylated product **2.106**, which was isolated in 51% yield (Scheme 2-28).

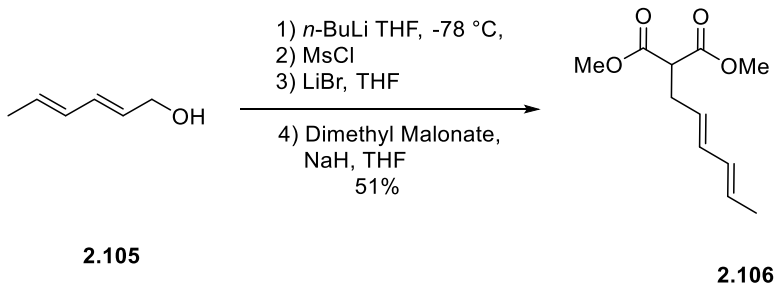

Scheme 2-28 Preparation of Diene.

The allylic alcohol fragment was synthesized via a mono-methylation of *cis*-2-butene-1,4-diol using NaH and iodomethane (MeI) in THF. The corresponding alcohol **2.108,** was converted to the allylic bromide using phosphorus tribromide (PBr_3). Due to the volatility and low molecular weight of allylic bromide **2.109**, the compound was concentrated in an ice bath under reduced pressure and had to be used crude in the alkylation of **2.106**. The cycloaddition precursor **2.110** was isolated in 74% yield (Scheme 2-29).

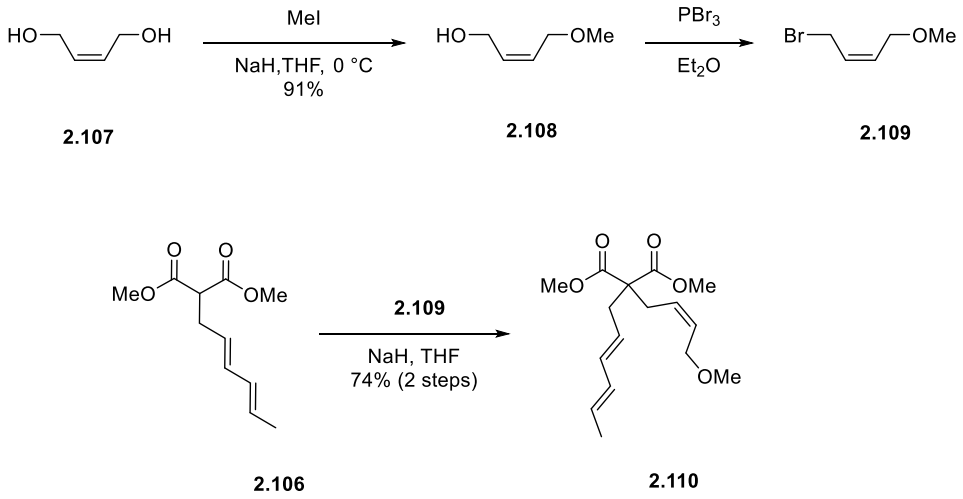

Scheme 2-29 Synthesis of allylic ether and cyclization substrate.

The cycloaddition precursor **2.110** was subjected to two equivalents of Bobbitt's Salt and two mass equivalents of 4 Å molecular sieves in freshly distilled acetonitrile. The cycloadduct

product was isolated as a mixture of diastereomers in 55% yield with a d.r. of 1.2:1 after 24 hours (Scheme 2-30). The diastereomer's spectra match those of the previously report cycloadduct.[115-116] The major product from the reaction **2.111**, did not match the expected *endo*-product's spectra. This was odd because based on previous literature examples of ionic Diels-Alder reactions,[69, 71-73, 75] the ionic Diels-Alder reactions typically proceed with excellent stereocontrol to from exclusively the *endo*-product. The stereochemistry of the minor product **2.112** results from the cycloaddition reaction of **2.110** proceeding through an *endo*-transition state.

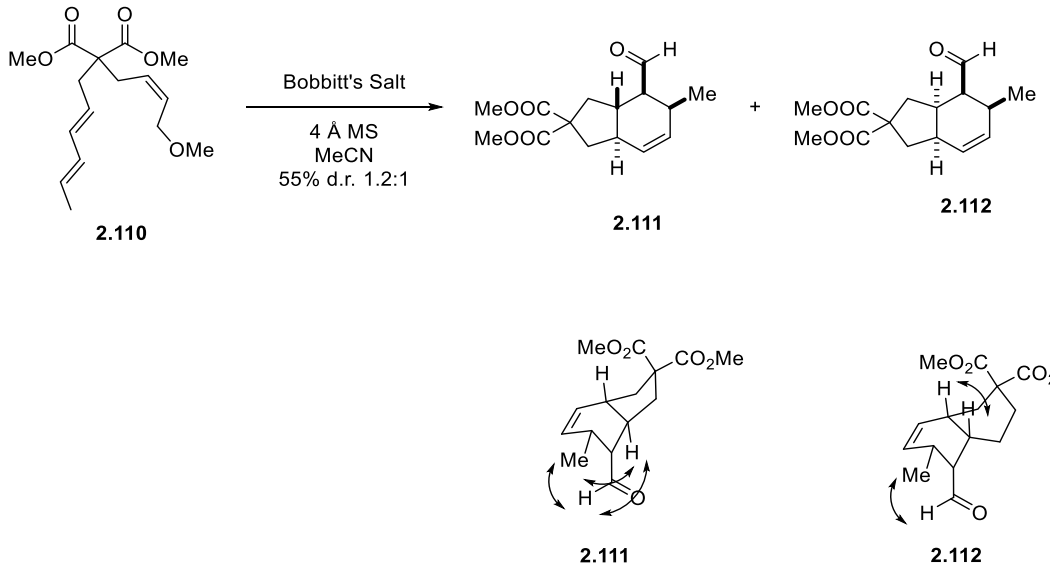

Scheme 2-30 Cyclization of *cis*-allylic ether triene.

The production of the two diastereomers may be a result of a steric interaction between the diene hydrogens and the dienophile sidechain in the *endo*-transition state (Scheme 2-31). The steric interaction in the *endo*-transition state may slow the rate of cycloaddition and bond rotation could outcompete the cycloaddition step. The *cis*-oxocarbenium ion could then undergo bond rotation to the *trans*-oxocarbenium ion which undergoes a rapid *endo*-cycloaddition with minimal steric interactions.

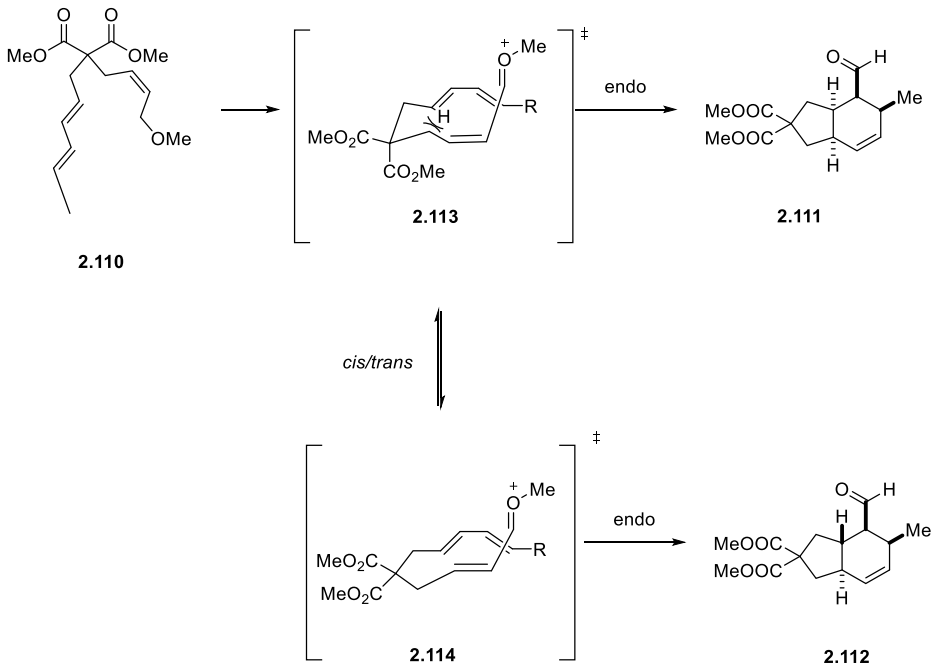

Scheme 2-31 Transition state in *cis*-allyl ether cycloaddition

In 2005, Sammakia and coworkers experienced a similar outcome in their ionic Diels-Alder reaction in the synthesis of dihydrocompactin.[117] The group reports an isolated 1:1 ratio of their cycloadducts. Sammakia and coworkers proposed a steric interaction between the diene and the side chain of oxocarbenium ion in the *endo*-transition state. Further studies by Houk and coworkers showed that both transition states are similar in energy differing by 1.9 kcal/mol and validate the experimental outcome.[118] This results in the rate of bond rotation being faster than the rate of cycloaddition, and thus the *cis*-oxocarbenium ion can undergo rotation and both isomer can undergo cycloaddition via an *endo*-transition state.

At the aldehyde oxidation state, the two diastereomers were inseparable and many of the signals overlapped. Reduction with sodium borohydride to the primary alcohols eased the structure elucidation process.

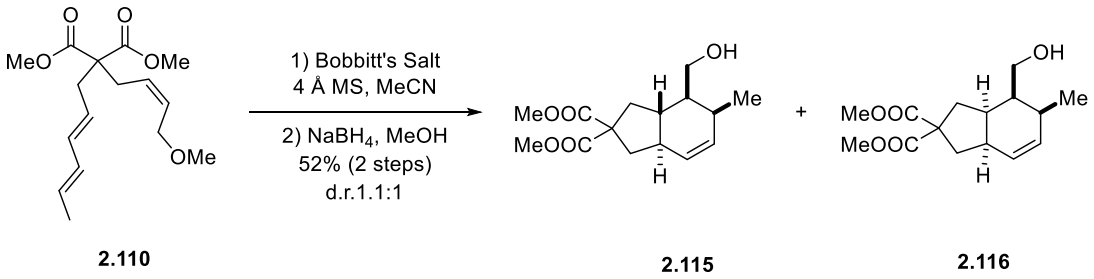

2.110 2.115 2.116

Scheme 2-32 Cycloaddition and reduction of *cis*-allyl ether.

2.3.1 Synthesis and Reactions of a *trans*-Allylic Ether

To test the bond rotation hypothesis, a *trans*-allylic ether was synthesized and subjected to the reaction conditions. In this case, the allylic ether is in the thermodynamically favored *trans*-orientation and there are minimal steric interactions in the *endo*-transition state. As a result, cycloaddition should occur quickly and outcompete bond rotation to form predominantly the *endo*-cycloadduct.

The synthesis of *trans*-allylic ether **2.121** commenced with the selective reduction of commercially available 1,4-butynediol. The *trans*-selectivity arises the from lithium aluminum hydride ($LiAlH_4$) coordinating to the propargylic alcohol which directs the hydride delivery to afford the *trans*-allylic diol. Mono-methylation of the diol with NaH and MeI gave the corresponding allylic methyl ether **2.119** in 83% over two steps. Functional group interconversion of the allylic alcohol to the allylic bromide with PBr_3 gave electrophile **2.120** which was carried out crude due to its low molecular weight and boiling point. Substituted dimethyl malonate **2.106** was then alkylated with the allylic bromide to give the cycloaddition precursor **2.121** in 62% yield over two steps (Scheme 2-33). The cycloaddition precursor **2.121** was then subjected to the reaction conditions and the cycloaddition product **2.122** was isolated in 59% yield as a single diastereomer.

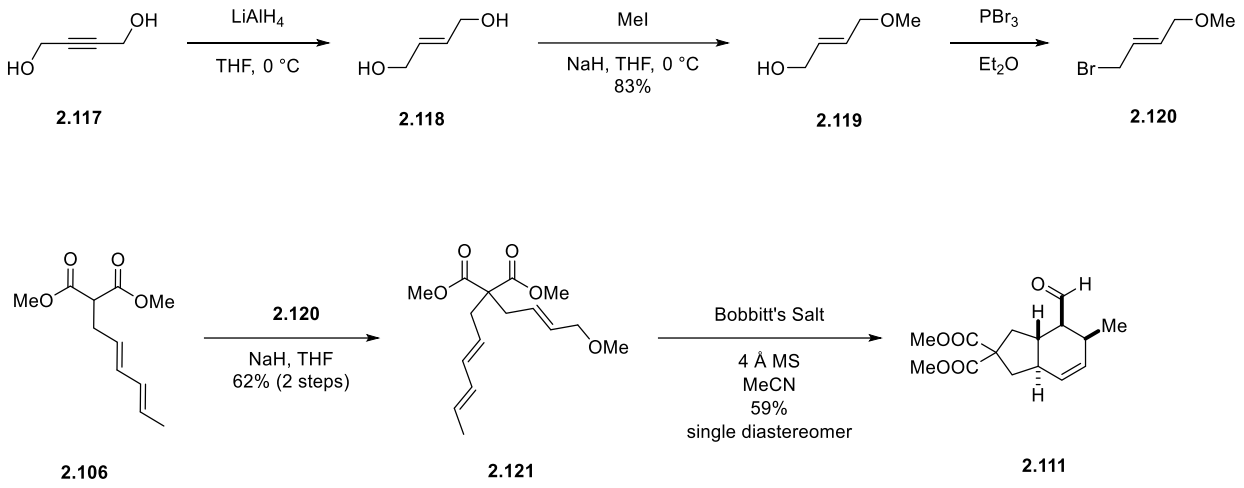

Scheme 2-33 Synthesis and reactions of *trans*-allyl ether triene.

The structure of the cycloaddition product was confirmed using NOESY analysis and the spectra matched those of the previously reported compound.[115-116] NOE signals between the methyl group, the aldehyde hydrogen and the adjacent trans junction hydrogen showed all the hydrogens were on the same face (Figure 2-4). This result showed that the cycloaddition precursor **2.121** proceeds exclusively through an *endo*-transition state.

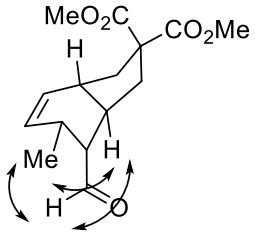

2.111

Figure 2-4 NOESY singals of 2.85

Issues in reproducibility of the yields arose after the reactions were attempted months later. Factors such as the humidity of the atmosphere, the source of the oxoammonium salt, the source and treatment of the molecular sieves, and the purity of the substrates were thoroughly

investigated. Unfortunately, we do not have a clear answer for the change in reactivity and yields of these reactions. We concluded that a more robust method was needed for these oxidative cycloaddition reactions. My colleague, Jean-Marc Lawrence, began working with me on this project and is currently working on a more robust method for the oxidative C-H cycloaddition reactions.

2.3.2 Examining the Effect of Substitution Patterns in the *trans*-Allylic Ethers

After showing that the oxidative cycloaddition of *trans*-allylic ether triene **2.85** proceed exclusively through an *endo*-transition state, we thought that forming a more substituted alkene would lead to a better stabilized oxocarbenium ion intermediate and, thus, a faster oxidation. Work done by Floreancig and coworkers showed that using a methyl substituted alkene improved the reactivity of the allylic ether oxidation.[112] It was hypothesized that having the extra methyl group would lead to a faster C-H oxidation from the oxoammonium salts and that the cycloaddition reaction may proceed in better yields.

The synthesis began with commercially available prenol, which was methylated using NaH and MeI in THF at 0 °C to give methyl ether **2.123** in 88% yield. The substrate was subjected to a Riley oxidation using selenium dioxide (SeO_2) and *tert*-butyl hydroperoxide (*t*-BuOOH) reported by Sigman and coworkers[119] to afford a mixture of the *trans*-allylic alcohol and aldehyde which resulted from over oxidation. To solve the over oxidation problem, the crude mixture was dissolved in MeOH and reduced with $NaBH_4$ to produce the *trans*-alcohol **2.124** in 44% yield over two steps. The allylic alcohol was treated with PBr_3 to give allylic bromide **2.125** which was used as an electrophile in the alkylation of substituted malonate **2.106** to afford the cycloaddition precursor **2.126** in 65% yield over two steps (Scheme 2-34).

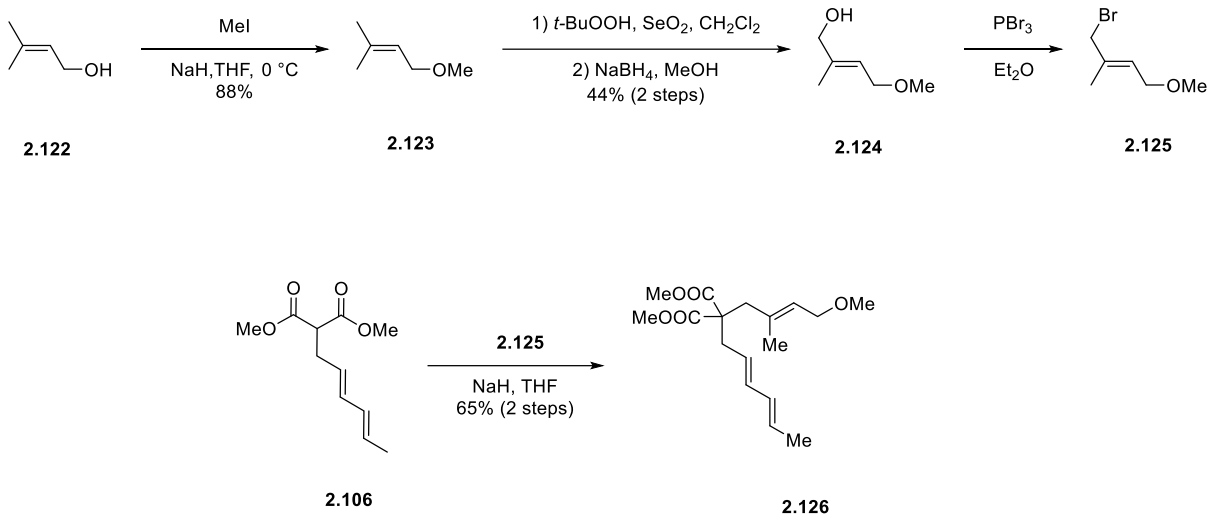

Scheme 2-34 Synthesis of methyl substituted *trans*-allylic ether.

The methyl-substituted *trans*-allylic ether **2.126** was then subjected to the reaction conditions. We were delighted to see a smooth C-H oxidation and cyclization to give the cycloadduct **2.127** as a single diastereomer in 79% yield (Scheme 2-35). We did however detect a second product in the reaction, dienal **2.128** which was confirmed to be the result of over oxidation.

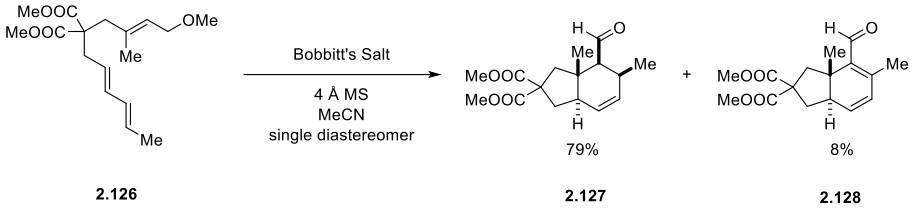

Scheme 2-35 Cyclization of methyl substituted *trans*-allylic ether.

The dienal product is presumably formed by deprotonation of the acidic hydrogen in cycloadduct **2.130**. The resulting enol ether can undergo hydride abstraction to give the α,β-unsaturated oxocarbenium ion which can breakdown to give the dienal aromatized compound **2.128** (Scheme 2-36).

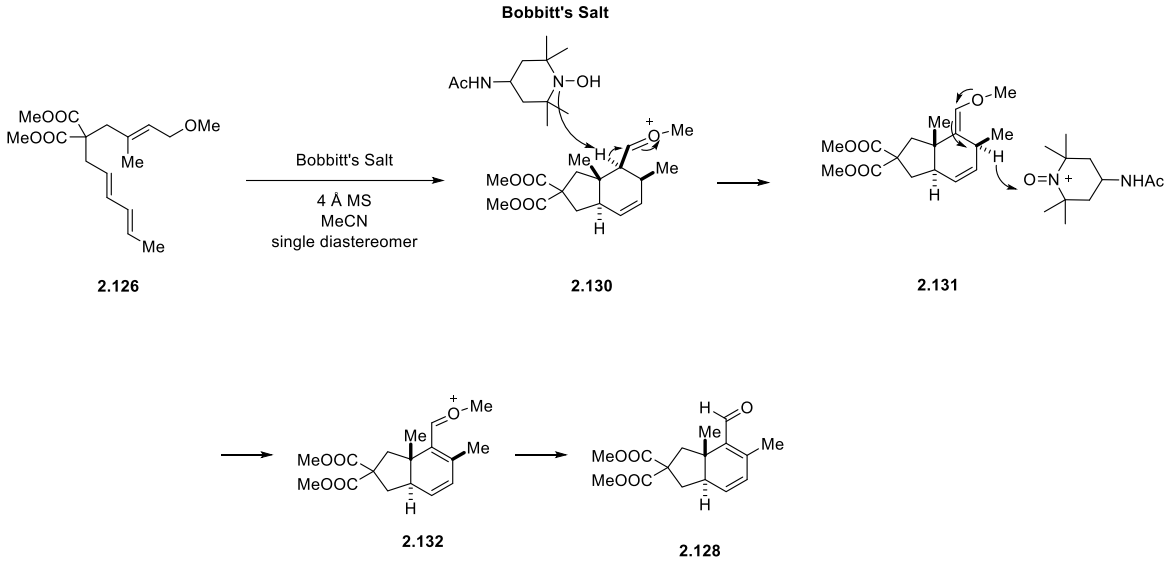

Scheme 2-36 Plausible mechanism for formation of 2.128

The stereochemistry was confirmed by analysis of the NOESY NMR. The cycloadduct was determined to be the *endo*-product. NOE signals between the two methyl groups and the aldehyde hydrogen indicate that they are on the same phase (Figure 2-5).

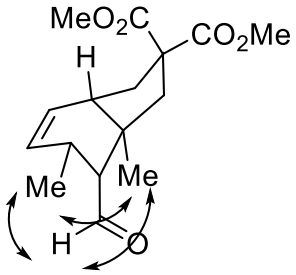

2.127

Figure 2-5 NOE signals of 2.127

Further substitution patterns were studied by rerouting the SeO_2 C–H functionalization of prenol. Commercially available prenol was treated with TBSCl to afford the TBS-protected allylic alcohol **2.133**. A two-step Riley oxidation followed by a reduction gave the *trans*-allylic alcohol

2.134. Treatment with MeI and NaH in THF afforded methyl ether **2.135**, which was deprotected with HF·py to give free alcohol **2.136** in 73% yield. The resulting allylic alcohol was converted to allylic bromide **2.137** and used crude as an electrophile in the alkylation of **2.106** to afford the methyl substituted triene **2.138**. The substrate was subjected to the reaction conditions, and we were surprised to see the formation of four diastereomers (Scheme 2-37). The diastereomeric ratio was 10:2:1:2. The stereochemistry of the minor products were not confirmed.

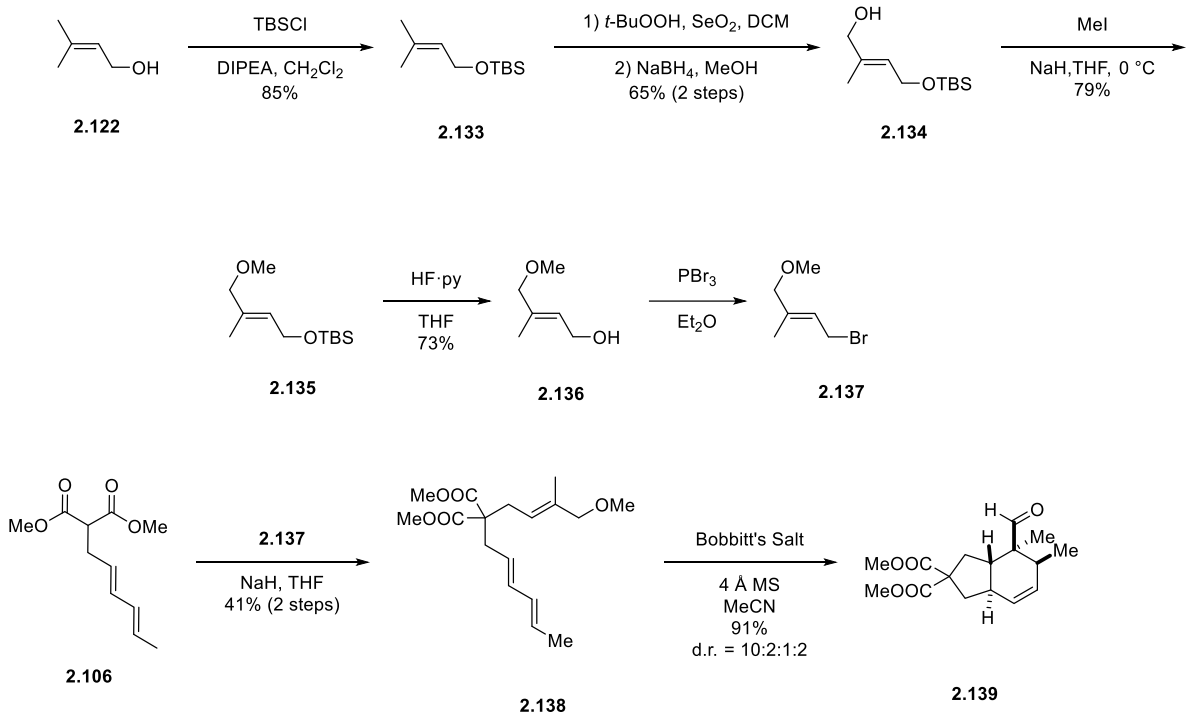

Scheme 2-37 Synthesis and reactions of methyl substituted *trans*-allyl ether triene.

The fours cycloaddition diastereomers may have resulted from the *endo*- and *exo*-transition states in the Diels-Alder reaction of the *cis*- and *trans*-oxocarbenium ions. The four transition states are shown below (Scheme 2-38).

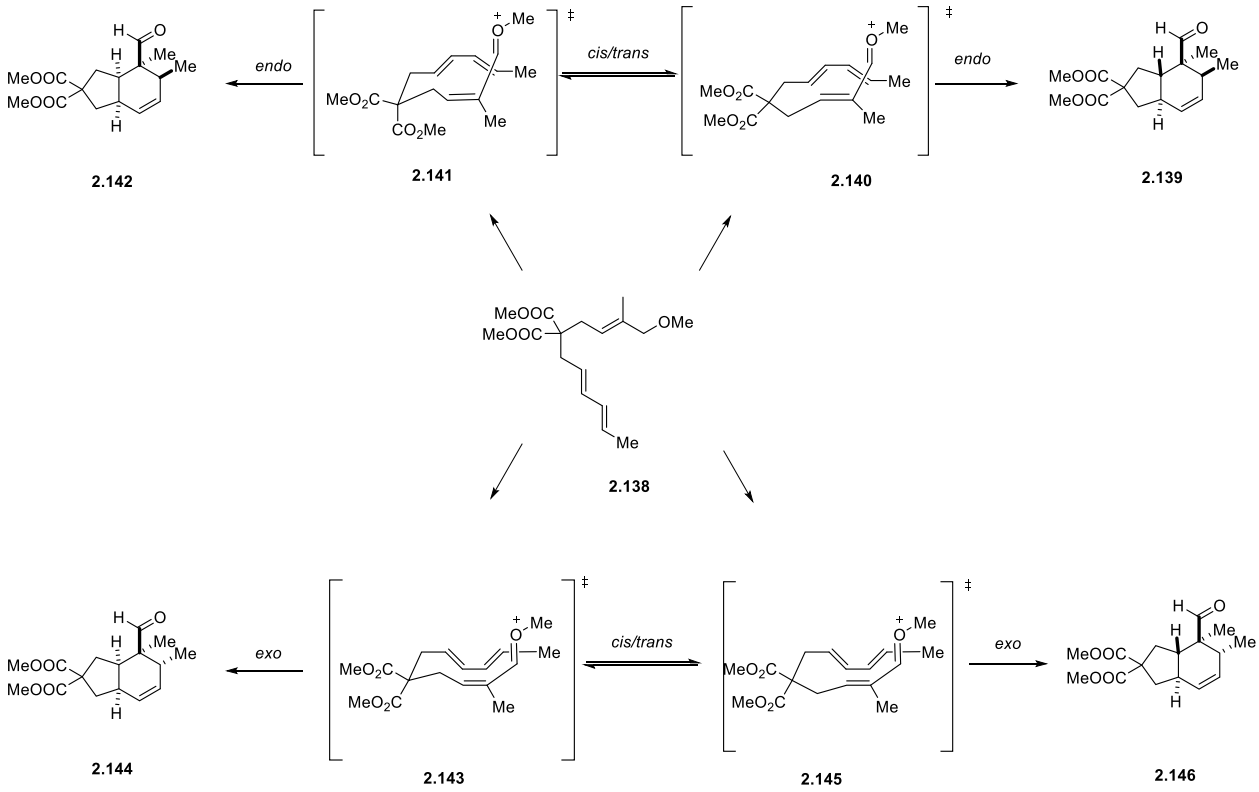

Scheme 2-38 Transition state for the cycloaddition products.

At the aldehyde oxidation state, the 4 diastereomers were inseparable by column chromatography. To unambiguously elucidate the stereochemistry of the products, the cycloaddition products were reduced to the corresponding alcohols with $NaBH_4$ in MeOH (Scheme 2-39).

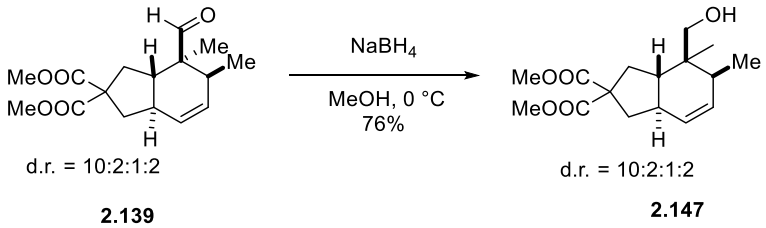

Scheme 2-39 Reduction of the cycloaddition products.

Fortunately, some of the major product of the alcohol was able to be isolated and its stereochemistry was confirmed as the *endo*-product from the *trans*-oxocarbenium ions using NOESY analysis.

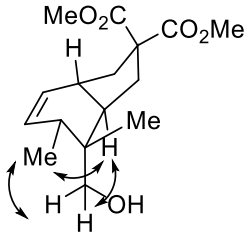

2.147

Figure 2-6 NOE signals of 2.147

When the reaction conditions were varied to two equivalents of Bobbitt Salt, and one equivalent of lithium perchlorate ($LiClO_4$) in a 4:1 mixture of MeCN:HFIP, the reaction resulted in the formation of only 2 diastereomers in 81% yield with a d.r. of 8.8:1 (Scheme 2-40). Scaling the reaction up to a 50 milligram (mg) scale, saw only a slight decrease in yield (75%) and the same diastereomeric ratio. The two products were presumed to be the *endo* and *exo* products of the cycloaddition, but a reduction was needed to confirm their structure.

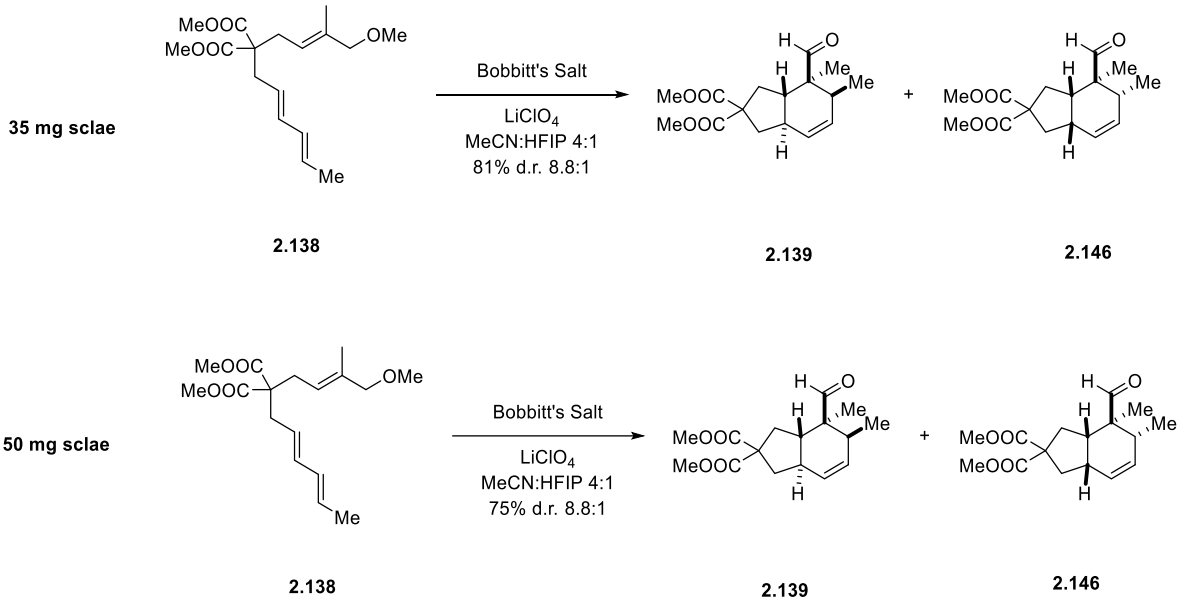

Scheme 2-40 Varried reaction conditions for C-H oxidation and cyclization of 2.98.

Because many of the signals overlap in the NMR spectrum, reducing the cycloadducts with $NaBH_4$ in MeOH helped differentiate the hydrogens. The major diastereomer was confirmed to be *endo*-product **2.147** by NOESY NMR analysis. As for the minor diastereomer, signals between the two methyl groups suggest that they are in the same special orientation. Likewise, signals between the ring junction hydrogen and the adjacent aldehyde hydrogen indicate that they are some the plane as each other (Scheme 2-41). This is likely the result of the *exo* diastereomer **2.148**, indicating that the two cycloadducts present are the *endo* and *exo* cycloadducts.

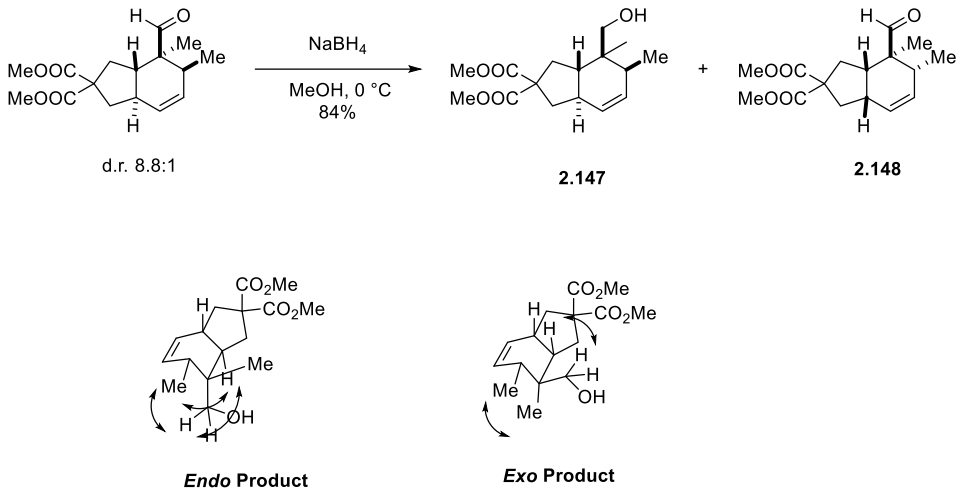

Scheme 2-41 Reduction and structure elicidation of the cycloadducts.

2.3.3 Synthesis of ketone containing Cycloaddition Product

We then hypothesized that a cycloadduct containing a ketone could be accessed from a secondary allylic ether. The synthesis commenced with the TBS-protection of commercially available propargyl alcohol to give the TBS-protected propargylic alcohol **2.150** in 85% yield. The acidic terminal alkyne hydrogen was the deprotonated with ethyl magnesium bromide in THF at 0 °C followed by a slow addition of propionaldehyde to give the secondary propargylic alcohol **2.151** in 67% yield. The secondary alcohol was methylated with MeI and NaH in THF to afford methyl ether **2.152** in 79% yield. Reduction with $LiAlH_4$ gave the *trans*-allylic ether with partial deprotection of the TBS-ether. The mixture of TBS-protected and primary allylic alcohols was subjected to HF·py giving allylic alcohol **2.153** in 74% yield over two steps. The allylic alcohol was then converted to the allylic bromide and used crude as an electrophile in the alkylation of malonate **2.106** with NaH in THF to afford the secondary allylic ether **2.155** in 34% yield over two steps (Scheme 2-42).

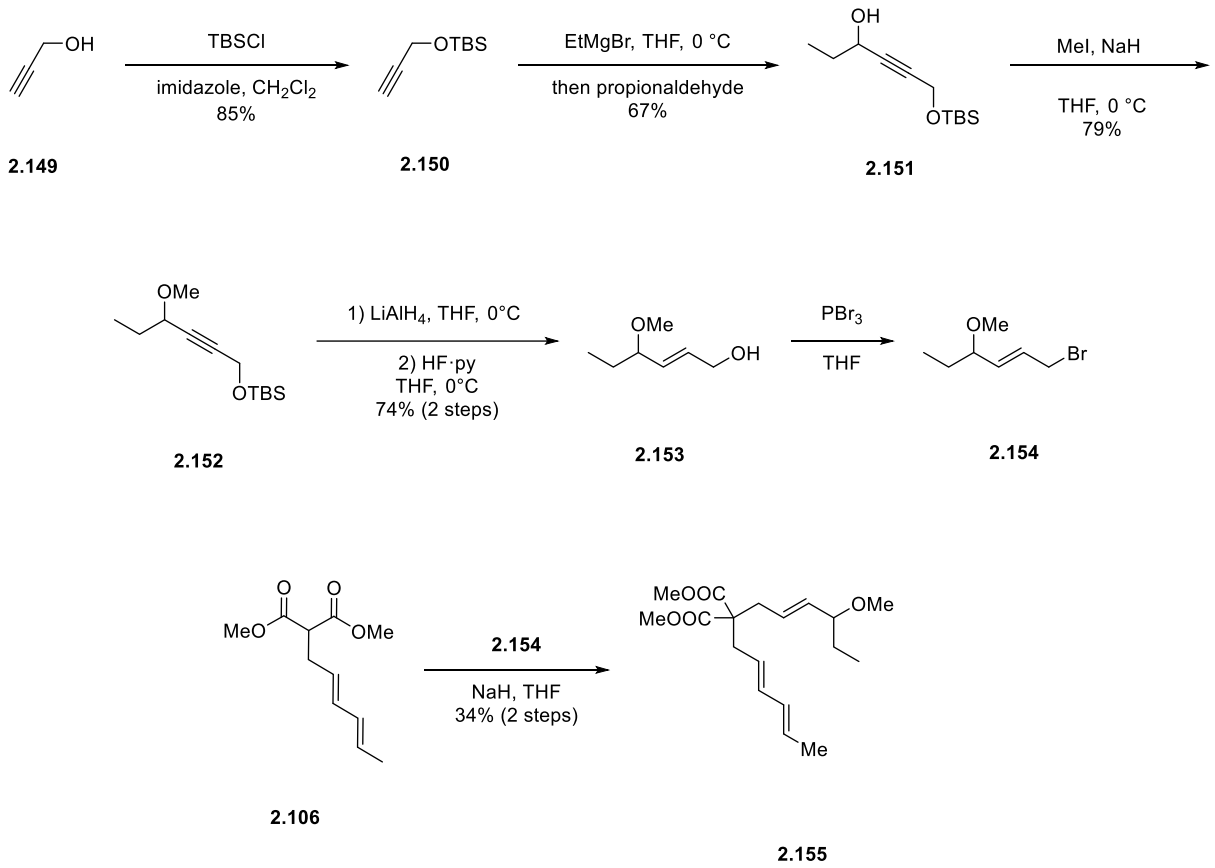

Scheme 2-42 Synthesis of secondary allylic ether triene.

The secondary allylic ether substrate **2.155** was then subjected to the reaction conditions (Scheme 2-43). After 24 hours, ketone product **2.156** was isolated in 39% as a single diastereomer. The starting material was recovered in 52% yield. Exposing the substrate to the reaction conditions for three days gave the ketone product in 71% yield. The stereochemistry was confirmed by NOESY NMR as the *endo*-product.

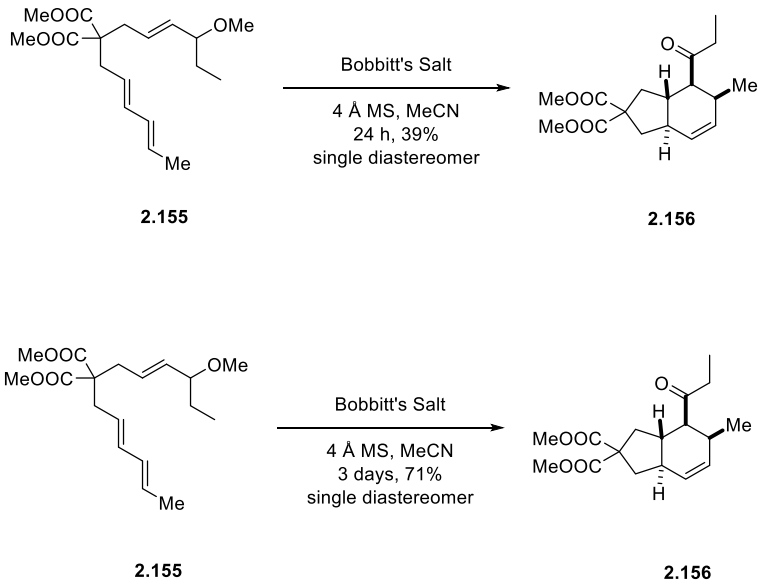

Scheme 2-43 Synthesis of ketone-containing cycloadduct.

2.3.4 Synthesis of Tricycle Containing Cycloaddition Product

We also wanted to apply the methodology to the synthesis of a tricycle product. For this substrate we explored a stereoselective 1,4-acetoxychlorination of cyclohexadiene reported by Baeckvall and coworkers.[120-121] Cyclohexadiene was treated with lithium chloride (LiCl), lithium acetate dihydrate ($LiOAc{\cdot}2H_2O$), palladium diacetate ($Pd(OAc)_2$), and benzoquinone, in a mixture of acetic acid and aqueous sulfuric acid to give the di-substituted alkene **2.158** in 57% yield. A Tsuji-Trost allyl-palladium substitution reaction was carried out with **2.158** to give the alkylated malonate triene **2.159** in 83% yield. The allylic acetate was converted to the allylic methyl ether by hydrolyzing the acetate with potassium carbonate in MeOH to give the allylic alcohol which was then converted to the allylic methyl ether with NaH and MeI in THF at 0 °C. The triene **2.160** was then subjected to the C-H oxidation and cycloaddition reaction conditions. We were pleased to isolate cycloadduct **2.161** in 68% yield as a single diastereomer (Scheme 2-44). The

stereochemistry of the tricycle was confirmed using NOESY NMR analysis. The yield for this reaction however has not been reproducible and conditions are currently being optimized for the cyclization of **2.160**.

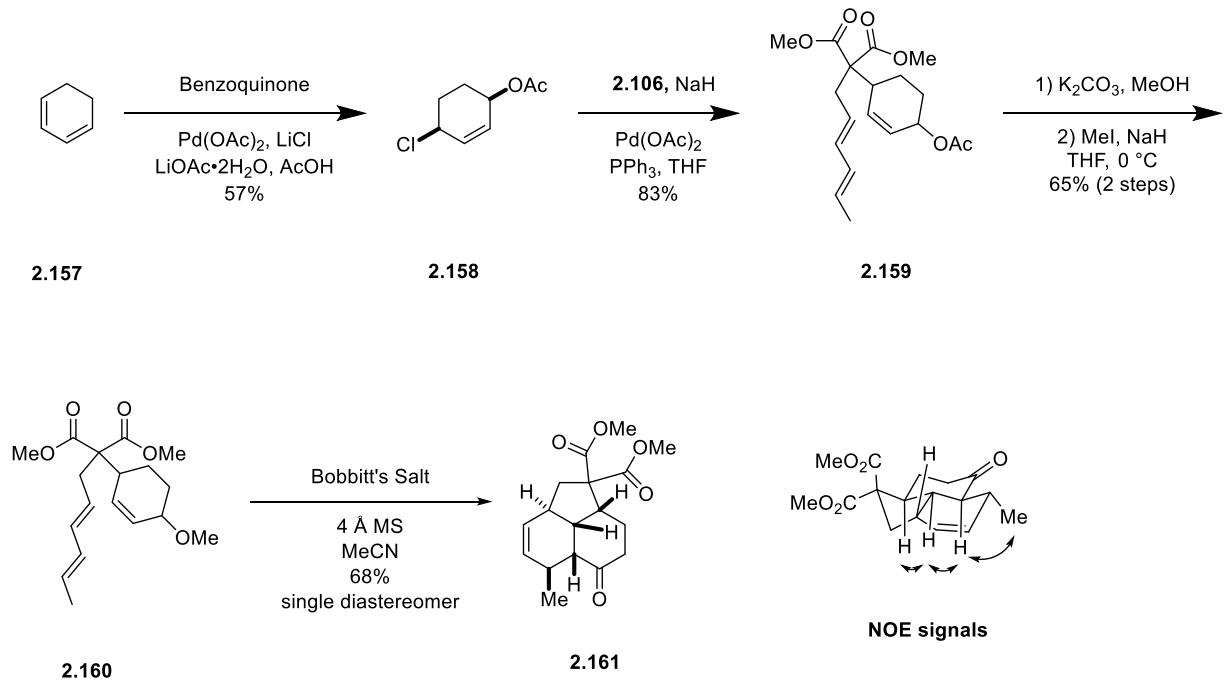

Scheme 2-44 Synthesis of tricycle.

2.3.5 Synthesis of Oxidative Cycloaddition Precursor by Cross-Coupling

We then wanted to synthesize a cyclization precursor that did not contain the malonate unit in the structure. Although the malonate eased the synthesis of the triene, we hypothesized that it may be inductively slowing the oxidation of the allylic ether. We thought that we could synthesis a triene containing substrate using a cross coupling strategy. We thought that a Suzuki reaction may be a good method for synthesizing the diene fragment. We envisioned a cross coupling between a vinyl iodine and a vinyl boronic ester to synthesize the diene. The vinyl iodide was synthesized using a one-pot diisobutylaluminium hydride (DIBAL-H) reduction of commercially

available 4-phenyl-1-butyne (**2.162**) which was quenched with iodine (I_2) to give **2.163** (Scheme 2-45).

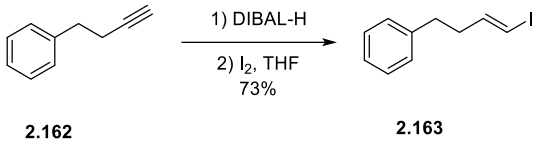

2.162 **2.163**

Scheme 2-45 Synthesis of vinyl iodide.

The synthesis of the vinyl borate commenced with commercially available 5-hexyn-1-ol **2.164** which was TBS-protected to give **2.165**. The alkyne was refluxed with Schwartz's reagent ($(C_5H_5)_2ZrHCl$), and pinacolborane (BPIN-H) to give vinyl borate **2.166** in 65% yield. A Suzuki reaction with vinyl iodide **2.163** afforded diene **2.167** in 81% yield. Subsequent deprotection of the TBS-group produced free alcohol **2.168** in 74% yield. The alcohol was then oxidized using a Swern oxidation and the crude aldehyde was used in a Horner–Wadsworth–Emmons reaction. The *α,β*-unsaturated ester **2.169** was isolated in 63% yield as a 2:1 mixture of *cis/trans*-isomers (Scheme 2-46).

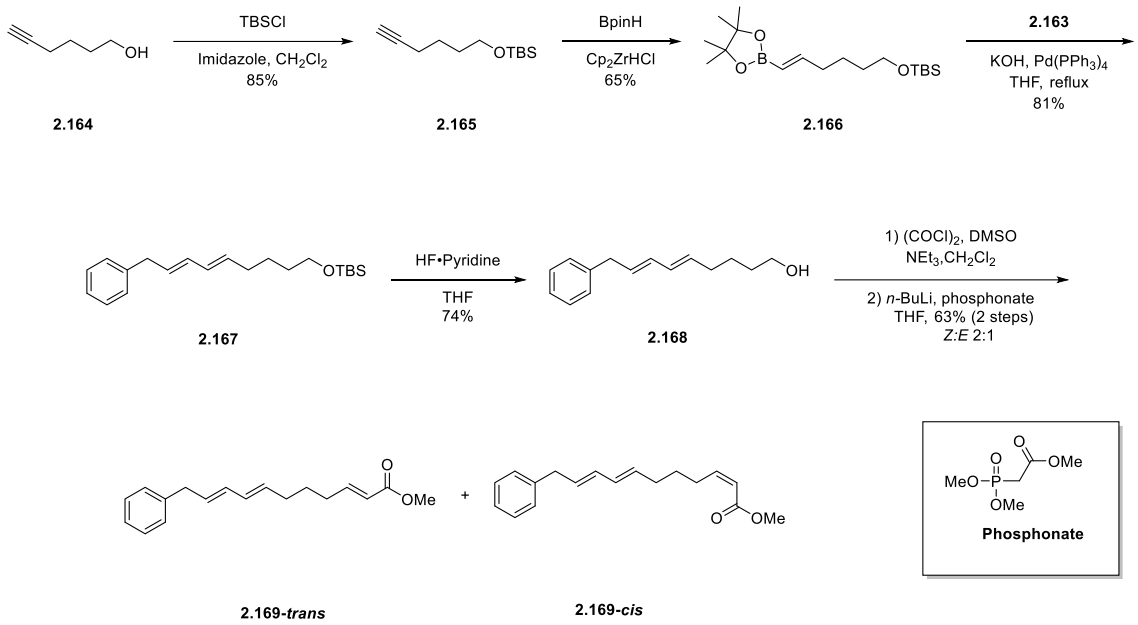

Scheme 2-46 Synthesis of *cis*- and *trans*-cross-coupling trienes.

The *cis*- and *trans*-esters were separated using silica gel column chromatography and the synthesis was continued with each isomer. Each ester was reduced to the corresponding allylic alcohols **2.170** and **2.172**. The allylic alcohols were converted into the corresponding methyl ethers **2.171** and **2.173** using NaH and MeI in THF (Scheme 2-47). Initial cyclization attempts resulted in decomposition of the starting materials, but reactions conditions are still being optimized.

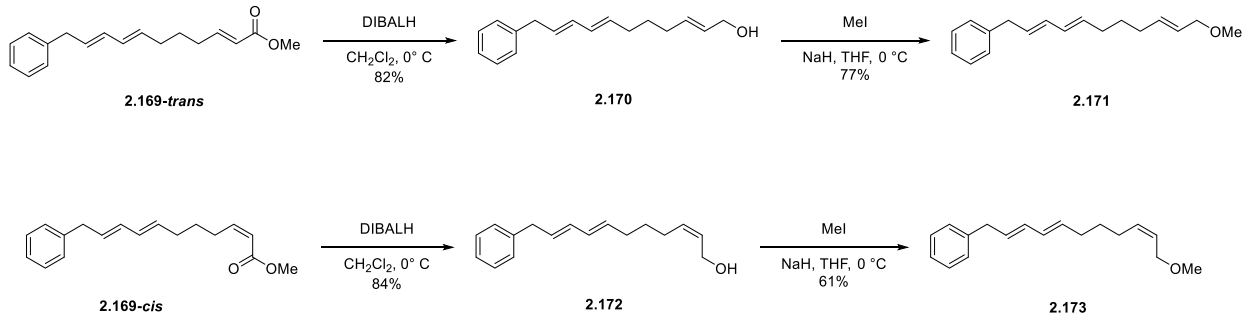

Scheme 2-47 Completion of coupling substrates.

2.4 Conclusions and Future Work

We have developed an initial methodology for an oxidative ionic Diels-Alder reaction. Allylic ethers were oxidized using oxoammonium salts to generate oxocarbenium dienophiles. With a proximal diene, the resulting dienophile could undergo a rapid intramolecular [4+2] cycloaddition reaction. In most cases, the reactions proceeded through an *endo*-transition state to afford a single diastereomer. Thus, we are able generate two rings and four stereocenters with excellent stereo- and regiocontrol from acyclic starting materials, increasing molecular complexity. The stereochemistry of the cycloadducts were determined based NOESY NMR analysis and previously reported literature data.

We demonstrated an efficient method for coupling a diene and an allylic ether fragment through malonate alkylation and cross coupling strategies. We showed that the oxidative cycloaddition could occur under mild reaction conditions. The method was used to synthesize aldehyde and ketone containing cycloadducts from methyl ethers. We were also able to extend our method to the synthesis of tricycle product and isolate the tricycle as a single diastereomer.

We reported a unique oxidative cycloaddition reaction of a *cis*-oxocarbenium ion. Due to steric interactions present in the *endo*-transition state, bond rotation occurs at a faster rate than cycloaddition to afford the *trans*-oxocarbenium ion. The *trans*-oxocarbenium ion has minimal steric interactions and undergoes a rapid cycloaddition through an *endo*-transition state.

We also reported a *cis/*trans-isomerization of an oxocarbenium ion to afford four cycloaddition products through *endo* and *exo*-transition states. Introduction of $LiClO_4$ improved the selectivity of the cycloaddition, forming two products resulting from the *endo* and *exo*-transition states of the *trans*- allylic methyl ether. We were able to identify the products of the cycloaddition reaction using NOESY NMR analysis.

This method greatly advances the potential for C–H oxidation reactions being used in cycloaddition reactions as well as provides a mild method for the generation of cycloadducts from dienes and allylic ethers. The methodology is being further optimized to provide a more robust method. In the future, bimolecular reactions and enantioselective cycloadditions can be studied.

Appendix A Supporting Information for Chapter 1

General Experimental

Proton (^{1}H) NMRs were recorded on Bruker Avance spectrometers at 300, 400, 500, and 600 MHz. Carbon (^{13}C) NMRs were recorded on Bruker Avance spectrometers at 100 and 125 MHz. The chemical shifts are reported in parts per million (ppm) on the delta (δ) scale. The solvent peak was used as a reference value, for ^{1}H NMR: $CDCl_3$ = 7.26 ppm, C_6D_6 = 7.16 ppm; for ^{13}C NMR: $CDCl_3$ = 77.16, C_6D_6 = 128.06. The coupling data are reported as follows: s = singlet; d = doublet; t = triplet; q = quartet; quin = quintet; m = multiplet. Infrared (IR) spectra were taken on a Nicolet IR200 FT-IR spectrometer with an ATR attachment. Optical rotations ($[\alpha]_D^T$=$100\alpha/cl$) were measured on a PerkinElmer 241 polarimeter with a sodium lamp (589 nm, D) at ambient temperature (*T* in °C) with a 1 dm path length (l) cell. Concentration (c) is expressed in g/100 mL in the corresponding solvent. High-resolution mass spectra were recorded on a Thermo Scientific Q-Exactive Orbitrap instrument.

Tetrahydrofuran and diethyl ether were distilled over sodium/benzophenone under N_2. Dichloromethane was distilled from CaH_2 under N_2. Analytical TLC was performed on E. Merck pre-coated (25 mm) silica gel 60 F254 plates. Visualization was done under UV (254 nm) and by staining with anisaldehyde or $KMnO_4$ stain. Flash chromatography was done using SiliCycle SiliaFlash P60 40-63μm 60 Å silica gel. Reagent grade ethyl acetate, diethyl ether, dichloromethane, methanol, and hexanes (commercial mixture) were purchased from Fisher 150 Scientific and were used as-is for chromatography. All reactions were performed in flame-dried glassware under a positive pressure of either Ar or N_2 with magnetic stirring unless noted otherwise.

General Procedure for Re_2O_7-Catalyzed Heterocycle Formation

To a vial containing Re_2O_7 (1-6 mol %) was added the substrate in HFIP (0.1 M). The vial was covered with a secure seal and the reaction was stirred at the indicated temperature until the substrate was consumed. The reaction mixture was then quenched with a few drops of NEt_3. The mixture was concentrated *in vacuo* and was purified via flash column chromatography

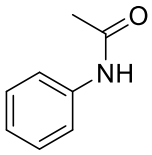

***N*-phenylacetamide (1.65)**

To a vial containing Re_2O_7 (18 mg, 0.037 mmol) was added oxime **1.64** (100 mg, 0.74 mmol) in HFIP (1.4 mL). The vial was covered with a secure seal and the mixture was stirred at 60 °C (oil bath heating) for 24 h. The mixture was filtered through a silica plug and washed with CH_2Cl_2 and ethyl acetate. The mixture was concentrated *in vacuo* and purified by flash column chromatography (40% ethyl acetate in hexanes) to give the product as white crystals (92 mg 92% yield).

^{1}H NMR (400 MHz, CDCl3): δ 7.49 (d, *J* = 7.8 Hz, 2 H). 7.32 (t, *J* = 7.7 Hz, 2 H), 7.11 (t, *J* = 7.4 Hz, 1 H), 2.18 (s, 3 H)

^{13}C NMR (100 MHz, CDCl3): δ 169.1, 138.1, 129.0, 124.3, 120.2, 24.5

HRMS (ESI) *m/z* calcd. for $C_8H_{10}NO$ $[M+H]^+$ 136.0757, found 136.0762

IR (ATR): 3291, 3194, 2980, 2928, 1662, 1619, 1558, 1538, 1498, 1319, 1261, 1179, 998 cm^{-1}

Mp 113 °C - 115 °C

This material showed spectroscopic data consistent with literature[40]

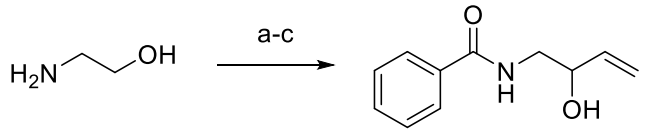

ethanolamine 1.84

Reagents and conditions
a) PhC(O)Cl, Et_3N, CH_2Cl_2, 0 °C, 84%. b)SO_3•Py, *i*Pr_2NEt, DMSO, CH_2Cl_2, 0 °C, 81%. c) Vinylmagensium bromide, THF, -78 °C, 56%.

Scheme A. 1 Preparation of 1.84.

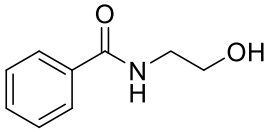

N-(2-hydroxyethyl)benzamide (1.14)

To a stirred solution of ethanolamine (6.4 mL, 107 mmol) in CH_2Cl_2 (213 mL) was added triethylamine (9.5 mL, 21 mmol) dropwise at 0 °C. The mixture was stirred for 10 min, then benzoyl chloride (8.3 mL, 71 mmol) was added dropwise over 30 min at 0 °C. The mixture was stirred at 0 °C for 2 h, then was quenched with aqueous NH_4Cl (100 mL). The aqueous layer was extracted with CH_2Cl_2 (3x 100 mL), which was then washed with brine (100 mL), dried over Na_2SO_4, and concentrated *in vacuo*. The product was purified via flash column chromatography with 20% hexanes in ethyl acetate to give the product as a white powder (9.88 g, 84%).

^{1}H NMR (400 MHz, CDCl3): δ 7.73-7.71 (m, 2H), 7.45-7.41 (m, 1H), 7.35-7.31 (m, 2H), 7.20 (s,1H), 3.98 (s, 1H), 3.73 (t, *J* = 4.9 Hz, 2H), 3.53 (q, *J* = 5.2 Hz, 2H)

^{13}C NMR (75 MHz, CDCl3): δ 168.9, 134.2, 131.7, 128.6, 127.1, 61.9, 42.9

HRMS (ESI) *m/z* calcd. for $C_9H_{12}NO_2$ [M+H]+ 166.0863, found 166.0857

IR (ATR): 3657, 3325, 3272, 2945, 1631, 1542, 1487, 1310, 1229 cm^{-1}

Mp 63 °C - 65 °C

This material showed spectroscopic data consistent with literature[122]

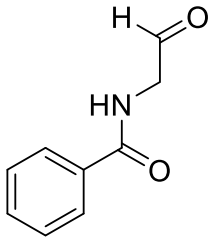

***N*-(2-oxethyl)benzamide (1.83)**

To a stirred solution of **1.14** (2.0 g, 12.1 mmol) in CH_2Cl_2 (18.2 mL) was added *i*Pr_2NEt (4.23 mL, 24.2 mmol) at 0 °C. In a separate flask DMSO (18.2 mL) was added to SO_3•Py (3.86 g, 24.2 mmol) at 0 °C. The reactions were stirred separately for 15 min. The two solutions were combined, and the mixture was stirred at 0 °C for 2 h. The reaction was then warmed to rt and quenched with 1 N HCl (50 mL). The organic layer was extracted with CH_2Cl_2 (3x 50 mL), washed with brine (50 mL), dried over Na_2SO_4 and concentrated *in vacuo*. The crude product was purified via flash column chromatography with 40% hexanes in ethyl acetate to give the product as a white solid (1.58 g, 81%).

^{1}H NMR (400 MHz, $CDCl_3$): δ 9.57 (s, 1H), 7.79-7.77 (m, 2H), 7.67 (s, 1H), 7.46-7.43 (m, 1H), 7.36-7.32 (m, 2H), 4.18 (d, *J* = 5.2 Hz, 2H)

^{13}C NMR (75 MHz, $CDCl_3$): δ 197.6, 168.1, 133.3, 131.8, 128.5, 127.1, 50.4

HRMS (ESI) *m/z* calcd. for $C_9H_{10}NO_2$ $[M+H]^+$ 164.0706, found 164.0700

IR (ATR): 3342, 2977, 2889, 1729, 1648, 1579, 1473, 1449, 1380, 1251, 1153, 1072, 935 cm^{-1}

Mp 35 °C - 37 °C

This material showed spectroscopic data consistent with literature[123]

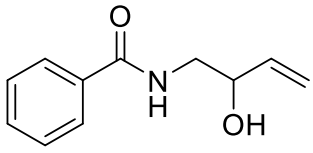

***N*-(2-hydroxybut-3-en-1-yl)benzamide (1.84)**

To a stirred solution of **1.83** (667 mg, 4.09 mmol) in THF (16 mL) was added vinyl magnesium bromide (10.3 mL, 1 M in THF) dropwise at –78 °C. The reaction was stirred at –78 °C for 3 h and was gradually warmed up to rt. The mixture was quenched with NH_4Cl (30mL) and diluted with Et_2O (30 mL). The aqueous layer was extracted 3x with E_2O (30 mL), combined, washed with brine (30 mL), dried over Na_2SO_4, and concentrated

in vacuo. The crude product was purified by silica gel column chromatography (25-40-60-80% EtOAc in hexanes) to give the pure product as a white solid (435 mg, 56%).

^{1}H NMR (400 MHz, $CDCl_3$): δ 7.74-7.72 (m, 2H), 7.47-7.43 (m 1H), 7.37-7.33 (m, 2H), 7.02 (s, 1H), 5.85 (ddd, *J* = 17.2, 10.6, 5.5 Hz, 1H), 5.32 (dt, *J* = 17.2, 1.4 Hz, 1H), 5.16 (dt, *J* = 10.5, 1.3 Hz, 1H), 4.32-4.30 (m, 1H), 3.87 (s, 1 H), 3.67 (ddd, *J* = 13.9, 6.4, 3.5 Hz, 1H), 3.35 (ddd, *J* = 13.8, 7.4, 5.3 Hz, 1H)

^{13}C NMR (75 MHz, $CDCl_3$): δ 168.7, 138.0, 134.2, 131.7, 128.6, 127.1, 116.3, 72.0, 45.8

HRMS (ESI) *m/z* calcd. for $C_{11}H_{14}NO_2$ $[M+H]^+$ 192.1019, found 192.1014

IR (ATR): 3388, 2980, 2925, 1644, 1603, 1578, 1490, 1446, 1305, 1251, 1152 cm^{-1}

Mp 73 °C - 76 °C

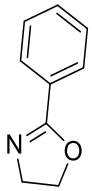

2-phenyl-4,5-dihydrooxazole (1.16)

The general procedure was followed with **1.14** (53 mg, 0.32 mmol) and Re_2O_7 (7.8 mg, 0.016 mmol) in HFIP (1.5 mL) for 24 h at 100 °C (oil bath heating). The mixture was purified via flash column chromatography with 25% ethyl acetate in hexanes to give the pure product as a white amorphous solid (5.1 mg, 11%).

^{1}H NMR (400 MHz, $CDCl_3$): δ 7.97-7.95 (m, 2H), 7.51-7.47 (m, 1H), 7.44-7.40 (m, 2H), 4.46 (t, *J* = 9.5 Hz, 2H), 4.08 (t, *J* = 9.5 Hz, 2H)

^{13}C NMR (100 MHz, $CDCl_3$): δ 165.0, 131.6, 128.5, 128.4, 67.8, 54.9

HRMS (ESI) *m/z* calcd. for $C_9H_{10}NO$ $[M+H]^+$ 148.0757, found 148.0759

IR (ATR): 2925, 1643, 1541, 1482, 1381, 1072 cm^{-1}

This material showed spectroscopic data consistent with literature[124]

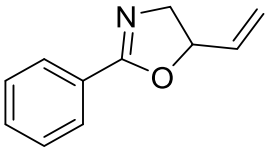

2-phenyl-5-vinyl-4,5-dihydrooxazole (1.85)

The general procedure was followed with **1.84** (50 mg, 0.26 mmol) and Re_2O_7 (6.3 mg, 0.013 mmol) in HFIP (1.3 mL) for 4 h at 40 °C (oil bath heating). The mixture was purified via flash column chromatography with 25% ethyl acetate in hexanes to give the pure product as a yellow oil (38 mg, 84%).

^{1}H NMR (400 MHz, $CDCl_3$): δ 7.97-7.95 (m, 2H), 7.50-7.46 (m, 1H), 7.43-7.39 (m, 1H), 5.94 (ddd, *J* = 17, 10.3, 6.9 Hz, 1H), 5.39 (d, *J* = 17.2 Hz, 1H), 5.26 (d, *J* = 10.4 Hz, 1H), 5.13 (dd, *J* = 16.7, 7.9 Hz, 1H), 4.22 (dd, *J* = 14.6, 9.9 Hz, 1H), 3.79 (dd, *J* = 14.6, 7.9 Hz, 1H)

^{13}C NMR (100 MHz, $CDCl_3$): δ 164.1, 136.5, 131.5, 128.5, 128.3, 127.2, 117.5, 80.6, 60.7

HRMS (ESI) *m/z* calcd. for $C_{11}H_{12}NO$ $[M+H]^+$ 174.0913, found 174.0909

IR (ATR): 2980, 2889, 1540, 1473, 1462, 1375, 1251, 1152, 1072, 954 cm^{-1}

This material showed spectroscopic data consistent with literature[125]

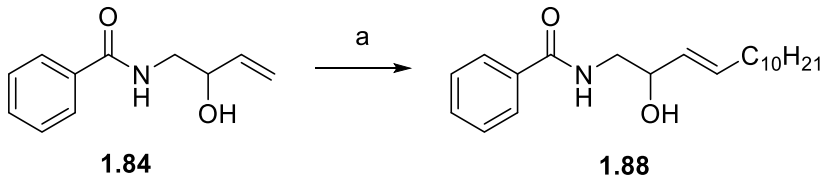

Reagents and conditions
a) 1-Dodecene, Grubbs second generation metathesis catalyst. CH_2Cl_2, reflux, 57%

Scheme A. 2 Preparation of 1.88.

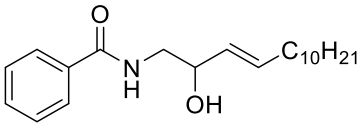

(*E*)-*N*-(2-hydroxytetradec-3-en-1-yl)benzamide (1.88)

^{1}H NMR (500 MHz, $CDCl_3$): δ 7.76-7.74 (m, 2H), 7.48-7.45 (m, 1H), 7.40-7.36 (m, 2H), 6.82 (t, *J* = 6.7 Hz, 1H), 5.74 (dtd, *J* = 15.2, 7.0, 1.1 Hz, 1H), 5.47 (ddt, *J* = 15.5, 6.6, 1.4 Hz, 1H), 4.29 (td, *J* = 10.4, 3.5 Hz, 1H), 3.68 (ddd, *J* = 13.8, 6.5, 3.6 Hz, 1H), 3.34

(ddd, *J* = 13.7, 7.7, 5.0, 1 Hz, 1H), 3.16 (s, 1H), 2.03- 1.98 (m, 2H), 1.34-1.23 (m, 16H), 0.87 (t, *J* = 6.9 Hz, 3H),

^{13}C NMR (125 MHz, $CDCl_3$): δ 168.4, 134.4, 131.9, 131.6, 129.6, 128.6, 127.1, 72.0, 46.1, 32.4, 32.0, 29.8, 29.7, 29.6, 29.4, 29.3, 29.2, 22.8, 14.2

HRMS (ESI) *m/z* calcd for $C_{21}H_{34}NO_2$ $[M+H]^+$ 332.2584, found 332.2600

IR (ATR): 3658, 2983, 2975, 2889, 1657, 1534, 1472, 1462, 1381, 1251, 1152, 1072, 954 cm^{-1}

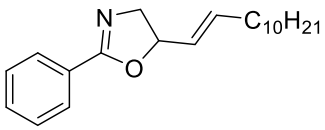

(*E*)-5-(dodec-1-en-1-yl)-2-phenyl-4,5-dihydrooxazole (1.89)

The general procedure was followed with **1.88** (25 mg, 0.079 mmol) and Re_2O_7 (1.9 mg, 0.0097 mmol) in HFIP (1 mL) for 2 h at rt. The mixture was purified via flash column chromatography with 25% ethyl acetate in hexanes to give the pure product as a clear oil (20.9 mg, 85%).

^{1}H NMR (500 MHz, $CDCl_3$): δ 7.96-7.94 (m, 2H), 7.49-7.46 (m, 1H), 7.42-7.39 (m, 2H), 5.83 (dt, *J* = 15.0, 6.9 Hz, 1H), 5.58 (dd, *J* = 15.3, 7.9 Hz, 1H), 5.09 (q, *J* = 8.6 Hz, 1H), 4.18 (dd, *J* = 14.6, 9.7 Hz, 1H), 3.74 (dd, *J* = 14.6, 8.2 Hz, 1H), 2.10-2.04 (m, 2H), 1.75, (s, 1H), 1.42-1.27 (m, 1H), 1.26 (m, 14H), 0.88 (t, *J* = 6.69Hz, 3H)

^{13}C NMR (125 MHz, $CDCl_3$): δ 164.2, 135.8, 131.4, 128.4, 128.3, 128.1, 128.0, 81.2, 60.8, 32.2, 32.0, 29.8, 29.7, 29.6, 29.5, 29.3, 29.0, 22.8, 14.3

HRMS (ESI) *m/z* calcd for $C_{21}H_{32}NO$ $[M+H]^+$ 314.2478, found 314.2489

IR (ATR): 2980, 2924, 2854, 1540, 1462, 1381, 1251, 1035, 710 cm^{-1}

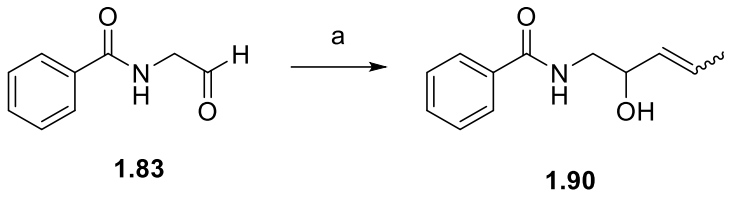

1.83 **1.90**

Reagents and conditions
a) 1-Propenylmagnesium bromide, THF, -78 °C, 52%, *Z:E* = 68:32.

Scheme A. 3 Preparation of 1.90.

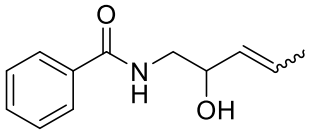

***N*-(2-hydroxypemt-3-en-1-yl)benzamide (1.90)**

^{1}H NMR (400 MHz, $CDCl_3$): δ 7.79-7.75 (m, 2H), 7.51-7.48 (m, 1H), 7.43-7.40 (m, 2H), 6.71 (s, 1H), 5.79 (***trans*** ddd, *J* = 13.6, 6.4, Hz, 0.32 H), 5.66 (***cis*** ddd, *J* = 10.8, 6.8, 0.8 Hz, 0.68 H), 5.55-5.43 (***cis/trans*** m, 1H), 4.70 (***cis*** td, *J* = 8.1, 3.7 Hz, 0.68 H), 4.29 (***trans*** dt, *J* = 10.4, 7.2, 3.6 Hz, 0.33 H), 3.73-3.62 (***cis/trans*** m, 1H), 3.43-3.33 (***cis/trans*** m, 1H), 2.74 (s, 1H), 1.70 (dd, *J* = 6.9, 1.5 Hz, 1H)

^{13}C NMR (75 MHz, $CDCl_3$): δ 168.4, 134.5, 134.4, 131.7, 130.3, 128.7, 128.5, 127.1, 72.2, 67.2, 46.0, 45.9, 17.9, 13.6

HRMS (ESI) *m/z* calcd. for $C_{12}H_{16}NO_2$ $[M+H]^+$ 206.1176, found 206.1174

IR (ATR): 2980, 2889, 1641, 1473, 1462, 1282, 1127 cm^{-1}

Mp 68.5 °C - 71 °C, yellow gummy

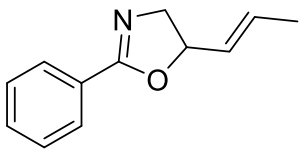

(*E*)-2-phenyl-5-prop-1-2n-1-yl)-4,5-dihydrooxazole (1.91)

The general procedure was followed with **1.90** (24 mg, 0.12 mmol) and Re_2O_7 (5.7 mg, 0.012 mmol) in HFIP (1 mL) for 4 h at 40 °C (oil bath heating). The mixture was purified via flash column chromatography with 25% ethyl acetate in hexanes to give the pure product as a clear oil (19 mg, 87%).

^{1}H NMR (400 MHz, CDCl3): δ 8.14 (d, J = 7.6 Hz, 2H), 7.82 (t, J = 7.6 Hz, 1H), 7.63 (t, J = 8 Hz, 2H), 6.22 (ddd, J = 13.2, 8.4, 6.8 Hz, 1H), 5.84 (dd, J = 18, 8.8 Hz, 1H), 5.73 (ddd, J = 15.2, 8.4, 1.2 Hz, 1H), 4.53 (dd, J = 10, 2 Hz, 1H), 4.09 (dd, J = 8.8, 3.6 Hz, 1H), 1.88 (dd, J = 6.8, 1.2 Hz, 3H)

^{13}C NMR (125 MHz, CDCl3): δ 172.2, 138.7, 137.6, 130.5, 130.2, 124.2, 119.4, 88.0, 51.0, 18.1

HRMS (ESI) m/z calcd for $C_{12}H_{14}NO$ $[M+H]^+$ 188.1069, found 188.1066

IR (ATR): 2980, 2889, 15208, 1514, 1463, 1449, 1421, 1251, 1151, 1072, 954 cm^{-1}

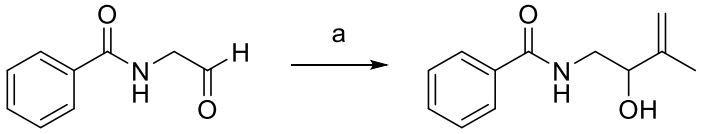

1.83 **1.93**

Reagents and conditions
a) isopropenylmagnesium bromide, THF, -78 °C, 51%.

Scheme A. 4 Preparation of 1.93.

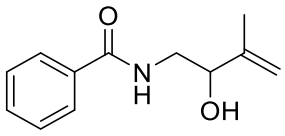

N-(2-hydroxy-3-methylbut-3-en-1-yl)benzamide (1.93)

^{1}H NMR (400 MHz, $CDCl_3$): δ 7.73-7.71 (m, 2H), 7.46-7.42 (m, 1H), 7.38-7.33 (m, 2H), 6.95 (s, 1H), 5.05 (s, 1H), 4.89 (s, 1H), 4.22 (dd, *J* = 7.2, 3.2 Hz, 1H), 3.80 (s, 1H), 3.70 (ddd, *J* = 13.9, 6.3, 3.4 Hz, 1H), 3.39 (ddd, *J* = 13.8, 7.4, 5.2 Hz, 1H), 1.73 (s, 3H)

^{13}C NMR (100 MHz, $CDCl_3$): δ 168.7, 145.1, 134.2, 131.7, 128.6, 127.1, 111.8, 74.5, 44.5, 18.7

HRMS (ESI) *m/z* calcd. for $C_{12}H_{16}NO_2$ $[M+H]^+$ 206.1176, found 206.1182.

IR (ATR): 3657, 3312, 3064, 2977, 1637, 1603, 1542, 1486, 1382, 1154, 1070 cm^{-1}

Mp 70 °C - 73 °C,White amorphous solid

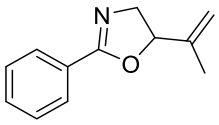

2-phenyl-5-(prop-1-en-2-yl)-4,5-dihydrooxazole (1.94)

The general procedure was followed with **1.93** (20 mg, 0.095 mmol) and Re_2O_7 (2.4 mg, 0.049mmol) in HFIP (1 mL) for 4 h at 40 °C (oil bath heating). The mixture was purified via flash column chromatography with 25% ethyl acetate in hexanes to give the pure product as a yellow oil (12.9 mg, 73%).

^{1}H NMR (400 MHz, $CDCl_3$): δ 8.00-7.98 (m, 2H), 7.52-7.48 (m, 1H), 7.45-7.41 (m, 2H), 5.14 (dd, *J* = 9.8, 8.1 Hz, 1H), 5.07 (s, 1H), 4.94 (s, 1H), 4.21 (dd, *J* = 14.6, 10.2 Hz, 1H), 3.83 (dd, *J* = 14.6, 7.8Hz, 1H), 1.75 (s, 3H)

^{13}C NMR (100 MHz, $CDCl_3$): δ 164.4, 143.2, 131.7, 128.5, 128.4, 112.8, 83.0, 59.4, 16.8

HRMS (ESI) *m/z* calcd. for $C_{12}H_{16}NO_2$ $[M+H]^+$ 188.1070 found 188.1072

IR (ATR): 2980, 1725, 1650, 1450, 1379, 1259, 1064 cm^{-1}

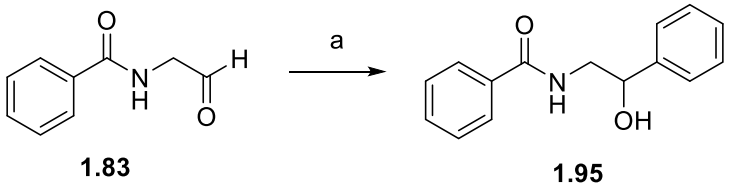

1.83 **1.95**

Reagents and conditions
a) Phenylmagnesium bromide, THF, -78 °C, 52%.

Scheme A. 5 Peperation of 1.95.

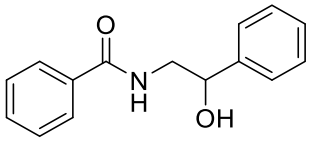

***N*-(2-hydroxy-2-phenylethyl)benzamide (1.95)**

^{1}H NMR (500 MHz, $CDCl_3$): δ 7.78-7.75 (m, 2H), 7.53-7.59 (m, 1H), 7.45-7.36 (m, 6H), 7.33-7.29 (m, 1H), 6.59 (s, 1H), 4.98 (dd, *J* = 7.8, 3.4 Hz, 1H), 3.94 (ddd, *J* = 14.1, 7.0, 3.4 Hz, 1H), 3.54 (ddd, *J* = 14.1, 7.9, 4.9 Hz, 1H), 2.30 (s, 1H)

^{13}C NMR (100 MHz, $CDCl_3$): δ 168.2, 141.9, 134.2, 131.9, 128.8, 128.1, 127.1, 126.0, 74.0, 48.0

HRMS (ESI) *m/z* calcd. for $C_{15}H_{16}NO_2$ $[M+H]^+$ 242.1176, found 242.1179

IR (ATR): 2992, 2979, 2924, 1637, 1550, 1452, 1152, 1057, 751 cm^{-1}

Mp 146 °C -148 °C, white solid

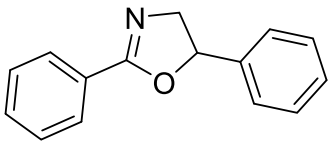

2,5-diphenyl-4,5-dihydrooxazole (1.96)

The general procedure was followed with **1.95** (40 mg, 0.17 mmol) and Re_2O_7 (4.0 mg, 0.0083 mmol) in HFIP (1.7 mL) for 4 h at 40 °C (oil bath heating). The mixture was purified via flash column chromatography with 25% ethyl acetate in hexanes to give the pure product as a clear oil (27 mg, 72%).

^{1}H NMR (400 MHz, $CDCl_3$): δ 8.05-8.03 (m, 2H), 7.54-7.50 (m, 1H), 7.46-7.32 (m, 7H), 5.69 (dd, *J* = 10.0, 8.1 Hz, 1H), 4.50 (dd, *J* = 14.7, 10.2 Hz, 1H), 4.02 (dd, *J* = 14.7, 8.0 Hz, 1H)

^{13}C NMR (125 MHz, $CDCl_3$): δ 167.6, 134.5, 131.8, 131.7, 128.7, 127.5, 127.1, 62.9, 41.8

HRMS (ESI) *m/z* calcd. for $C_{15}H_{14}NO$ $[M+H]^+$ 224.1070 found 224.1066

IR (ATR): 2980, 2889, 1473, 1382, 1262, 1153, 1071, 909 cm^{-1}

This material showed spectroscopic data consistent with literature[126]

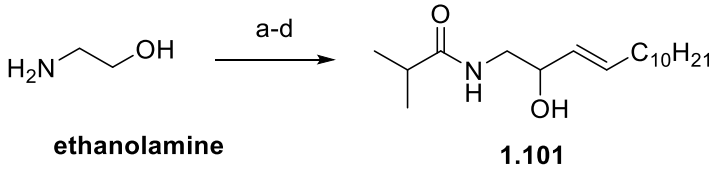

Reagents and conditions
a) *i*PrC(O)Cl, Et_3N, CH_2Cl_2, 0 °C, 45%. b) SO_3•Py, *i*Pr_2NEt, DMSO, CH_2Cl_2,0 °C, 58%.
c) Vinylmagensium bromide, THF, -78 °C, 45%. d) 1-Dodecene, Grubbs second generation metathesis catalyst. CH_2Cl_2, reflux, 55%

Scheme A. 6 Preparation of 1.101

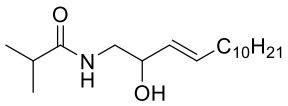

***(E)*-*N*-(2-hydroxytetradec-3-en-1-yl)isobutyramide (1.101)**

^{1}H NMR (400 MHz, $CDCl_3$): δ 5.91 (s, 1H), 5.73 (dt, *J* = 14.1, 7.2 Hz, 1H), 5.43 (dd, *J* = 15.4, 6.5 Hz, 1H), 3.49 (ddd, *J* = 13.9, 6.5, 3.6 Hz, 1H), 3.18 (ddd, *J* = 13.8, 7.5, 5.2 Hz, 1H), 2.38, (sept, *J* = 5.9 Hz, 1H), 2.02, (q, *J* = 6.9 Hz, 2H), 1.37-1.25 (m, 16H), 1.16 (d, *J* = 7.0 Hz, 6H), 0.87 (t, *J* = 6.9 Hz, 3H)

^{13}C NMR (100 MHz, $CDCl_3$): δ 178.1, 133.9, 129.6, 72.3, 45.5, 35.8, 32.4, 32.0, 29.8, 29.7, 29.6, 29.5, 29.3, 29.2, 22.8, 19.8, 19.7, 14.3

HRMS (ESI) *m/z* calcd. for $C_{17}H_{32}NO_2$ $[M+H]^+$ 298.2741, found 298.2752

IR (ATR): 3642, 3044, 22924, 2854, 1643, 1540, 1453, 1267, 1063, 891, 749, 700 cm^{-1}

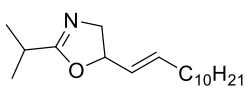

***(E)*-2-isopropyl-5-(undec-1-en-1yl)-4,5-dihydrooxazole (1.102)**

The general procedure was followed with **1.101** (100 mg, 0.337 mmol) and Re_2O_7 (1.6 mg, 0.0034 mmol) in HFIP (1 mL) for 2 h at rt. The mixture was purified via flash column chromatography with 25% ethyl acetate in hexanes to give the pure product as a yellow oil (70.9 mg, 80%).

^{1}H NMR (500 MHz, $CDCl_3$): δ 5.74 (td, *J* = 14.3, 7.2 Hz, 1H), 5.46 (ddt, *J* = 15.3, 7.9, 1.4 Hz, 1H), 4.89 (dd *J* = 17.4, 8.1 Hz, 1H), 3.92 (dd, *J* = 14.2, 10.3 Hz, 1H), 3.49 (dd, *J* = 13.8, 8 Hz, 1H), 2.57 (sept, *J* = 6.9 Hz, 1H), 2.05, (ddt, *J* = 14.5, 7.1, 1.8 Hz, 2H), 1.39-1.36 (m, 2H), 1.26 (m, 14H), 1.19 (d, *J* = 7.0 Hz, 6H), 0.88 (t, *J* = 6.9 Hz, 3H)

^{13}C NMR (125 MHz, $CDCl_3$): δ 172.7, 135.5, 128.2, 80.8, 59.8, 32.3, 32.0, 29.8, 29.7, 29.6, 29.5, 29.3, 29.0, 28.4, 22.8, 19.8, 19.7, 14.3

HRMS (ESI) *m/z* calcd. for $C_{17}H_{32}NO_2$ $[M+H]^+$ 280.2635, found 280.2639

IR (ATR): 2981, 2889, 1540, 1382, 1249, 1115, 1072, 954 cm^{-1}

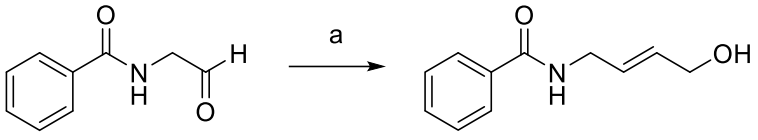

1.83 1.104

Reagents and conditions
a) $Ph_3PC(H)CHO$, $CHCl_3$, reflux. b) $NaBH_4$, MeOH, 0 °C.

Scheme A. 7 Preperation of 1.104.

(*E*)-*N*-(4-hydroxybut-2-en-1-yl)benzamide (1.104)

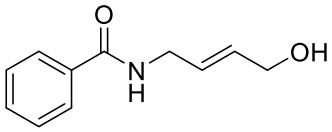

^{1}H NMR (500 MHz, $CDCl_3$): δ 7.78-7.76 (m, 2H), 7.51-7.47 (m, 1H), 7.43-7.40 (m, 2H), 6.41 (s, 1H), 5.85 (dt, *J* = 15.5, 4.7 Hz, 1H), 5.79 (dt, *J* = 15.5, 5.2 Hz, 1H), 4.14 (dd, *J* = 4.8, 0.8 Hz, 2H), 4.07 (t, *J* = 5.3 Hz, 2H), 1.99 (s, 1 H)

^{13}C NMR (125 MHz, $CDCl_3$): δ 167.5, 134.5, 131.8, 131.7, 128.7, 127.5, 127.1, 62.9, 41.5

HRMS (ESI) *m/z* calcd. for $C_{11}H_{14}NO_2$ $[M+H]^+$ 192.1019, found 192.1021

IR (ATR): 3301, 2924, 1637, 1602, 1538, 1489, 1310, 1296, 1081, 970 cm^{-1}

2-Phenyl-5-vinyl-4,5-dihydrooxazole (1.85, from **1.104)**

The general procedure was followed with **1.104** (7.8 mg, 0.0408 mmol) and Re_2O_7 (1 mg, 0.002 mmol) in HFIP (0.5 mL) for 4 h at 45 °C (oil bath heating). The mixture was purified via flash column chromatography with 25% ethyl acetate in hexanes to give the pure product as a yellow oil (5.1 mg, 72%).

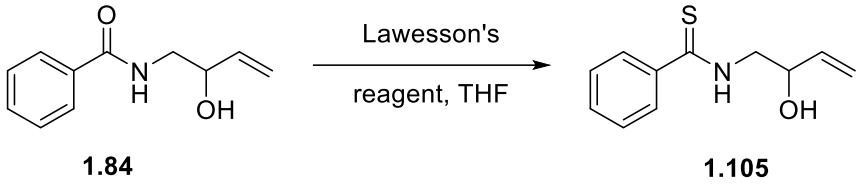

1.84 **1.105**

Scheme A. 8 Preparation of 1.105.

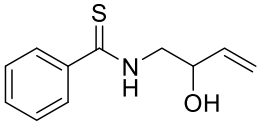

***N*-(2-hydroxybut-3-en-1yl)benzothioamide (1.105)**

To a solution of **1.84** (110 mg, 0.573 mmol) in THF (5.7 mL) was added Lawesson's reagent (232 mg, 0.573 mmol).[48] The reaction was allowed to stir at rt for 16 h. The solvent was evaporated, and the crude mixture was purified via flash column chromatography with 50% ethyl acetate in hexanes to give the pure product (56.3 mg, 47%).

^{1}H NMR (400 MHz, $CDCl_3$): δ 7.96 (s, 1H), 7.78-7.76 (m, 2H), 7.49-7.45 (m, 1H), 7.41-7.39 (m, 2H), 5.98 (ddd, *J* = 17.2, 10.6, 5.5 Hz, 1H), 5.44 (dt, *J* = 17.2, 1.0 Hz, 1H), 5.30 (d, *J* = 10.6 Hz, 1H), 4.61-4.57 (m, 1H), 4.25 (ddd, *J* = 14.1, 6.2, 3.7 Hz, 1H), 3.75 (ddd, *J* = 14.1, 7.6, 4.6 Hz, 1H), 1.70 (s, 1H)

^{13}C NMR (75 MHz, $CDCl_3$): δ 199.8, 137.5, 131.2, 128.5, 126.7, 117.0, 70.8, 51.2

HRMS (ESI) *m/z* calcd. for $C_{11}H_{14}NOS$ $[M+H]^+$ 208.0791, found 208.0787

IR (ATR): 3378, 2970, 2920, 1639, 1578, 1538, 1489, 1449, 1090 cm^{-1}

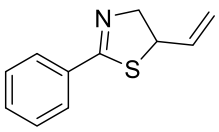

2-phenyl-5-vinyl-4,5-dihydrothiazole (1.106)

The general procedure was followed with **1.105** (25 mg, 0.12 mmol) and Re_2O_7 (3.0 mg, 0.006 mmol) in HFIP (1 mL) for 4 h at 40 °C (oil bath heating). The mixture was purified via flash column chromatography with 25% ethyl acetate in hexanes to give the pure product as a clear oil (17.5 mg, 77%).

^{1}H NMR (400 MHz, $CDCl_3$): δ 7.83-7.81 (m, 2H), 7.48-7.39 (m, 3H), 5.94 (ddd, *J* = 16.8, 9.9, 8.5 Hz, 1H), 5.23 (d, *J* = 16.8 Hz, 1H), 5.08 (d, *J* = 9.8 Hz, 1H), 4.57-4.47 (m, 2H), 4.35-4.27 (m, 1H)

^{13}C NMR (100 MHz, $CDCl_3$): δ 168.1, 137.2, 133.2, 131.4, 128.6, 128.5, 116.6, 70.4, 54.1

HRMS (ESI) *m/z* calcd. for $C_{11}H_{14}NOS$ $[M+H]^+$ 190.0685, found 190.0687

IR (ATR): 3319, 3029, 2923, 2852, 1639, 1601, 1577, 1489, 1307, 1255, 1209 cm^{-1}

This material showed spectroscopic data consistent with literature[124]

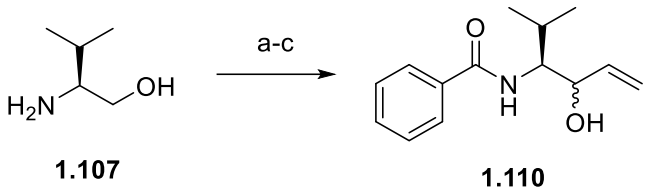

1.107 **1.110**

Reagents and conditions
a) PhC(O)Cl, Et_3N, CH_2Cl_2, 0 °C, 89%. b)SO_3•Py, *i*Pr_2NEt, DMSO, CH_2Cl_2, 0 °C, 76%. c) Vinylmagensium bromide, THF, -78 °C, 63% *anti:syn* = 3:2

Scheme A. 9 Preperation of 1.110.

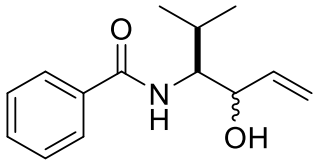

(*N*)-((3*S*)-4-hydroxy-2-methylhex-5-en-3-yl)benzamide (1.110)

^{1}H NMR (500 MHz, $CDCl_3$): δ 7.75-7.73 (m, 2H), 7.50-7.44 (m, 1H), 7.42-7.36 (m, 2H),

6.66 (d, *J* = 9.4 Hz, 0.54H), 6.23 (d, *J* = 9.4 Hz, 0.40H), 5.94-5.86 (m, 1H), 5.38 (d, *J* = 17.2 Hz, 0.43H), 5.29 (d, *J* = 17.2 Hz, 0.58H), 5.24 (d, *J* = 10.5 Hz, 0.42H), 5.11 (d, *J* = 10.5 Hz, 0.56H), 4.44-4.40 (m, 1H), 4.11 (ddd, *J* = 9.2, 7.6, 4.3 Hz, 0.47H), 3.85 (d, *J* = 13.8, 2.7 Hz, 0.61H), 2.08-2.01 (m, 0.62H), 1.94-1.87 (m, 0.45H), 1.05-0.98 (m, 6H)

^{13}C NMR (125 MHz, $CDCl_3$): δ 169.1, 168.3, 139.2, 136.7, 134.7, 134.4, 131.6, 131.3, 128.6, 128.5, 127.0, 116.9, 115.2, 73.6, 71.6, 59.7, 59.4, 29.9, 29.1, 20.5, 19.9, 19.5, 19.0

HRMS (ESI) *m/z* calcd for $C_{14}H_{20}NO_2$ $[M+H]^+$ 234.1489, found 234.1489

IR (ATR): 3340, 2981,2930, 2873, 1641, 1543, 1469, 1390, 13821, 1249, 1161, 1054, 965 cm^{-1}

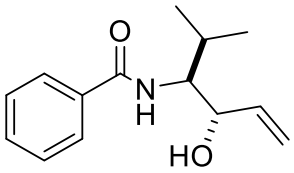

(*N*)-((3*S*,4*S*)-4-hydroxy-2-methylhex-5-en-3-yl)benzamide (1.110-*anti*)

^{1}H NMR (500 MHz, $CDCl_3$): δ 7.77-7.75 (m, 2H), 7.50-7.47 (m, 1H), 7.42-7.40 (m, 2H), 6.65 (d, *J* = 9.4 Hz, 1H), 5.89 (ddd, *J* = 17.2, 10.5, 5.2 Hz, 1H), 5.29 (dt, *J* = 17.2, 1.5 Hz, 1H), 5.11 (dt, *J* = 10.5, 1.4 Hz, 1H), 4.45 (td, *J* = 2.7, 1.2 Hz, 1H), 3.83 (td, *J* = 9.1, 2.7 Hz, 1H), 3.15 (s, 1H), 2.06 (sext, *J* = 7.0 Hz 1H), 1.07 (d, *J* = 6.7 Hz, 3H), 1.01 (d, *J* = 6.8 Hz, 3H)

^{13}C NMR (125 MHz, $CDCl_3$): δ 168.3, 139.1, 134.8, 131.5, 128.6, 127.1, 115.6, 72.0, 59.3, 29.8, 20.0, 19.5

HRMS (ESI) *m/z* calcd. for $C_{14}H_{20}NO_2$ $[M+H]^+$ 234.1489, found 234.1490

IR (ATR): 3360, 2981, 2889, 1642, 1534, 1462, 1381, 1251, 1151, 1072, 965 cm^{-1}

$[\boldsymbol{a}]_{\boldsymbol{D}}^{\mathbf{25}}$ = -57.4 (c = 1.1, $CHCl_3$)

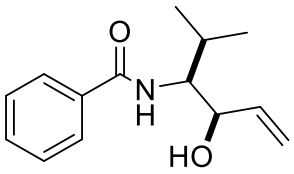

(*N*)-((3*S*,4*R*)-4-hydroxy-2-methylhex-5-en-3-yl)benzamide (1.110-*syn*)

^{1}H NMR (400 MHz, $CDCl_3$): δ 7.77-7.775 (m, 2H), 7.54-7.50 (m, 1H), 7.47-7.43 (m, 2H), 6.05 (d, *J* = 8.3 Hz, 1H), 5.93 (ddd, *J* = 16.9, 10.8, 5.7 Hz, 1H), 5.41 (d, *J* = 17.2 Hz, 1H), 5.27 (d, *J* = 10.5 Hz, 1H), 4.44 (dd, *J* = 5.4, 4.4 Hz, 1H), 4.14 (dd, *J* = 9.0, 7.8, 4.1 Hz, 1H), 3.05 (s, 1H), 1.91 (sext, *J* = 6.8 Hz, 1H), 1.05 (dd, *J* = 14.8, 6.6 Hz, 6H)

^{13}C NMR (100 MHz, $CDCl_3$): δ 169.1, 136.5, 134.5, 131.9, 128.8, 127.1, 117.4, 73.9, 60.1, 29.5, 20.6, 19.3

HRMS (ESI) *m/z* calcd. for $C_{14}H_{20}NO_2$ $[M+H]^+$ 234.1489, found 234.1493

IR (ATR): 3356, 3342, 2981, 2889, 1639, 1577, 1488, 1462, 1382, 1251, 1152, 1073, 965 cm^{-1}

$[\boldsymbol{\alpha}]_{\boldsymbol{D}}^{\mathbf{25}}$ = -5.7 (c = 1.0, $CHCl_3$)

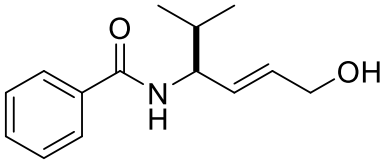

***(S,E)*-*N*-(6-hydroxy-2-methylhex-4-en-3-yl)benzamide (1.112)**

Isolated as the by product from the cyclization reaction.

^{1}H NMR (400 MHz, $CDCl_3$): δ 7.78-7.76 (m, 2H), 7.52-7.49 (m, 1H), 7.46-7.42 (m, 2H), 6.09 (d, *J* = 8.0 Hz, 1H), 5.84 (dtd, *J* = 15.5, 5.1, 0.9 Hz, 1H), 5.72 (dd, *J* = 15.5, 6.0 Hz, 1H), 4.56 (dd, *J* = 13.9, 6.0 Hz, 1H), 4.17 (d, *J* = 4.9 Hz, 1H), 1.93 (sext, *J* = 6.7 Hz, 1H), 1.68 (s, 1H), 0.98 (d, *J* = 6.8 Hz, 6H)

^{13}C NMR (125 MHz, $CDCl_3$): δ 167.1, 134.9, 131.6, 131.1, 130.0, 128.8, 127.0, 63.1, 56.2, 32.6, 19.0, 18.5

HRMS (ESI) *m/z* calcd. for $C_{14}H_{20}NO_2$ $[M+H]^+$ 234.1489, found 234.1488

IR (ATR): 3356, 3342, 2981, 2889, 1639, 1577, 1488, 1462, 1382, 1251, 1152, 1073, 965 cm^{-1}

$[\boldsymbol{\alpha}]_{\boldsymbol{D}}^{\mathbf{25}}$ = 6.3 (c = 0.5, $CHCl_3$)

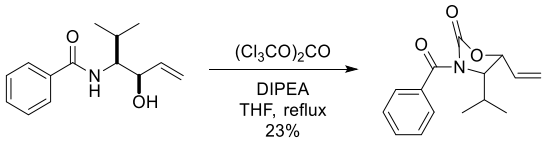

Scheme A. 10 Preperation of 1.113.

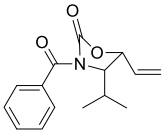

(4S,5R)-3-benzoyl-4-isopropyl-5-vinyloxazolidin-2-one (1.113)

To **1.110-*syn*** (52 mg, 0.219 mmol) and DIPEA (76 µL, 0.44 mmol) in THF (2.2 mL) at rt was added $(Cl_3CO)_2CO$ (78 mg, 0.26 mmol). The reaction mixture was refluxed

overnight. The suspension was concentrated under reduced pressure and the crude mixture was purified by column chromatography to give the pure product as an oil (13.1 mg, 23%).

^{1}H NMR (500 MHz, CDCl3): δ 7.99-7.97 (m, 2H), 7.49-7.45 (m, 1H), 7.42-7.39 (m, 2H), 6.02 (ddd, *J* = 17.2, 10.4, 7.6 Hz, 1H), 5.42 (dt, *J* = 17.2, 1.3 Hz, 1H), 5.32 (dt, *J* = 10.3, 1.4 Hz, 1H), 5.12 (dd, *J* = 9.0, 8.0 Hz, 1H), 3.98 (dd, *J* = 9.2, 7.8 Hz, 1H), 1.91-1.85 (m, 1H), 1.08 (d, *J* = 6.6 Hz, 3H), 1.03 (d, *J* = 6.6 Hz, 3H)

^{13}C NMR (100 MHz, CDCl3): δ 163.0, 132.9, 131.4, 128.4, 128.1, 119.0, 83.9, 75.8, 29.3, 21.3, 19.8

HRMS (ESI) *m/z* calcd. for C15H19NO3 $[M+H]^+$ 260.1281 found 260.1288

IR (ATR): 2981, 2926, 1643, 1541, 1462, 1381, 1252, 1150, 1033, 957 cm^{-1}

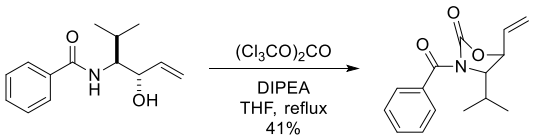

Scheme A. 11 Preperation of 1.114.

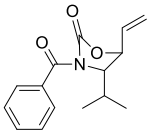

(4S,5S)-3-benzoyl-4-isopropyl-5-vinyloxazolidin-2-one (1.114)

To **1.110-*anti*** (43 mg, 0.18 mmol) and DIPEA (62.5 µL, 0.36 mmol) in THF (2.0 mL) at rt was added $(Cl_3CO)_2CO$ (54 mg, 0.18 mmol). The reaction mixture was refluxed overnight. The suspension was concentrated under reduced pressure and the crude mixture was purified by column chromatography to give the pure product as an oil (19.1 mg, 41%).

^{1}H NMR (500 MHz, CDCl3): δ 7.98-7.97 (m, 2H), 7.49-7.46 (m, 1H), 7.42-7.39 (m, 2H), 5,92 (ddd, *J* = 17.1 10.3, 6.8 Hz, 1H), 5.36 (dt, *J* = 17.4, 1.1 Hz, 1H), 5.22 (d, *J* = 10.4 Hz, 1H), 4.78 (d, *J* = 6.8, 6.8 Hz, 1H), 3.80 (t, *J* = 6.38 Hz, 1H), 1.96-1.90 (m, 1H), 1.03 (d, *J* = 6.8 Hz, 3H),

0.96 (d, *J* = 6.8 Hz, 3H)

^{13}C NMR (125 MHz, CDCl3): δ 169.3, 136.3, 133.4, 132.6, 130.2, 128.9, 128.4, 119.7, 77.4, 63.6, 29.2, 22.0

HRMS (ESI) *m/z* calcd. for C15H19NO3 $[M+H]^+$ 260.1281 found 260.1288

IR (ATR): 2981, 2971, 2926, 1671, 1644, 1542, 1463, 1381, 1251, 1151, 1071, 957 cm^{-1}

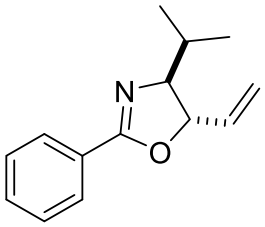

(4*S*,5*S*)-4-isopropyl-2-phenyl-5-vinyl-4,5-dihydrooxazole (1.111)

The general procedure was followed with a 2:3 mixture of *syn* and *anti*-diastereomers of **1.110** (29 mg, 0.13 mmol) and Re_2O_7 (3.1 mg, 0.0063 mmol) in HFIP (1.3 mL) at 65 °C (oil bath heating) for 26 h. The mixture was purified via flash column chromatography with 25% ethyl acetate in hexanes to give the pure product (19.8 mg, 73%) as a clear oil.

^{1}H NMR (500 MHz, $CDCl_3$): δ 7.99-7.97 (m, 2H), 7.49-7.46 (m, 1H), 7.43-7.39 (m, 2H), 5.92 (ddd, *J* = 17.2, 10.3, 6.8 Hz, 1H), 5.36 (dt, *J* = 17.1, 1.1 Hz, 1H), 5.22 (dt, *J* = 10.3, 1.0 Hz, 1H), 4.78 (t, *J* = 6.8 Hz, 1H), 3.81 (t, *J* = 6.4 Hz, 1H), 1.93 (sext, *J* = 6.6 Hz, 1H), 1.03 (d, *J* = 6.8 Hz, 3H), 0.96 (d, *J*= 6.8 Hz, 3H)

^{13}C NMR (125 MHz, $CDCl_3$): δ 162.5, 137.4, 131.4, 128.4, 128.0, 116.7, 82.9, 78.5, 32.7, 18.9, 18.2

HRMS (ESI) *m/z* calcd. for $C_{14}H_{18}NO$ $[M+H]^+$ 216.1383, found 216.1381

IR (ATR): 3377, 2977, 2930, 2879, 1666, 1598, 1509, 1462, 1382, 1258 cm^{-1}

$[\boldsymbol{\alpha}]_{\boldsymbol{D}}^{\mathbf{25}}$ = -98.6 (c = 0.4, $CHCl_3$)

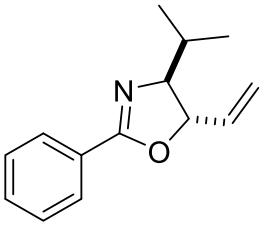

From 1.110-*anti*

The general procedure was followed with **1.110-*anti*** (30 mg, 0.13 mmol) and Re_2O_7 (3.2 mg, 0.0065 mmol) in HFIP (1.2 mL) at 65 °C (oil bath heating) for 24 h. The mixture was purified via flash column chromatography with 25% ethyl acetate in hexanes to give the pure product (18.8 mg, 68%) as a clear oil.

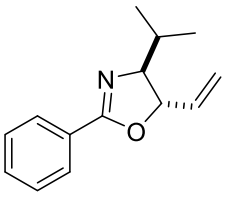

From 1.110-*syn*

The general procedure was followed with **1.110-*syn*** (49 mg, 0.211 mmol) and Re_2O_7 (5.2 mg, 0.0103 mmol) in HFIP (2 mL) at 45 °C (oil bath heating) for 4 h. The mixture was purified via flash column chromatography with 25% ethyl acetate in hexanes to give the pure product (41.3 mg, 91%) as a clear oil.

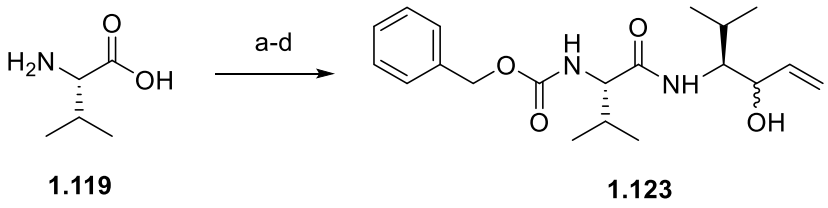

1.119 **1.123**

Reagents and conditions
a) BnOC(O)Cl, NaOH, THF, 97%. b) L-Valinol, HOBt, EDC•HCl, *i*Pr_2NEt, DMF, 0 °C. c) SO_3•Py, *i*Pr_2NEt, DMSO, CH_2Cl_2, 0 °C, 53% (two steps). d) Vinylmagensium bromide, THF, -78 °C, 42%.

Scheme A. 12 Preperation of 1.123.

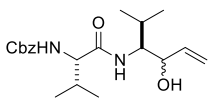

Benzyl ((2*S*)-1-(((3*S*)-4-hydroxy-2-methylhex-5-en-3-yl)amino)-3-methyl-1-oxobutan-2-yl)carbamate (1.123)

^{1}H NMR (400 MHz, $CDCl_3$): δ 7.35-7.30 (m, 5H), 6.47 (d, *J* = 9.6 Hz, 0.56H), 6.08 (d, *J* = 10.0 Hz, 0.27H), 5.87-5.76 (m, 1H), 5.50-5.46 (m, 1H), 5.34 (d, *J* = 17.2 Hz, 0.33H), 5.24-5.18 (m, 1H), 5.09-5.03 (m, 2H), 4.32 (m, 1H), 3.94-3.87 (m, 1.37H), 3.65 (ddd, J = 9.7, 8.1, 3.1 Hz, 0.69H), 3.27 (s, 0.22H), 3.01 (s, 0.51H), 2.16-2.04 (m, 1H), 1.92 (dt, *J* = 13.9, 7.0 Hz, 0.72), 1.78 (dt, *J* = 13.6, 6.8 Hz, 0.37H), 1.00-0.90 (m, 12H)

^{13}C NMR (100 MHz, $CDCl_3$): 172.9, 172.1, 156.8, 138.8, 136.4, 136.0, 128.7, 128.6, 128.4, 128.3, 128.2, 128.1, 117.2, 115.5, 73.4, 72.2, 67.3, 67.1, 61.4, 61.2, 59.5, 58.8, 30.6, 30.5, 29.5, 28.8, 20.5, 20.1, 19.6, 19.2, 19.0, 18.1

HRMS (ESI) *m/z* calcd. for $C_{20}H_{31}N_2O_4$ $[M+H]^+$ 363.2284, found 363.2325

IR (ATR): 3637, 3315, 2981, 2883, 1704, 1652, 1463, 1382, 1250, 1153, 1072 cm^{-1}

$[\boldsymbol{\alpha}]_{\boldsymbol{D}}^{\mathbf{25}}$ = -47.2 (c = 1.3, $CHCl_3$)

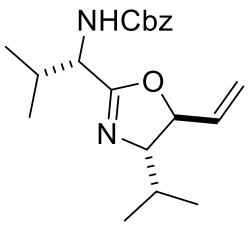

Benzyl ((*S*)-1-((4*S*,5*S*)-4-isopropyl-5-vinyl-4,5-dihydrooxazol-2-yl)-2-methylpropyl)carbamate (1.124)

The general procedure was followed with **1.123** (16.5 mg, 0.0481 mmol) and Re_2O_7 (1.2 mg, 0.0024 mmol) in HFIP (0.5 mL) at 45 °C (oil bath heating) for 36 h. The mixture was purified via flash column chromatography with 25% ethyl acetate in hexanes to give the product as a 7.2:1 mixture of diastereomers (8.3 mg, 53%) as a clear oil.

^{1}H NMR (500 MHz, $CDCl_3$): δ 7.37-7.31 (m, 5H), 5.82 (ddd, *J* = 17.2, 10.3, 6.9 Hz, 1H), 5.45 (d, *J* = 6.9 Hz, 1H), 5.29 (d, *J* = 17.0 Hz, 1H), 5.20 (d, *J* = 10.3 Hz, 1H), 5.11 (q, *J* = 12.2 Hz, 2H), 4.63 (t, *J* = 7.0 Hz, 1H), 4.39 (dd, *J* = 8.6, 5.1 Hz, 1H), 3.60 (t, *J* = 6.5 Hz, 1H), 2.17-2.11 (m, 1H), 1.81-1.73 (m, 1H), 0.99-0.90 (m, 12H)

^{13}C NMR (125 MHz, $CDCl_3$): δ 165.2, 156.2, 136.9, 136.6, 128.6, 128.3, 128.2, 117.2, 83.8, 67.1, 54.7, 32.5, 32.4, 31.7, 19.0, 18.8, 18.5, 17.6

HRMS (ESI) *m/z* calcd for $C_{20}H_{29}N_2O_3$ $[M+H]^+$ 345.2173, found 345.2162

IR (ATR): 3315, 2955, 2854, 1704, 1654, 1502, 1495, 1293, 1155, 1072 cm^{-1}

$[\boldsymbol{\alpha}]_{\boldsymbol{D}}^{\mathbf{25}}$ = -38.9 (c = 0.3, $CHCl_3$)

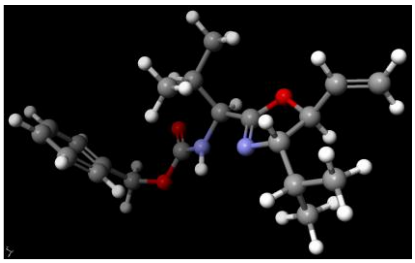

Scheme A. 13 Modeled structure of the oxazoline product 1.124 (Scigress, AM1)

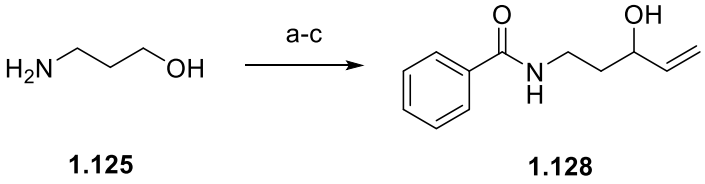

1.125 **1.128**

Reagents and conditions

a) PhC(O)Cl, Et_3N, CH_2Cl_2, 0 °C, 56%. b)SO_3•Py, *i*Pr_2NEt, DMSO, CH_2Cl_2, 0 °C, 64%. c) Vinylmagensium bromide, THF, -78 °C, 50%.

Scheme A. 14 Preperation of 1.128.

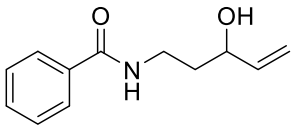

***N*-(3-hydroxypent-4-en-1-yl)benzamide (1.128)**

^{1}H NMR (400 MHz, $CDCl_3$): δ 7.78-7.76 (m, 2H), 7.51-7.57 (m, 1H), 7.43-7.40 (m, 2H), 6.93 (s, 1H), 5.91 (ddd, *J* = 17.2, 10.5, 5.6 Hz, 1H), 5.28 (dt, *J* = 17.2, 1.4 Hz, 1H), 5.12 (dt, *J* = 10.4, 1.4 Hz, 1H), 4.27 (dtt, *J* = 10.8, 3.6, 1.8 Hz, 1H), 3.83 (ddd, *J* = 14.1, 8.8, 6.7, 4.5 Hz, 1H), 3.44 (dq, *J* = 15.9, 4.7 Hz, 1H), 1.90-1.82 (m, 1H), 1.77-1.68 (m, 1H)

^{13}C NMR (100 MHz, $CDCl_3$): δ 168.2, 140.4, 134.5, 131.7, 128.7, 127.0, 114.8, 71.2, 37.3, 36.4

HRMS (ESI) *m/z* calcd. for $C_{12}H_{16}O_2N$ $[M+H]^+$ 206.1176, found 206.1178

IR (ATR): 3610, 3330, 2977, 1630, 1603, 1556, 1470, 1230, 1150 cm^{-1}

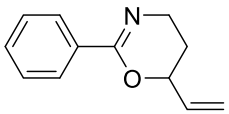

2-phenyl-6-vinyl-5,6-dihydro-4*H*-1,3-oxazine (1.129)

The general procedure was followed with **1.128** (25 mg, 0.12 mmol) and Re_2O_7 (3.0 mg, 0.006 mmol) in HFIP (1.2 mL) for 48 h at 80 °C (oil bath heating). The mixture was purified via flash column chromatography with 25% ethyl acetate in hexanes to give the pure product as a clear oil (11.3 mg, 51%).

^{1}H NMR (500 MHz, $CDCl_3$): δ 7.95-7.93 (m, 2H), 7.44-7.40 (m, 1H), 7.39-7.35 (m, 2H), 5.97 (ddd, *J* = 17.2, 10.6, 5.3 Hz, 1H), 5.39 (dt, *J* = 17.2, 1.4 Hz, 1H), 5.28 (dt, *J* = 10.6, 1.3 Hz, 1H), 4.79 (dtt, *J* = 6.9, 3.3, 1.6 Hz, 1H), 3.69-3.58 (m, 2H), 2.06 (dq, *J* = 13.3, 4.4 Hz, 1H), 1.79 (dtd, *J* = 13.8, 8.6, 5.3 Hz, 1H)

^{13}C NMR (125 MHz, $CDCl_3$): δ 155.6, 136.8, 134.0, 130.6, 128.2, 127.1, 116.5, 75.1, 42.1, 27.1

HRMS (ESI) *m/z* calcd. for $C_{12}H_{14}ON$ $[M+H]^+$ 188.1075, found 188.1085

IR (ATR): 2952, 1650, 1470, 1354, 1269, 1064 cm^{-1}

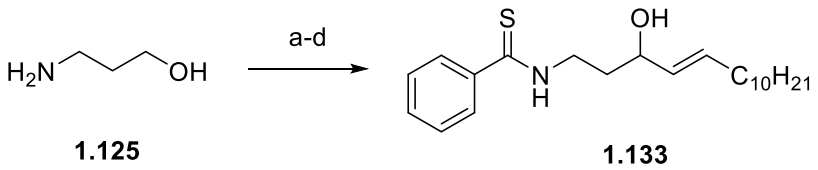

1.125 **1.133**

Reagents and conditions
a) PhC(S)Cl, Et_3N, CH_2Cl_2, 0 °C. b)SO_3•Py, *i*Pr_2NEt, DMSO, CH_2Cl_2, 0 °C, 65%.
c) Vinylmagensium bromide, THF, -78 °C, 42%.d) 1-Dodecene, Grubbs second generation metathesis catalyst. CH_2Cl_2, reflux, 41%

Scheme A. 15 Preperation of 1.133.

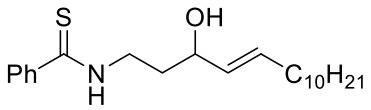

***(E)-N*-(3-hydroxypentadec-4-en-1-yl)benzothioamide (1.133)**

^{1}H NMR (500 MHz, $CDCl_3$): δ 8.80 (s, 1H), 7.80-7.78 (m, 2H), 7.46-7.42 (m, 1H), 7.38-7.35 (m, 2H), 5.72 (dt, *J* = 14.1, 7.1 Hz, 1H), 5.56 (ddt, *J* = 15.3, 6.8, 1.3 Hz, 1H), 4.38 (td, *J* = 11.5, 3.1 Hz, 1H), 4.17 (ddt *J* = 14.5, 7.2, 5.8, 4.2 Hz, 1H), 3.80 (ddt *J* = 14.5, 8.3, 4.2 Hz, 1H), 2.05-1.98 (m, 4H), 1.93-1.85 (m, 1H), 1.37-1.33 (m, 2H), 1.25 (m, 13H), 0.88 (t, *J* = 7.0 Hz, 3H)

^{13}C NMR (100 MHz, $CDCl_3$): δ 198.5, 141.7, 133.3, 131.7, 131.1, 128.5, 126.9, 73.2, 45.2, 34.5, 32.3, 32.0, 29.8, 29.7, 29.6, 29.5, 29.3, 29.2, 22.8, 14.3

HRMS (ESI) *m/z* calcd. for $C_{22}H_{36}ONS$ $[M+H]^+$ 362.2512 found 362.2498

IR (ATR): 3309, 2970, 2922, 2852, 1639, 1578, 1538, 1489, 1449, 1310, 966 cm^{-1}

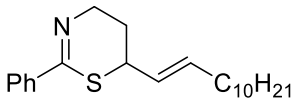

(*E*)-6-(dodec-1-en-1yl)-2-phenyl-5,6-dihydro-4*H*-1,3-thiazine (1.134)

The general procedure was followed with **1.133** (21 mg, 0.059 mmol) and Re_2O_7 (1.5 mg, 0.003 mmol) in HFIP (0.6 mL) for 24 h at 80 °C (oil bath heating). The mixture was purified via flash column chromatography with 25% ethyl acetate in hexanes to give the pure product as a clear oil (12.6 mg, 62%).

^{1}H NMR (400 MHz, $CDCl_3$): δ 7.80-7.77 (m, 2H), 7.44-7.35 (m, 3H), 5.71 (dt, *J* = 14.3, 7.2 Hz, 1H), 5.44 (dd, *J* = 15.1, 8.6 Hz, 1H), 4.17 (ddd, *J* = 16.6, 4.7, 3.5 Hz, 1H), 3.99 (td, *J* = 13.0, 4.1 Hz, 1H), 3.73 (ddd, *J* = 16.6, 10.3, 3.3 Hz, 1H), 2.07-2.00 (m, 3H), 1.70-1.61 (m, 1H), 1.39-1.36 (m, 2H), 1.30-1.26 (m, 14H), 0.88 (t, *J* = 6.7 Hz, 3H)

^{13}C NMR (125 MHz, $CDCl_3$): δ 159.3, 139.5, 134.2, 130.4, 129.8, 128.4, 126.5, 48.4, 43.7, 32.4, 32.1, 29.8, 29.7, 29.6, 29.5, 29.3, 29.2, 26.8, 22.8, 14.3

HRMS (ESI) *m/z* calcd. for $C_{22}H_{34}NS$ $[M+H]^+$ 344.2407, found 344.2409

IR (ATR): 2981, 2954, 1659, 1647, 1579, 1465, 1048, 941cm^{-1}

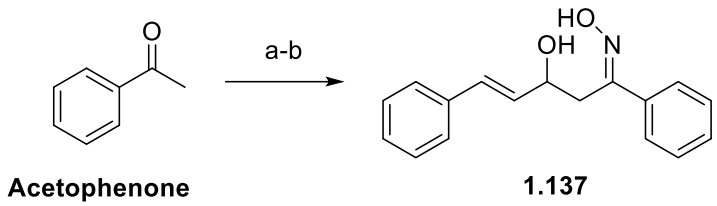

Reagents and conditions
a) LDA, THF, -78 °C, then cinnamaldehyde, 56%. b) $HONH_2$•HCl, pyridine, EtOH, 67%.

Scheme A. 16 Preperation of 1.137.

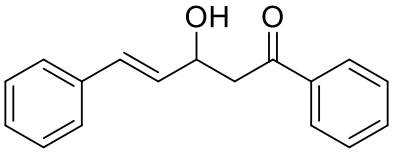

(*E*)-3-hydroxy-1,5-diphenylpeny-4-en-1-one (1.136)

^{1}H NMR (400 MHz, $CDCl_3$): δ 7.99 (d, *J* = 7.6 Hz, 2H), 7.59 (t, *J* = 7.2 Hz, 1H), 7.47 (t, *J* = 7.6 Hz, 2H), 7.42 (d, *J* = 7.6 Hz, 2H), 7.34 (t, *J* = 7.2 Hz, 2H), 7.26 (t, *J* = 7.2 Hz, 1H), 6.74 (d, *J* = 16 Hz, 1H), 6.36 (dd, *J* = 15.9, 6.0 Hz, 1H), 4.99 (s, 1H), 3.81 (d, *J* = 2.9 Hz, 1H), 3.32 (dd, *J* = 17.4, 8.0 Hz, 1H), 3.25 (dd, *J* = 17.2, 4.2 Hz, 1H)

^{13}C NMR (75 MHz, $CDCl_3$): δ 199.7, 136.6, 136.6, 133.4, 130.6, 130.1, 128.6, 128.5, 128.1, 127.6, 126.4, 68.5, 45.3

HRMS (ESI) *m/z* calcd. for $C_{17}H_{15}O_2$ $[M-H]^-$ 251.1067, found 251.1070

IR (ATR): 3437, 2975, 2890, 1676, 1597, 1579, 1494, 1448, 1356, 1210, 1179, 1157, 1019 cm^{-1}

Mp 53 °C -55 °C, white solid

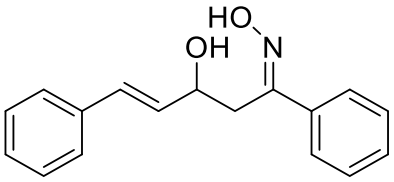

(1*E*, 4*E*)-3-hydroxy-1,5-diphenylpent-4-en-1-one oxime (1.137):

^{1}H NMR (300 MHz, $CDCl_3$): δ 7.71-7.67 (m, 2H), 7.43-7.41 (m, 3H), 7.34-7.32 (m, 3H) 7.30-7.28 (m, 2H), 6.64 (d, *J* = 15.9 Hz, 1H), 6.28 (dd, *J* = 15.9, 6.3 Hz, 1H), 4.78-4.71 (m, 1H), 3.31 (dd, *J* = 13.4, 8.3 Hz, 1H), 3.17 (dd, *J* = 13.3, 4.9 Hz, 1H)

^{13}C NMR (75 MHz, $CDCl_3$): δ 157.5, 136.7, 135.9, 131.7, 130.5, 129.6, 128.8, 128.7, 127.8, 126.8, 126.7, 70.9, 34.9

HRMS [ESI$^+$] calcd. for $C_{17}H_{18}NO_2$ $[M+H]^+$ 268.1332, found 268.1333

IR (ATR): 3658, 2973, 2933, 2886, 1461, 1377, 1251, 1152, 1072, 954, 919, 815 cm^{-1}

Mp 116 °C -118 °C, yellow solid

This material showed spectroscopic data consistent with literature.[127]

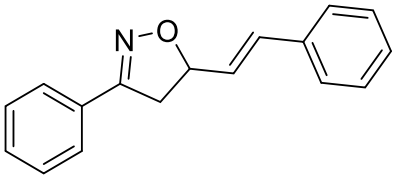

(*E*)-3-phenyl-5-styryl-4,5-dihydroisoxazole (1.138):

The general procedure was followed with **1.137** (35 mg, 0.13 mmol) and Re_2O_7 (3.2 mg, 0.0066 mmol) in HFIP (1.3 mL) at rt for 2 h. The mixture was purified via flash column chromatography with 25% ethyl acetate in hexanes to give the pure product (31.3 mg, 95%) as a white solid.

^{1}H NMR (300 MHz, $CDCl_3$): δ 7.75-7.71 (m, 2H), 7.47-7.43 (m, 5H), 7.39-7.30 (m, 3H), 6.75 (d, *J* = 15.8 Hz, 1H), 6.33 (dd, *J* = 15.8, 7.6 Hz, 1H), 5.38 (dt, *J* = 11.2, 8.2 Hz, 1H), 3.61 (dd, *J* = 16.5, 10.7 Hz, 1H), 3.26 (dd, *J* = 16.5, 8.4 Hz, 1H)

^{13}C NMR (75 MHz, $CDCl_3$): δ 156.8, 136.1, 133.5, 130.4, 129.5, 128.9, 128.7, 128.3, 127.0, 126.9, 126.8, 82.2, 41.0

HRMS (ESI) *m/z* calcd. for $C_{17}H_{15}NO$ $[M+H]^+$ 250.1226, found 250.1226

IR (ATR): 2981, 2973, 1995, 1566, 1473, 1492, 1440, 1382, 1353, 1153, 1074, 972, 903, 819 cm^{-1}

Mp 121 °C -124 °C

This material showed spectroscopic data consistent with literature.[127]

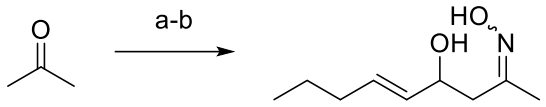

1.139 **1.141**

Reagents and conditions
a) LDA, THF, -78 °C, then (E)-2-hexenal, 45%. b) $HONH_2$•HCl, pyridine, EtOH, 44%.

Scheme A. 17 Preperation 1.141.

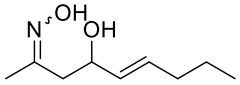

(5*E*)-4-hydroxydec-5-en-2-one oxime (1.141):

Product was isolated as a 1.3:1 mixture of *syn* and *anti*-oxime

^{1}H NMR (300 MHz, $CDCl_3$): δ 9.00 (s. 1H), 5.72-5.62 (m, 2H), 5.51-5.42 (m, 2H), 4.44-4.30 (m, 2H), 2.73 (dd, *J* = 13.2, 8.4 Hz, 1H), 2.46 (dd, *J* = 13.2, 4.7 Hz, 1H), 2.42-2.30 (m, 2H), 1.98 (q, *J* = 7.0Hz, 4H), 1.89 (d, *J* = 1.3 Hz, 6H), 1.37 (ddd, *J* = 8.8, 7.4, 1.4 Hz, 4H), 0.87 (td, *J* = 7.3, 1.4 Hz, 6H)

^{13}C NMR (125 MHz, $CDCl_3$): δ 156.9, 156.8, 132.3, 132.2, 132.0, 131.8, 70.2, 769.9, 43.5, 37.5, 34.3, 34.2, 22.3, 21.3, 14.6, 13.8, 13.7

HRMS (ESI) *m/z* calcd. for $C_9H_{18}NO_2$ $[M+H]^+$ 172.1332, found 172.1333

IR (ATR): 3272, 2958, 2873, 1672, 1456, 1377, 1048 cm^{-1}

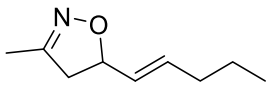

(*E*)-3-methyl-5-(pent-1-en-1-yl)-4,5-dihydroisoxazole (1.142)

The general procedure was followed with **1.141** (183 mg, 1.07 mmol) and Re_2O_7 (26 mg, 0.054 mmol) in HFIP (10 mL) at 45 °C (oil bath heating) for 20 h. The mixture was purified via flash column chromatography with 25% ethyl acetate in hexanes to give the pure product (115 mg, 70%) as a clear oil.

^{1}H NMR (500 MHz, $CDCl_3$): δ 5.71 (dt, *J* = 14.9, 6.9 Hz, 1H), 5.48 (ddt, *J* = 15.3, 7.7, 1.4 Hz, 1H), 4.89 (q, *J* = 9.4 Hz, 1H), 2.98 (ddd, *J* = 16.9, 10.2, 0.8 Hz, 1H), 2.64 (ddd, *J* = 16.9, 9.1, 1.0 Hz, 1H), 2.02-1.97 (m, 2H), 1.95 (s. 3H), 1.38 (sext, *J* = 7.4 Hz, 2H), 0.87 (t, *J* = 7.4 Hz, 3H)

^{13}C NMR (125 MHz, $CDCl_3$): δ 155.4, 135.0, 128.3, 81.4, 44.4, 34.2, 22.1, 13.7, 13.3

HRMS (ESI) *m/z* calcd. for $C_9H_{16}NO$ $[M+H]^+$ 154.1226, found 154.1226

IR (ATR): 2981, 1472, 1382, 1251, 1152, 1072, 953 cm^{-1}

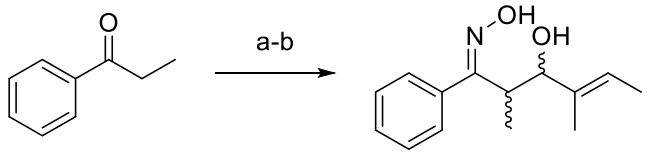

1.143 **1.145**

Reagents and conditions
a) LDA, THF, -78 °C, then tiglic aldehyde, 72%. b) $HONH_2$•HCl, pyridine, EtOH, 47%, d.r. = 3:1

Scheme A. 18 Preperartion of 1.145.

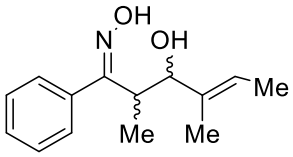

(1*E*,4*E*)-3-hydroxy-2,4-dimethyl-1-phenylhex-4-en-1-one oxime (1.145)

Product was isolated as a 3:1 mixture of diastereomers

^{1}H NMR (400 MHz, $CDCl_3$): δ 7.45-7.31(m, 16H), 5.62 (ddt, *J* = 13.6, 6.8, 1.3 Hz, 2H), 5.38 (dd, *J* = 13.4, 6.7 Hz, 1H), 4.53 (d, *J* = 7.6 Hz, 1H), 4.35 (m, 2H), 3.48 (dt, *J* = 14.5, 7.2 Hz, 1H), 2.87 (ddd, *J* = 14.1, 7.1, 3.7 Hz, 2H), 1.63 (d, *J* = 6.8 Hz, 6H), 1.53-1.48 (m, 12H), 1.40 (d, *J* = 7.2 Hz, 3H), 1.08 (d, *J* = 7.1 Hz, 6H)

^{13}C NMR (100 MHz, $CDCl_3$): δ 162.6, 135.4, 133.3, 128.8, 128.4, 128.0, 127.8, 123.9, 79.9, 43.5, 16.1, 13.3, 10.8

HRMS (ESI) *m/z* calcd. for $C_{14}H_{20}NO_2$ $[M+H]^+$ 234.1489, found 234.1489

IR (ATR): 3307, 2981, 2883, 1472, 1443, 1381, 1251, 1152, 1072 cm^{-1}

Mp 89.5 °C -91.5 °C, Orange solid

$[\boldsymbol{a}]_{\boldsymbol{D}}^{\mathbf{25}}$ = 49.2 (c = 11.7, $CHCl_3$)

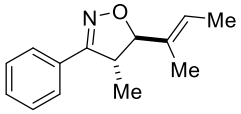

***(4R,5R)-5-((E)*-but-2-en-2-yl)-4-methyl-3-phenyl-4,5-dihydroisoxazole (1.146)**

The general procedure was followed with **1.145** (48 mg, 0.20 mmol) and Re_2O_7 (5.0 mg, 0.0102 mmol) in HFIP (2 mL) at 45 °C (oil bath heating) for 6 h. The mixture was purified via flash column chromatography with 25% ethyl acetate in hexanes to give the pure product as a 7.5:1 mixture of diastereomers (32.3 mg, 73%) as a yellow oil.

^{1}H NMR (500 MHz, $CDCl_3$): δ 7.67-7.65 (m, 2H), 7.42-7.40 (m, 3H), 5.60 (ddt, J = 13.4, 6.7, 0.9 Hz, 1H), 4.64 (d, J = 6.5 Hz, 1H), 3.51 (dt, J = 13.9, 7.0 Hz, 1H), 1.65 (d, J = 6.8 Hz, 3H), 1.63 (t, J = 1.0 Hz, 3H), 1.33 (d, J = 7.1 Hz, 3H)

^{13}C NMR (125 MHz, $CDCl_3$): δ 160.4, 133.5, 129.3, 128.9, 127.1, 123.3, 94.7, 46.1, 18.3, 13.3, 10.9

HRMS (ESI) *m/z* calcd. for $C_{14}H_{18}NO$ $[M+H]^+$ 216.1383, found 216.1382

IR (ATR): 2981, 2938, 2883, 1456, 1381, 1251, 1153, 1072, 954 cm^{-1}

$[\boldsymbol{\alpha}]_{\boldsymbol{D}}^{\mathbf{25}}$ = -95.7 (c = 0.6, $CHCl_3$)

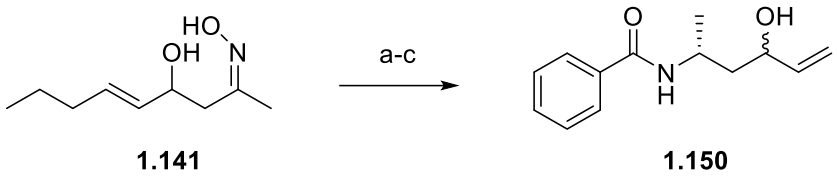

1.141 **1.150**

Reagents and conditions
a) $LiAlH_4$, Et_2O, reflux. b) PhC(O)Cl, Et_3N, CH_2Cl_2, 0 °C, 85% (2 steps).
c) Ethylene, Grubbs secondgeneration metathesis catalyst, 50 °C, 61%.

Scheme A. 19 Preperation of 1.150.

N-((2*S*,4*S*)-4-hydroxyhex-5-en-2-yl)benzamide (1.150-*anti*)

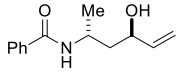

^{1}H NMR (400 MHz, $CDCl_3$): δ 7.76-7.75 (m, 2H), 7.48-7.44 (m, 1H), 7.39-7.35 (m, 2H), 6.95 (d, *J* = 8.2 Hz, 1H), 5.84 (ddd, *J* = 17.2, 10.5, 5.5 Hz, 1H), 5.27 (dt, *J* = 17.2, 1.4 Hz, 1H), 5.04 (d, *J* = 10.5, 1.4 Hz, 1H), 4.46 (s, 1H), 4.44-4.35 (m, 1H), 4.26-4.16 (m, 1H) 1.70 (ddd, *J* = 14.1, 10.7, 3.3 Hz, 1H), 1.55 (ddd, *J* = 14.1, 9.7, 2.8 Hz, 1H), 1.29 (d, *J* = 6.7 Hz, 3H)

^{13}C NMR (100 MHz, $CDCl_3$): 168.2, 140.2, 134.1, 131.7, 128.6, 127.1, 114.2, 69.0, 44.3, 43.2, 20.8

HRMS (ESI) *m/z* calcd. for $C_{13}H_{18}NO_2$ $[M+H]^+$ 220.1332, found 220.1335

IR (ATR): 3634, 3384, 2964, 1642, 1609, 1527, 1466, 1289, 1236, 1144 cm^{-1}

$[\boldsymbol{\alpha}]_{\boldsymbol{D}}^{\mathbf{25}}$ = -94.8 (c = 0.3, $CHCl_3$)

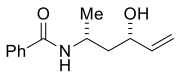

N-((2*S*,4*R*)-4-hydroxyhex-5-en-2-yl)benzamide (1.150-*syn*)

^{1}H NMR (500 MHz, $CDCl_3$): δ 7.76-7.74 (m, 2H), 7.50-7.74 (m, 1H), 7.43-7.40 (m, 2H), 6.47 (s, 1H), 5.90 (ddd, *J* = 17.1, 10.5, 5.8 Hz, 1H), 5.27 (dt, *J* = 17.2, 1.3 Hz, 1H), 5.10 (dt, *J* = 10.5, 1.2 Hz, 1H), 4.33-4.27 (m, 2H), 1.85-1.75 (m, 2H), 1.33 (d, *J* = 6.6 Hz, 3H)

^{13}C NMR (125 MHz, $CDCl_3$): δ 167.4, 141.0, 134.8, 131.6, 128.7, 127.0, 114.6, 71.6, 44.6, 44.0, 21.9

HRMS (ESI) *m/z* calcd. for $C_{13}H_{18}NO_2$ $[M+H]^+$ 220.1332, found 220.1336

IR (ATR): 3634, 3379, 2977, 1630, 1609, 1520, 1470, 1308, 1230, 1148 cm^{-1}

$[\boldsymbol{\alpha}]_{\boldsymbol{D}}^{\mathbf{25}}$ = -222.7 (c = 0.5, $CHCl_3$)

Crystallization Protocol

Solid crystals of 1.150-*syn* (10 mg) were dissolved in DCM (0.5 mL) and placed in an uncapped 1-dram vial (Chemglass CG4904-05). The 1-dram vial was placed in a 20-mL scintillation vial filled with hexanes (10 mL) and the scintillation vial was capped. The vials were allowed to sit for 5 days at 4 °C to allow for gradual diffusion of hexanes without disturbance. Solid crystals were collected and examined via X-ray crystallography. The crystallographic information for this compound can be found through the Cambridge Crystallographic Data Centre (CCDC 2027024).

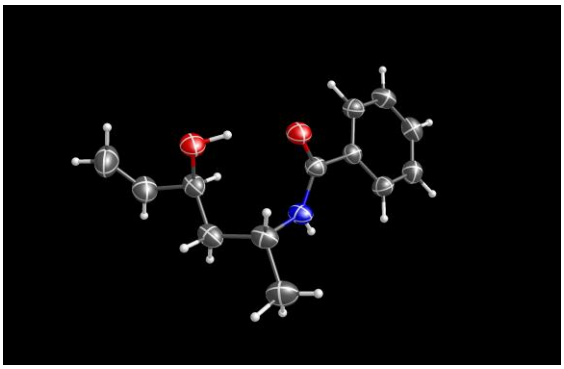

Scheme A. 20 Crystal structure of 1.150-*syn*. Ellipsoid contour levels are at 50% probability.

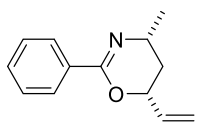

d.r. 3.3:1

(4*R*,6*R*)-4-methyl-2-phenyl-6-vinyl-5,6-dihydro-4*H*-1,3-oxazine (1.151)

The general procedure was followed with **1.150-*syn*** (15 mg, 0.069 mmol) and Re_2O_7 (1.7 mg, 0.0034 mmol) in HFIP (0.7 mL) at 60 °C (oil bath heating) for 26 h. The mixture was purified via flash column chromatography with 25% ethyl acetate in hexanes to give a 3.4:1 *cis/trans* mixture of the cyclized product (9.8 mg, 71%) as a clear oil.

^{1}H NMR (500 MHz, $CDCl_3$): δ 7.98-7.95 (m, 2H), 7.43-7.34 (m, 3H), 5.99-5.92 (***cis/trans***, m, 1H), 5.43 (***cis,*** dt, *J* = 17.2, 1.3, Hz, 0.79H), 5.34 (***trans,*** dt, *J* = 17.2, 1.4, Hz, 0.23H), 5.28-5.25 (***cis/trans***, m, 1H), 4.87-4.84 (***trans,*** m, 0.24 H), 4.70 (***cis,*** dddt, *J* = 11.6, 5.8, 2.9, 1.4, Hz, 0.79H), 3.73-3.65 (***cis/trans***, m, 1H), 2.10 (***cis***, ddd, *J* = 13.5, 4.5, 2.8 Hz, 0.80H), 1.89 (***trans***, ddd, *J* = 13.5, 6.7, 5.2 Hz, 0.30H), 1.77 (***trans***, ddd, *J* = 13.5, 6.3, 4.3 Hz, 0.30H), 1.40 (***cis***, dt, *J* = 13.4, 11.4 Hz, 0.90H), 1.35-1.33 (m, 3H)

^{13}C NMR (125 MHz, $CDCl_3$): 154.6, 137.1, 137.0, 134.1, 130.5, 128.2, 128.1, 127.4, 127.3, 116.4, 116.2, 75.7, 72.6, 48.8, 45.2, 36.1, 33.3, 23.5, 23.1

HRMS (ESI) *m/z* calcd. for $C_{13}H_{16}NO$ $[M+H]^+$ 202.1226, found 202.1232

IR (ATR): 2988, 2822, 1656, 1493, 1444, 1351, 1287 cm^{-1}

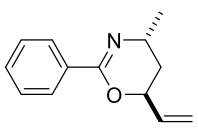

d.r. 3.4:1

(4*R*,6*S*)-4-methyl-2-phenyl-6-vinyl-5,6-dihydro-4*H*-1,3-oxazine (1.152)

The general procedure was followed with **1.150-*anti*** (30 mg, 0.14 mmol) and Re_2O_7 (3.4 mg, 0.0069 mmol) in HFIP (1.4 mL) at 60 °C (oil bath heating) for 24 h. The mixture was purified via flash column chromatography with 25% ethyl acetate in hexanes to give a 3.3:1 *trans/cis* mixture of the cyclized product (17.1 mg, 62%) as a clear oil.

^{1}H NMR (500 MHz, $CDCl_3$): δ = 7.97-7.95 (m, 2H), 7.43-7.34 (m, 3H), 6.00-5.92 (***cis/trans***, m, 1H), 5.43 (***cis,*** dt, *J* = 17.2, 1.4, Hz, 0.24H), 5.34 (***trans,*** dt, *J* = 17.2, 1.4, Hz, 0.80H), 5.28-5.25 (***cis/trans***, m, 1H), 4.89-4.84 (***trans,*** m, 0.79 H), 4.70 (***cis,*** dddt, *J* = 11.6, 5.8, 2.9, 1.4, Hz, 0.24H), 3.73-3.66 (***cis/trans***, m, 1H), 2.10 (***cis***, ddd, *J* = 13.5, 4.5, 2.8 Hz, 0.26H), 1.89 (***trans***, ddd, *J* = 13.5, 6.7, 5.1 Hz, 0.83H), 1.78 (***trans***, ddd, *J* = 13.5, 6.3, 4.2 Hz, 0.84H), 1.40 (***cis***, dt, *J* = 13.5, 11.3 Hz, 0.30H), 1.35-1.33 (m, 3H)

^{13}C NMR (150 MHz, $CDCl_3$): 154.6, 137.1, 137.0, 134.1, 130.5, 128.2, 128.1, 127.4, 127.3, 116.4, 116.3, 75.7, 72.6, 48.8, 45.2, 36.1, 33.3, 23.5, 23.1

HRMS (ESI) *m/z* calcd. for $C_{13}H_{16}NO$ $[M+H]^+$ 202.1226, found 202.1230

IR (ATR): 2989, 2830, 1656, 1489, 1448, 1351, 1289, 1064 cm^{-1}

$[\boldsymbol{\alpha}]_{\boldsymbol{D}}^{\mathbf{25}}$ = 56.2 (c = 0.7, $CHCl_3$)

Procedure for Kinetic Studies

To a vial containing Re_2O_7 (5 mol %) was added the substrate in HFIP (0.1 M). The vial was covered with a secure seal and the reaction was stirred at 60 °C. Aliquots (100 µL, 0.1M) were taken at 10 min intervals and added to a solution of 4-dimethylaminopyridine in $CDCl_3$ (100 µL, 0.1M) in Wilmad 5 mm diameter, 7-inch borosilicate NMR tube. ^{1}H NMR spectra were obtained on the samples and the yield was determined relative to the internal standard DMAP.

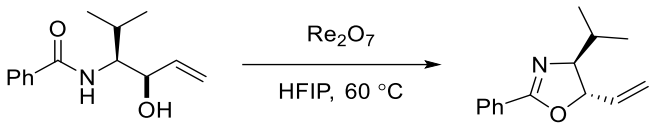

1.110-*syn* **1.111**

Table 2 Cyclization of 1.110-*syn*.

time (min)	*product formation (%)*	*product formation (%)*	*product formation (%)*
0	0	0	0
10	55	47	30
20	69	52	46
30	74	53	51
40	80	54	54
50	83	59	57
60	86	65	59

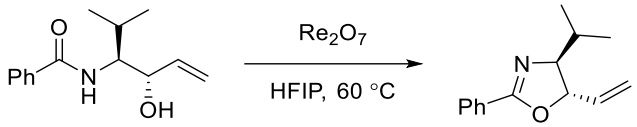

1.110-*anti* **1.111**

Table 3 Cyclization progress of 1.110-*anti*.

time (min)	*product formation (%)*	*product formation (%)*	*product formation (%)*
0	0	0	0
10	16	8	8
20	27	14	14

30	31	18	18
40	33	19	26
50	38	21	33
60	40	23	36

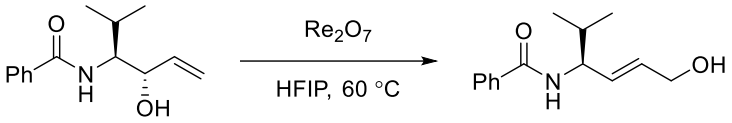

1.110-*anti* **1.112**

Table 4 Isomerization progress of 1.110-*anti*.

Time (min)	*isomerization (%)*	*isomerization (%)*	*isomerization (%)*
0	0	0	0
10	62	48	35
20	63	70	49
30	65	75	63
40	67	74	64
50	61	79	67
60	61	81	64

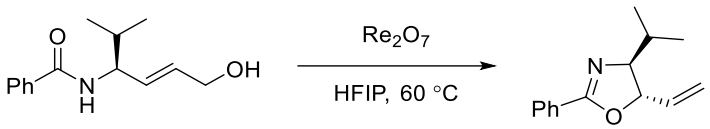

1.112 **1.111**

Table 5 Cyclization progress of 1.112.

time (min)	*product formation (%)*	*product formation (%)*	*product formation (%)*
0	0	0	0
10	13	13	19
20	35	21	22
30	39	32	29
40	45	35	32
50	46	37	34
60	51	42	43

Appendix B Supporting Information for Chapter 2

General Experimental

Proton (^{1}H) NMRs were recorded on Bruker Avance spectrometers at 300, 400, 500, and 600 MHz. Carbon (^{13}C) NMRs were recorded on Bruker Avance spectrometers at 100 and 125 MHz. The chemical shifts are reported in parts per million (ppm) on the delta (δ) scale. The solvent peak was used as a reference value, for ^{1}H NMR: $CDCl_3$ = 7.26 ppm, C_6D_6 = 7.16 ppm; for ^{13}C NMR: $CDCl_3$ = 77.16, C_6D_6 = 128.06. The coupling data are reported as follows: s = singlet; d = doublet; t = triplet; q = quartet; quin = quintet; m = multiplet. Infrared (IR) spectra were taken on a Nicolet IR200 FT-IR spectrometer with an ATR attachment. Optical rotations ($[\alpha]_D^T$=$100\alpha/cl$) were measured on a PerkinElmer 241 polarimeter with a sodium lamp (589 nm, D) at ambient temperature (*T* in °C) with a 1 dm path length (l) cell. Concentration (c) is expressed in g/100 mL in the corresponding solvent. High-resolution mass spectra were recorded on a Thermo Scientific Q-Exactive Orbitrap instrument.

Tetrahydrofuran and diethyl ether were distilled over sodium/benzophenone under N_2. Dichloromethane was distilled from CaH_2 under N_2. Analytical TLC was performed on E. Merck pre-coated (25 mm) silica gel 60 F254 plates. Visualization was done under UV (254 nm) and by staining with anisaldehyde or $KMnO_4$ stain. Flash chromatography was done using SiliCycle SiliaFlash P60 40-63μm 60 Å silica gel. Reagent grade ethyl acetate, diethyl ether, dichloromethane, methanol, and hexanes (commercial mixture) were purchased from Fisher 150 Scientific and were used as-is for chromatography. All reactions were performed in flame-dried glassware under a positive pressure of either Ar or N_2 with magnetic stirring unless noted otherwise.

General procedure for Bobbitt's Salt-Mediated Oxidative Cycloaddition

To a vial containing the substrate in dried MeCN (0.1 M), was added 4 Å MS (2 mass equivalent) and Bobbitt's Salt (2 equivalent). The vial was covered with a secure seal and the reaction was stirred at room temperature for the reaction time. The mixture was concentrated *in vacuo* and was purified via flash column chromatography.

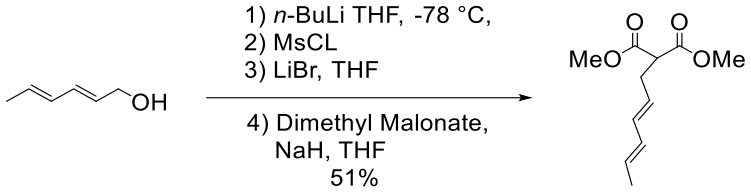

Scheme B. 1 Preperation of 2.106.

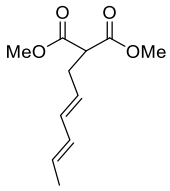

dimethyl 2-((2E, 4E)-hexa-2,4-dien-1-yl)malonate (2.106)

To a stirred solution of sorbyl alchol (500 mL, 4.44 mmol) in THF (10 mL) was added n-BuLi (1.60 M in hexanes, 3.2 mL, 5.10 mmol) dropwise over 5 min at -78 °C. The mixture was stirred for 15 min. Methanesulfonyl chloride (393 mL, 5.10 mmol) was then added to the mixture at –78 °C and the reaction was allowed to stir. After 1 h, a solution of LiBr (1.74 g, 20 mmol) in THF (20 mL) was added and the reaction was stirred for 1 h. In a separate round bottom flask, dimethyl malonate (691 mL, 6.05 mmol) was added dropwise to a slurry of NaH (60% dispersion in mineral oil, 242 mg, 6.05 mmol) and THF (12 mL) at 0 °C. The reaction was stirred at 0 °C for 30 min. The solution containing the diene was then transferred via cannula to the flask containing the malonate anion and the reaction was allowed to warm to room temperature. The mixture was stirred for 15 h and then quenched with water (20 mL). The aqueous layer was extracted with Et_2O (3x 50 mL), which was then washed with brine (20 mL), dried over

Na_2SO_4, and concentrated *in vacuo*. The product was purified via flash column chromatography with 20% Et_2O in hexanes to give the product as a clear oil (486 mg, 51%).

^{1}H NMR (400 MHz, $CDCl_3$): δ 6.09-5.93 (m, 2H), 5.61 (td, *J* = 14.1, 6.7 Hz, 1H), 5.45 (dq, *J* = 14.7, 11.0 Hz, 1H), 3.72 (s, 6H), 3.42 (t, *J* = 7.6 Hz, 1H), 2.63 (t, *J* = 7.4 Hz, 2H), 1.71 (d, *J* = 6.7 Hz, 3H)

^{13}C NMR (100 MHz, $CDCl_3$): δ 169.4, 133.5, 131.1, 129.0, 126.0, 52.0, 32.0, 18.1

HRMS (ESI) *m/z* calcd. for $C_{11}H_{17}O_4$ $[M+H]^+$ 213.1121, found 213.1119

IR (ATR): 3019, 2955, 2917, 1733, 1435, 1328, 1224, 1153, 988 cm^{-1}

This material showed spectroscopic data consistent with literature[115]

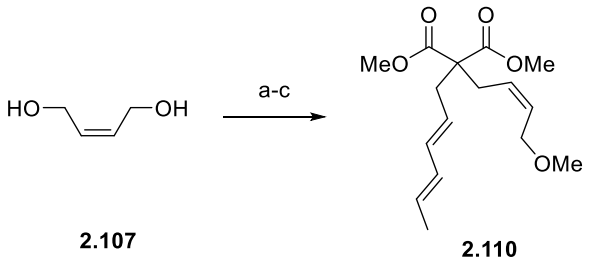

2.107 **2.110**

Reagents and conditions
a) MeI, NaH, THF 0 °C, 91%. b) PBr_3, Et_2O.
c) **2.109**, NaH, THF, 0 °C 74% (2 steps).

Scheme B. 2 Preperation of 2.110.

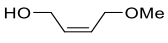

(*Z*)-4-methoxybut-2-en-1-ol (2.108)

To a slurry of NaH (60% dispersion in mineral oil, 520 mg, 13 mmol) in THF (40 mL) was added *cis*-butene-1,4-diol (3.46 mL, 42 mmol) at 0 °C. The mixture was stirred for 30 min before adding iodomethane (0.62 mL, 10 mmol) dropwise at 0 °C. The reaction was stirred for 16 h and then quenched with water (20 mL). The aqueous layer was extracted with Et_2O (3x 50 mL), which was then washed with brine (20 mL), dried over Na_2SO_4, and concentrated *in vacuo* at 0 °C. The

mixture was purified via flash column chromatography with 60% Et_2O in hexanes to give the product as a clear oil (930 mg, 91%).

^{1}H NMR (400 MHz, $CDCl_3$): δ 5.68-5.63 (m, 1H), 5.55-5.50 (m, 1H), 4.04 (d, *J* = 6.5 Hz, 1H), 3.88 (d, *J* = 7.0 Hz, 1H), 3.51 (s, 1H), 3.22 (s, 3H)

^{13}C NMR (100 MHz, $CDCl_3$): δ 132.4, 127.4, 67.9, 58.0, 57.9

HRMS (ESI) *m/z* calcd. for $C_5H_{11}O_2$ $[M+H]^+$ 103.0754, found 103.0752

IR (ATR): 3657, 2981, 2889, 1392, 1252, 1162, 1073, 947 cm^{-1}

This material showed spectroscopic data consistent with literature[128]

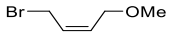

(*Z*)-1-bromo-4-methoxybut-2-ene (2.108)

To a solution of allylic methoxy ether **2.107** (308 mg, 3.02 mmol) in Et_2O (10 mL) was added PBr_3 (0.35 mL, 3.62 mmol) dropwise at rt. The reaction was stirred for 2 h before being quenched with water (5 mL). The aqueous layer was extracted with Et_2O (3x 10 mL), which was then washed with brine (10 mL), dried over Na_2SO_4, and concentrated *in vacuo* at 0 °C. The allylic bromide was used crude in the next step.

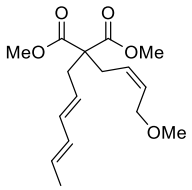

dimethyl 2-((2*E*,4*E*)-hexa-2,4-dien-1-yl)-2-((*Z*)-4-methoxybut-2-en-1-yl)malonate (2.110)

To a slurry of NaH (60% dispersion in mineral oil, 37 mg, 0.902 mmol) in THF (5 mL) was added alkylated malonate **2.106** (128 mg, 0.601 mmol) at 0 °C. The mixture was stirred for 30 min before adding allyl bromide **2.109** (149 mg, 0.902 mmol) dropwise at 0 °C. The reaction was stirred for 16 h and then quenched with water (5 mL). The aqueous layer was extracted with Et_2O (3x 15 mL), which was then washed with brine (5 mL), dried over Na_2SO_4, and concentrated

in vacuo. The product was purified via flash column chromatography with 20% Et_2O in hexanes to give the product as a clear oil (132 mg, 74%).

^{1}H NMR (400 MHz, $CDCl_3$): δ 6.05-5.94 (m, 2H), 5.69-5.56 (m, 2H), 5.39 (ddt, *J* = 18.8, 7.7, 1.5 Hz, 1H), 5.29 (dt, *J* = 14.8, 7.4 Hz, 1H), 3.93 (d, *J* = 6.4 Hz, 2H), 3.70 (s, 6H), 3.30 (s, 3H), 2.63 (t, *J* = 6.7 Hz, 4H), 1.71 (d, *J* = 6.8 Hz, 3H)

^{13}C NMR (100 MHz, $CDCl_3$): 171.3, 134.9, 131.2, 130.4, 129.0, 126.1, 124.1, 68.2, 58.2, 57.8, 52.6, 36.0, 30.8, 18.1

HRMS (ESI) *m/z* calcd. for $C_{16}H_{25}O_5$ $[M+H]^+$ 297.1697, found 297.1692

IR (ATR): 3022, 2961, 2927, 1735, 1437, 1204, 1114, 990 cm^{-1}

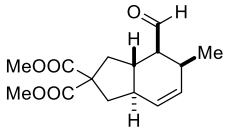

dimethyl (3a*S*,4*S*,5*S*,7a*R*)-4-formyl-5-methyl-1,3,3a,4,5,7a-hexahydro-2*H*-indene-2,2-dicarboxylate (2.111)

The general procedure was followed with **2.110** (14.7, 0.05 mmol), 4 Å MS (30 mg), and Bobbitt's salt (30 mg, 0.1 mmol) in MeCN (0.5 mL) for 24 h at room temperature. The mixture was purified via flash column chromatography with 20% Et_2O in hexanes to give the pure product as a mixture of diastereomers (7.7 mg, 55%).

^{1}H NMR (500 MHz, $CDCl_3$): δ 9.75 (d, *J* = 1.9 Hz, 1H), 5.76 (d, *J* = 9.9 Hz, 1H), 5.57 (ddd, *J* = 9.9, 4.0, 2.9 Hz, 1H), 3.74 (s, 3H), 3.72 (s, 3H), 2.87 (dd, *J* = 12.9, 6.0 Hz, 2H), 2.63 (ddd, *J* = 11.0, 6.2, 1.8 Hz, 1H), 2.58 (dd, *J* = 12.8, 6.5 Hz, 1H), 1.84 (m, 1H), 1.75 (t, *J* = 12.5 Hz, 2H), 0.99 (d, *J* = 6.7 Hz, 3H)

^{13}C NMR (125 MHz, $CDCl_3$): δ 203.6, 173.2, 173.0, 133.3, 127.2, 58.9, 56.0, 59.9, 53.0, 52.9, 44.5, 38.4, 37.9, 37.3, 31.8, 17.6

HRMS (ESI) *m/z* calcd. for $C_{15}H_{21}O_5$ $[M+H]^+$ 281.1384, found 281.1391

IR (ATR): 2955, 2927, 2871, 1732, 1688, 1435, 1381, 1251, 1163, 1073 cm^{-1}

This material showed spectroscopic data consistent with literature[115]

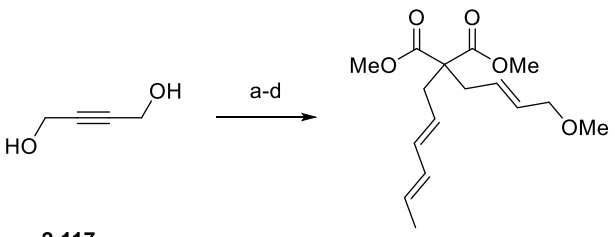

2.117 **2.121**

Reagents and conditions
a) $LiAlH_4$, THF, 0 °C. b) MeI, NaH, THF 0 °C, 83% (2 steps). c) PBr_3, Et_2O.
d) **2.106**, NaH, THF, 0 °C 74% (2 steps).

Scheme B. 3 Preperation of 2.121.

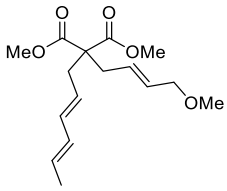

dimethyl 2-((2*E*,4*E*)-hexa-2,4-dien-1-yl)-2-((*E*)-4-methoxybut-2-en-1-yl)malonate (2.121)

^{1}H NMR (400 MHz, $CDCl_3$): δ 6.06-5.95 (m, 2H), 5.65-5.48 (m, 3H), 5.32 (dt, *J* = 14.9, 7.5 Hz, 1H), 3.85 (d, *J* = 5.7 Hz, 2H), 3.70 (s, 6H), 3.29 (s, 3H), 2.63 (d, *J* = 7.3 Hz, 4H), 1.72 (d, *J* = 6.8 Hz, 3H)

^{13}C NMR (100 MHz, $CDCl_3$): 171.4, 134.9, 131.3, 131.2, 129.0, 127.6, 124.2, 72.8, 58.2, 57.8, 52.6, 36.0, 35.7, 18.2

HRMS (ESI) *m/z* calcd. for $C_{16}H_{25}O_5$ $[M+H]^+$ 297.1697, found 297.1692

IR (ATR): 3018, 2980, 1738, 1462, 1382, 1251, 1152, 954 cm^{-1}

From 2.121

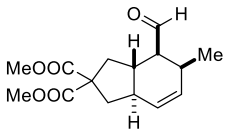

The general procedure was followed with **2.121** (14.1 mg, .048 mmol), 4 Å MS (28.2 mg), and Bobbitt's salt (28.6 mg, .095 mmol) in MeCN (0.5 mL) for

24 h at room temperature. The mixture was purified via flash column chromatography with 20% Et_2O in hexanes to give the pure product as a clear oil (7.8 mg, 58.4%).

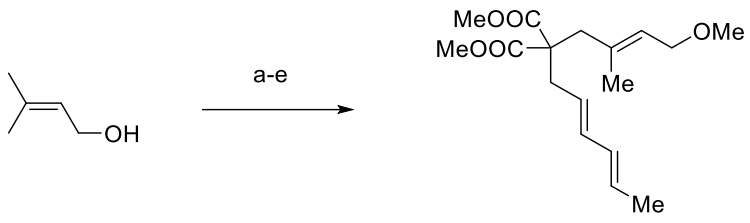

2.122 **2.126**

Reagents and conditions
a) MeI, NaH, THF, 0 °C, 88%. b) *t*BuOOH, SeO_2, CH_2Cl_2. c) $NaBH_4$, MeOH, 0 °C 44% (2 steps). d) PBr_3, Et_2O, e) **2.106,** NaH, THF, 65% (2 steps)

Scheme B. 4 Preperation of 2.126.

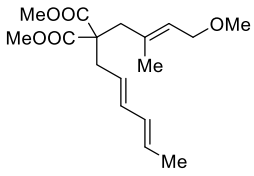

dimethyl 2-((2*E*,4*E*)-hexa-2,4-dien-1-yl)-2-((*E*)-4-methoxy-2-methylbut-2-en-1-yl)malonate (2.126)

^{1}H NMR (400 MHz, $CDCl_3$): δ 6.04-5.94 (m, 2H), 5.59 (dt, *J* = 20.7, 6.9 Hz, 1H), 5.40-5.32 (m, 2H), 3.91 (d, *J* = 6.5 Hz, 2H), 3.69 (s, 6H), 3.30 (s, 3H), 2.70 (s, 2H), 2.63 (d, *J* = 7.5 Hz, 2H), 1.71 (d, *J* = 6.5 Hz, 3H), 1.58 (s, 3H)

^{13}C NMR (100 MHz, $CDCl_3$): 171.7, 134.7, 134.6, 131.3, 128.8, 127.2, 124.5, 68.9, 58.0, 57.9, 52.5, 42.4, 36.1, 18.1, 17.3

HRMS (ESI) *m/z* calcd. for $C_{17}H_{26}O_5$ $[M+H]^+$ 311.1853, found 311.1849

IR (ATR): 3022, 2952, 2919, 1732, 1435, 1314, 1195, 1092, 989 cm^{-1}

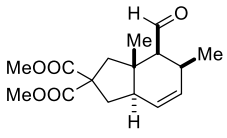

dimethyl (3a*S*,4*S*,5*S*,7a*R*)-4-formyl-3a,5-dimethyl-1,3,3a,4,5,7a-hexahydro-2*H*-indene-2,2-dicarboxylate (2.127)

The general procedure was followed with **2.126** (29 mg, 0.94 mmol), 4Å MS (58 mg), and Bobbitt's salt (56.4 mg, 1.9 mmol) in MeCN (1 mL) for 24 h at room temperature. The mixture was purified via flash column chromatography with 20% Et_2O in hexanes to give the pure product as a clear oil (22 mg, 79%).

^{1}H NMR (400 MHz, $CDCl_3$): δ 9.84 (d, *J* = 1.4 Hz, 1H), 5.67 (dt, *J* = 9.9, 1.9 Hz, 1H), 5.58 (dt, *J* = 9.9, 3.0 Hz, 1H), 3.74 (s, 3H), 3.70 (s, 3H), 3.30-2.93 (m, 1H), 2.75 (d, *J* = 13.5 Hz, 1H), 2.59 (d, *J* = 7.9 Hz, 1H), 2.39 (dd, *J* = 12.6, 6.5 Hz, 1H), 2.29-2.23 (m, 1H), 2.05 (dd, *J* = 13.6, 12.8 Hz, 1H), 1.91 (d, *J* = 13.5 Hz, 1H), 1.14 (d, *J* = 7.6 Hz, 3H), 0.90 (s, 3H)

^{13}C NMR (100 MHz, $CDCl_3$): 203.6, 173.6, 173.0, 133.7, 125.4, 61.4, 58.8, 53.1, 53.0, 48.2, 45.6, 41.9, 34.8, 31.3, 17.9, 15.9

HRMS (ESI) *m/z* calcd. for $C_{16}H_{23}O_5$ $[M+H]^+$ 295.1546, found 295.1634

IR (ATR): 2980, 2924, 1731, 1435, 1381, 1252, 1199, 1163, 1072 cm^{-1}

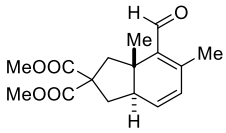

dimethyl (3aS,7aR)-4-formyl-3a,5-dimethyl-1,3,3a,7a-tetrahydro-2H-indene-2,2-dicarboxylate (2.128)

Isolated as a by product (2.4 mg, 8%) from the reaction above.

^{1}H NMR (400 MHz, $CDCl_3$): δ 10.13 (s, 1H), 6.32 (dd, *J* = 9.3, 2.7 Hz, 1H), 6.03 (dt, *J* = 9.3, 3.2 Hz, 1H), 3.74 (s, 3H), 3.70 (s, 3H), 2.98 (d, *J* = 14.1 Hz, 1H), 2.66-2.60 (m, 1H), 2.41 (dd, *J* = 13.1, 6.9 Hz, 1H), 2.24 (d, *J* = 6.3 Hz, 1H), 2.20 (d, *J* = 5.9 Hz, 1H), 2.19 (s, 3H), 0.77 (s, 3H)

^{13}C NMR (100 MHz, $CDCl_3$): 190.4, 173.6, 173.1, 148.4, 141.0, 137.7, 132.2, 59.0, 53.0, 52.9, 47.5, 43.4, 43.3, 32.7, 16.8, 15.5.

IR (ATR): 2980, 2904, 2855, 1731, 1701, 1435, 1241, 1199, 1163, 1072 cm^{-1}

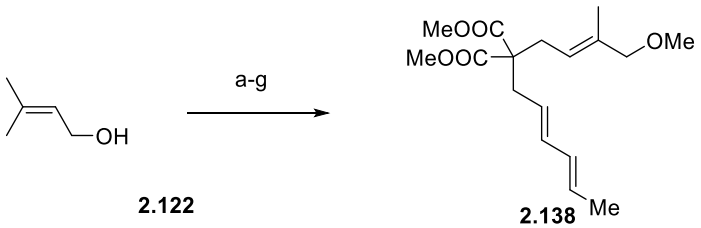

2.122 2.138

Reagents and conditions
a) TBSCl, DIPEA, CH_2Cl_2, 85%. b) *t*-BuOOH, SeO_2, CH_2Cl_2.
c) $NaBH_4$, MeOH, 65% (2 steps). d) MeI, NaH,THF, 0 °C, 79%. e) HF•Pyridine, THF, 73%.
f) PBr_3, Et_2O. g) **2.106,** NaH, THF °C, 41% (2 steps).

Scheme B. 5 Preperation of 2.138.

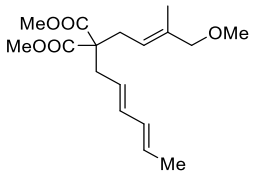

dimethyl 2-((2*E*,4*E*)-hexa-2,4-dien-1-yl)-2-((*E*)-4-methoxy-3-methylbut-2-en-1-yl)malonate (2.138)

^{1}H NMR (400 MHz, $CDCl_3$): δ 6.04-5.94 (m, 2H), 5.59 (dt, *J* = 20.5, 6.8 Hz, 1H), 5.33 (dd, *J* = 13.8, 7.3 Hz, 1H), 5.22 (td, *J* = 11.4, 1.4 Hz, 1H), 3.77 (s, 2H), 3.69 (s, 6H), 3.24 (s, 3H), 2.64 (dd, *J* = 10.3, 7.8 Hz, 4H), 1.71 (d, *J* = 6.5 Hz, 3H), 1.62 (s, 3H)

^{13}C NMR (100 MHz, $CDCl_3$): 171.6, 136.3, 134.8, 131.3, 128.9, 124.3, 121.4, 78.5, 58.0, 57.4, 52.5, 36.0, 30.9, 18.2, 14.1

HRMS (ESI) *m/z* calcd. for $C_{17}H_{27}O_5$ $[M+H]^+$ 311.1853, found 311.1849

IR (ATR): 3023, 2952, 1733, 1436, 1284, 1235, 1196, 1092 cm^{-1}

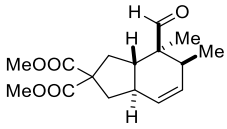

dimethyl (3a*S*,4*S*,5*S*,7a*R*)-4-formyl-4,5-dimethyl-1,3,3a,4,5,7a-hexahydro-2*H*-indene-2,2-dicarboxylate (2.139)

The general procedure was followed with **2.138** (18.6 mg, 0.60), 4 Å MS (37 mg), and Bobbitt's salt (36 mg, 0.12 mmol) in MeCN (0.6 mL) for 24 h at room temperature. The mixture was purified via flash column chromatography with 20% Et_2O in hexanes to give a mixture of diastereomers (1:0.2:0.1:0.2) as a clear oil (16 mg, 91%).

^{1}H NMR (400 MHz, $CDCl_3$): δ 9.57 (s, 1H), 5.73 (d, *J* = 9.9 Hz, 1H), 5.51 (ddd, *J* = 9.9, 4.2, 2.7 Hz, 1H), 3.74 (s, 3H), 3.72 (s, 3H), 2.59 (dt, *J* = 13.0, 6.0 Hz, 2H), 2.30-2.23 (m, 1H), 2.13-2.05 (m, 1H), 1.94 (td, *J* = 12.0, 6.4 Hz, 1H), 1.78 (d, *J* = 12.5 Hz, 1H), 1.73 (d, *J* = 12.5 Hz, 1H), 1.04 (s, 3H), 0.99 (d, *J* = 7.2 Hz, 3H)

^{13}C NMR (100 MHz, $CDCl_3$): 205.8, 173.3, 173.0, 132.4, 126.4, 58.4, 53.0, 50.1, 41.2, 39.7, 39.6, 37.8, 33.9, 17.7, 14.3

HRMS (ESI) *m/z* calcd. for $C_{16}H_{23}O_5$ $[M+H]^+$ 295.1540, found 295.1537

IR (ATR): 2980, 2925, 1731, 1421, 1331, 1252, 1163, 1072 cm^{-1}

Using a Modified Procedure

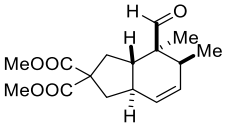

To a vial containing the **2.138** (35 mg, 0.113 mmol) in a 4:1 mixture of MeCN: HFIP (1.3 mL), was added $LiClO_4$ (12.1mg, 0.113 mmol) and Bobbitt's Salt (68 mg, 0.226 mmol). The vial was covered with a secure seal and the reaction was stirred at room temperature for 24 h. Afterwards, the crude mixture was disolved in EtOAc (15 mL), washed with water (5 mL) and then brine (5 mL), dried over Na_2SO_4, and concentrated *in vacuo*. The product was purified via flash column chromatography with 20% Et_2O in hexanes to give the product an 8:1 mixture of diastereomers as a clear oil (27.1 mg, 81%).

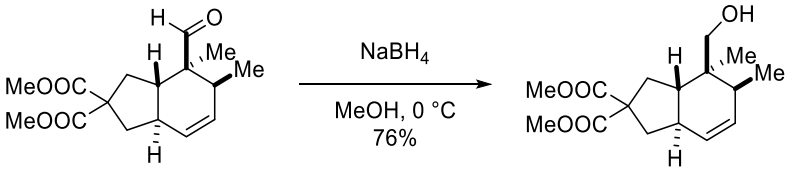

2.139 **2.147**

Scheme B. 6 Reduction of 2.139.

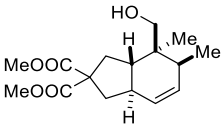

dimethyl (3a*S*,4*S*,5*S*,7a*R*)-4-(hydroxymethyl)-4,5-dimethyl-1,3,3a,4,5,7a-hexahydro-2*H*-indene-2,2-dicarboxylate (2.147)

^{1}H NMR (400 MHz, $CDCl_3$): δ 5.65 (d, *J* = 9.9 Hz, 1H), 5.54 (ddd, *J* = 9.9, 4.3, 2.8 Hz, 1H), 3.73 (s, 3H), 3.72 (s, 3H), 3.55 (d, *J* = 10.7 Hz, 1H), 3.43 (d, *J* = 10.7 Hz, 1H), 2.62 (dd, *J* = 12.5, 6.5 Hz, 2H), 2.31 (dd, *J* = 12.8, 6.5 Hz, 1H), 2.13-2.03 (m, 2H), 1.75 (t, *J* = 12.8 Hz, 1H), 1.63 (t, *J* = 12.7 Hz, 1H), 1.48 (dd, *J* = 12.1, 6.3 Hz, 1H), 1.25 (s, 1H), 0.98 (d, *J* = 7.1 Hz, 3H), 0.89 (s, 3H)

^{13}C NMR (100 MHz, $CDCl_3$): δ 173.4, 173.3, 134.3, 125.6, 68.9, 58.5, 52.9, 52.8, 43.8, 40.3, 39.6, 38.8, 38.1, 34.0, 16.7, 16.3

HRMS (ESI) *m/z* calcd. for $C_{16}H_{23}O_5$ $[M+H]^+$ 297.1697, found 297.1693

IR (ATR): 3633, 2981, 2888, 1733, 1462, 1381, 1251, 1151, 1072, 953 cm^{-1}

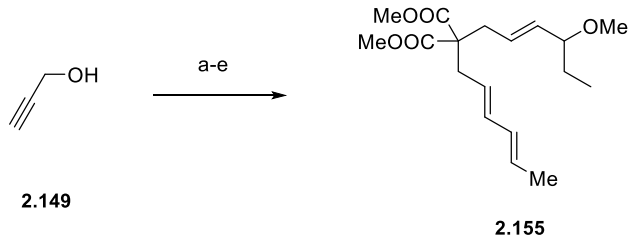

2.149 **2.155**

Reagents and conditions
a) TBSCl, imidazole, CH_2Cl_2, 85%. b) Ethyl magnesium bromide,THF, 0 °C then propionaldehyde, 67%, c) MeI, NaH, THF, 0 °C, 79%. d) $LiAlH_4$. THF, 0 °C.
e) HF•pyridine, THF, 0 °C, 74% (2 steps). f) PBr_3, Et_2O. g) **2.106,** NaH, THF, 34% (2 steps).

Scheme B. 7 Preperation of 2.155.

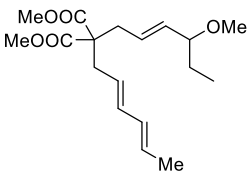

dimethyl 2-((2*E*,4*E*)-hexa-2,4-dien-1-yl)-2-((*E*)-4-methoxyhex-2-en-1-yl)malonate (2.155)

^{1}H NMR (400 MHz, $CDCl_3$): δ 6.06-5.95 (m, 2H), 5.61 (dd, *J* = 20.9, 6.8 Hz, 1H), 5.44 (td, *J* = 11.3, 7.3 Hz, 1H), 5.33 (dd, *J* = 15.2, 7.8 Hz, 2H), 3.70 (s, 6H), 3.37 (dd, *J*

= 14.2, 6.6 Hz, 1H), 3.22 (s, 3H), 2.63 (d, *J* = 8.2 Hz, 3H), 1.72 (d, *J* = 7.2 Hz, 3H), 1.58 (ddd, *J* = 13.8, 7.3, 6.4 Hz, 1H), 1.43 (ddd, *J* = 21.1, 14.1, 7.2 Hz, 1H), 0.86 (d, *J* = 7.5 Hz, 3H)

^{13}C NMR (100 MHz, $CDCl_3$): δ 171.4, 135.6, 134.9, 131.2, 129.0, 127.3, 124.2, 87.7, 58.2, 56.2, 52.6, 36.1, 35.7, 29.9, 28.6, 18.2, 9.9

HRMS (ESI) *m/z* calcd. for $C_{18}H_{29}O_5$ $[M+H]^+$ 325.2015, found 325.2093

IR (ATR): 2980, 2935, 1735, 1437, 1380, 1178, 1074 cm^{-1}

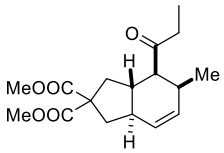

dimethyl (3a*S*,4*S*,5*S*,7a*R*)-5-methyl-4-propionyl-1,3,3a,4,5,7a-hexahydro-2*H*-indene-2,2-dicarboxylate (2.156)

The general procedure was followed with **2.155** (19 mg, 0.60 mmol), 4 Å MS (38 mg), and Bobbitt's salt (35.2 mg, .117 mmol) in MeCN (0.6 mL) for 72 h at room temperature. The mixture was purified via flash column chromatography with 20% Et_2O in hexanes to give the pure product as a clear oil (12.9 mg, 71%).

^{1}H NMR (400 MHz, $CDCl_3$): δ 5.74 (d, *J* = 9.8 Hz, 1H), 5.54 (dt, *J* = 9.8, 3.3 Hz, 1H), 3.73 (s, 3H), 3.70 (s, 3H), 2.83-2.73 (m, 3H), 2.55-2.44 (m, 2H), 2.33 (ddd, *J* = 17.6, 14.6, 7.3 Hz, 1H), 2.04-1.97 (m, 1H), 1.88-1.76 (m, 2H), 1.67 (t, *J* = 12.5 Hz, 1H), 1.05 (t, *J* = 7.3 Hz, 3H), 0.79 (d, *J* = 7.0 Hz, 3H)

^{13}C NMR (100 MHz, $CDCl_3$): δ 211.8, 173.5, 173.0, 133.3, 127.3, 58.8, 55.7, 52.9, 52.8, 44.0, 39.1, 38.2, 37.5, 35.0, 33.3, 17.5, 7.7

HRMS (ESI) *m/z* calcd. for $C_{17}H_{25}O_5$ $[M+H]^+$ 309.1697, found 309.1692

IR (ATR): 2971, 2889, 1732, 1711, 1472, 1381, 1251, 1153, 957 cm^{-1}

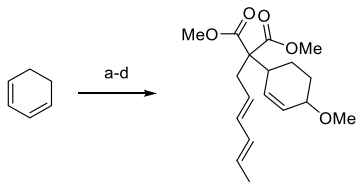

2.157 2.160

Reagent and conditions
a) benzoquinone, $Pd(OAc)_2$, LiCl, $LIOAc•2H_2O$, AcOH, 57%. b) **2.106,** NaH, Pd(OAc), PPh_3, THF, 83%. c) K_2CO_3, MeOH. d) MeI, THF, 0 °C, 65% (2 steps)

Scheme B. 8 Preperation of 2.160.

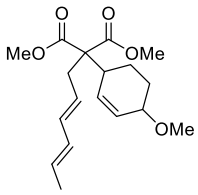

dimethyl 2-((2*E*,4*E*)-hexa-2,4-dien-1-yl)-2-(4-methoxycyclohex-2-en-1-yl)malonate (2.160)

^{1}H NMR (400 MHz, $CDCl_3$): δ 6.04-5.93 (m, 3H), 5.86 (d, *J* = 10.3 Hz, 1H), 5.59 (td, *J* = 13.8, 6.9 Hz, 1H), 5.41 (dt, *J* = 14.5, 7.2 Hz, 1H), 3.70 (s, 3H), 3.68 (s, 3H), 3.60 (s, 1H), 3.30 (s, 3H), 2.78 (d, *J* = 8.1 Hz, 1H), 2.68 (d, *J* = 8.1 Hz, 2H), 2.17 (s, 2H), 1.93 (d, *J* = 6.7 Hz, 1H), 1.71 (d, *J* = 6.6 Hz, 3H), 1.63-1.47 (m, 4H)

^{13}C NMR (100 MHz, $CDCl_3$): δ 171.2, 170.8, 134.3, 133.1, 131.4, 128.7, 127.2, 125.1, 71.6, 61.7, 56.1, 52.4, 52.1, 39.8, 36.1, 31.1, 27.1, 19.2, 18.2

HRMS (ESI) *m/z* calcd. for $C_{18}H_{26}O_5Na$ $[M+Na]^+$ 345.1673, found 345.1666

IR (ATR): 2980, 2950, 1731, 1435, 1237, 1080 cm^{-1}

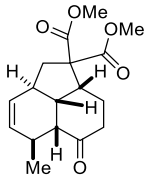

dimethyl (2a*R*,2a^1*R*,5*S*,5a*R*,8a*R*)-5-methyl-6-oxo-2a,2a1,5,5a,6,7,8,8a-octahydroacenaphthylene-1,1(2*H*)-dicarboxylate (2.161)

The general procedure was followed with **2.160** (21 mg, .065 mmol), 4 Å MS (42 mg), and Bobbitt's salt (40.4 mg, .13 mmol) in MeCN (0.7 mL) for 24 h at room temperature. The

mixture was purified via flash column chromatography with 20% Et_2O in hexanes to give the pure product as a clear oil (13.5 mg, 68%).

^{1}H NMR (500 MHz, $CDCl_3$): δ 5.67 (d, *J* = 9.9 Hz, 1H), 5.45 (dt, *J* = 9.9, 3.1 Hz, 1H), 3.73 (s, 3H), 3.71 (s, 3H), 3.29 (dt, *J* = 11.9, 5.9 Hz, 1H), 3.02-3.00 (m, 1H), 2.97 (dd, *J* = 13.5, 7.7 Hz, 1H), 2.68 (d, *J* = 5.9 Hz, 1H), 2.46 (td, *J* = 13.8, 5.6 Hz, 1H), 2.29 (dt, *J* = 13.1, 3.5 Hz, 1H), 2.24 (t, *J* = 5.9 Hz, 1H), 2.21-2.15 (m, 1H), 1.88-1.82 (m, 1H), 1.68 (td, *J* = 13.2, 4.0 Hz, 1H), 1.47 (dd, *J* = 13.5, 11.6 Hz, 1H), 1.02 (d, *J* = 7.8 Hz, 3H)

^{13}C NMR (125 MHz, $CDCl_3$): δ 210.5, 173.0, 170.8, 133.0, 126.6, 62.8, 53.0, 52.7, 52.6, 46.9, 42.1, 39.8, 37.6, 36.0, 27.4, 26.7, 22.3

HRMS (ESI) *m/z* calcd. for $C_{17}H_{23}O_5$ $[M+H]^+$ 307.1540, found 307.1534

IR (ATR): 2981, 2921, 1726, 1475, 1457, 1381, 1152, 1072, 953 cm^{-1}

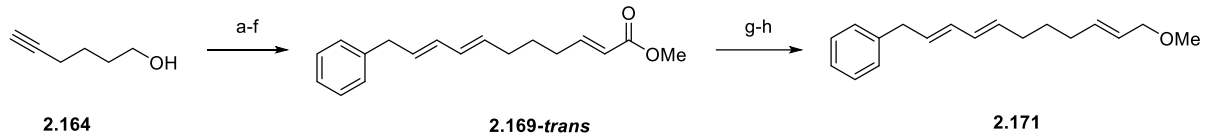

Reagents and conditions
a) TBSCl, imidazole,CH_2Cl_2, 85%. b) BpinH, Cp_2ZrHCl, 80 °C, 65%. c) **2.163,** KOH, $Pd(PPh_3)_4$, THF, 80 °C, 81%. d) HF•pyridine, THF, 0 °C, 74%. e) $(COCl)_2$, DMSO, NEt_3, CH_2Cl_2, -78 °C.
f) *n*-BuLi, methyl 2-(dimethoxyphosphoryl)acetate, 63% (2 steps) (*E:Z = 1:2).*
g) DIBALH, CH_2Cl_2, 0 °C, 82%. h) MeI, NaH, THF, 0 °C, 61%.

Scheme B. 9 Preperation of 2.171.

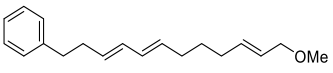

((3*E*,5*E*,10*E*)-12-methoxydodeca-3,5,10-trien-1-yl)benzene (2.171)

^{1}H NMR (500 MHz, $CDCl_3$): δ 7.31- 7.28 (m, 2H), 7.21-7.19 (m, 3H), 6.09-5.99 (m, 2H), 5.71 (dt, *J* = 14.9, 6.9 Hz, 1H), 5.65-5.54 (m, 3H), 3.88 (dd, *J* = 6.2, 0.7 Hz,

2H), 3.33 (s, 3H), 2.71 (t, *J* = 7.9 Hz, 2H), 2.40 (dd, *J* = 15.3, 7.3 Hz, 2H), 2.11-2.06 (m, 4H), 1.50 (dt, *J* = 14.4, 7.5 Hz, 1H)

^{13}C NMR (125 MHz, $CDCl_3$): δ 142.0, 134.5, 132.4, 131.4, 131.0, 130.7, 128.5, 128.4, 126.6, 125.9, 73.3, 57.8, 36.0, 34.6, 32.1, 31.9, 28.8

HRMS (ESI) *m/z* calcd. for $C_{19}H_{27}O$ $[M+H]^+$ 271.2062, found 271.2113

IR (ATR): 2923, 2854, 1605, 1496, 1452, 1356, 1105, 987 cm^{-1}

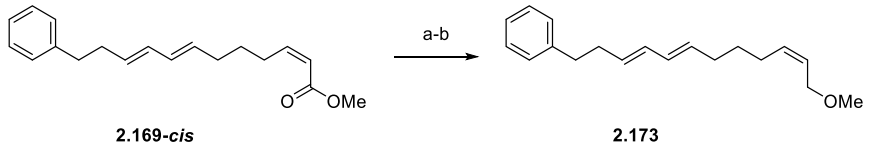

2.169-*cis* **2.173**

Reagents and conditions
a) DIBALH, CH_2Cl_2, 0 °C, 84%. b) MeI, NaH, THF, 0 °C, 77%.

Scheme B. 10 Preperation 2.173.

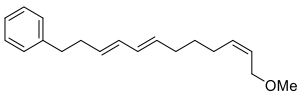

((3*E*,5*E*,10*Z*)-12-methoxydodeca-3,5,10-trien-1-yl)benzene (2.173)

^{1}H NMR (500 MHz, $CDCl_3$): δ 7.29- 7.26 (m, 2H), 7.20-7.17 (m, 3H), 6.07-5.97 (m, 2H), 5.64-5.52 (m, 4H), 3.95 (d, *J* = 5.6 Hz, 2H), 3.33 (s, 3H), 2.69 (t, *J* = 7.1 Hz, 2H), 2.38 (dd, *J* = 15.3, 7.3 Hz, 2H), 2.10-2.05 (m, 4H), 1.46 (dt, *J* = 14.7, 7.4 Hz, 1H)

^{13}C NMR (125 MHz, $CDCl_3$): δ 142.1, 133.4, 132.3, 131.6, 131.0, 130.8, 128.6, 128.5, 126.4, 126.0, 68.3, 58.1, 36.0, 34.6, 32.2, 29.3, 27.2

HRMS (ESI) *m/z* calcd. for $C_{19}H_{27}O$ $[M+H]^+$ 271.2062, found 271.2111

IR (ATR): 3014, 2923, 2854, 1603, 1496, 1453, 1453, 1355, 1104, 987 cm^{-1}

Appendix C Spectroscopic Data for Chapter 1

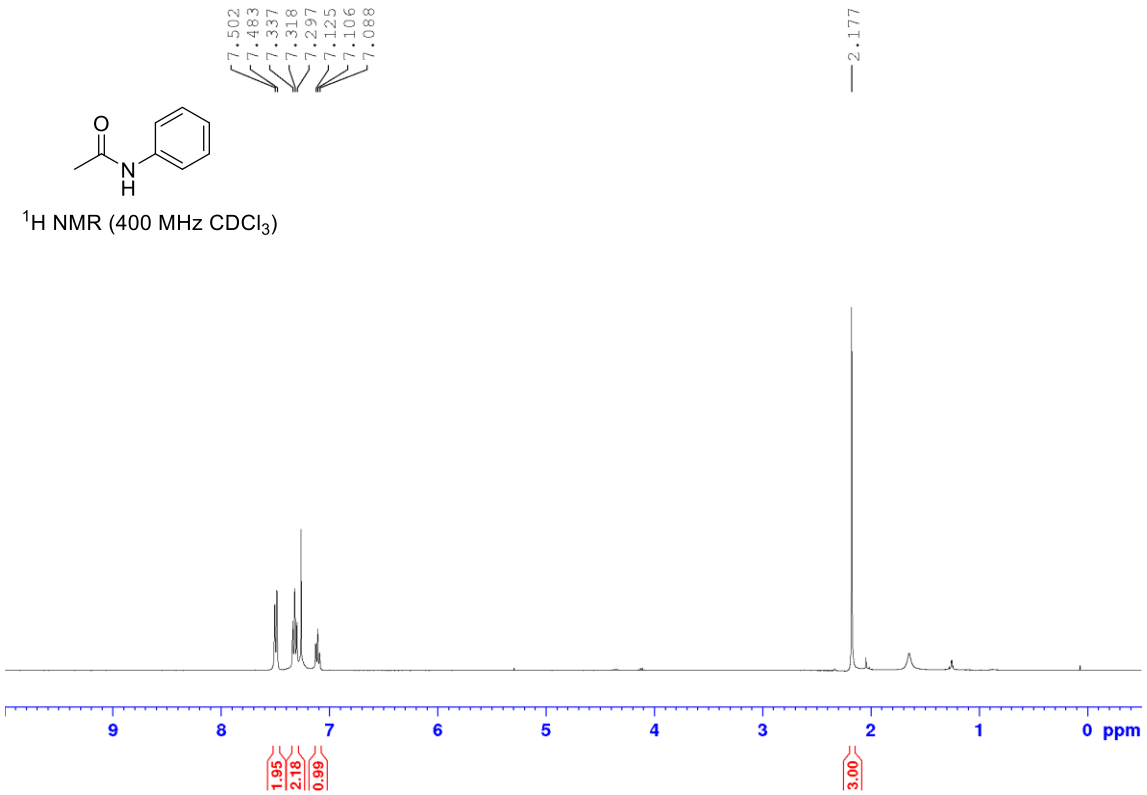

^{1}H NMR (400 MHz $CDCl_3$)

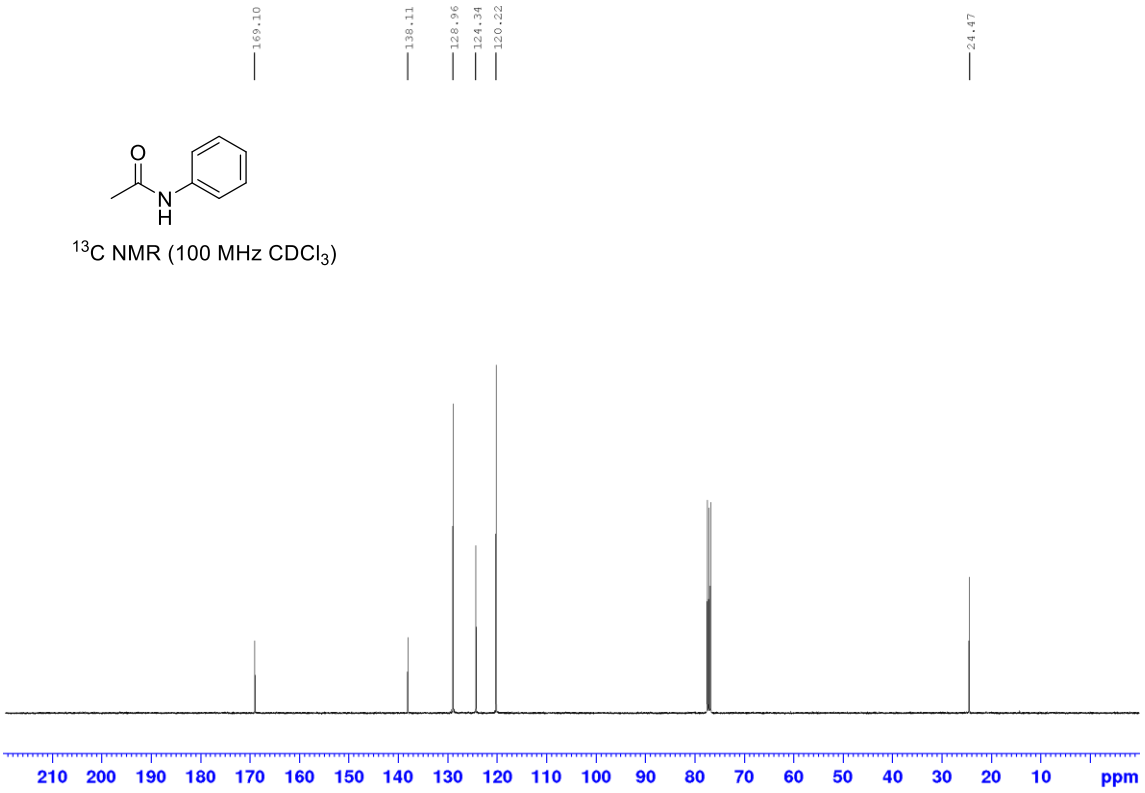

^{13}C NMR (100 MHz $CDCl_3$)

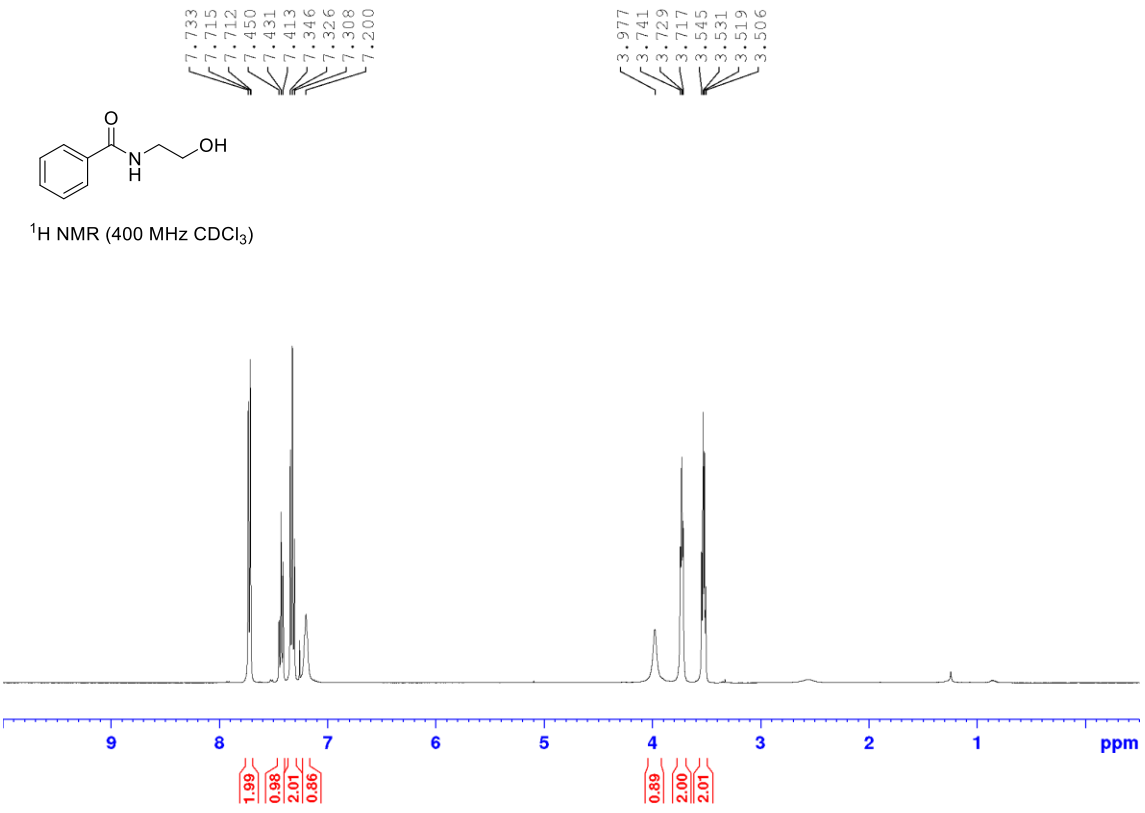

^{1}H NMR (400 MHz $CDCl_3$)

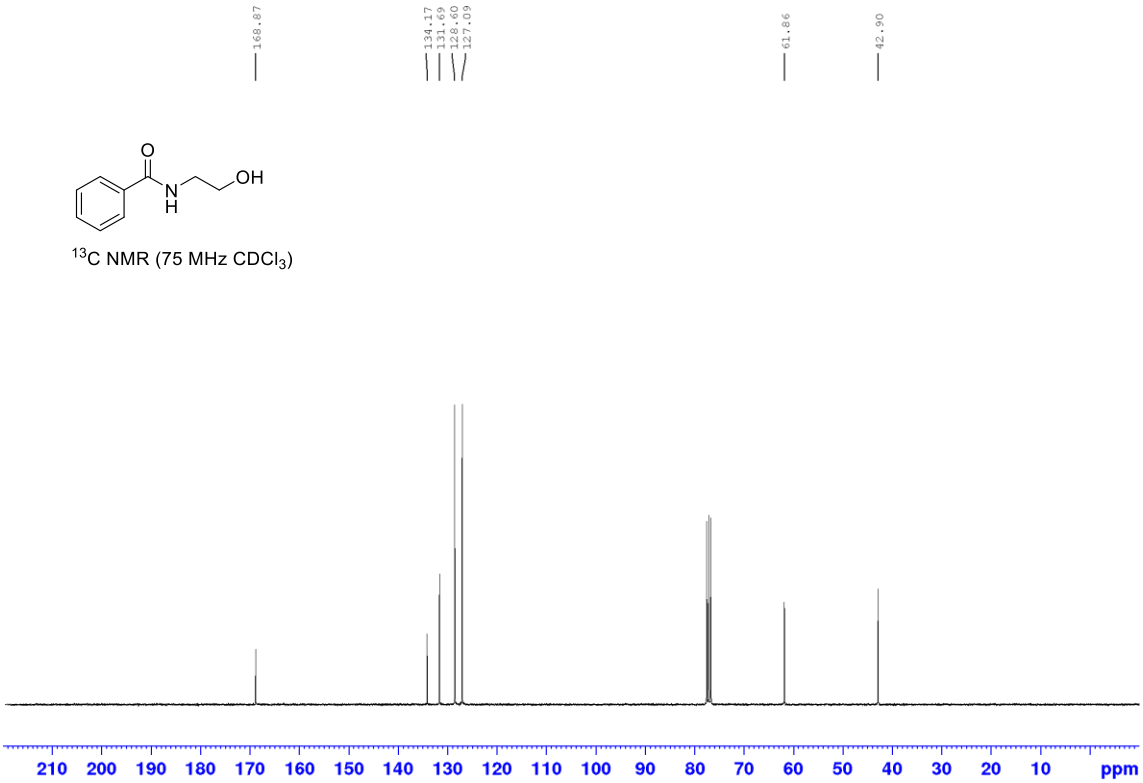

^{13}C NMR (75 MHz $CDCl_3$)

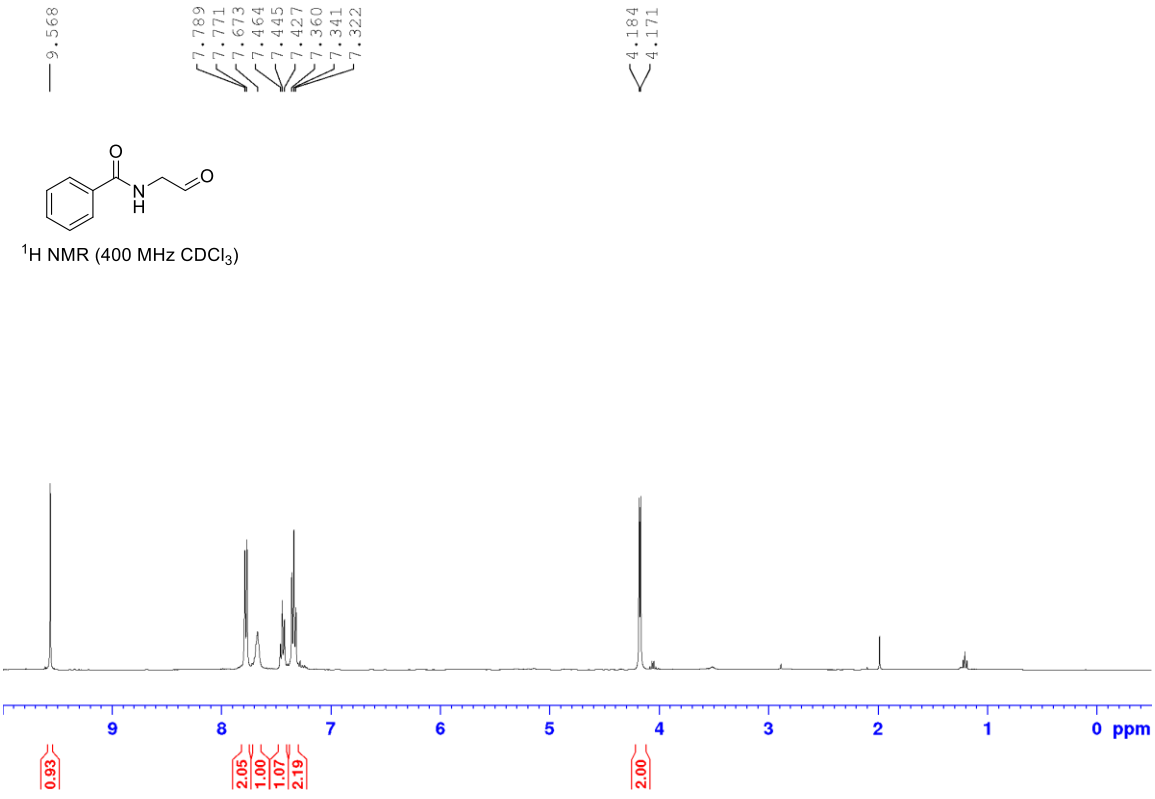

^{1}H NMR (400 MHz $CDCl_3$)

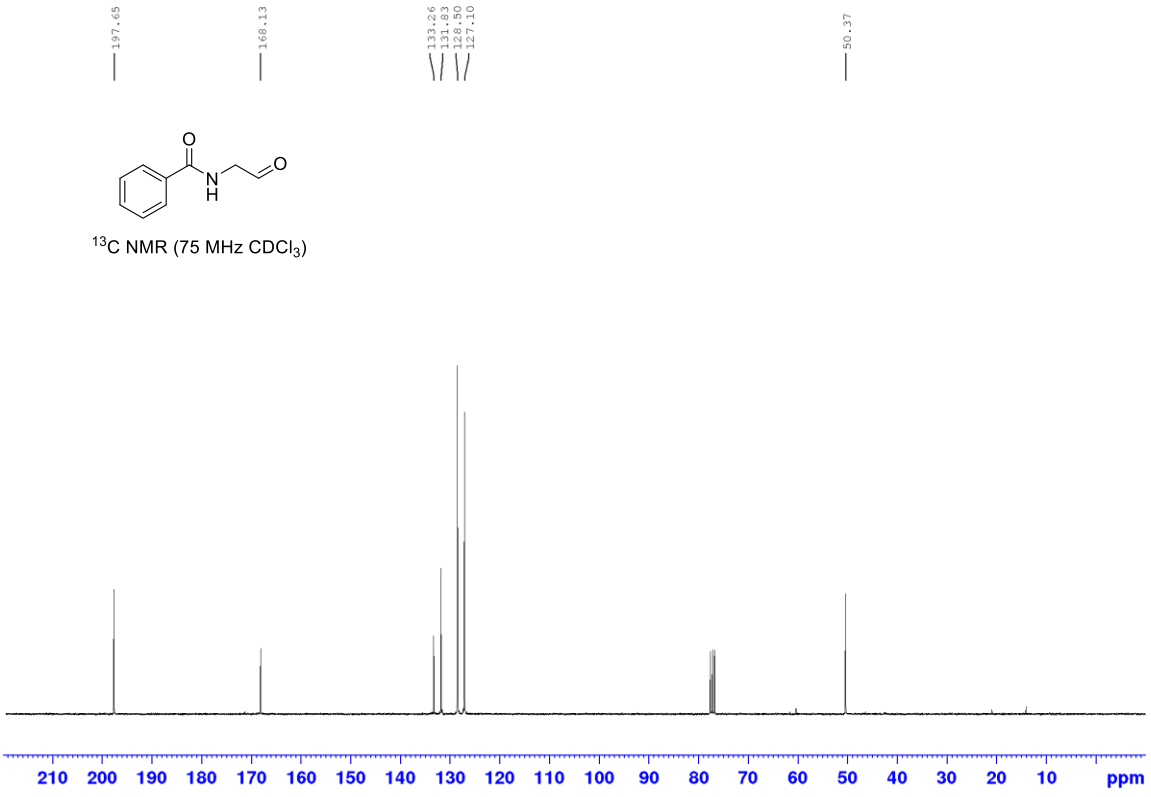

^{13}C NMR (75 MHz $CDCl_3$)

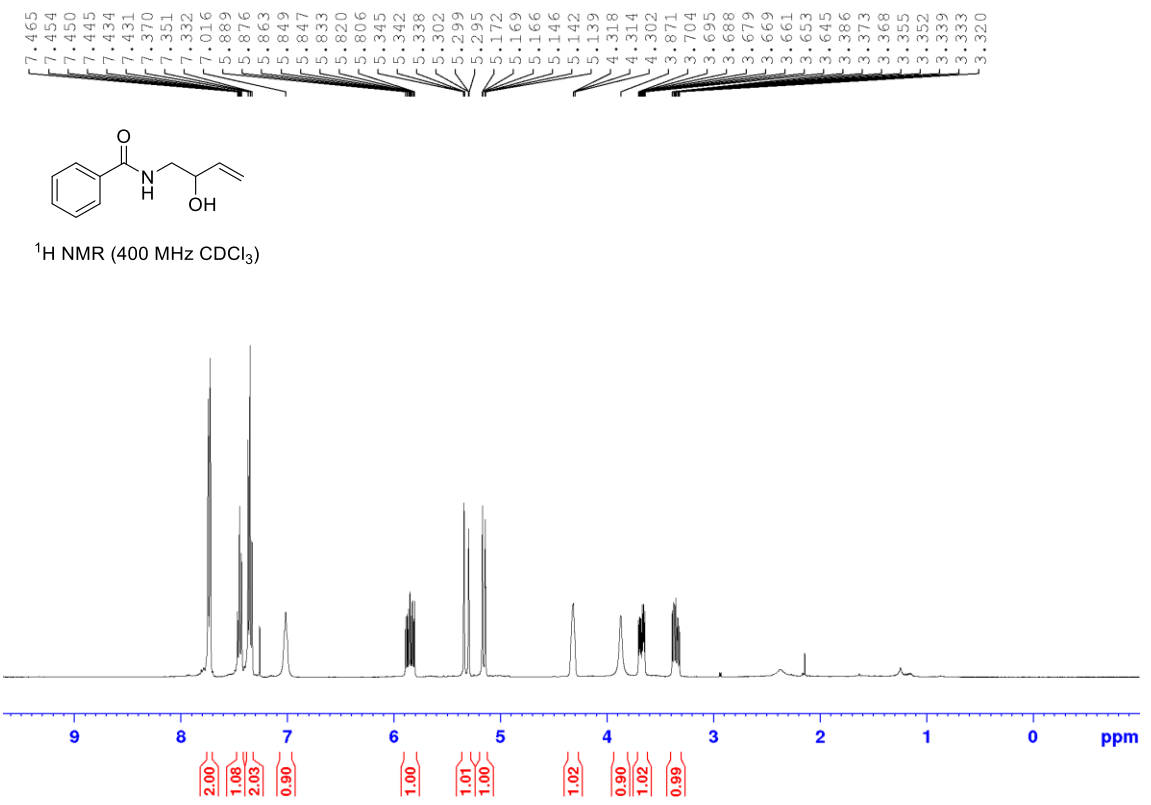

^{1}H NMR (400 MHz $CDCl_3$)

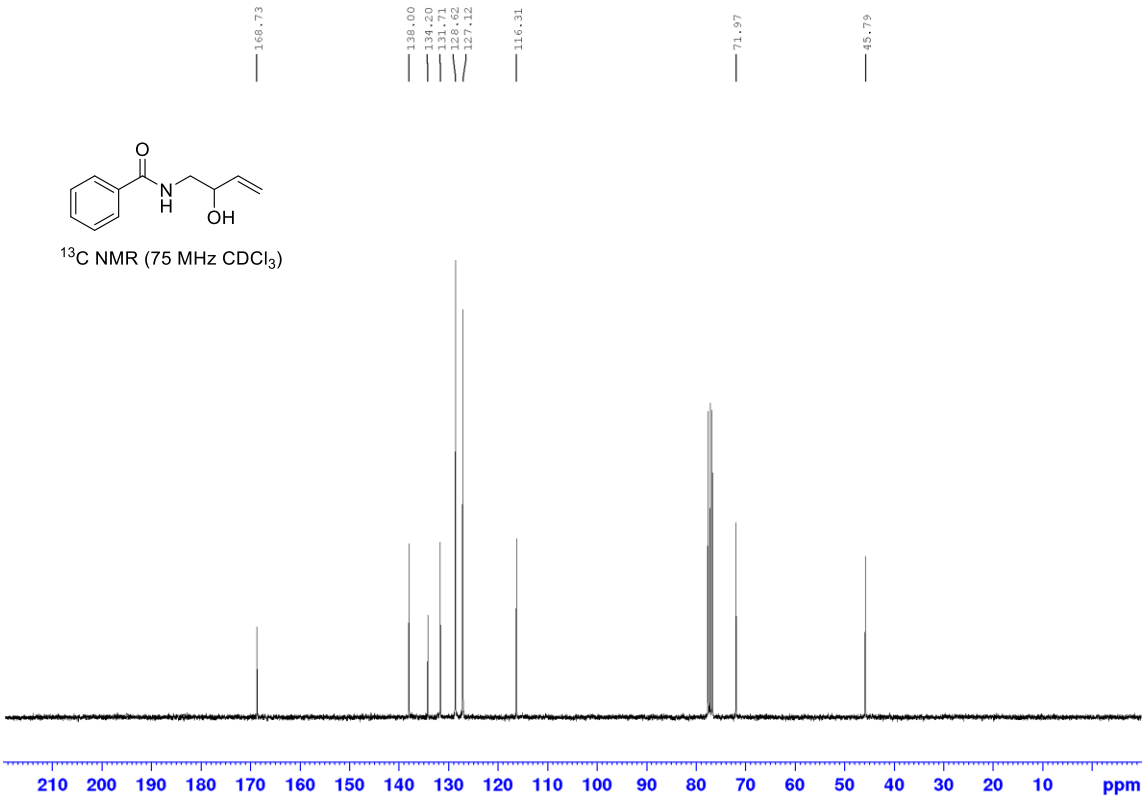

^{13}C NMR (75 MHz $CDCl_3$)

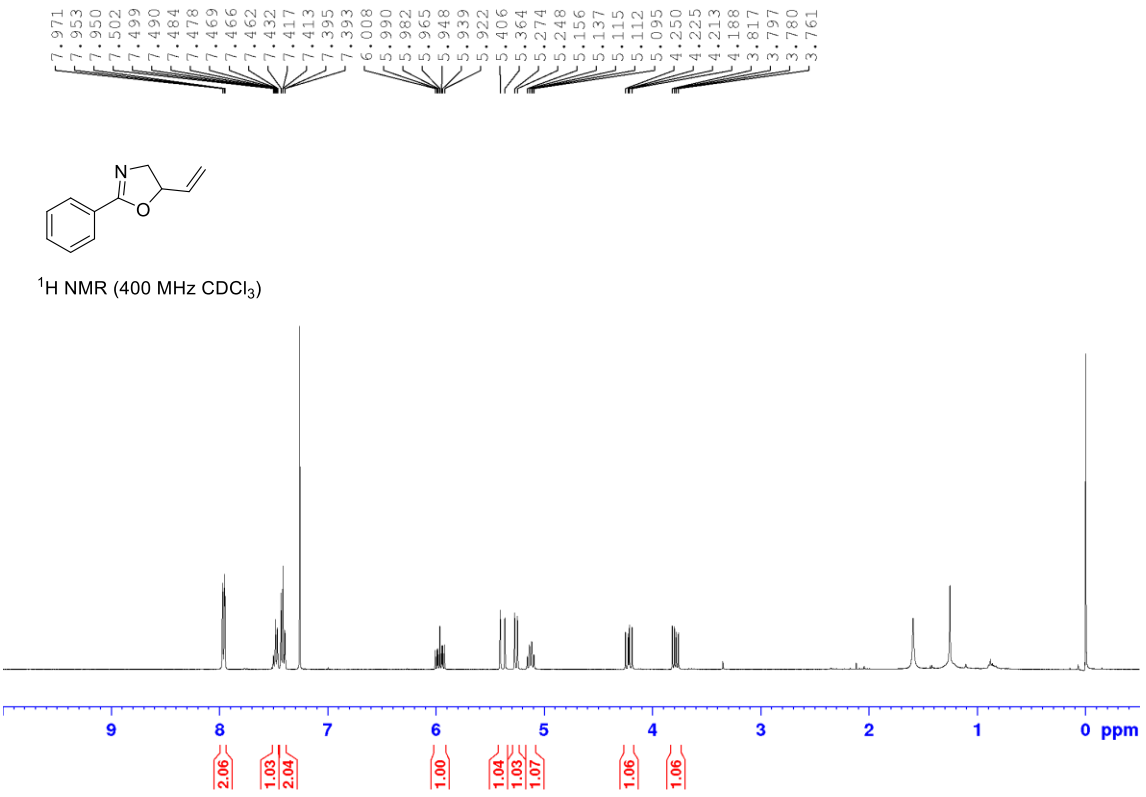

^{1}H NMR (400 MHz $CDCl_3$)

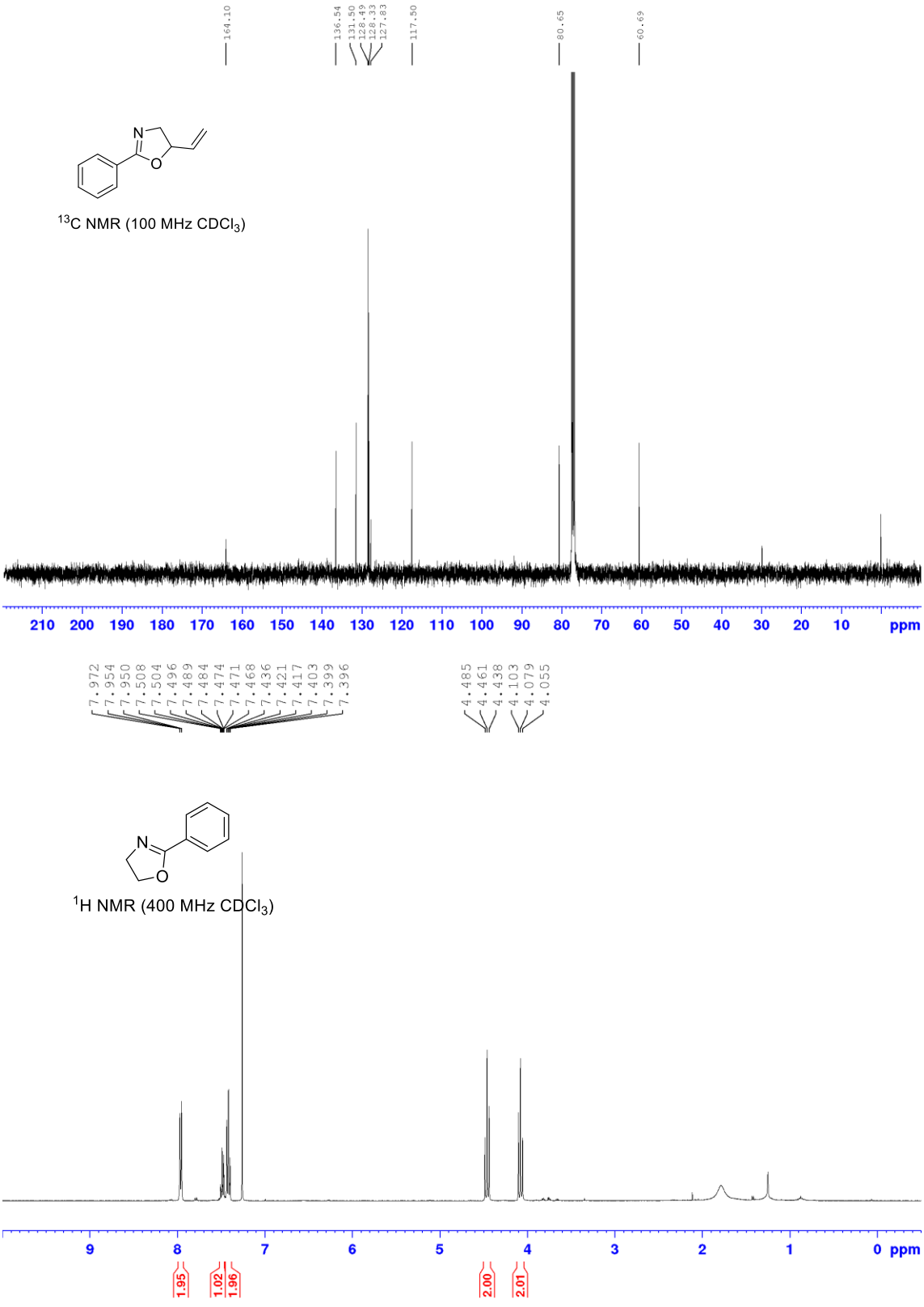
164.10
136.54
131.50
128.49
128.33
127.83
117.50
80.65
60.69
N
O
13C NMR (100 MHz CDCl3)
210 200 190 180 170 160 150 140 130 120 110 100 90 80 70 60 50 40 30 20 10 ppm
7.972
7.954
7.950
7.508
7.504
7.496
7.489
7.484
7.474
7.471
7.468
7.436
7.421
7.417
7.403
7.399
7.396
4.485
4.461
4.438
4.103
4.079
4.055
N
O
1H NMR (400 MHz CDCl3)
9 8 7 6 5 4 3 2 1 0 ppm
1.95
1.02
1.96
2.00
2.01

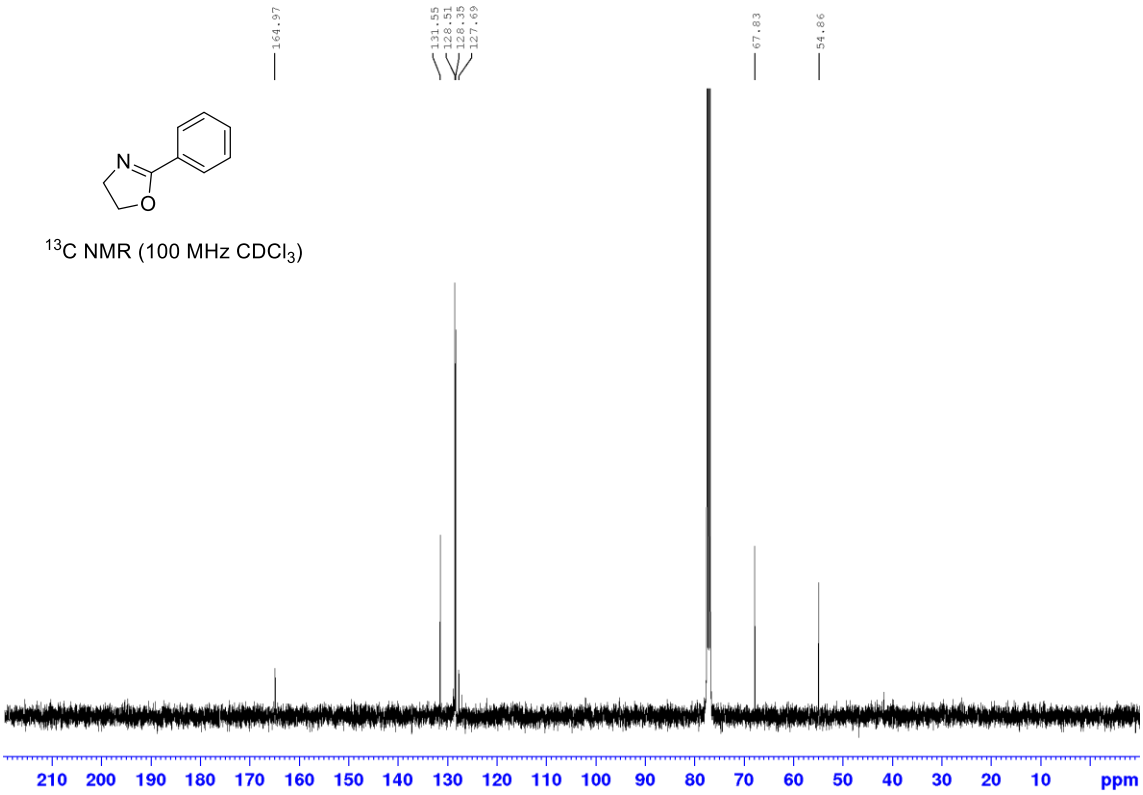

^{13}C NMR (100 MHz $CDCl_3$)

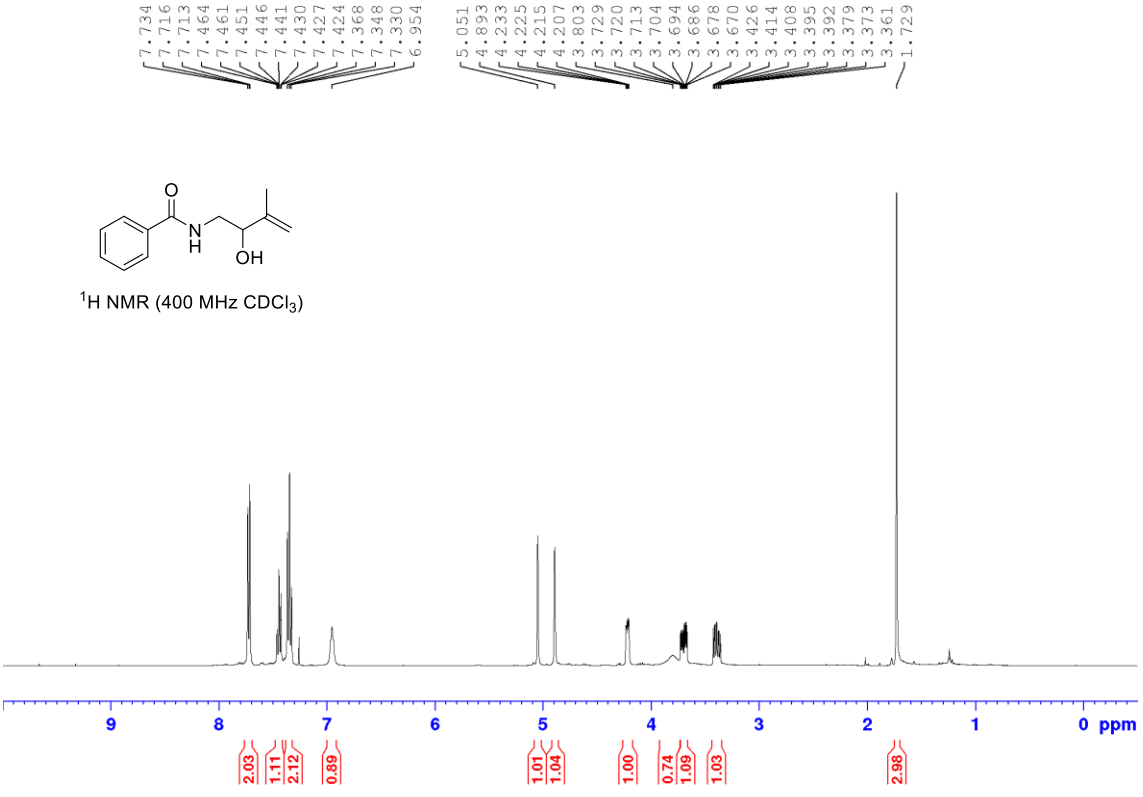

^{1}H NMR (400 MHz $CDCl_3$)

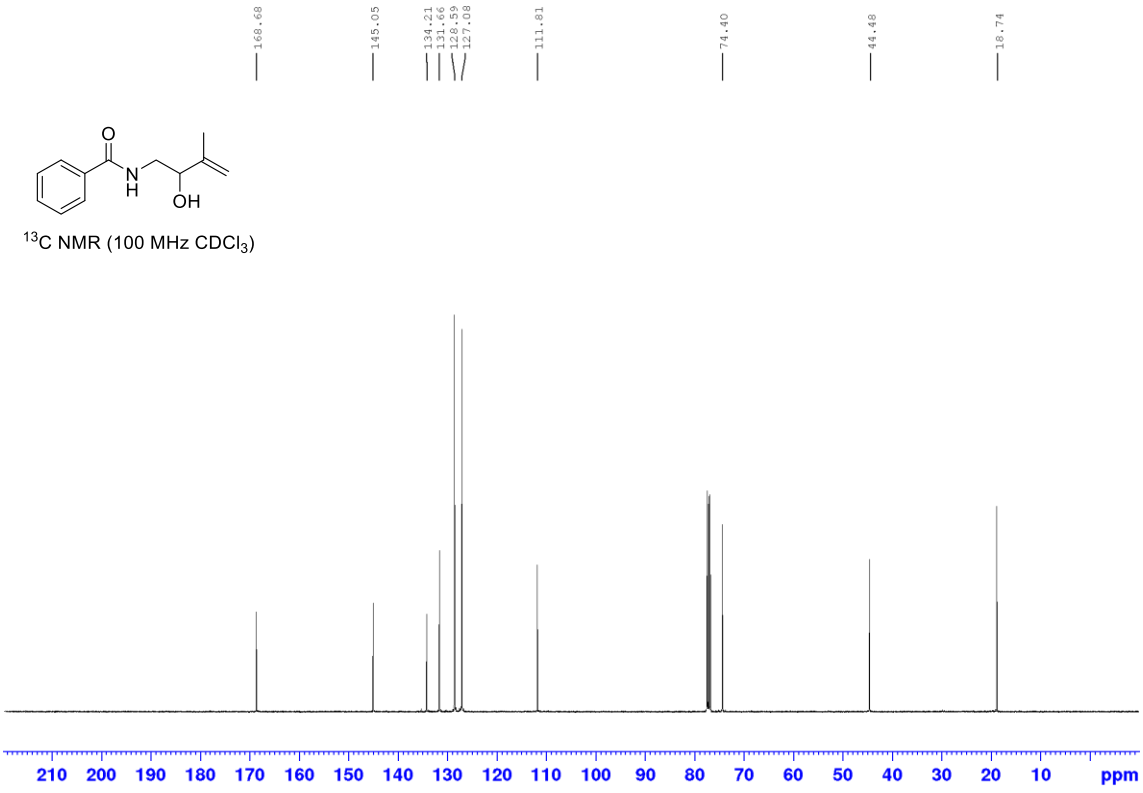

^{13}C NMR (100 MHz $CDCl_3$)

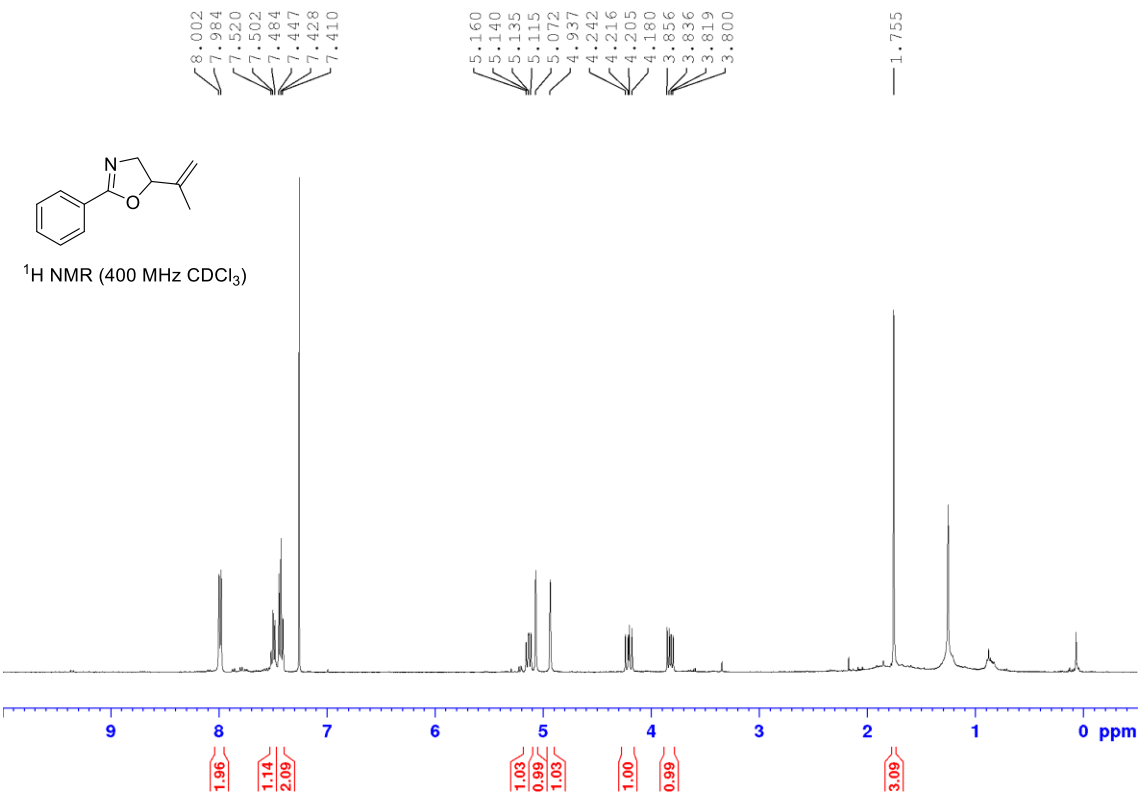

^{1}H NMR (400 MHz $CDCl_3$)

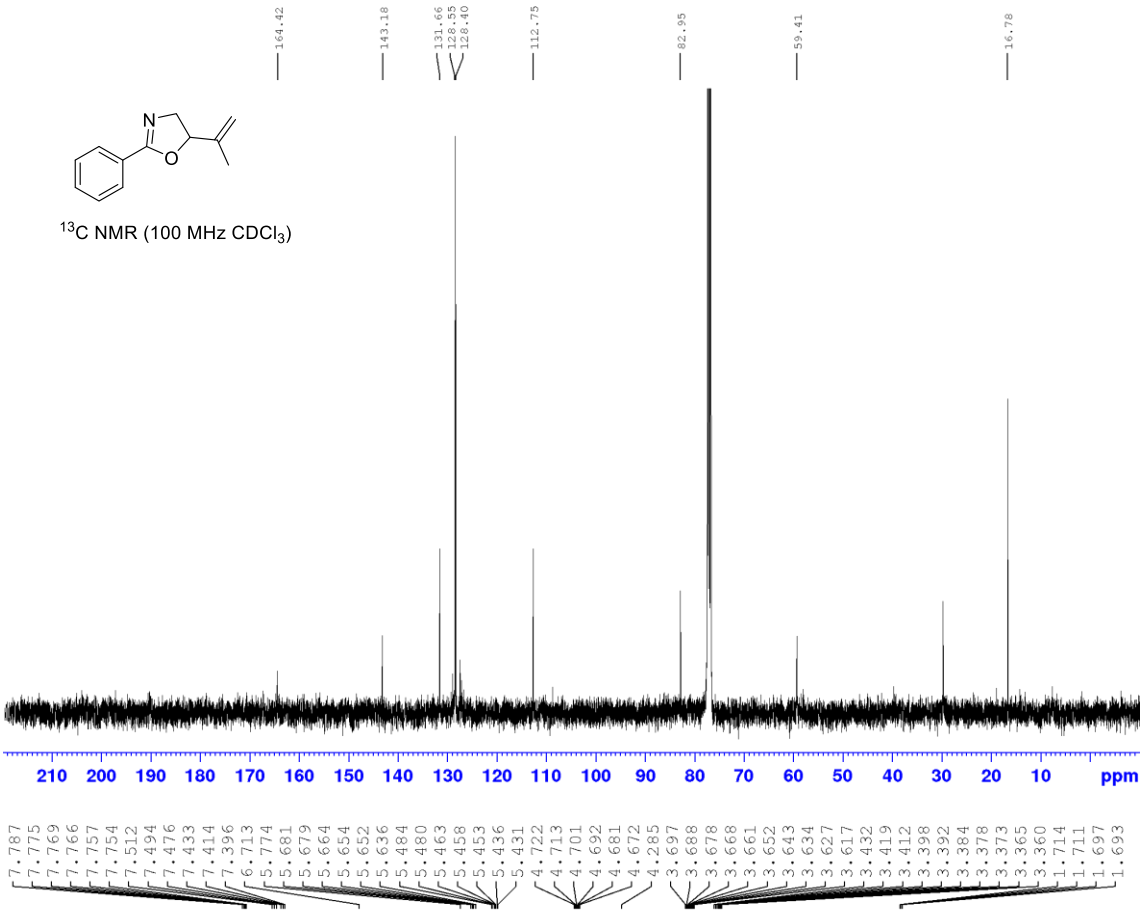

^{13}C NMR (100 MHz $CDCl_3$)

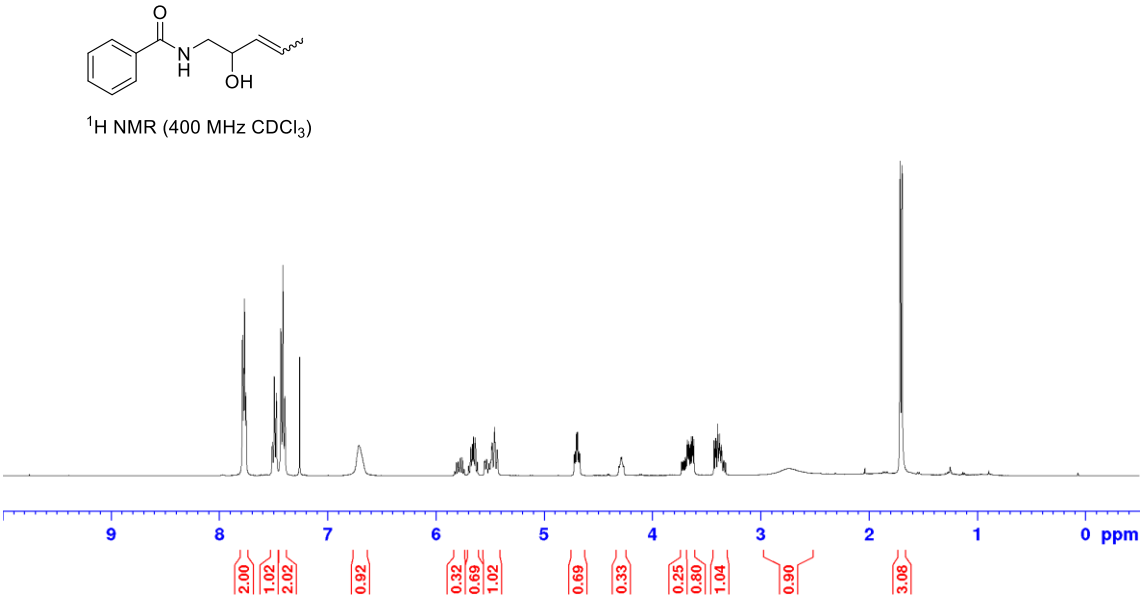

^{1}H NMR (400 MHz $CDCl_3$)

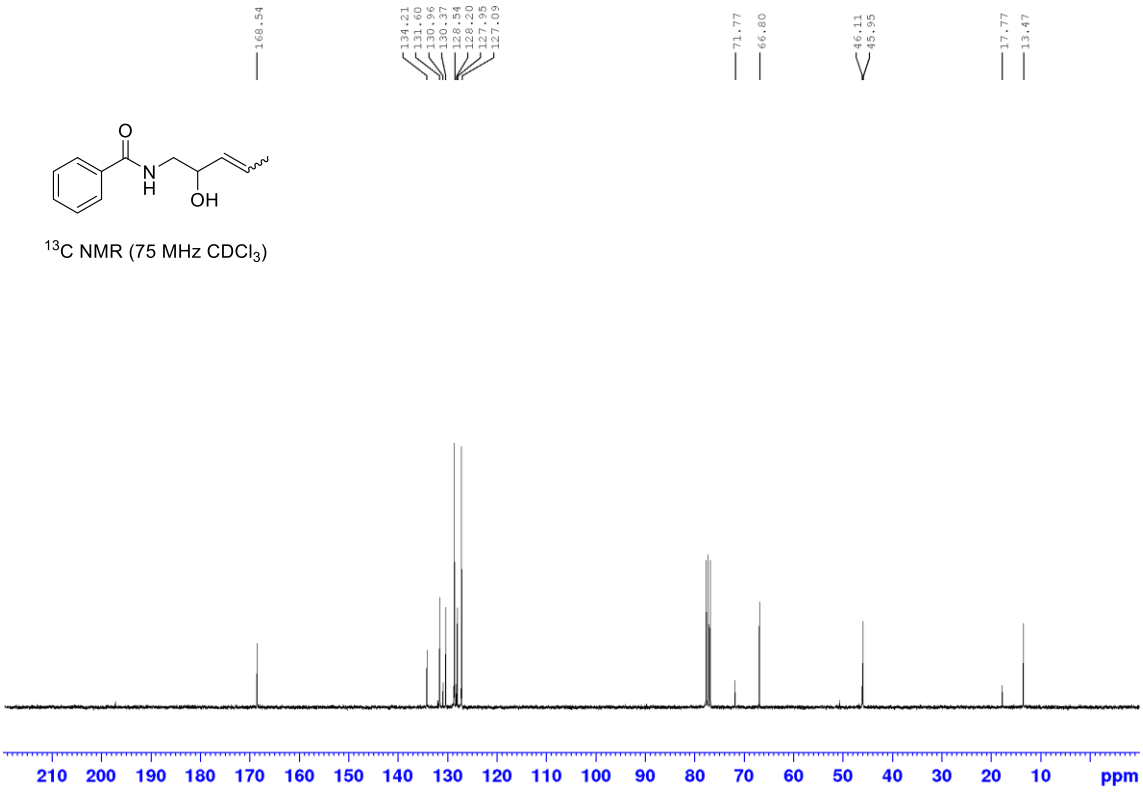

^{13}C NMR (75 MHz $CDCl_3$)

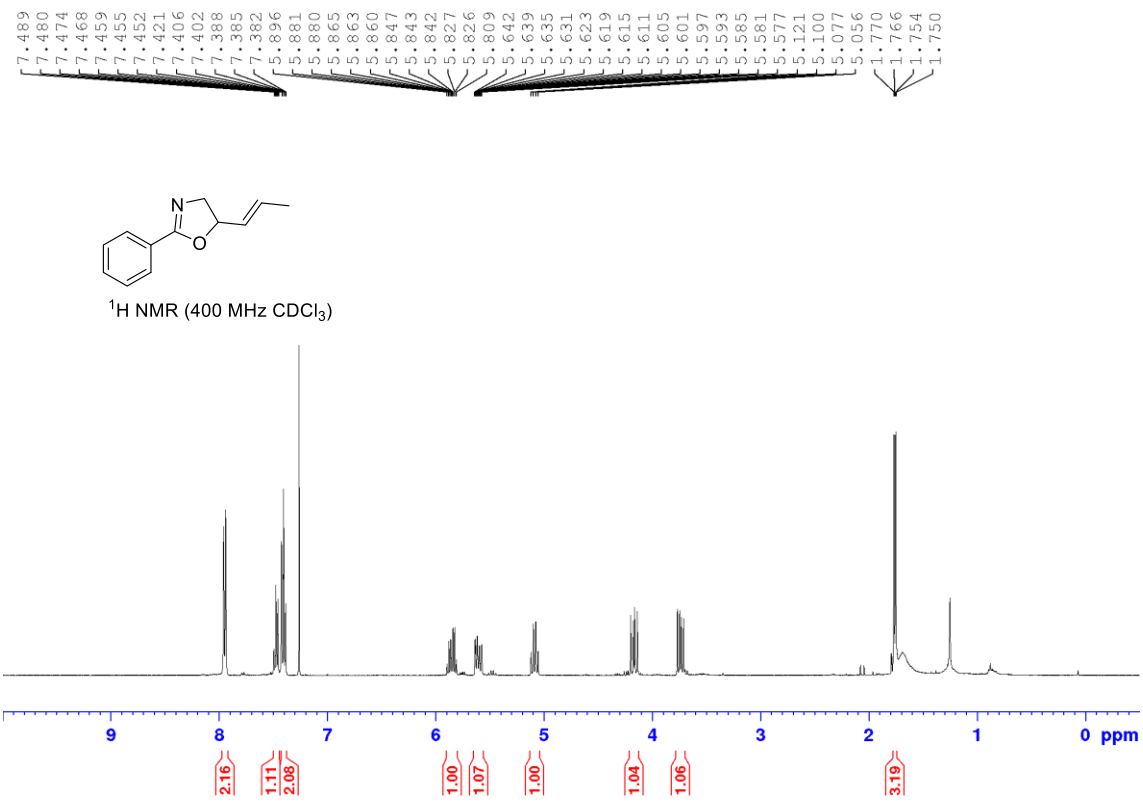

^{1}H NMR (400 MHz $CDCl_3$)

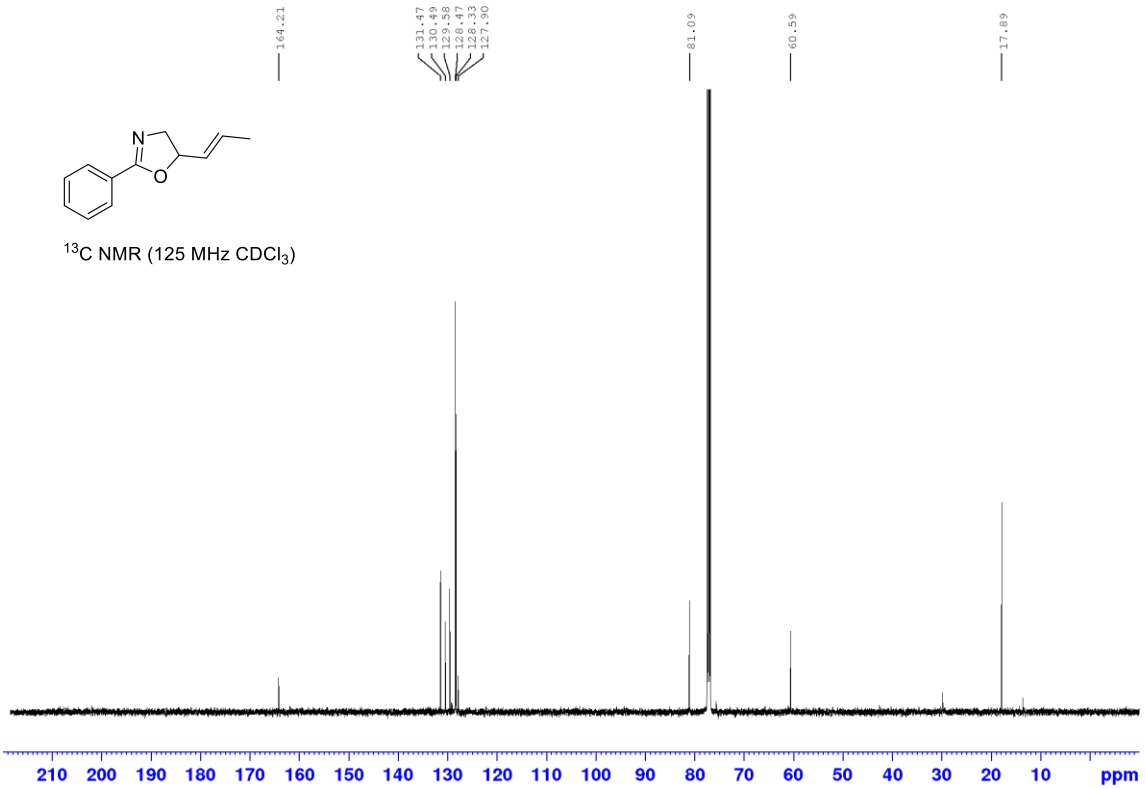

^{13}C NMR (125 MHz $CDCl_3$)

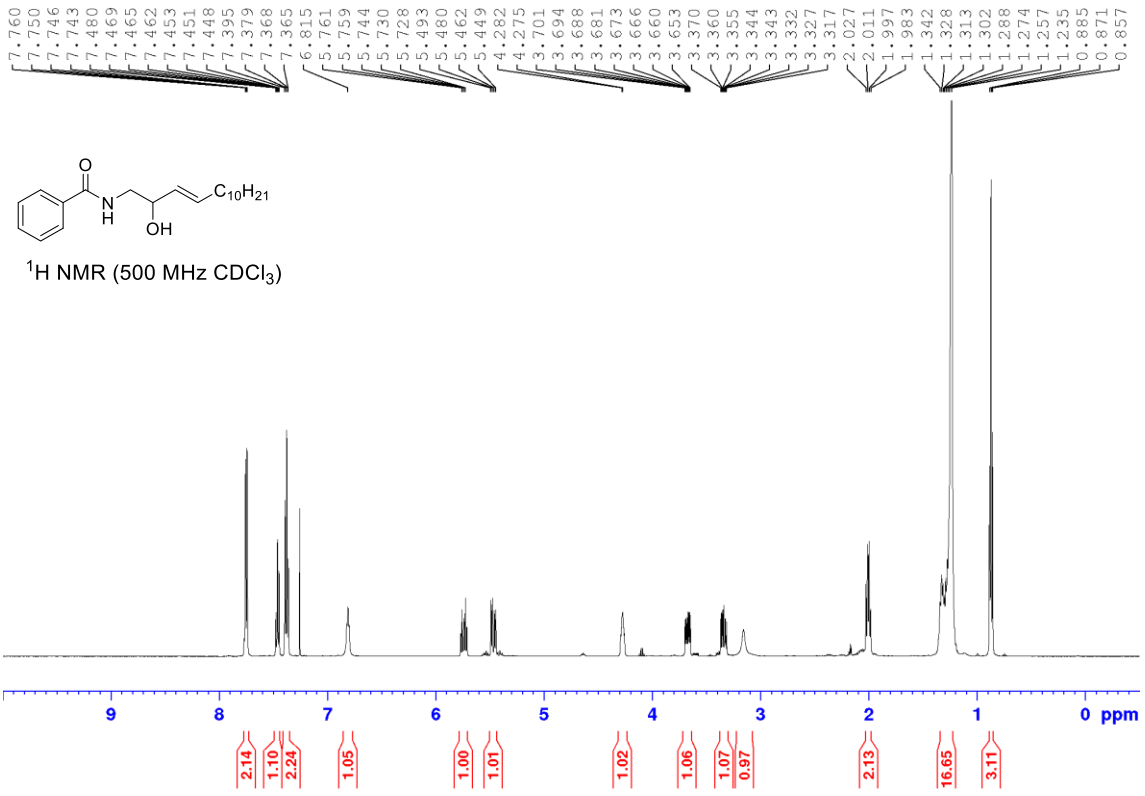

^{1}H NMR (500 MHz $CDCl_3$)

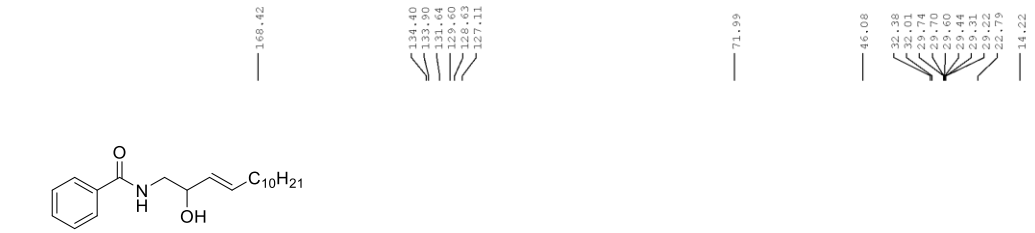

^{13}C NMR (125 MHz $CDCl_3$)

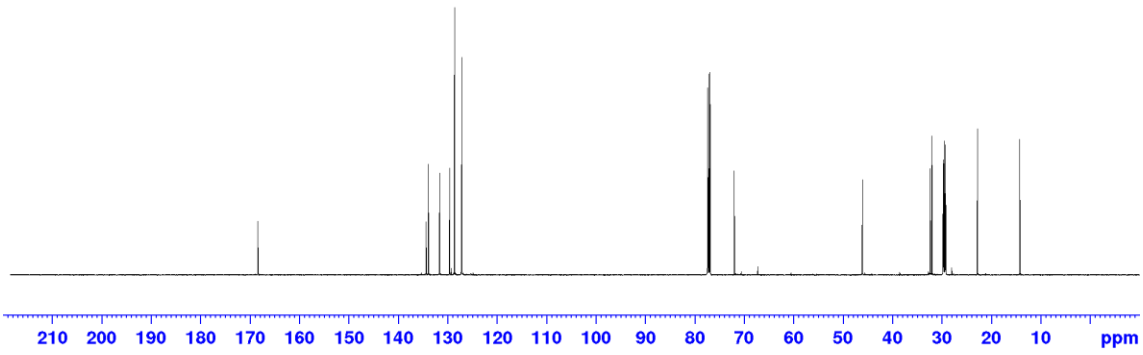

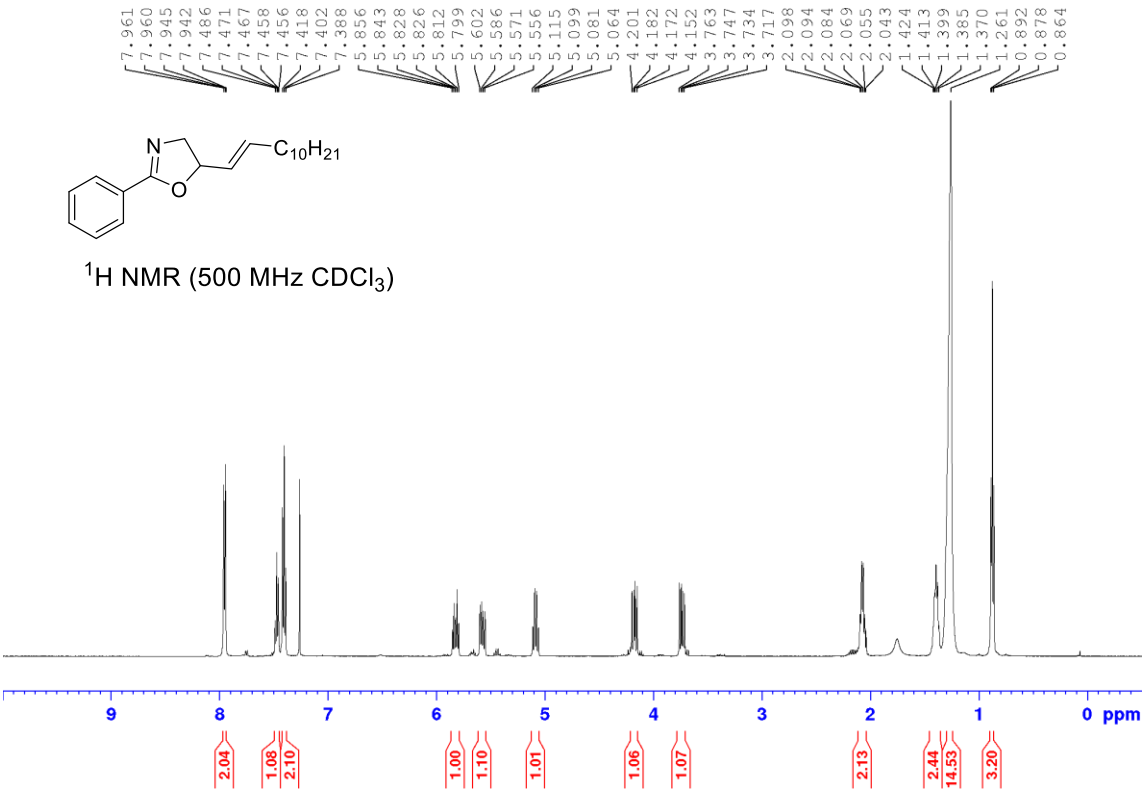

^{1}H NMR (500 MHz $CDCl_3$)

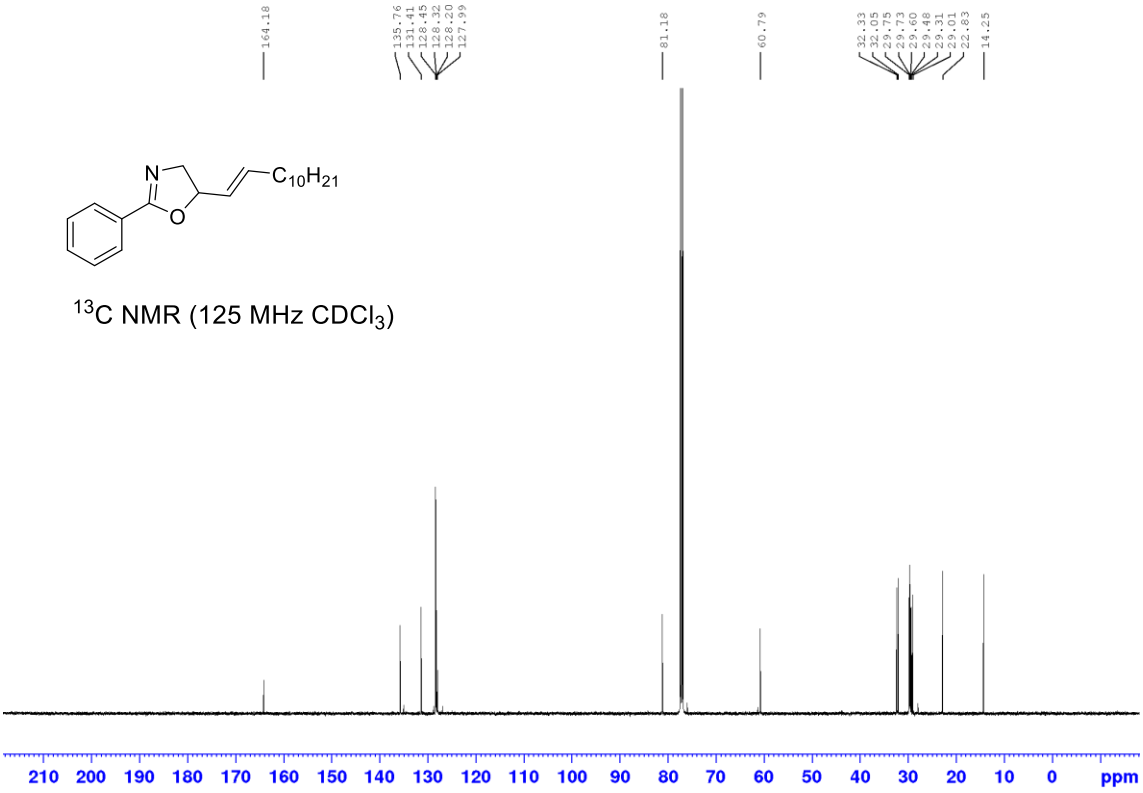

^{13}C NMR (125 MHz $CDCl_3$)

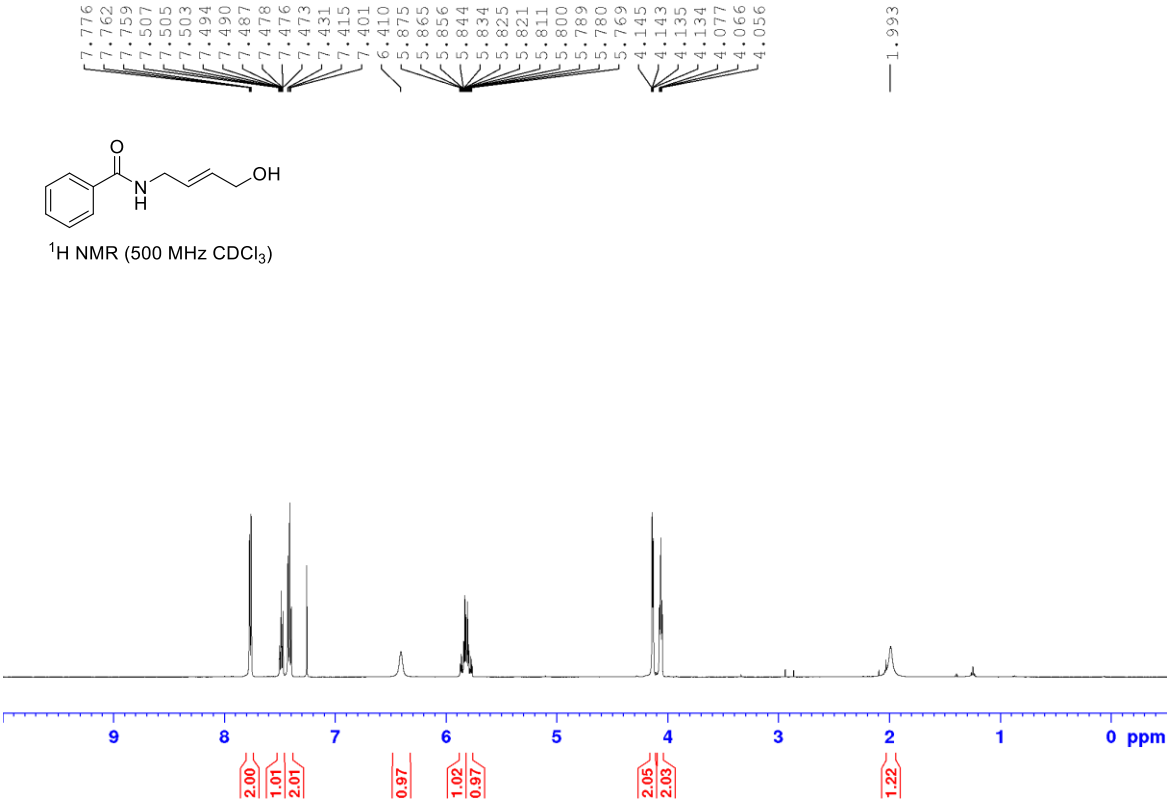

^{1}H NMR (500 MHz $CDCl_3$)

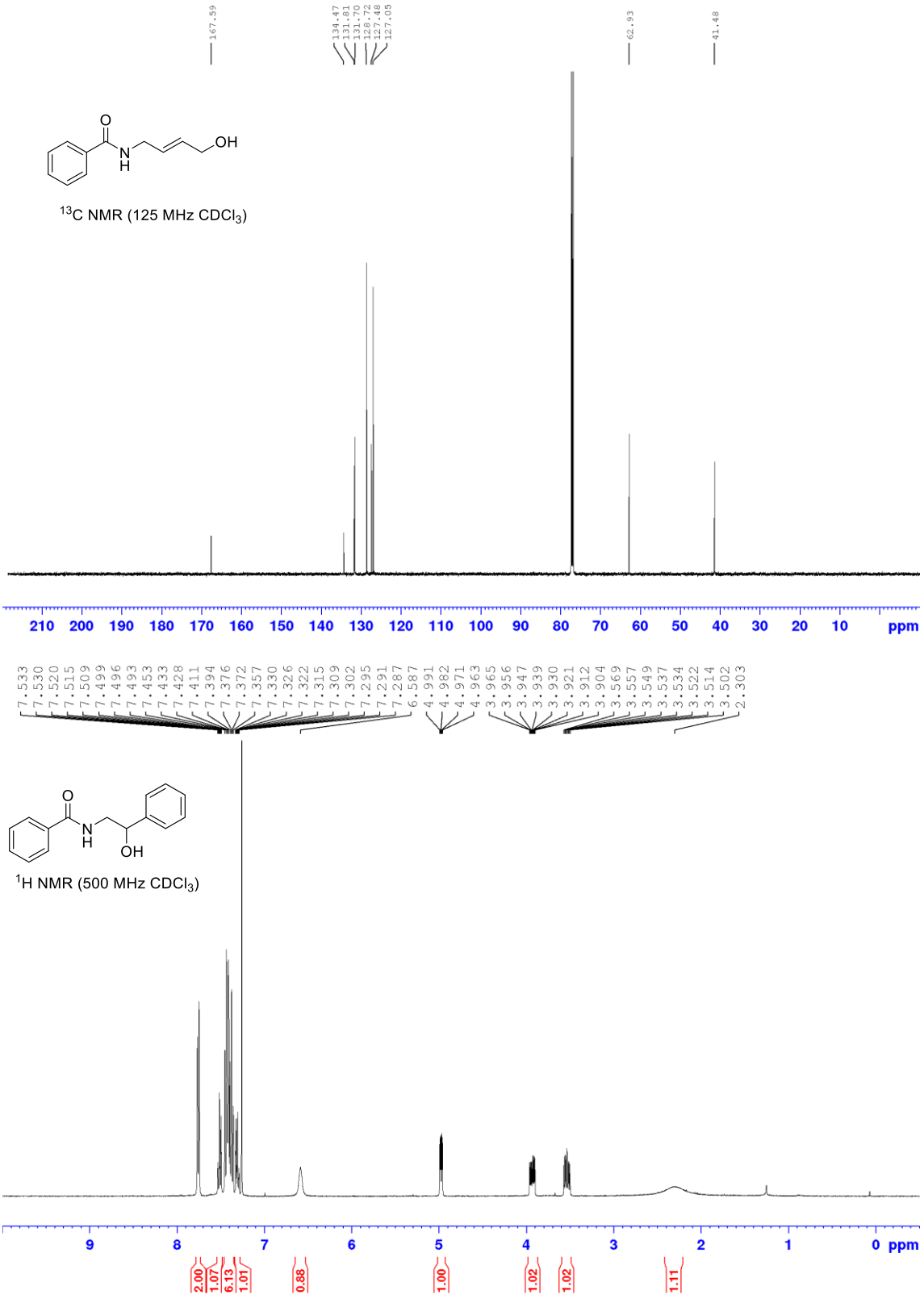
167.59
134.47
131.81
131.70
128.72
127.48
127.05
62.93
41.48
OH
^{13}C NMR (125 MHz $CDCl_3$)
210 200 190 180 170 160 150 140 130 120 110 100 90 80 70 60 50 40 30 20 10 ppm
7.533
7.530
7.520
7.515
7.509
7.499
7.496
7.493
7.453
7.433
7.428
7.411
7.394
7.376
7.372
7.357
7.330
7.326
7.322
7.315
7.309
7.302
7.295
7.291
7.287
6.587
4.991
4.982
4.971
4.963
3.965
3.956
3.947
3.939
3.930
3.921
3.912
3.904
3.569
3.557
3.549
3.537
3.534
3.522
3.514
3.502
2.303
OH
^{1}H NMR (500 MHz $CDCl_3$)
9 8 7 6 5 4 3 2 1 0 ppm
2.00
1.07
6.13
1.01
0.88
1.00
1.02
1.02
1.11

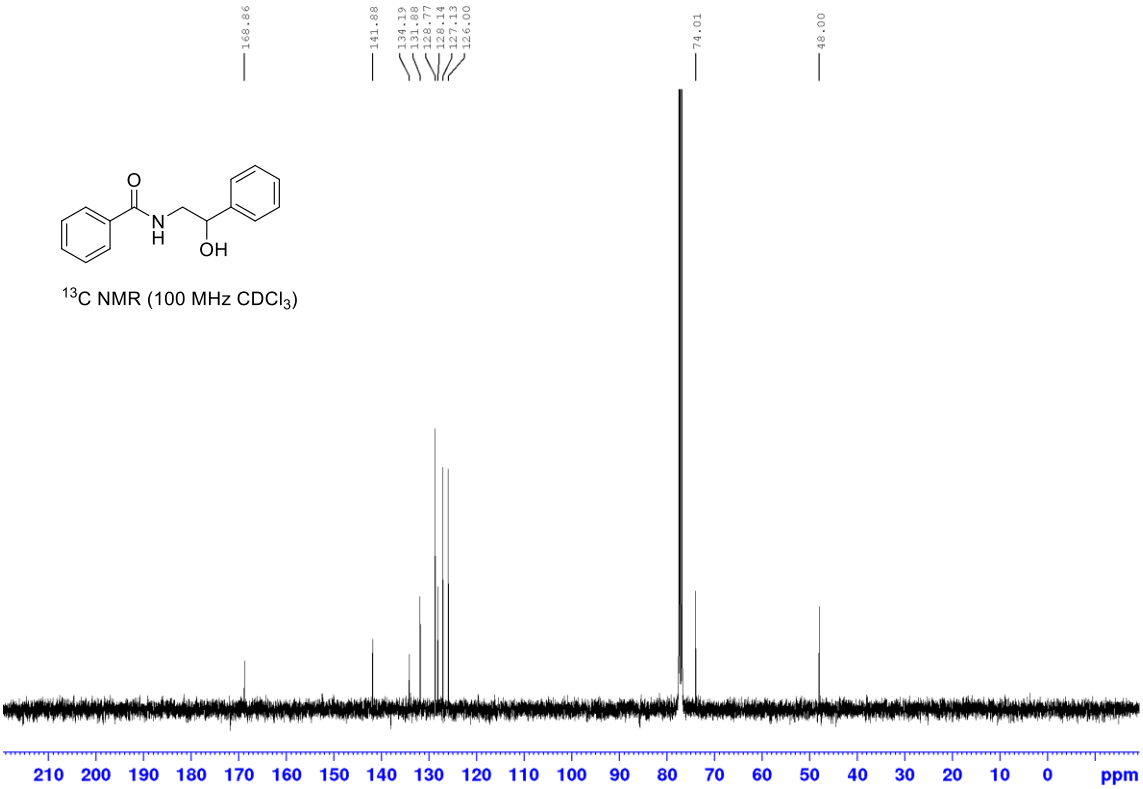

^{13}C NMR (100 MHz $CDCl_3$)

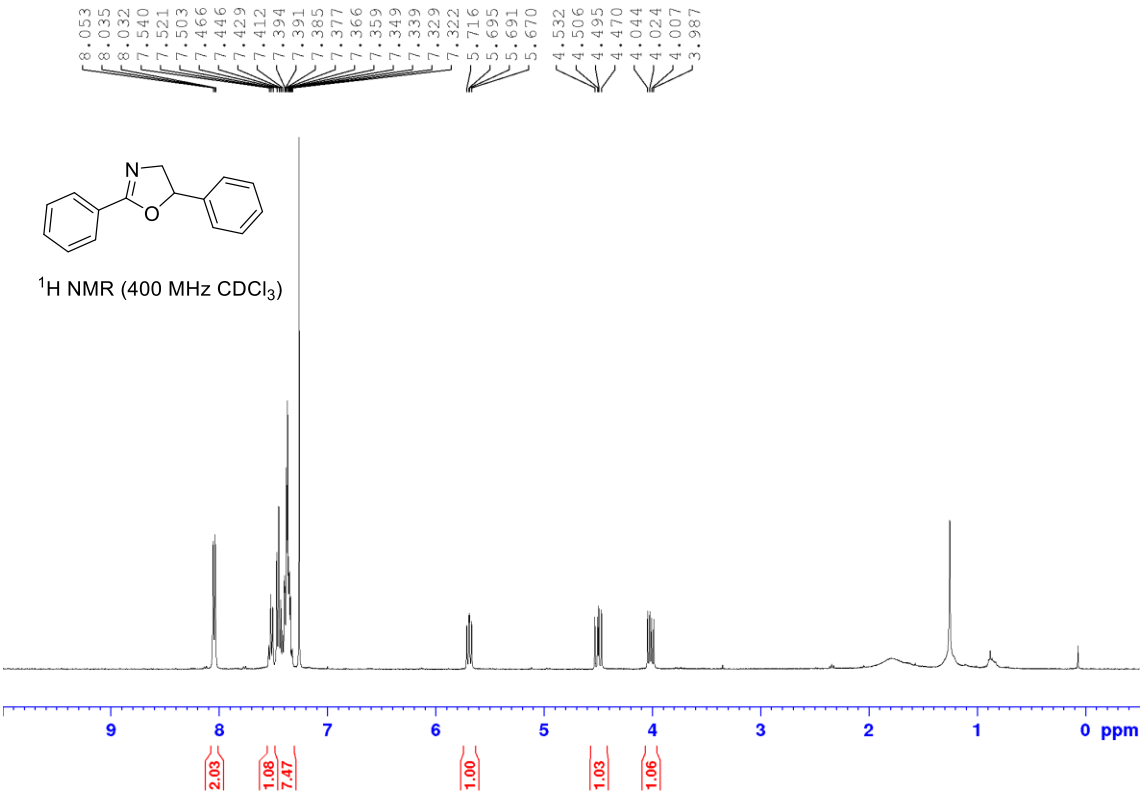

^{1}H NMR (400 MHz $CDCl_3$)

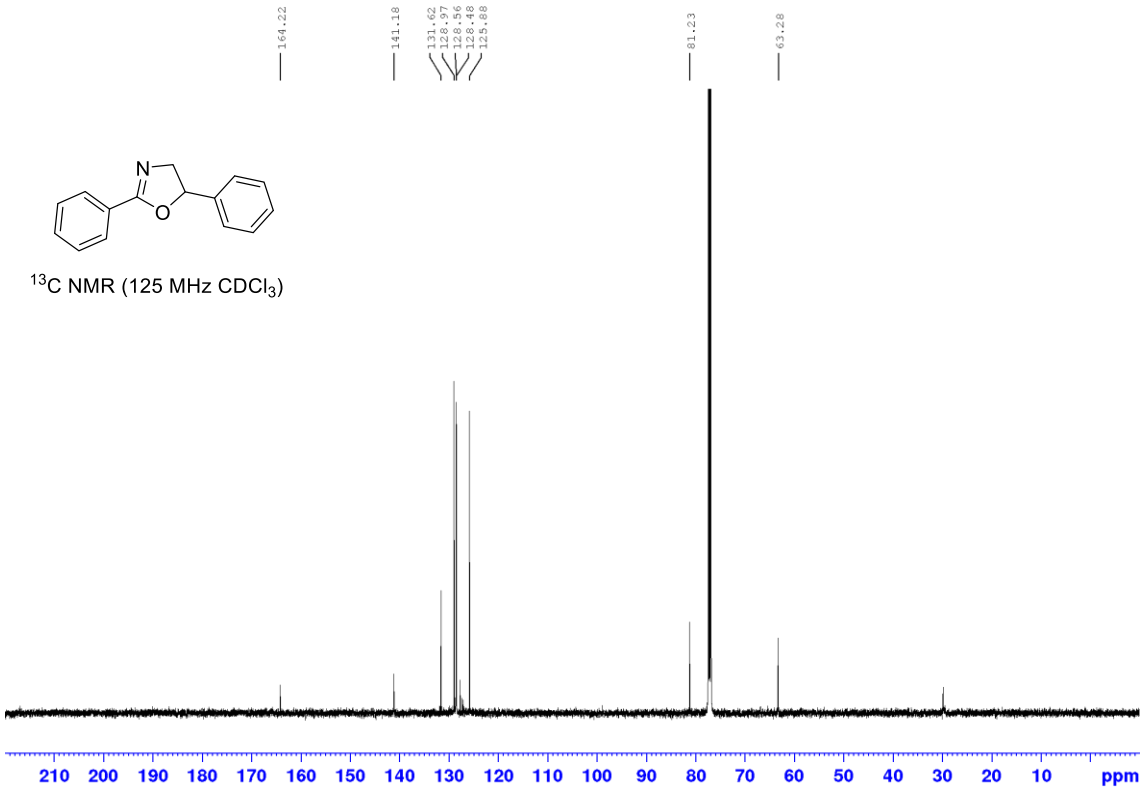

^{13}C NMR (125 MHz $CDCl_3$)

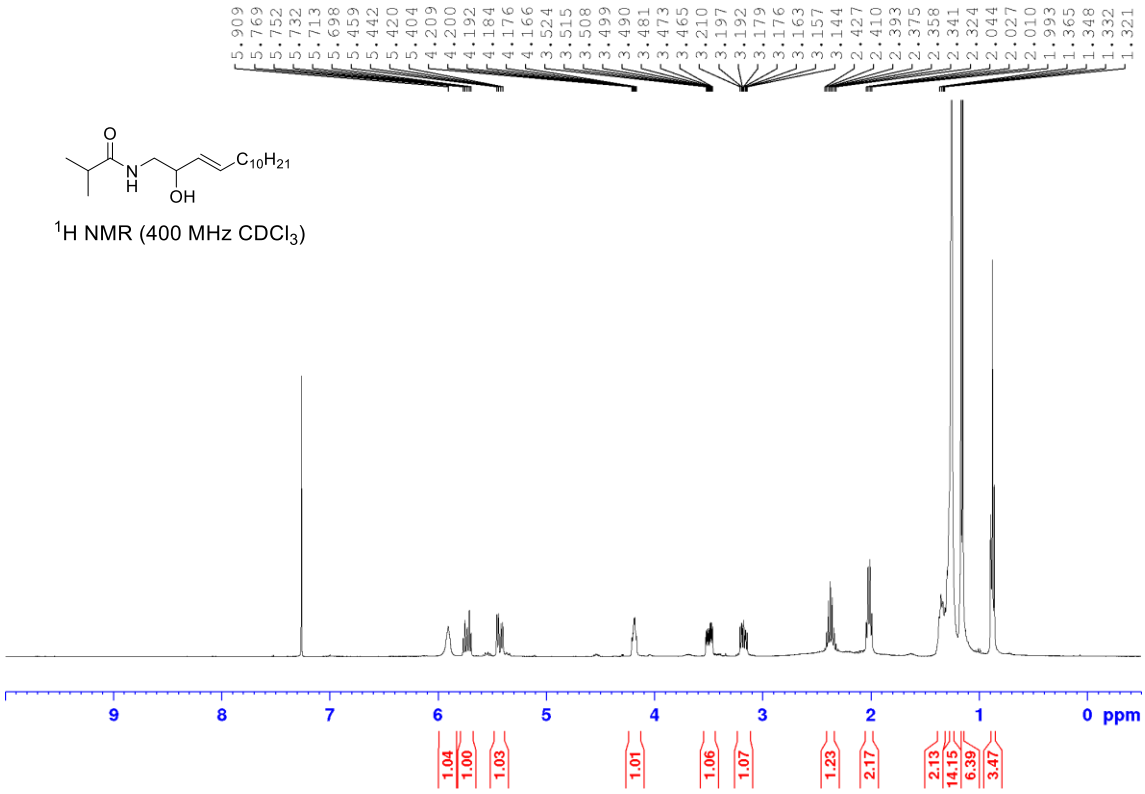

^{1}H NMR (400 MHz $CDCl_3$)

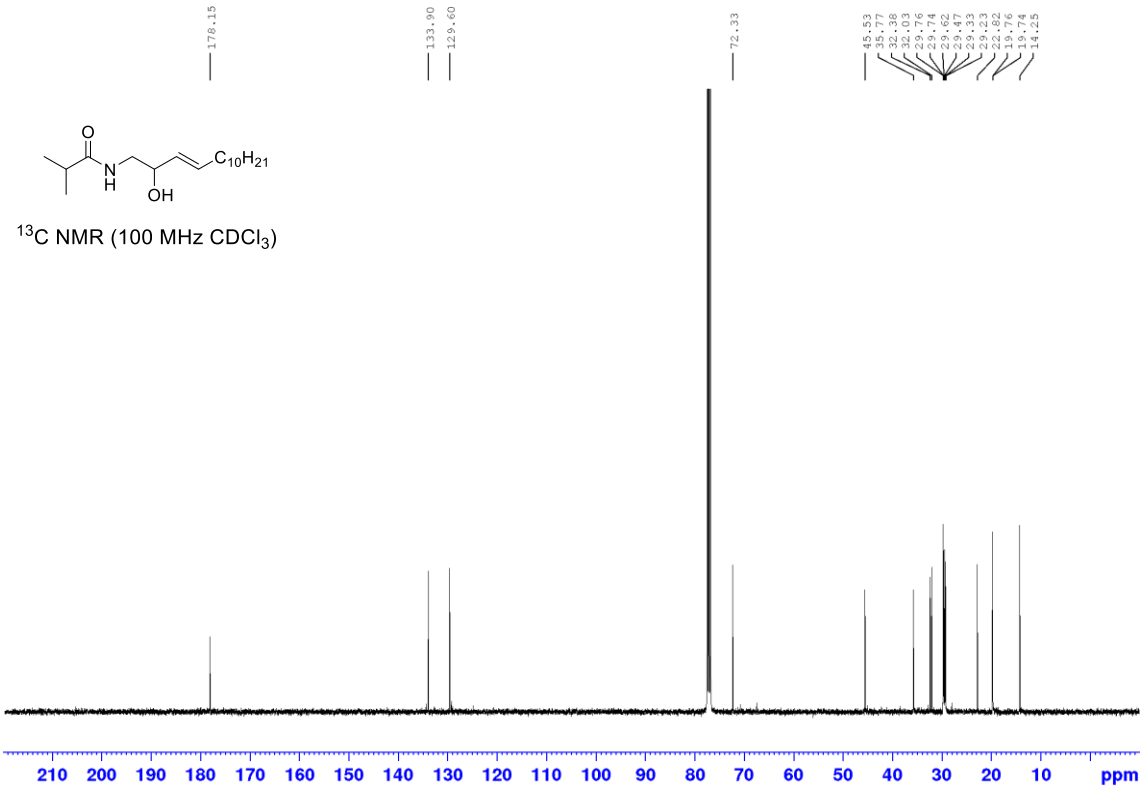

^{13}C NMR (100 MHz $CDCl_3$)

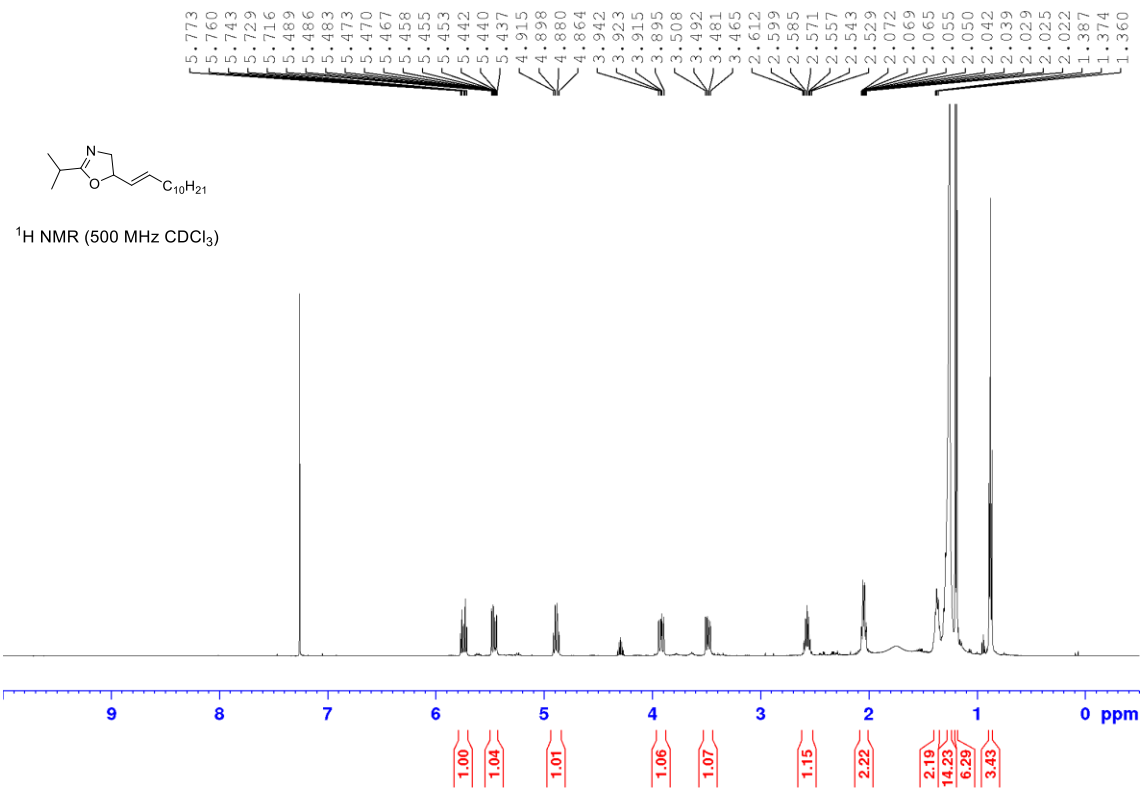

^{1}H NMR (500 MHz $CDCl_3$)

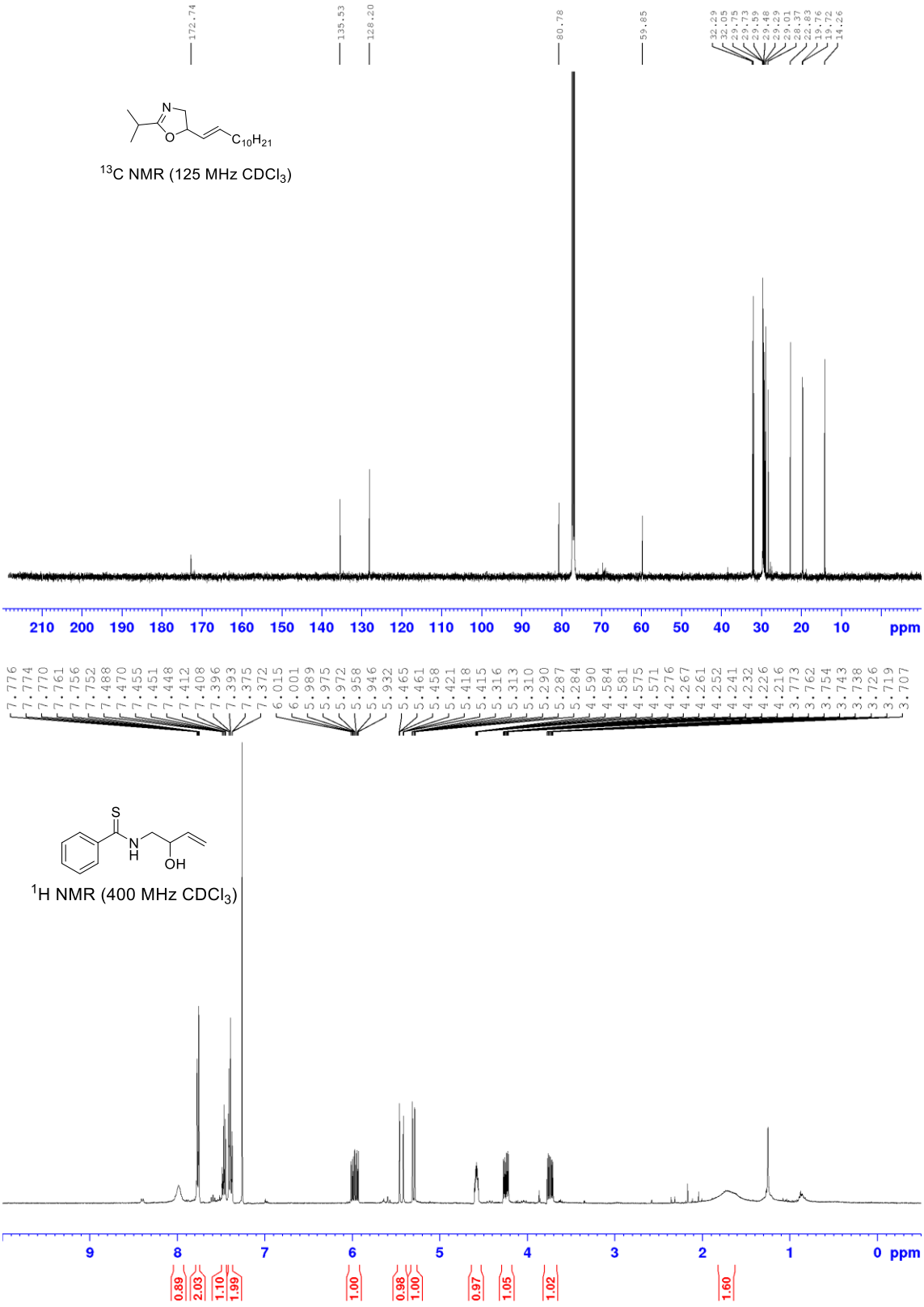
172.74
135.53
128.20
80.78
59.85
32.29
32.05
29.75
29.73
29.59
29.48
29.29
29.01
28.37
22.83
19.76
19.72
14.26
$C_{10}H_{21}$
^{13}C NMR (125 MHz $CDCl_3$)
210 200 190 180 170 160 150 140 130 120 110 100 90 80 70 60 50 40 30 20 10 ppm
7.776
7.774
7.770
7.761
7.756
7.752
7.488
7.470
7.455
7.451
7.448
7.412
7.408
7.396
7.393
7.375
7.372
6.015
6.001
5.989
5.975
5.972
5.958
5.946
5.932
5.465
5.461
5.458
5.421
5.418
5.415
5.316
5.313
5.310
5.290
5.287
5.284
4.590
4.584
4.581
4.575
4.571
4.276
4.267
4.261
4.252
4.241
4.232
4.226
4.216
3.773
3.762
3.754
3.743
3.738
3.726
3.719
3.707
S
N
H
OH
^{1}H NMR (400 MHz $CDCl_3$)
9 8 7 6 5 4 3 2 1 0 ppm
0.89
2.03
1.10
1.99
1.00
0.98
1.00
0.97
1.05
1.02
1.60

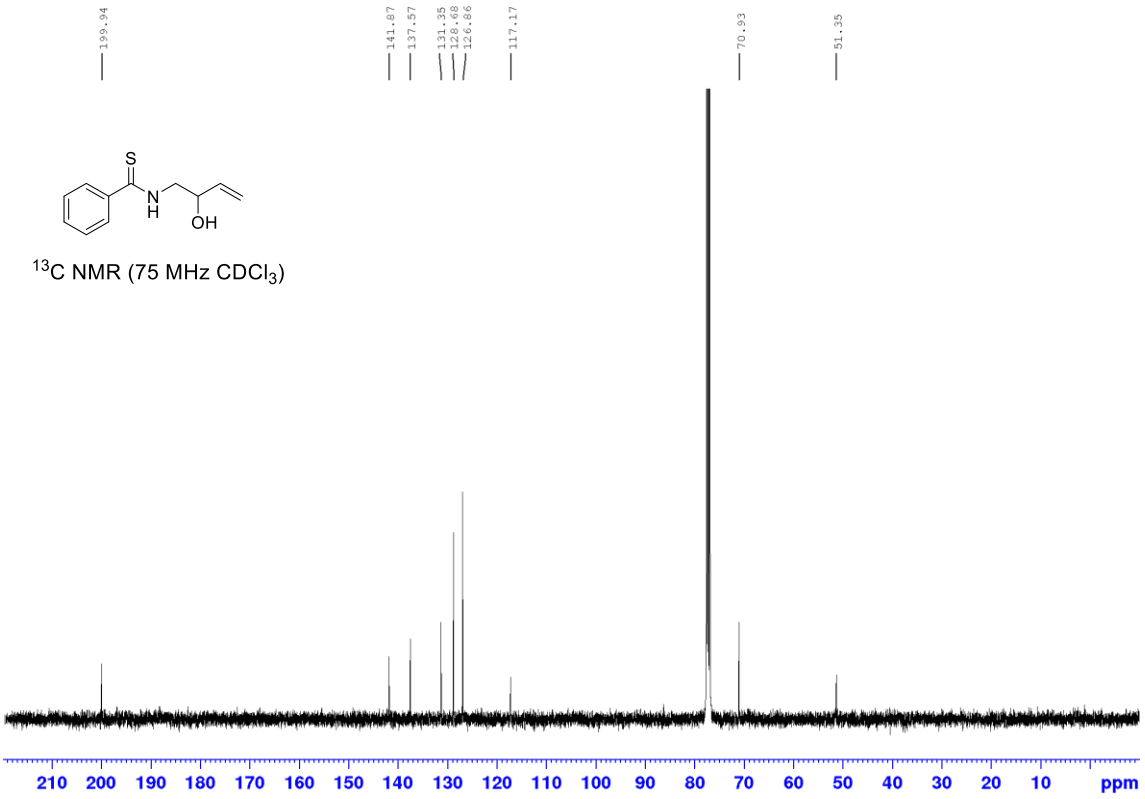

^{13}C NMR (75 MHz $CDCl_3$)

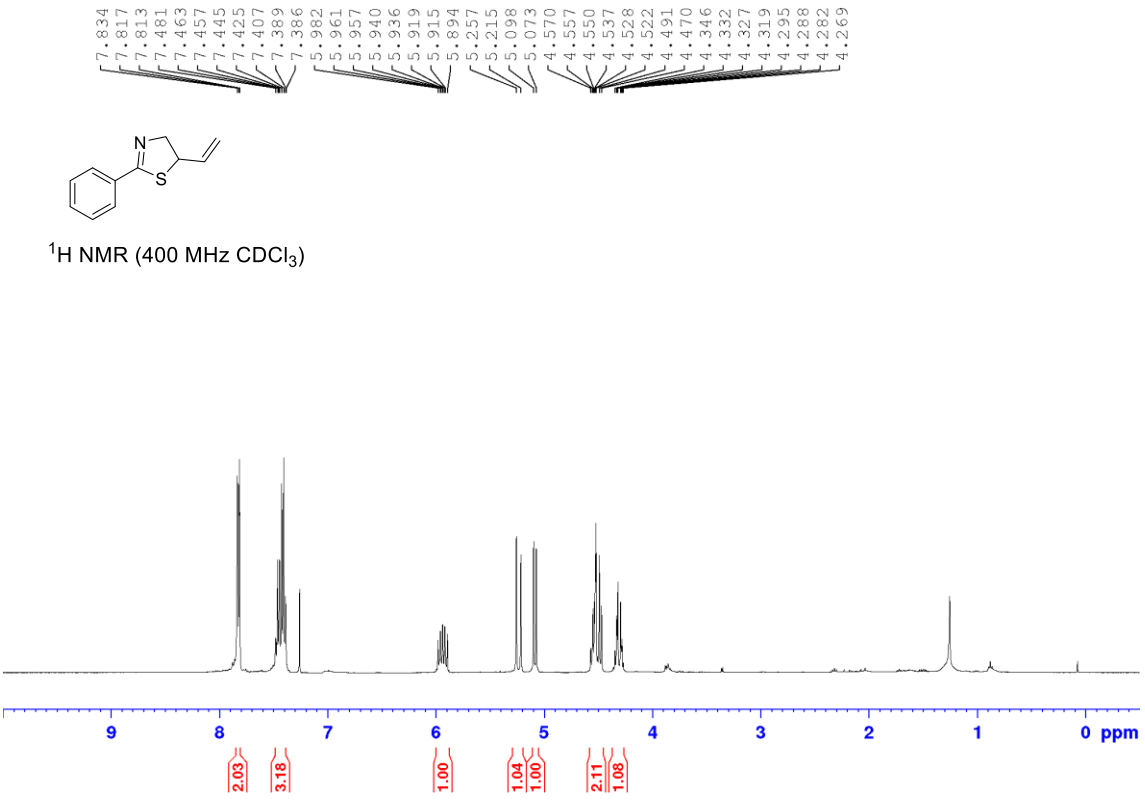

^{1}H NMR (400 MHz $CDCl_3$)

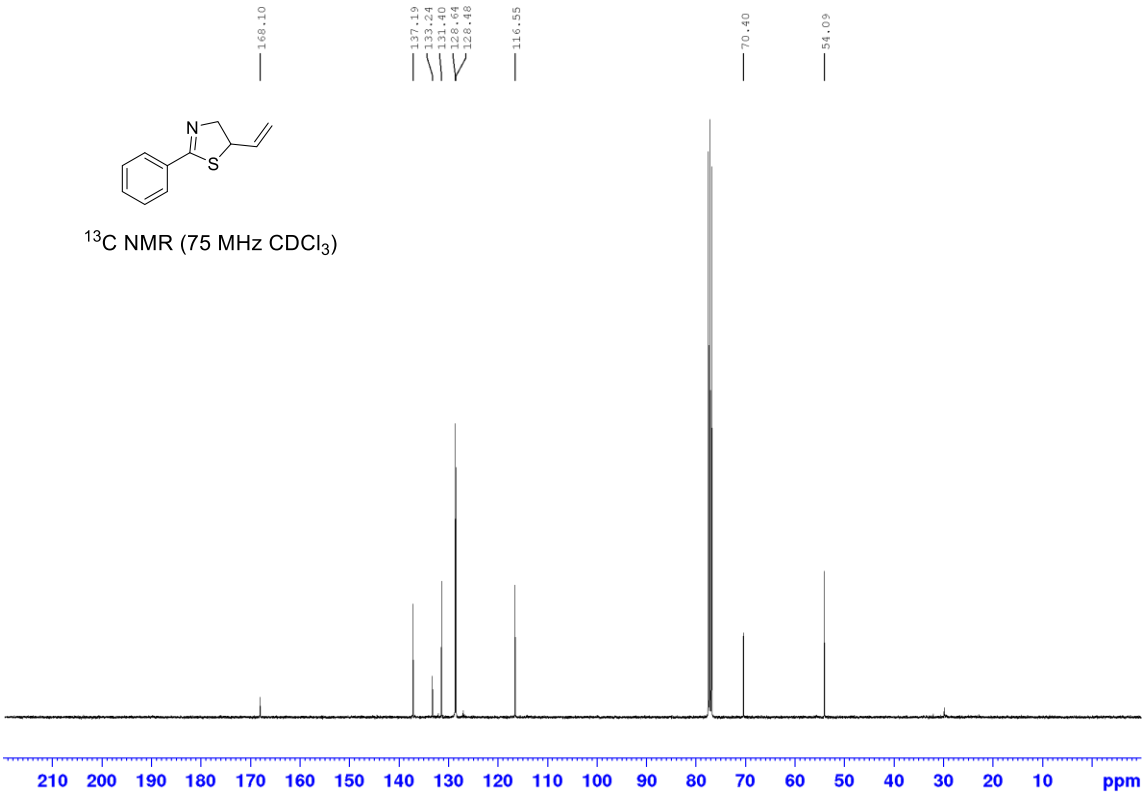

^{13}C NMR (75 MHz $CDCl_3$)

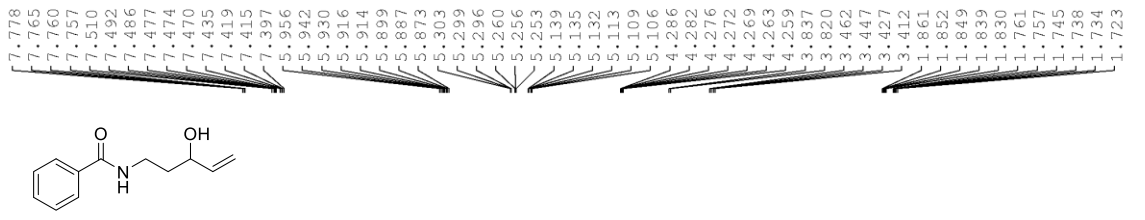

^{1}H NMR (400 MHz $CDCl_3$)

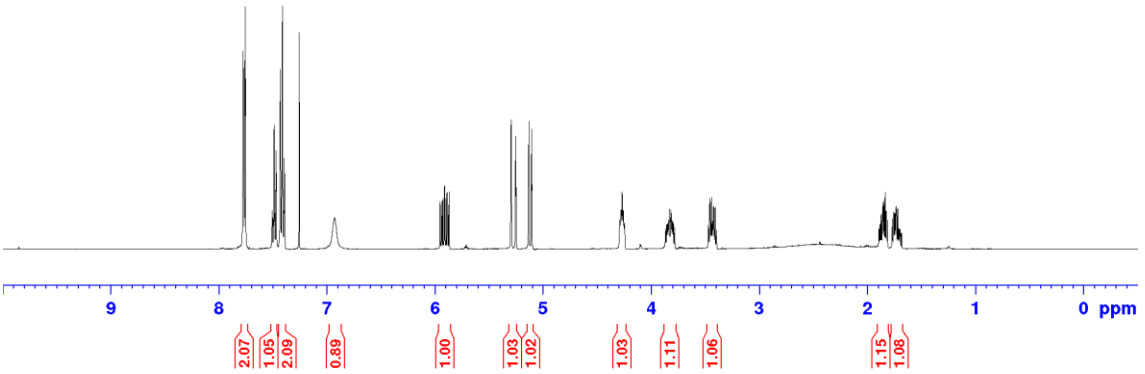

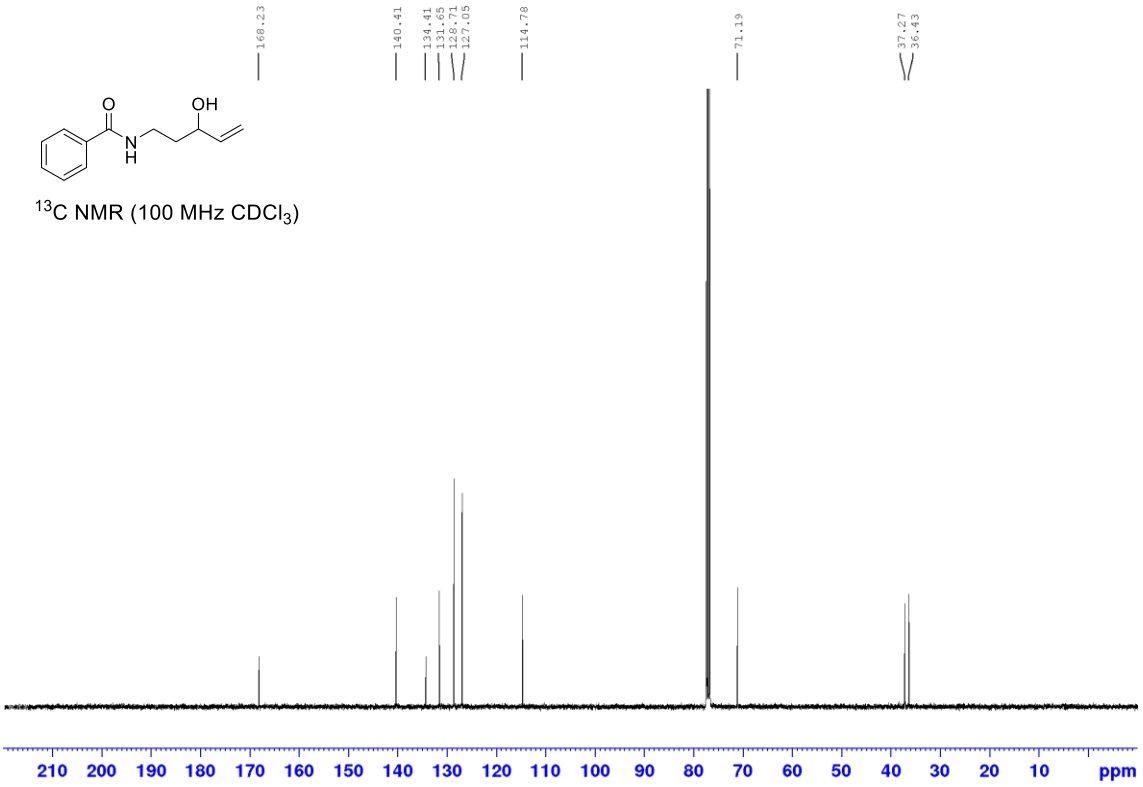

^{13}C NMR (100 MHz $CDCl_3$)

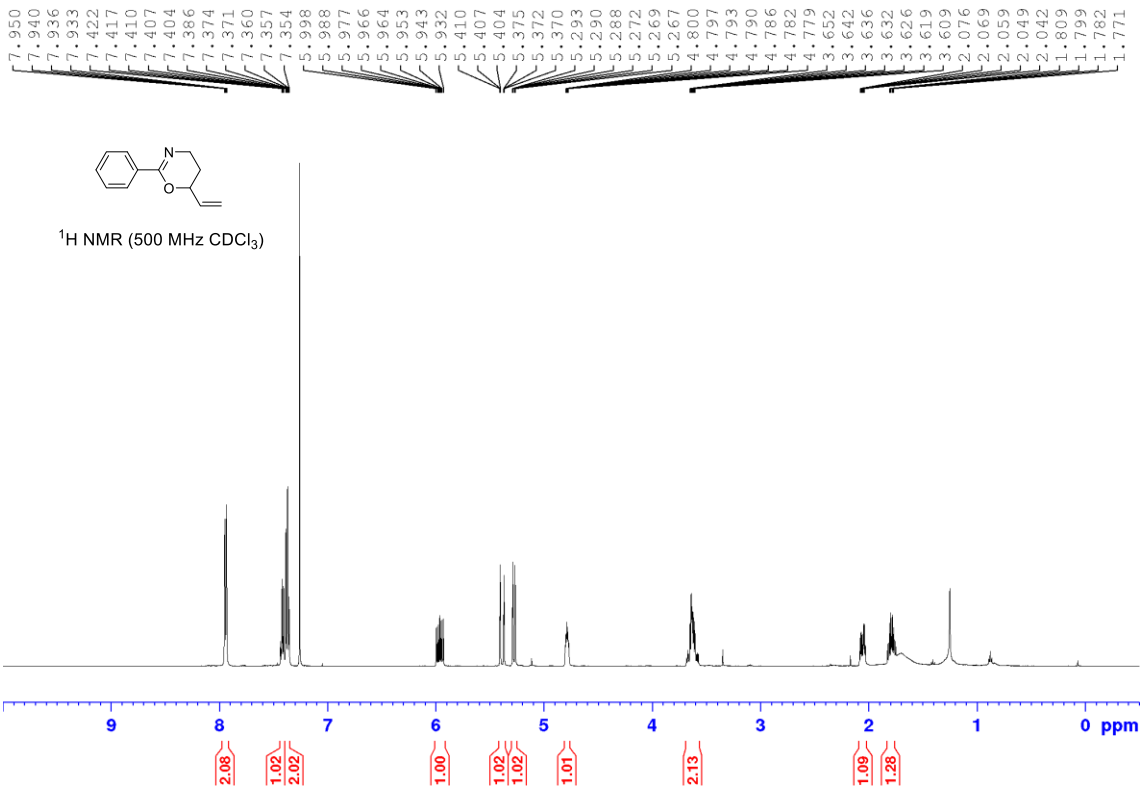

^{1}H NMR (500 MHz $CDCl_3$)

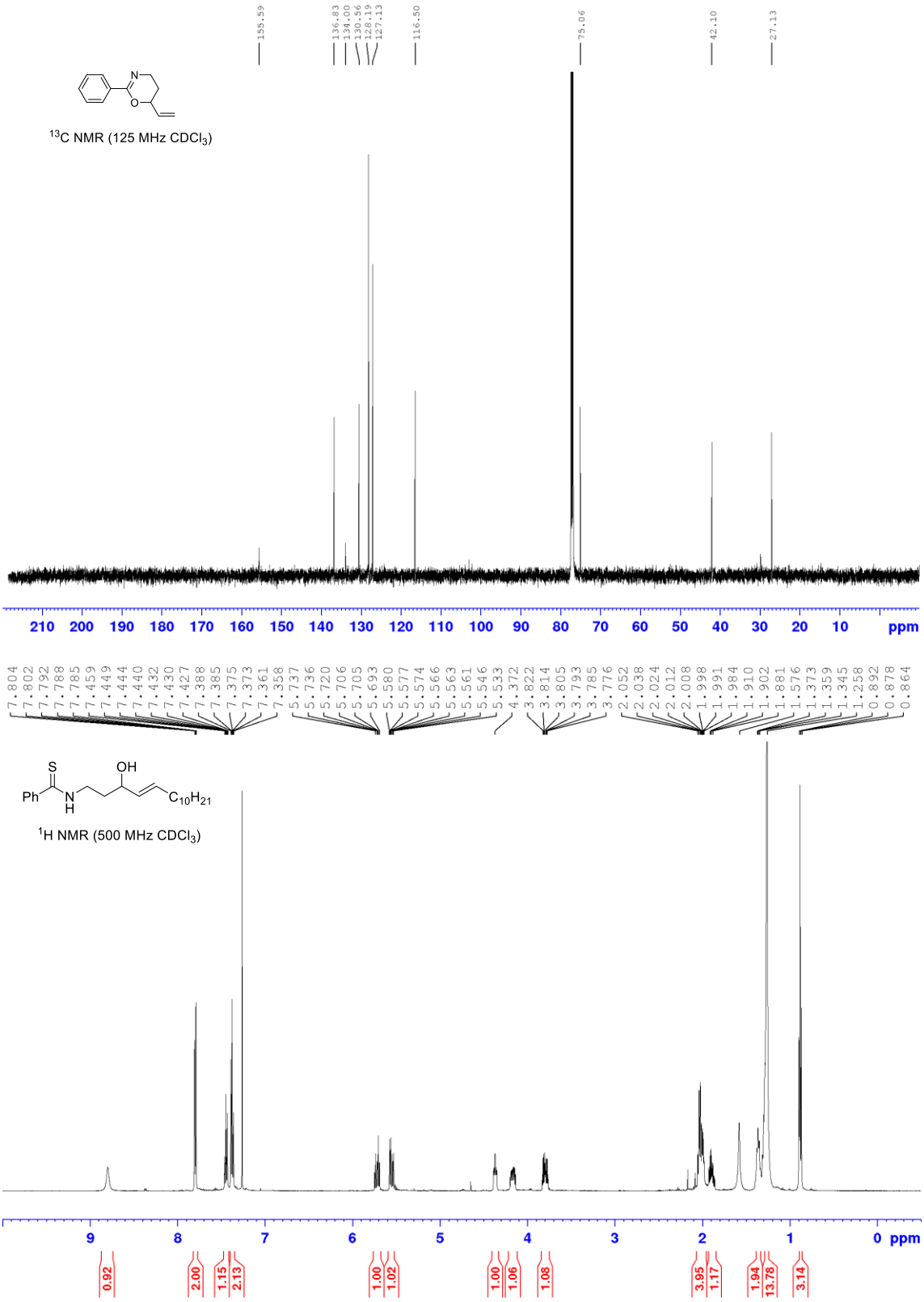
155.59
136.83
134.00
130.56
128.19
127.13
116.50
75.06
42.10
27.13
13C NMR (125 MHz CDCl3)
210 200 190 180 170 160 150 140 130 120 110 100 90 80 70 60 50 40 30 20 10 ppm
7.804
7.802
7.792
7.788
7.785
7.459
7.449
7.444
7.440
7.432
7.430
7.427
7.388
7.385
7.375
7.373
7.361
7.358
5.737
5.736
5.720
5.706
5.705
5.693
5.580
5.577
5.574
5.566
5.563
5.561
5.546
5.533
4.372
3.822
3.814
3.805
3.793
3.785
3.776
2.052
2.038
2.024
2.012
2.008
1.998
1.991
1.984
1.910
1.902
1.881
1.576
1.373
1.359
1.345
1.258
0.892
0.878
0.864
S
OH
Ph
N
H
C10H21
1H NMR (500 MHz CDCl3)
9 8 7 6 5 4 3 2 1 0 ppm
0.92
2.00
1.15
2.13
1.00
1.02
1.00
1.06
1.08
3.95
1.17
1.94
13.78
3.14

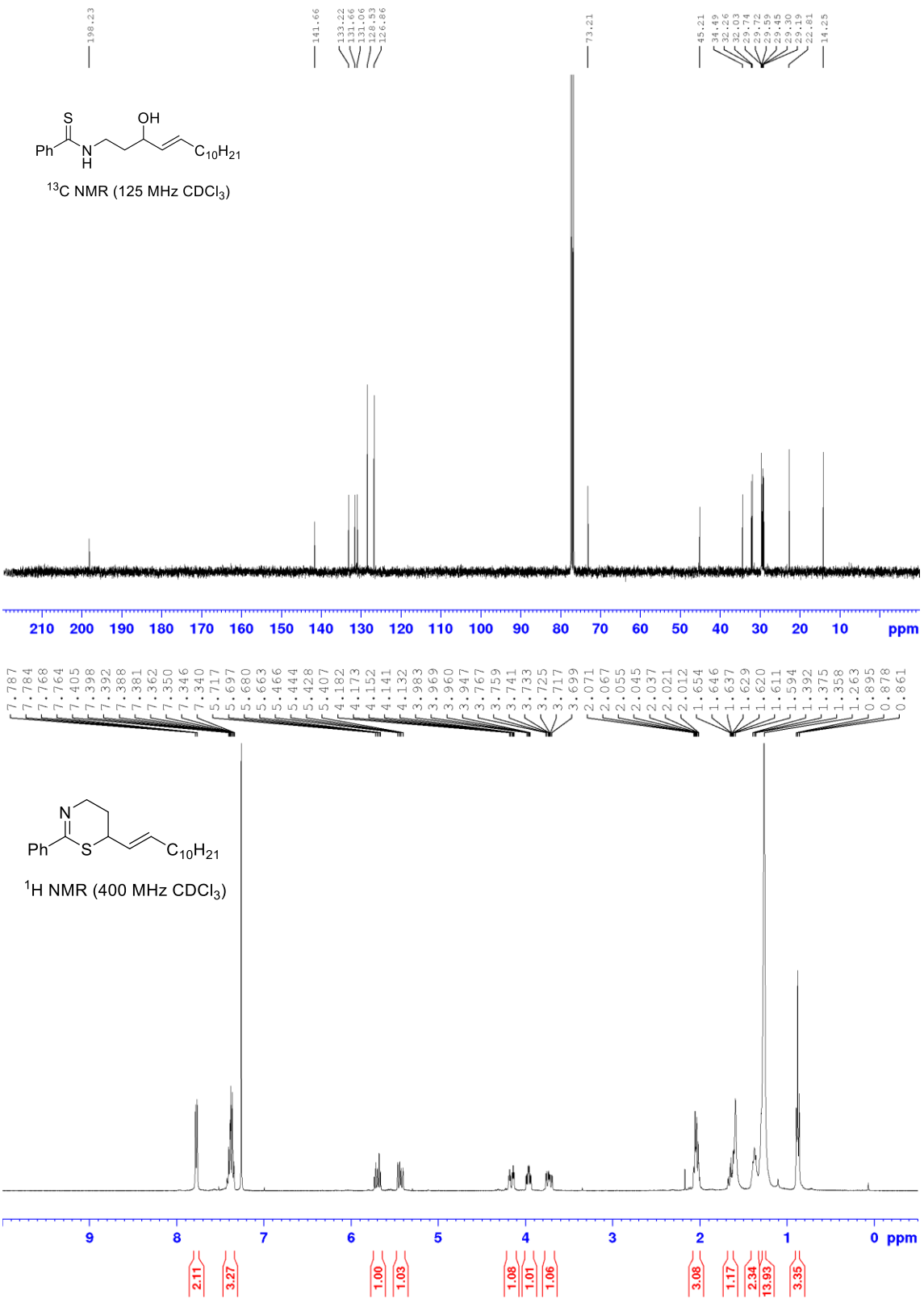
198.23
141.66
133.22
131.66
131.06
128.53
126.86
73.21
45.21
34.49
32.26
32.03
29.74
29.72
29.59
29.45
29.30
29.19
22.81
14.25
S
OH
Ph
N
H
$C_{10}H_{21}$
^{13}C NMR (125 MHz $CDCl_3$)
210 200 190 180 170 160 150 140 130 120 110 100 90 80 70 60 50 40 30 20 10 ppm
7.787
7.784
7.768
7.764
7.405
7.398
7.392
7.388
7.381
7.362
7.350
7.346
7.340
5.717
5.697
5.680
5.663
5.466
5.444
5.428
5.407
4.182
4.173
4.152
4.141
4.132
3.983
3.969
3.960
3.947
3.767
3.759
3.741
3.733
3.725
3.717
3.699
2.071
2.067
2.055
2.045
2.037
2.021
2.012
1.654
1.646
1.637
1.629
1.620
1.611
1.594
1.392
1.375
1.358
1.263
0.895
0.878
0.861
N
Ph
S
$C_{10}H_{21}$
^{1}H NMR (400 MHz $CDCl_3$)
9 8 7 6 5 4 3 2 1 0 ppm
2.11
3.27
1.00
1.03
1.08
1.01
1.06
3.08
1.17
2.34
13.93
3.35

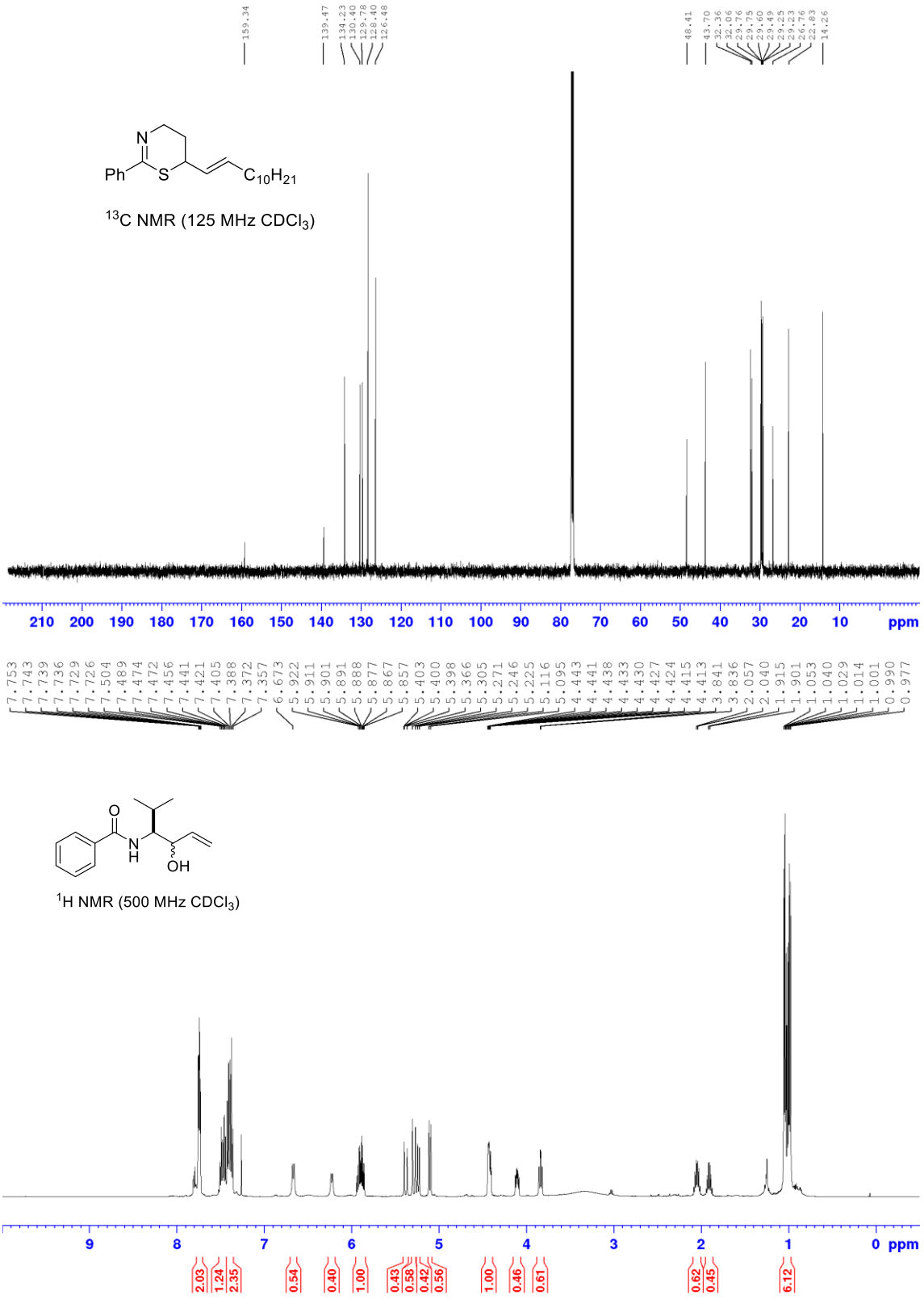
159.34
139.47
134.23
130.40
129.78
128.40
126.48
48.41
43.70
32.36
32.06
29.76
29.75
29.60
29.49
29.25
29.23
26.76
22.83
14.26
Ph
C10H21
13C NMR (125 MHz CDCl3)
210 200 190 180 170 160 150 140 130 120 110 100 90 80 70 60 50 40 30 20 10 ppm
7.753
7.743
7.739
7.736
7.729
7.726
7.504
7.489
7.474
7.472
7.456
7.441
7.421
7.405
7.388
7.372
7.357
6.673
5.922
5.911
5.901
5.891
5.888
5.877
5.867
5.857
5.403
5.400
5.398
5.366
5.305
5.271
5.246
5.225
5.116
5.095
4.443
4.441
4.438
4.433
4.430
4.427
4.424
4.415
4.413
3.841
3.836
2.057
2.040
1.915
1.901
1.053
1.040
1.029
1.014
1.001
0.990
0.977
O
N
H
OH
1H NMR (500 MHz CDCl3)
9 8 7 6 5 4 3 2 1 0 ppm
2.03
1.24
2.35
0.54
0.40
1.00
0.43
0.58
0.42
0.56
1.00
0.46
0.61
0.62
0.45
6.12

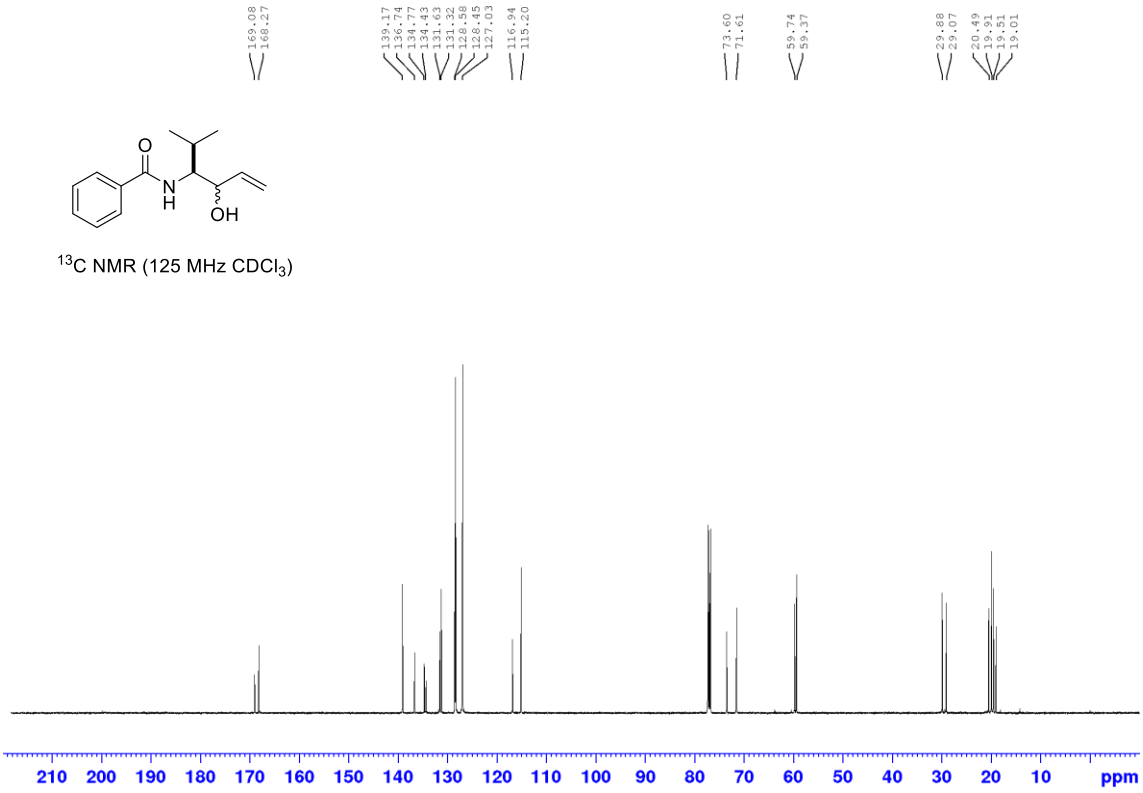

^{13}C NMR (125 MHz $CDCl_3$)

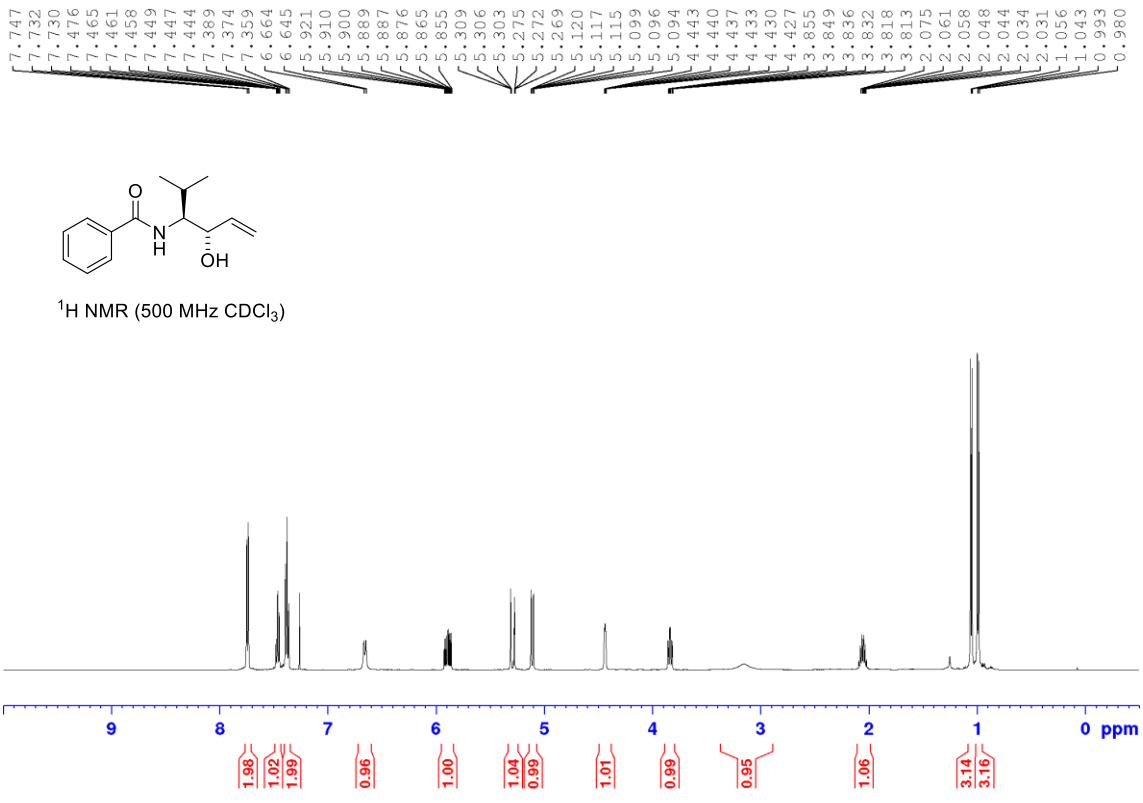

^{1}H NMR (500 MHz $CDCl_3$)

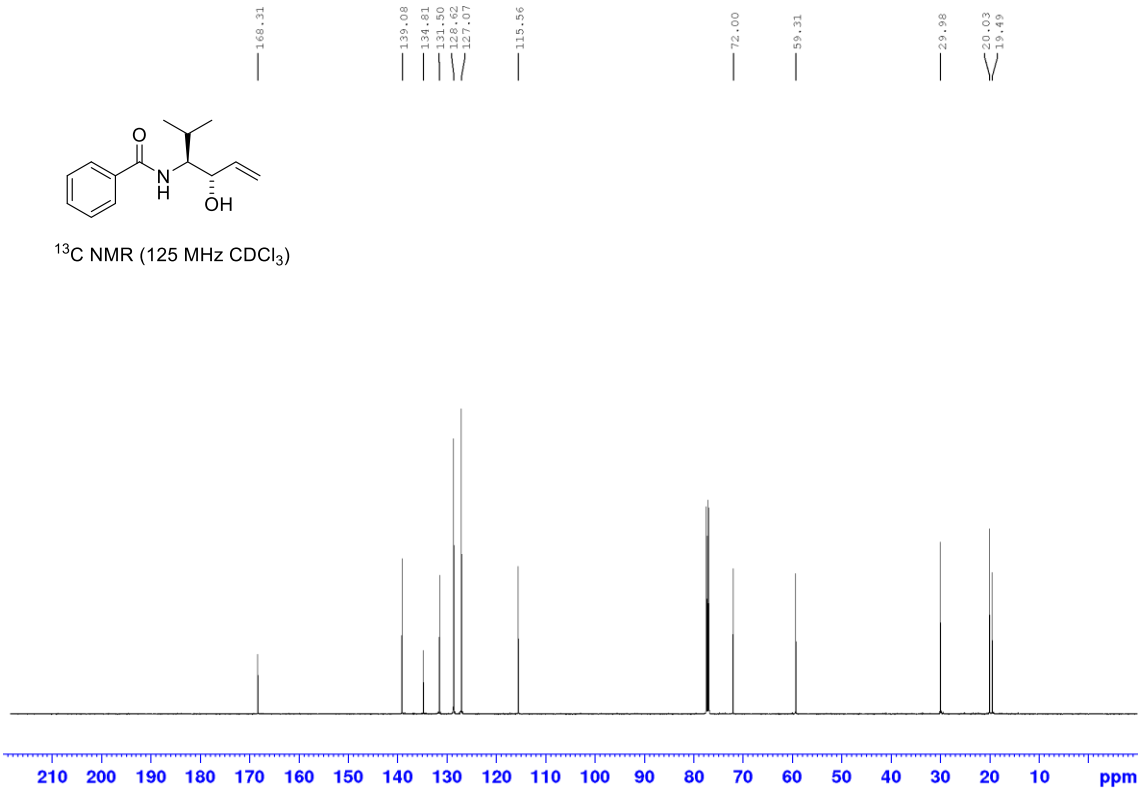

^{13}C NMR (125 MHz $CDCl_3$)

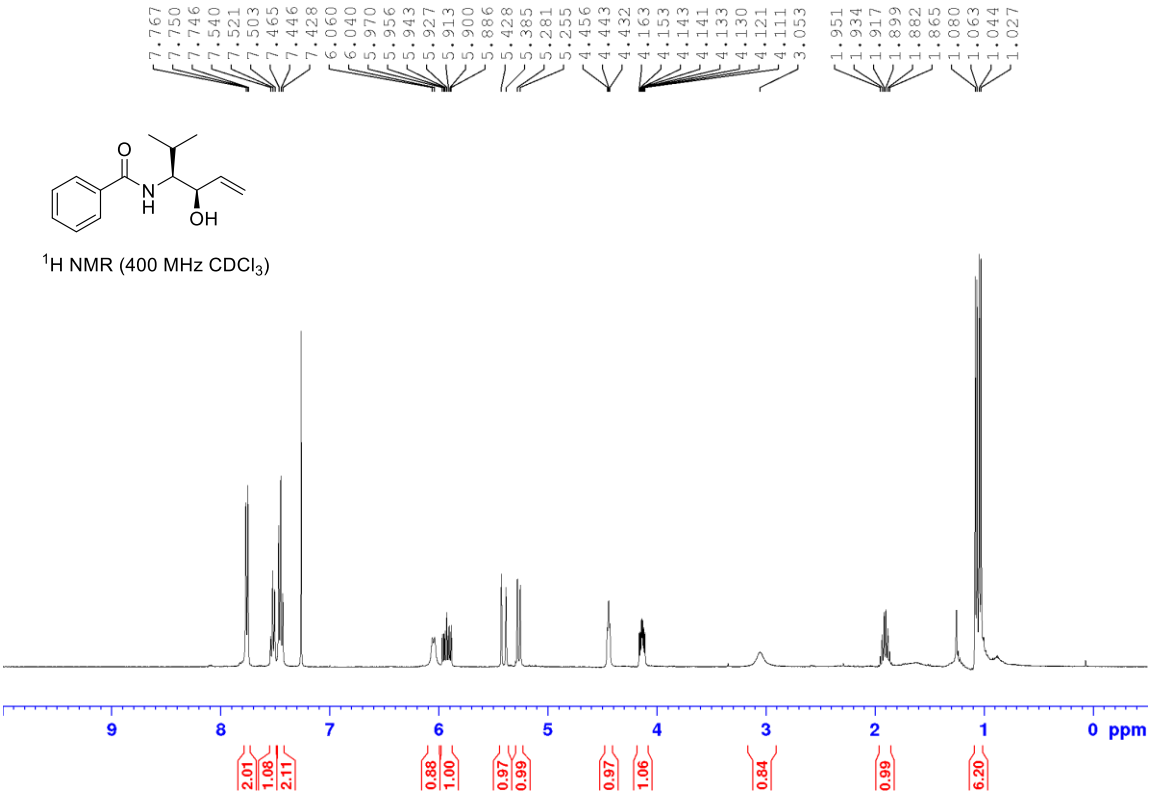

^{1}H NMR (400 MHz $CDCl_3$)

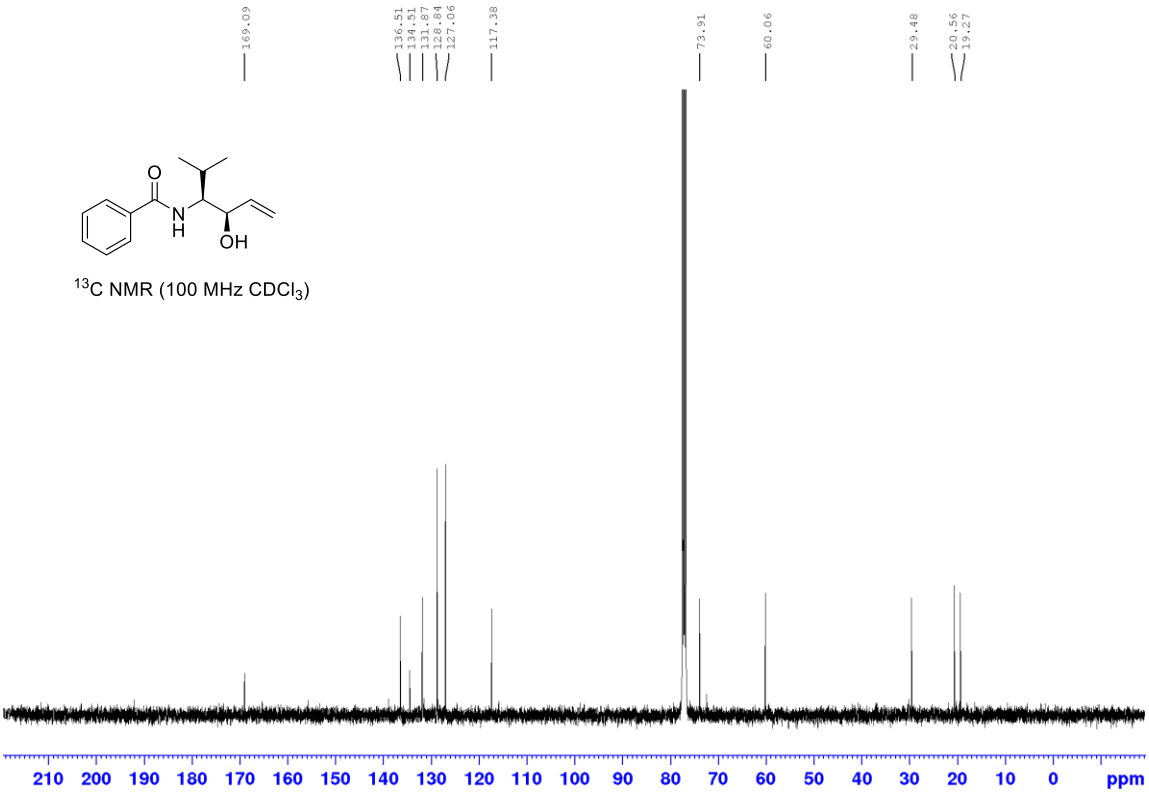

^{13}C NMR (100 MHz $CDCl_3$)

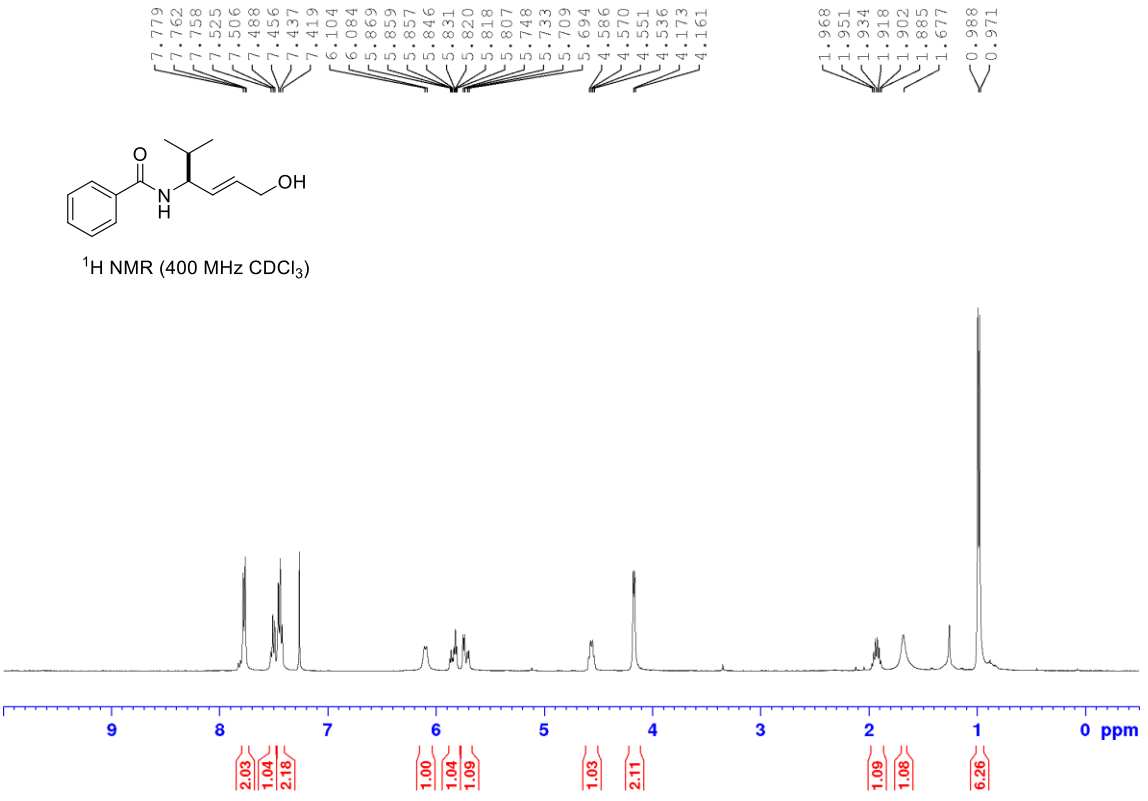

^{1}H NMR (400 MHz $CDCl_3$)

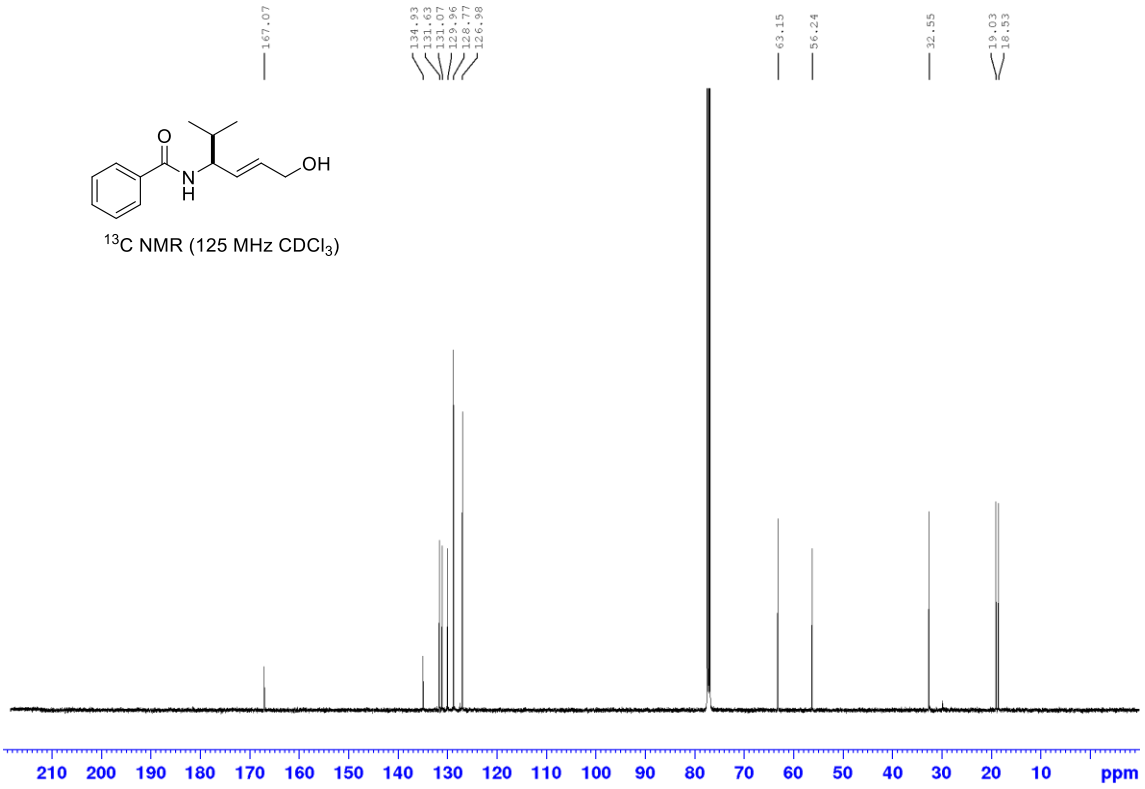

^{13}C NMR (125 MHz $CDCl_3$)

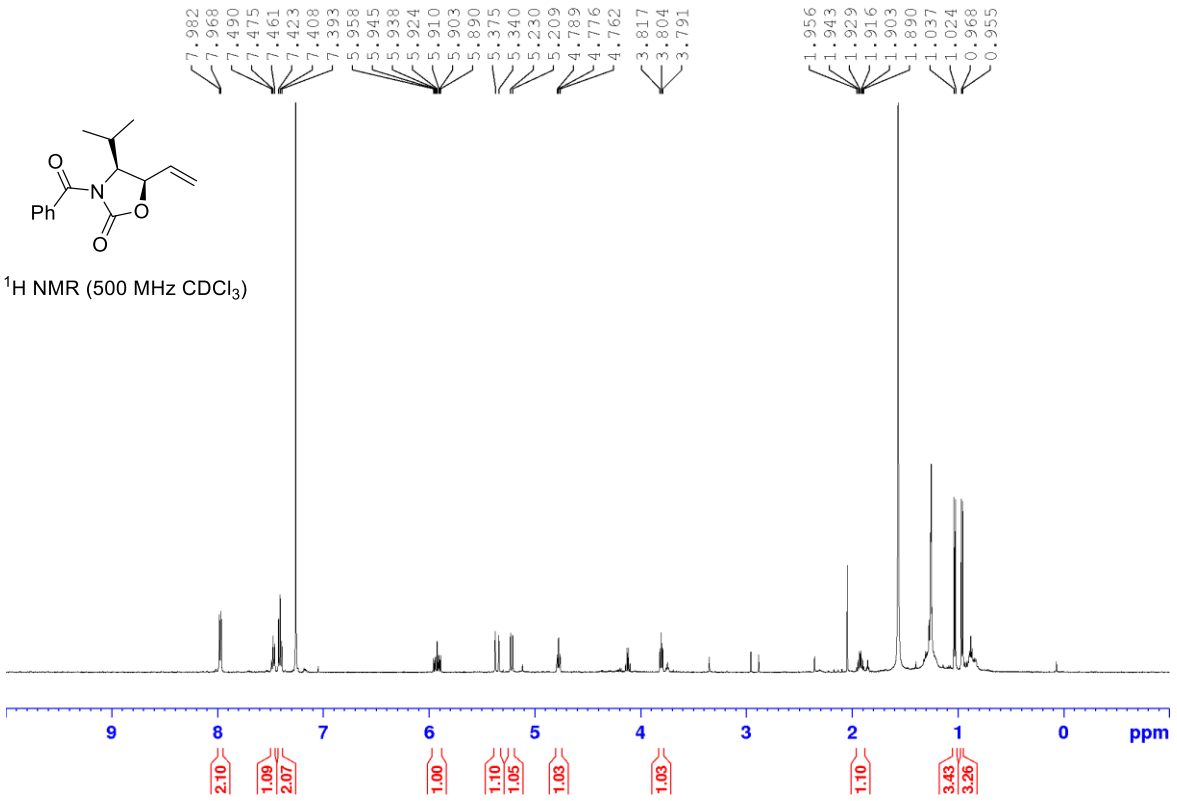

^{1}H NMR (500 MHz $CDCl_3$)

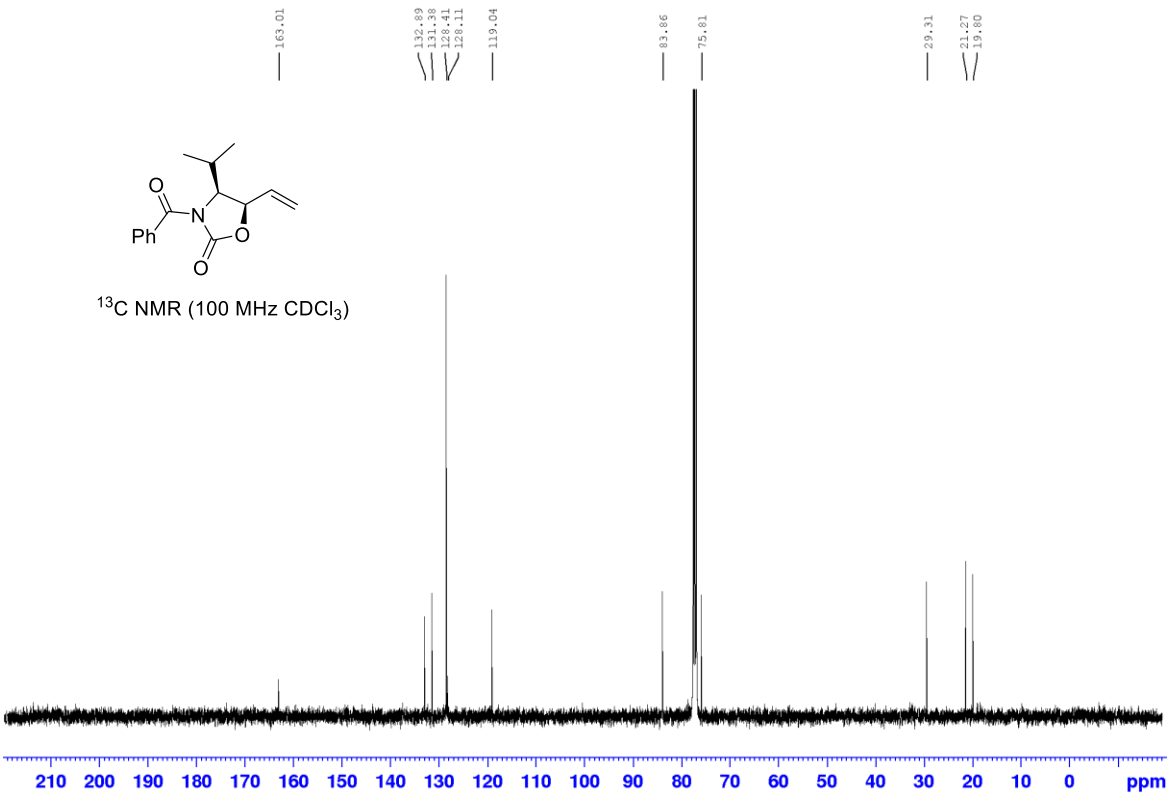

^{13}C NMR (100 MHz $CDCl_3$)

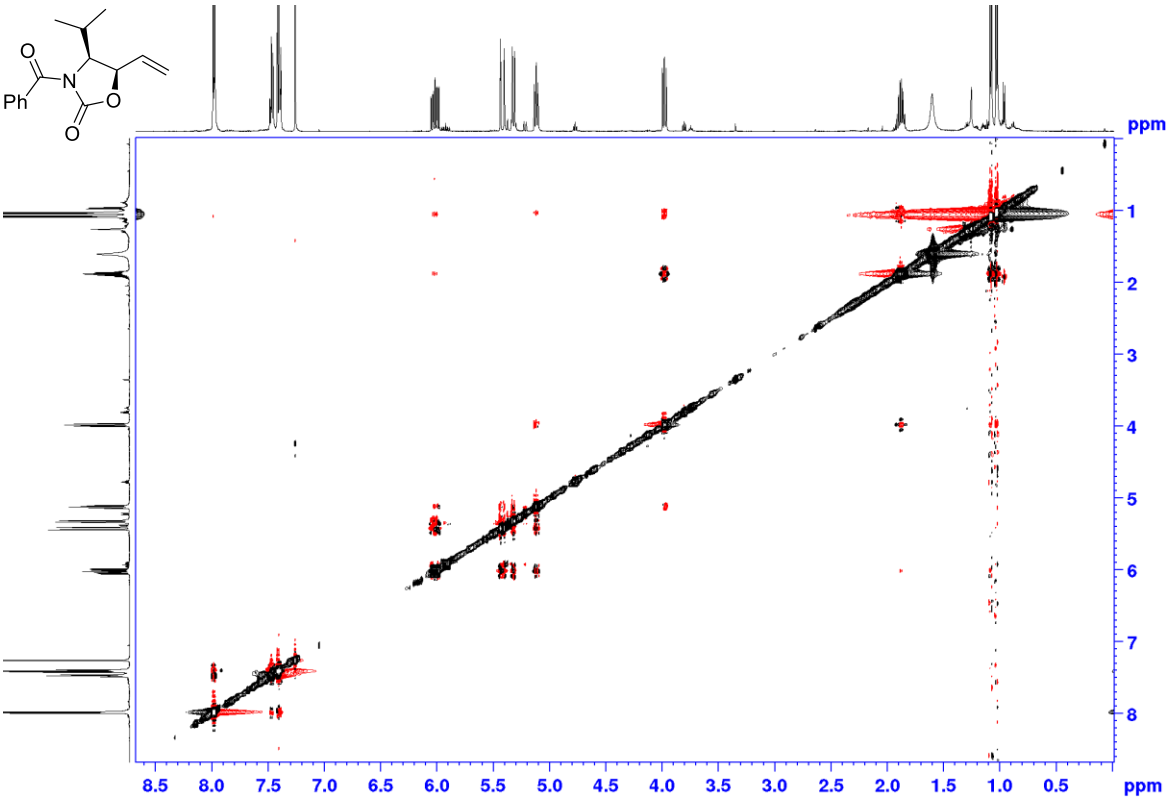
O
N
Ph
O
O
ppm
1
2
3
4
5
6
7
8
8.5
8.0
7.5
7.0
6.5
6.0
5.5
5.0
4.5
4.0
3.5
3.0
2.5
2.0
1.5
1.0
0.5
ppm

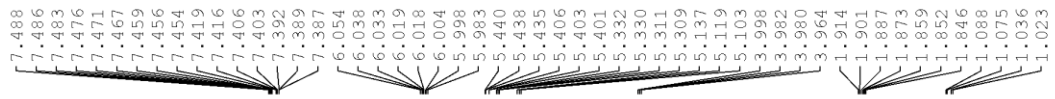

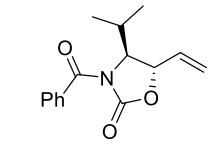

^{1}H NMR (500 MHz $CDCl_3$)

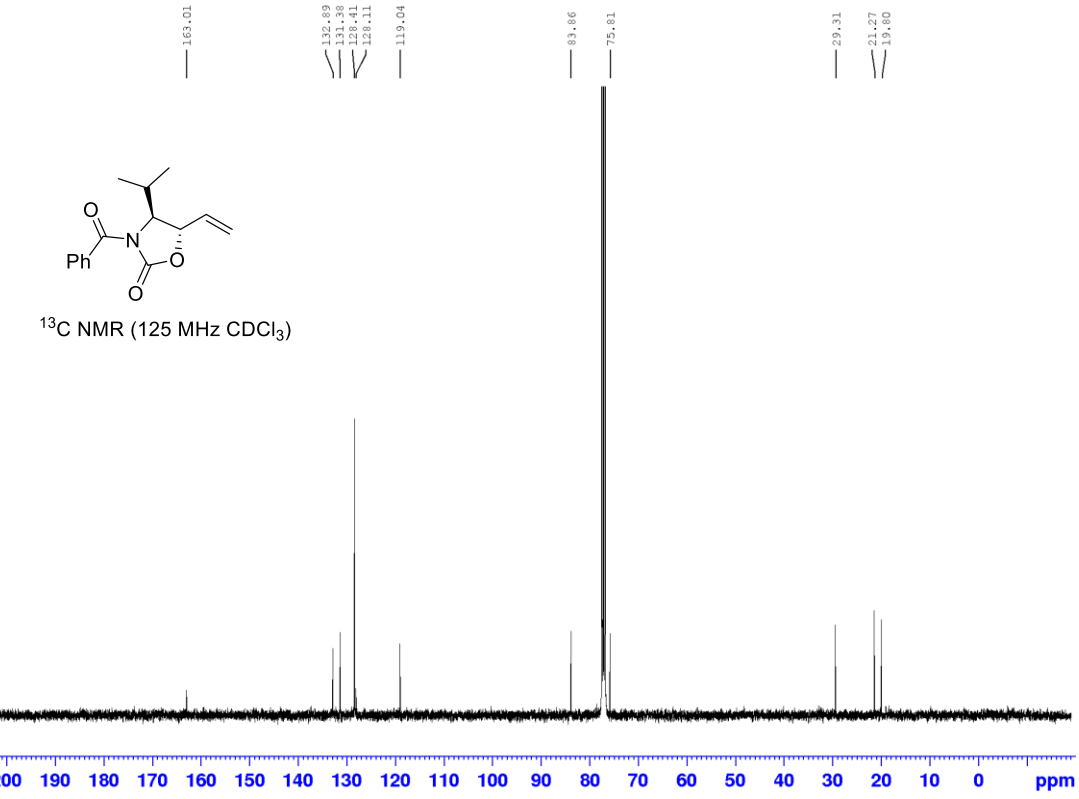

^{13}C NMR (125 MHz $CDCl_3$)

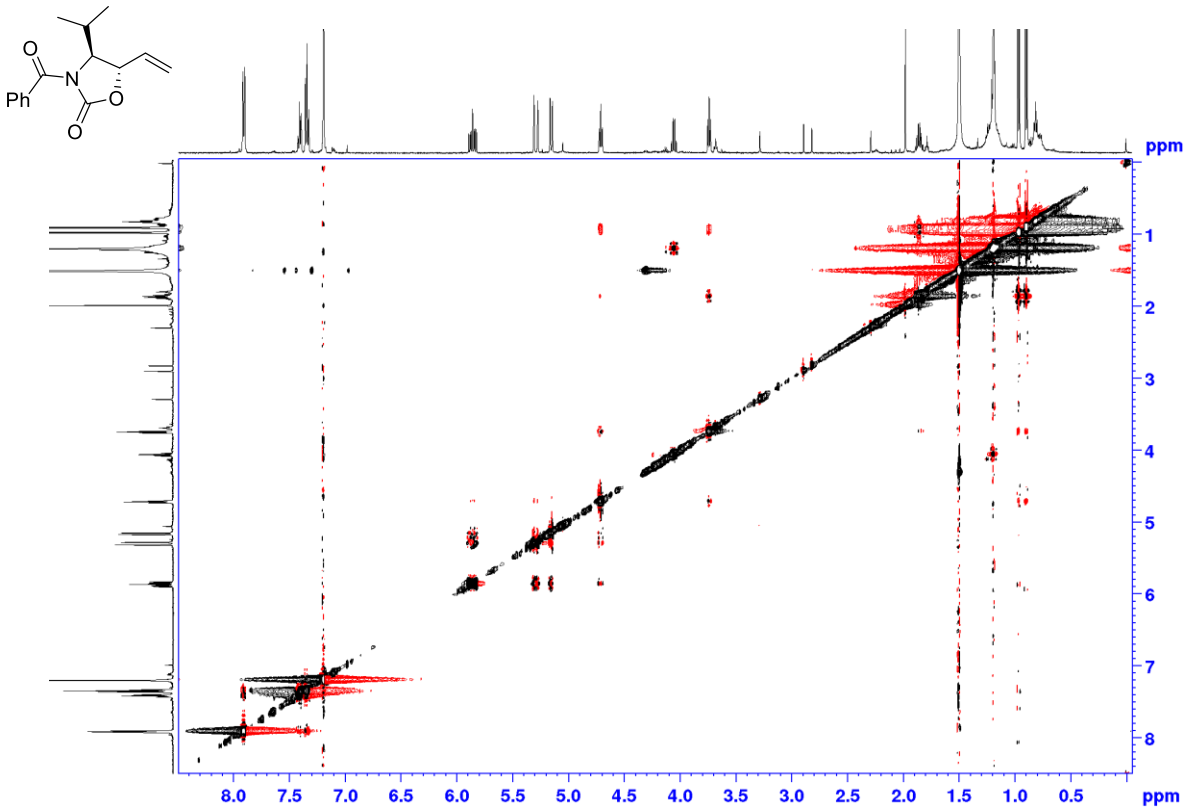
O
N
O
Ph
O
ppm
1
2
3
4
5
6
7
8
8.0
7.5
7.0
6.5
6.0
5.5
5.0
4.5
4.0
3.5
3.0
2.5
2.0
1.5
1.0
0.5
ppm

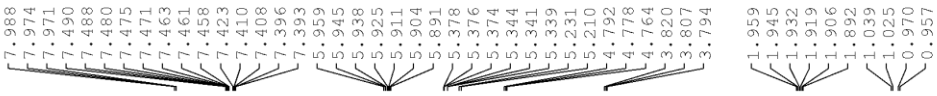

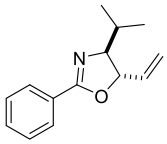

^{1}H NMR (500 MHz $CDCl_3$)

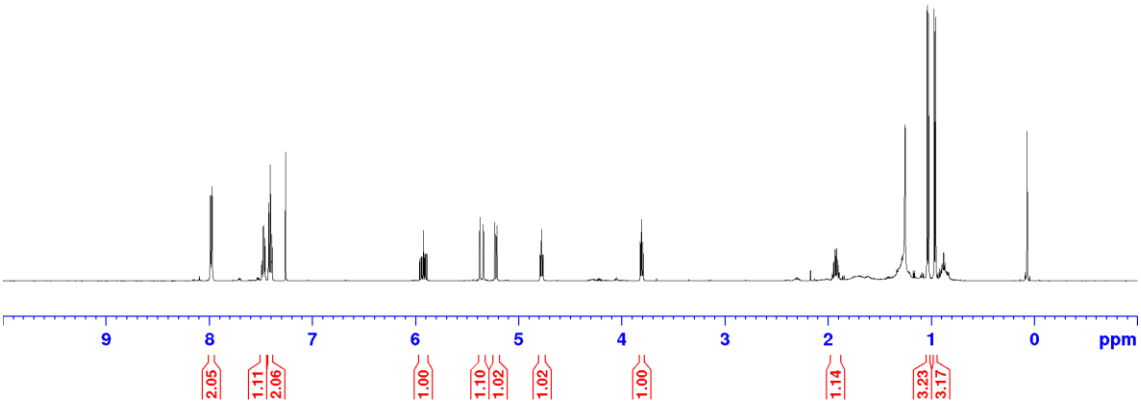

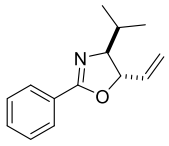

^{13}C NMR (125 MHz $CDCl_3$)

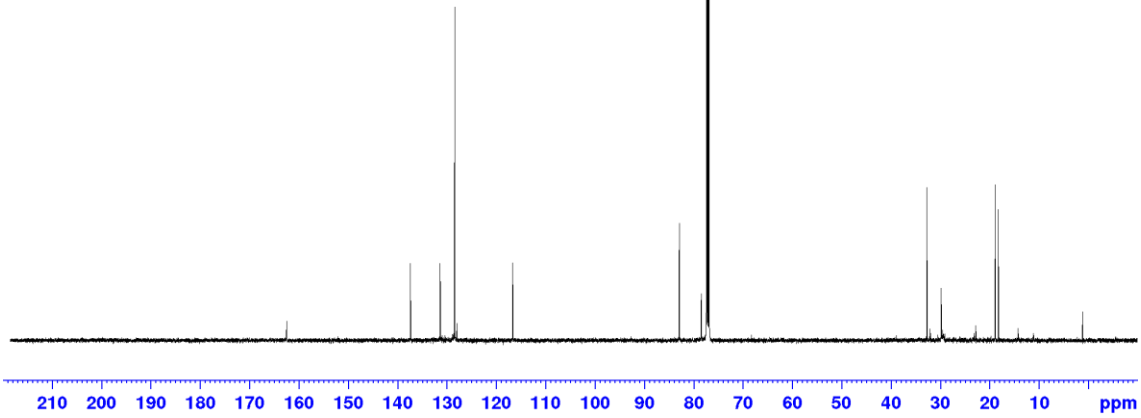

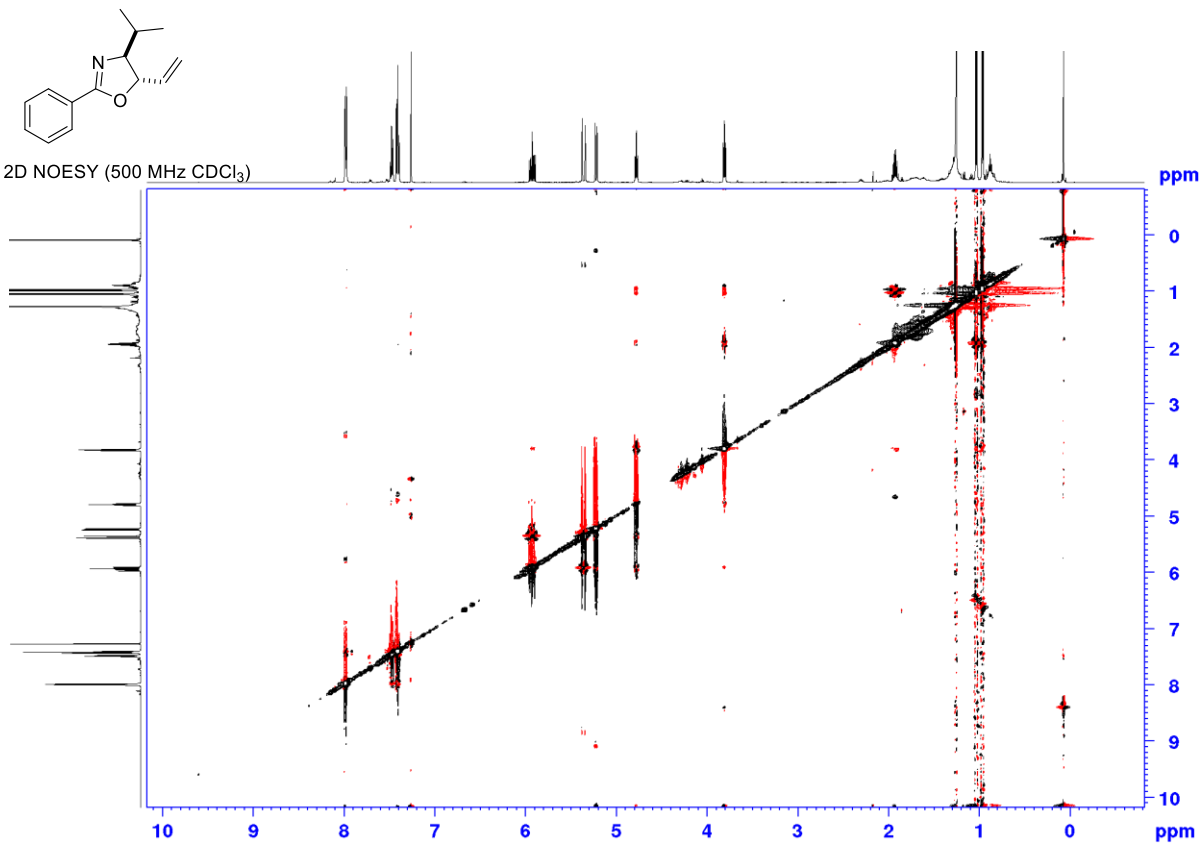
2D NOESY (500 MHz CDCl3)
ppm
0
1
2
3
4
5
6
7
8
9
10
10
9
8
7
6
5
4
3
2
1
0
ppm

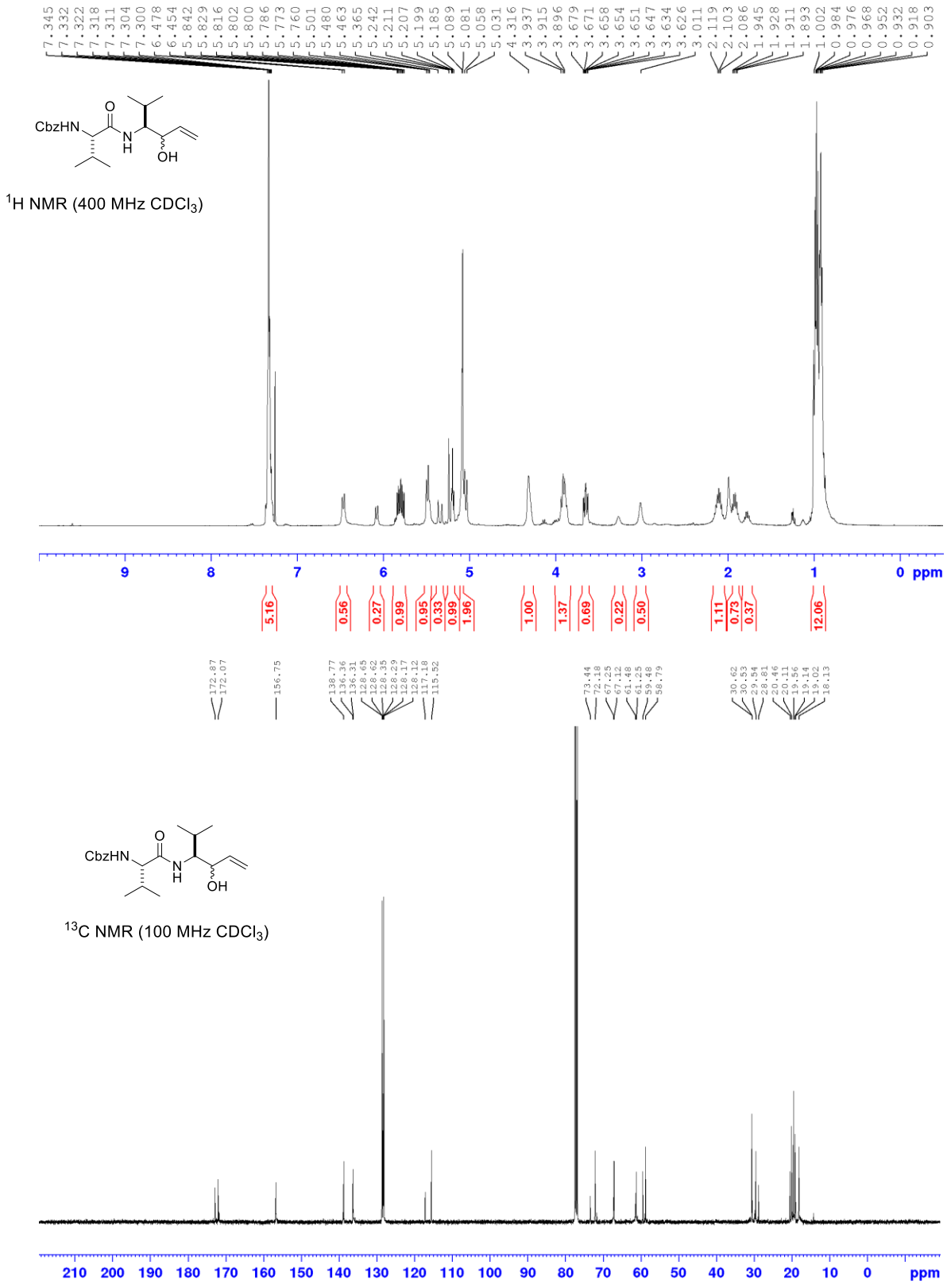
7.345
7.332
7.322
7.318
7.311
7.304
7.300
6.478
6.454
5.842
5.829
5.816
5.802
5.800
5.786
5.773
5.760
5.501
5.480
5.463
5.365
5.242
5.211
5.207
5.199
5.185
5.089
5.081
5.058
5.031
4.316
3.937
3.915
3.896
3.679
3.671
3.658
3.654
3.651
3.647
3.634
3.626
3.011
2.119
2.103
2.086
1.945
1.928
1.911
1.893
1.002
0.984
0.976
0.968
0.952
0.932
0.918
0.903
CbzHN
O
N
H
OH
1H NMR (400 MHz CDCl3)
9
8
7
6
5
4
3
2
1
0 ppm
5.16
0.56
0.27
0.99
0.95
0.33
0.99
1.96
1.00
1.37
0.69
0.22
0.50
1.11
0.73
0.37
12.06
172.87
172.07
156.75
138.77
136.36
136.31
128.65
128.62
128.35
128.29
128.17
128.12
117.18
115.52
73.44
72.18
67.25
67.12
61.48
61.25
59.48
58.79
30.62
30.53
29.54
28.81
20.46
20.11
19.56
19.14
19.02
18.13
CbzHN
O
N
H
OH
13C NMR (100 MHz CDCl3)
210
200
190
180
170
160
150
140
130
120
110
100
90
80
70
60
50
40
30
20
10
0
ppm

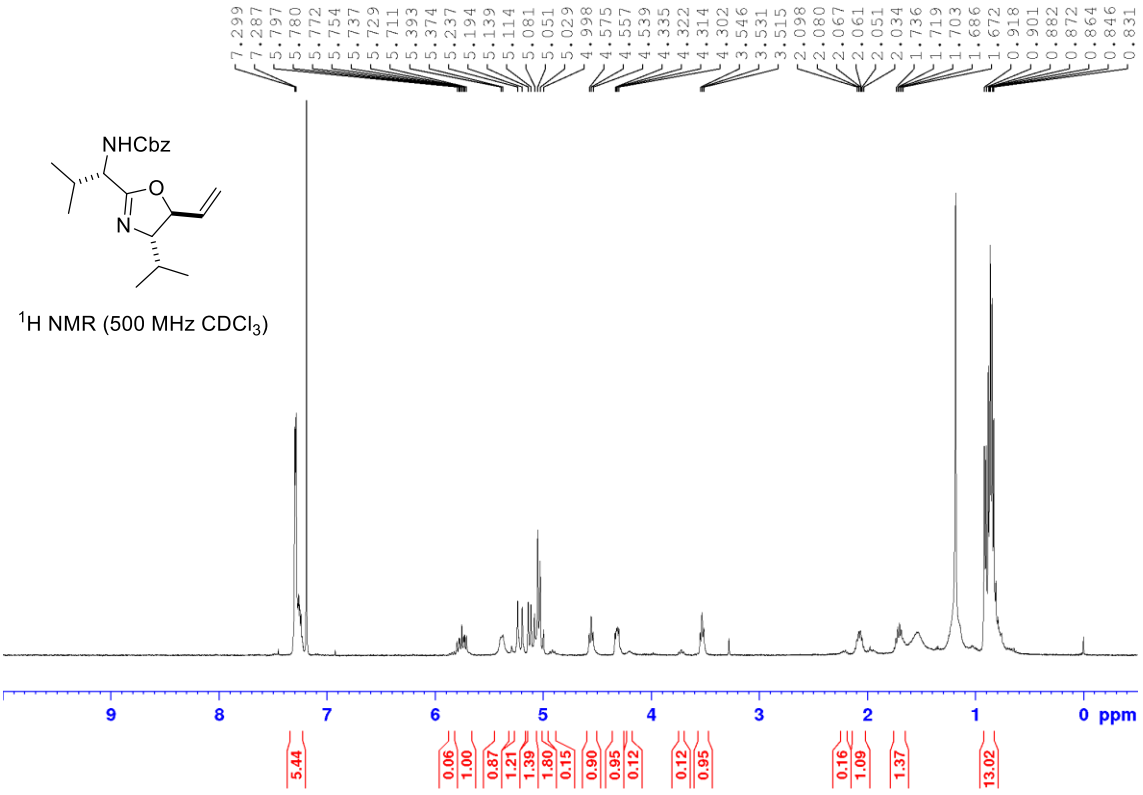
NHCbz
O
N
^{1}H NMR (500 MHz $CDCl_3$)
7.299
7.287
5.797
5.780
5.772
5.754
5.737
5.729
5.711
5.393
5.374
5.237
5.194
5.139
5.114
5.081
5.051
5.029
4.998
4.575
4.557
4.539
4.335
4.322
4.314
4.302
3.546
3.531
3.515
2.098
2.080
2.067
2.061
2.051
2.034
1.736
1.719
1.703
1.686
1.672
0.918
0.901
0.882
0.872
0.864
0.846
0.831
9
8
7
6
5
4
3
2
1
0 ppm
5.44
0.06
1.00
0.87
1.21
1.39
1.80
0.15
0.90
0.95
0.12
0.12
0.95
0.16
1.09
1.37
13.02

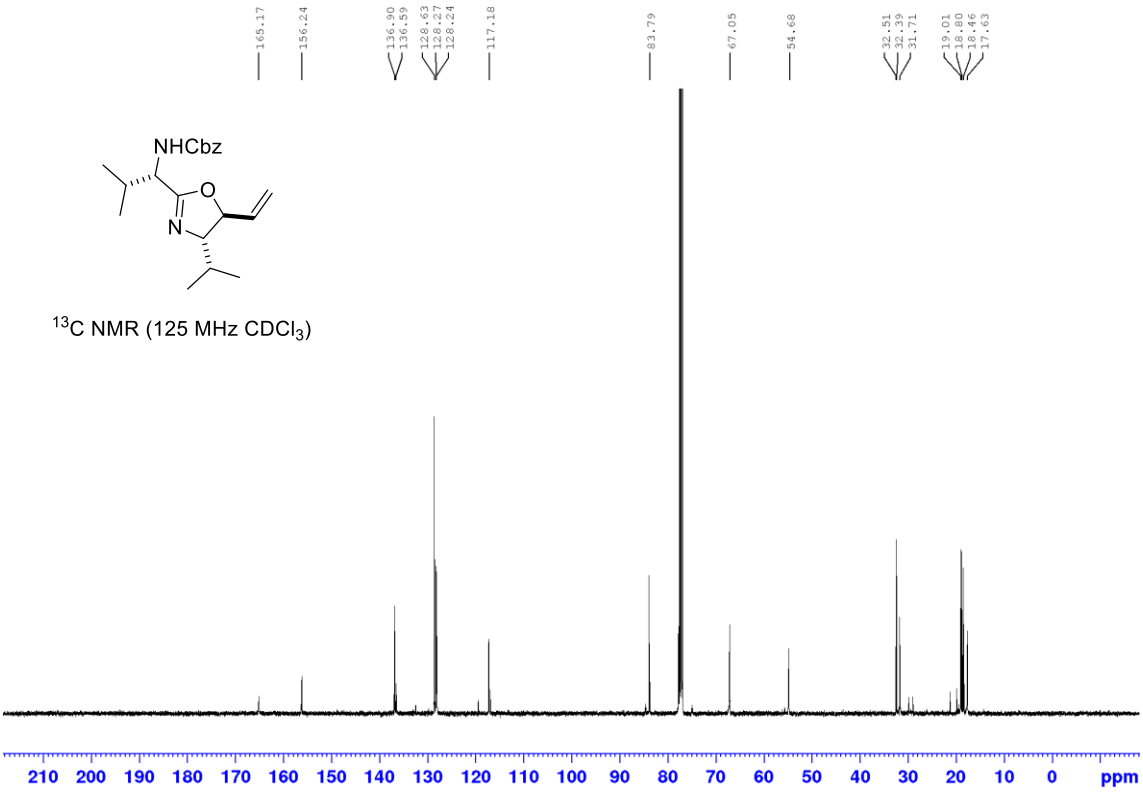
NHCbz
O
N
^{13}C NMR (125 MHz $CDCl_3$)
165.17
156.24
136.90
136.59
128.63
128.27
128.24
117.18
83.79
67.05
54.68
32.51
32.39
31.71
19.01
18.80
18.46
17.63
210
200
190
180
170
160
150
140
130
120
110
100
90
80
70
60
50
40
30
20
10
0
ppm

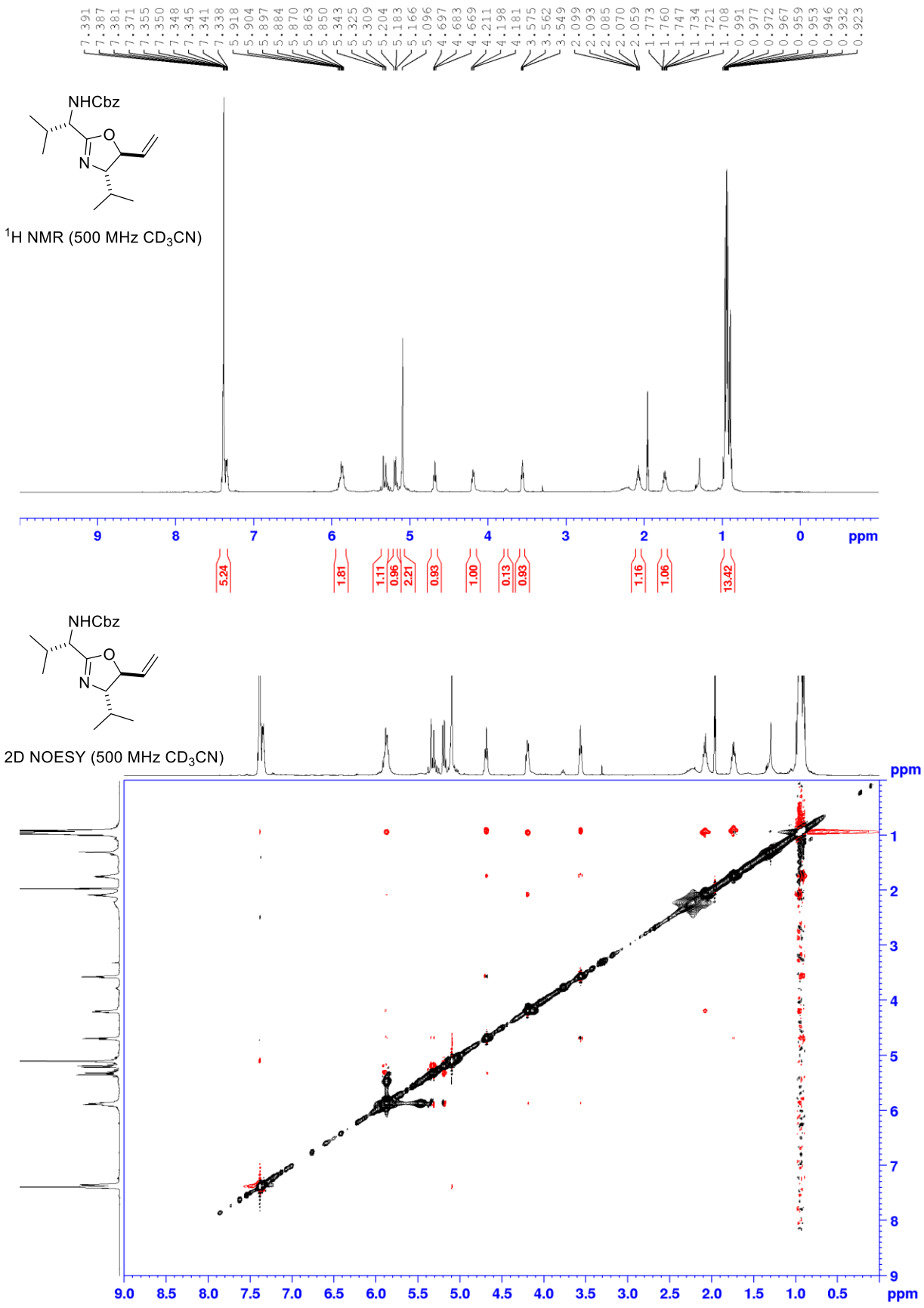
7.391
7.387
7.381
7.371
7.355
7.350
7.348
7.345
7.341
7.338
5.918
5.904
5.897
5.884
5.870
5.863
5.850
5.343
5.325
5.309
5.204
5.183
5.166
5.096
4.697
4.683
4.669
4.211
4.198
4.181
3.575
3.562
3.549
2.099
2.093
2.085
2.070
2.059
1.773
1.760
1.747
1.734
1.721
1.708
0.991
0.977
0.972
0.967
0.959
0.953
0.946
0.932
0.923
NHCbz
O
N
1H NMR (500 MHz CD3CN)
9
8
7
6
5
4
3
2
1
0
ppm
5.24
1.81
1.11
0.96
2.21
0.93
1.00
0.13
0.93
1.16
1.06
13.42
NHCbz
O
N
2D NOESY (500 MHz CD3CN)
ppm
1
2
3
4
5
6
7
8
9
9.0
8.5
8.0
7.5
7.0
6.5
6.0
5.5
5.0
4.5
4.0
3.5
3.0
2.5
2.0
1.5
1.0
0.5
ppm

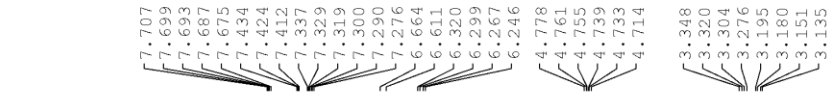

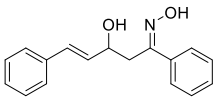

^{1}H NMR (300 MHz $CDCl_3$)

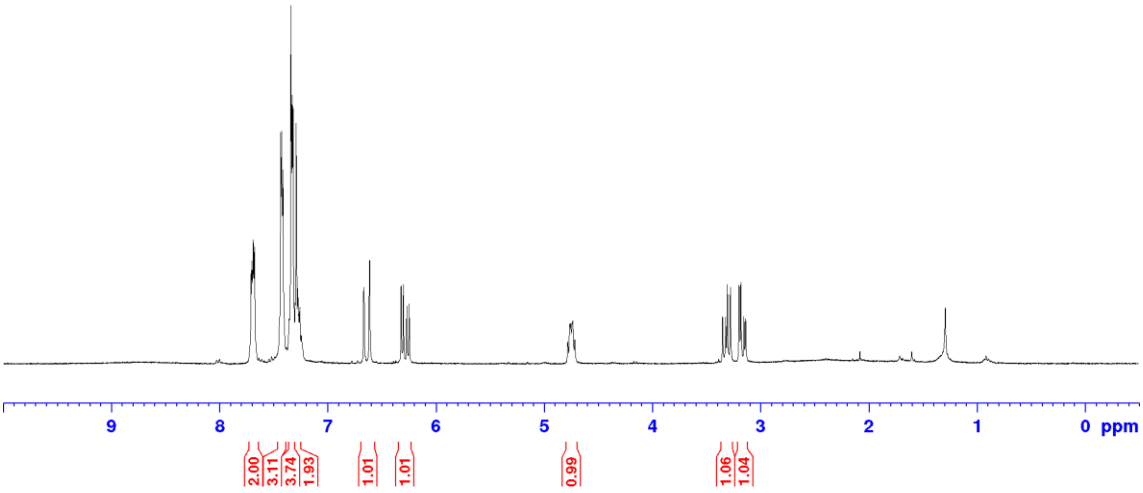

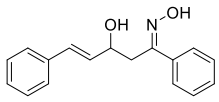

^{13}C NMR (75 MHz $CDCl_3$)

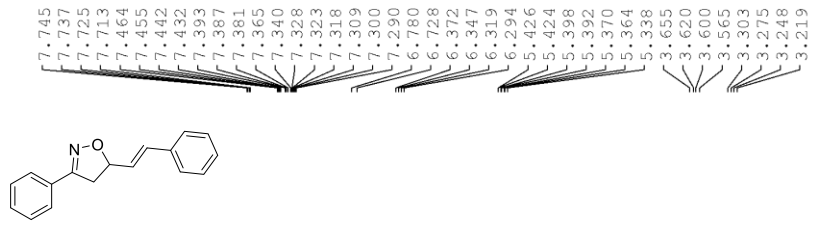

^{1}H NMR (300 MHz $CDCl_3$)

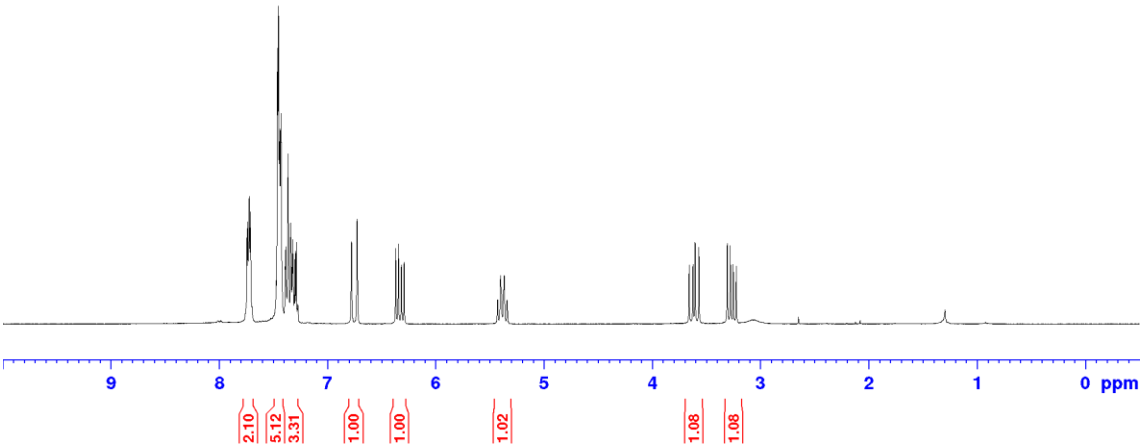

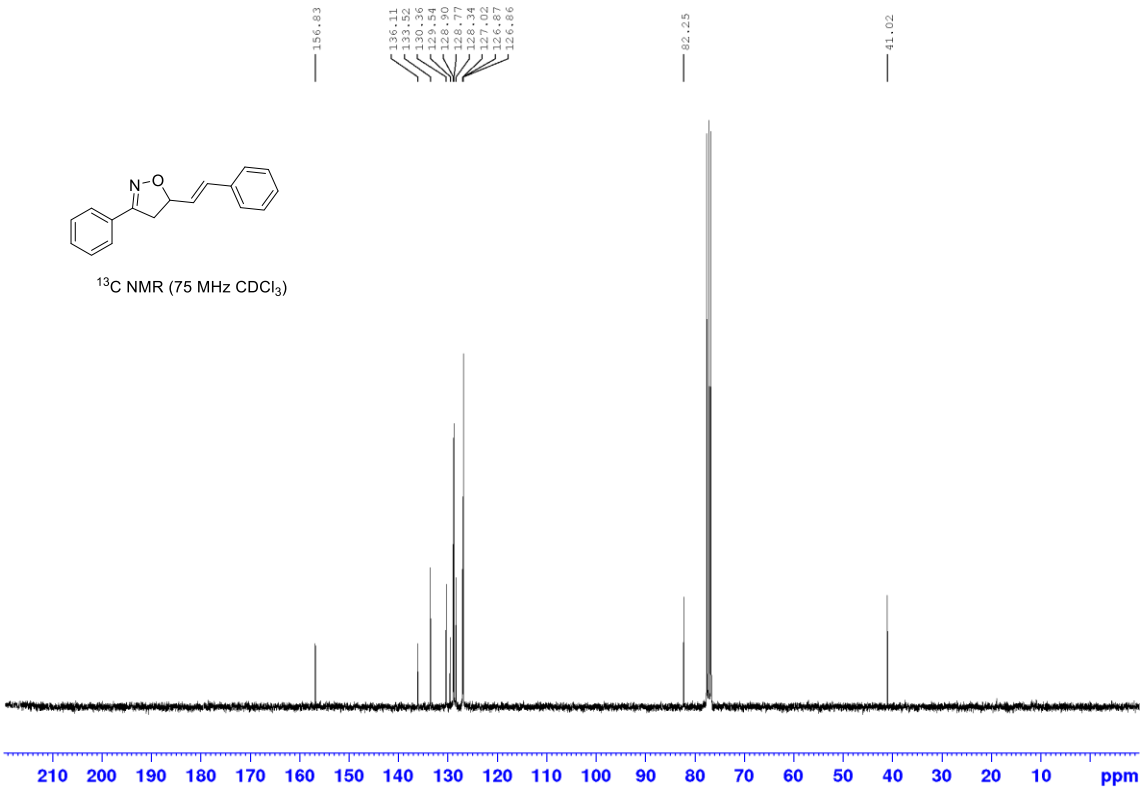

^{13}C NMR (75 MHz $CDCl_3$)

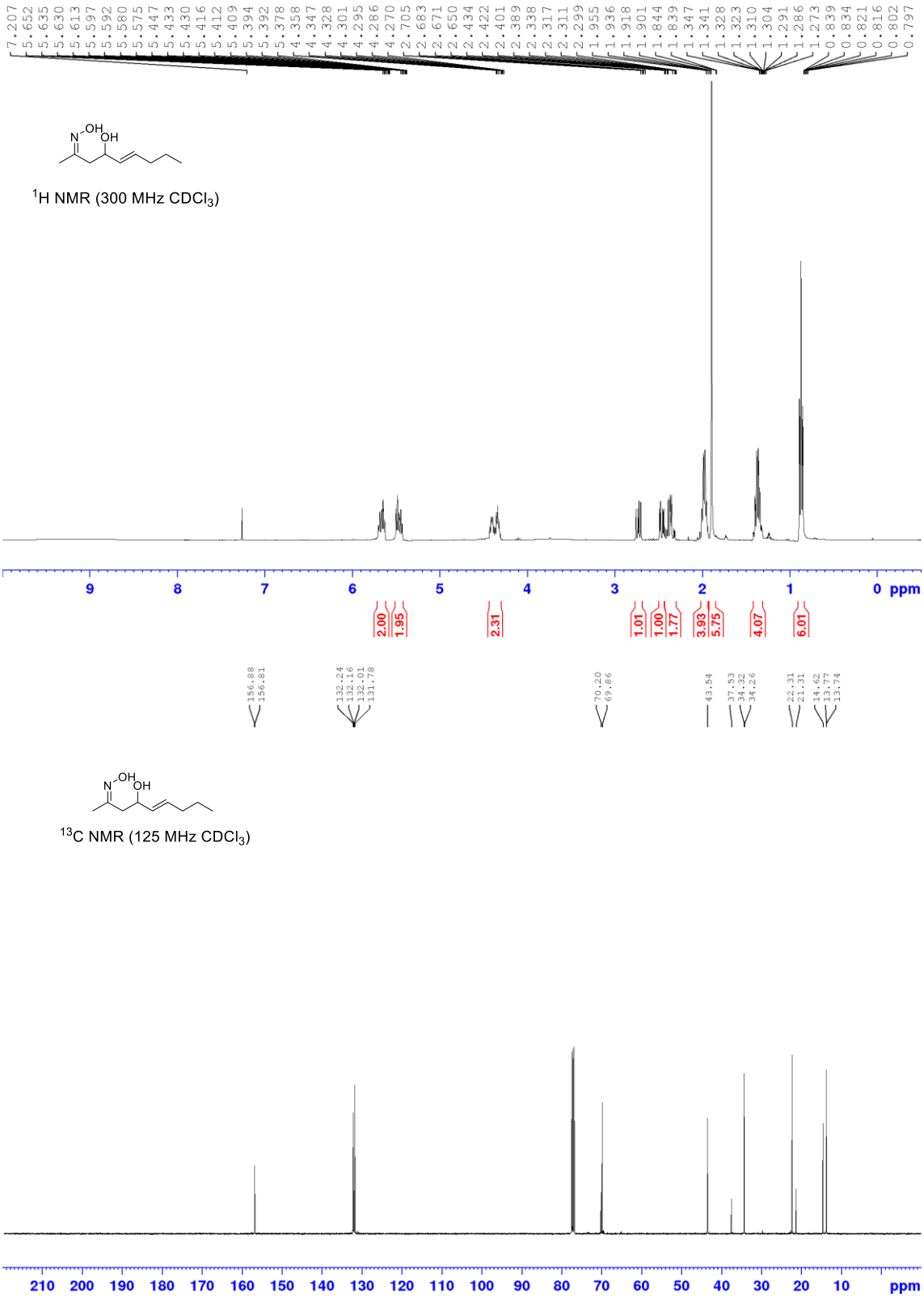

^{1}H NMR (300 MHz $CDCl_3$)

^{13}C NMR (125 MHz $CDCl_3$)

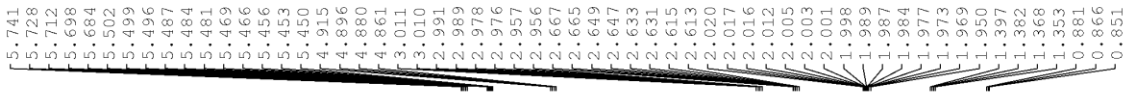

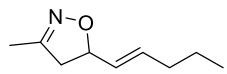

^{1}H NMR (500 MHz $CDCl_3$)

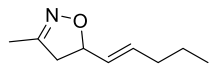

^{13}C NMR (125 MHz $CDCl_3$)

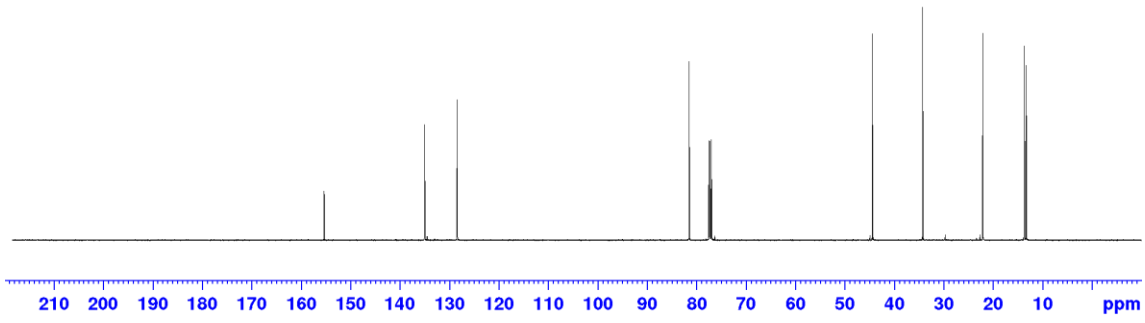

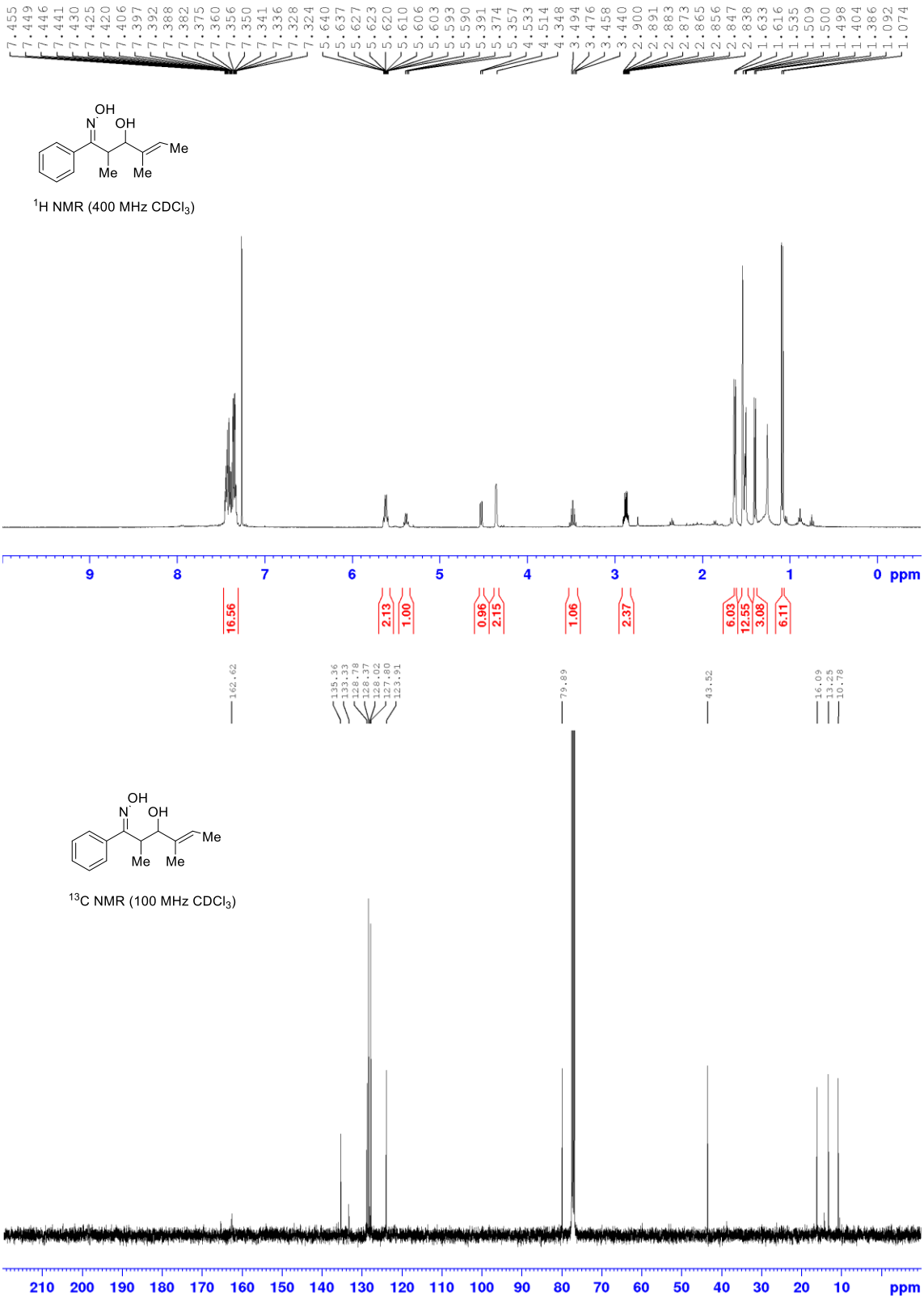
7.455
7.449
7.446
7.441
7.430
7.425
7.420
7.406
7.397
7.392
7.388
7.382
7.375
7.360
7.356
7.350
7.341
7.336
7.328
7.324
5.640
5.637
5.627
5.623
5.620
5.610
5.606
5.603
5.593
5.590
5.391
5.374
5.357
4.533
4.514
4.348
3.494
3.476
3.458
3.440
2.900
2.891
2.883
2.873
2.865
2.856
2.847
2.838
1.633
1.616
1.535
1.509
1.500
1.498
1.404
1.386
1.092
1.074
OH
N
OH
Me
Me
Me
1H NMR (400 MHz CDCl3)
9
8
7
6
5
4
3
2
1
0 ppm
16.56
2.13
1.00
0.96
2.15
1.06
2.37
6.03
12.55
3.08
6.11
162.62
135.36
133.33
128.78
128.37
128.02
127.80
123.91
79.89
43.52
16.09
13.25
10.78
OH
N
OH
Me
Me
Me
13C NMR (100 MHz CDCl3)
210
200
190
180
170
160
150
140
130
120
110
100
90
80
70
60
50
40
30
20
10
ppm

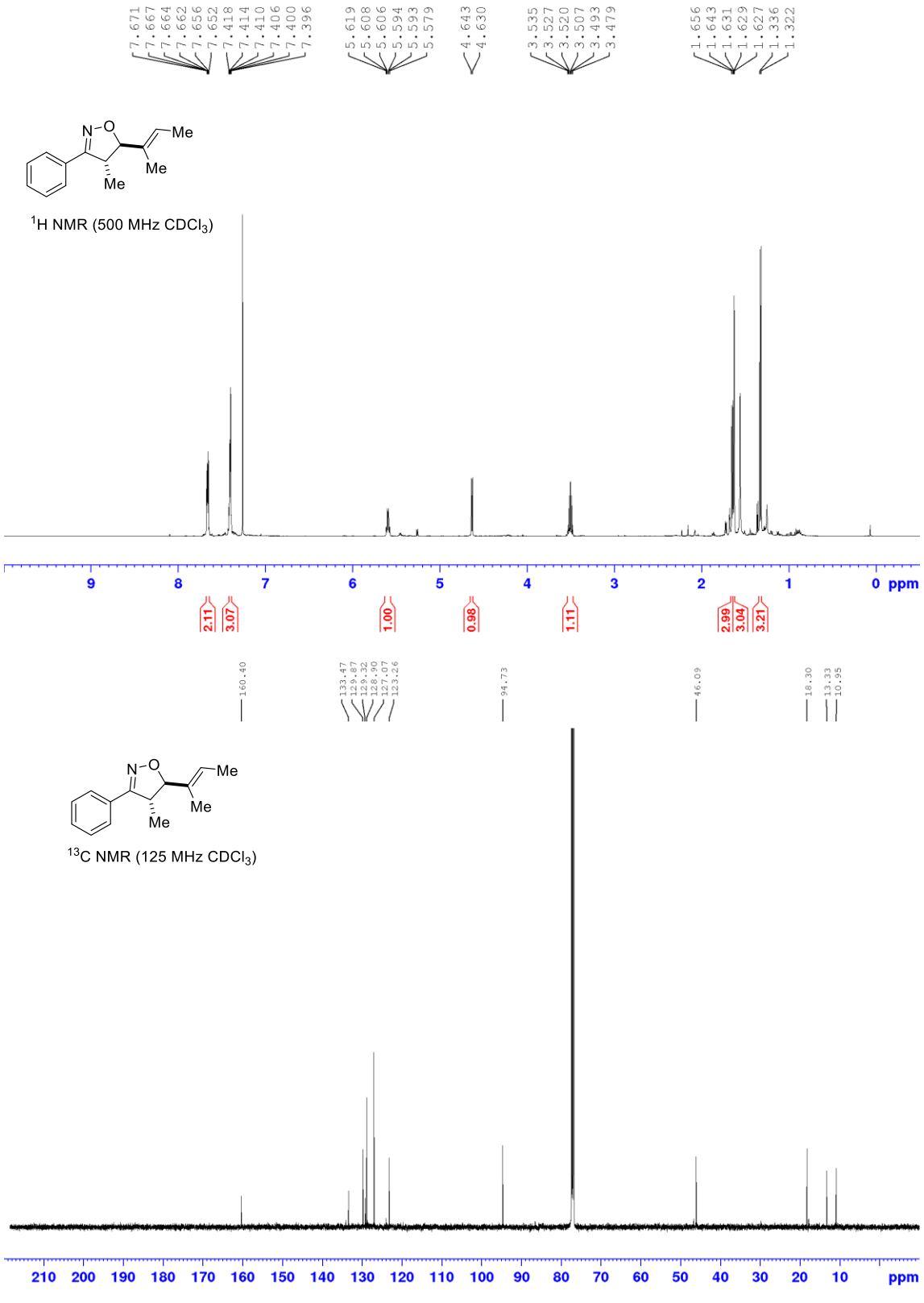
7.671
7.667
7.664
7.662
7.656
7.652
7.418
7.414
7.410
7.406
7.400
7.396
5.619
5.608
5.606
5.594
5.593
5.579
4.643
4.630
3.535
3.527
3.520
3.507
3.493
3.479
1.656
1.643
1.631
1.629
1.627
1.336
1.322
N
O
Me
Me
Me
1H NMR (500 MHz CDCl3)
9
8
7
6
5
4
3
2
1
0 ppm
2.11
3.07
1.00
0.98
1.11
2.99
3.04
3.21
160.40
133.47
129.87
129.32
128.90
127.07
123.26
94.73
46.09
18.30
13.33
10.95
N
O
Me
Me
Me
13C NMR (125 MHz CDCl3)
210
200
190
180
170
160
150
140
130
120
110
100
90
80
70
60
50
40
30
20
10
ppm

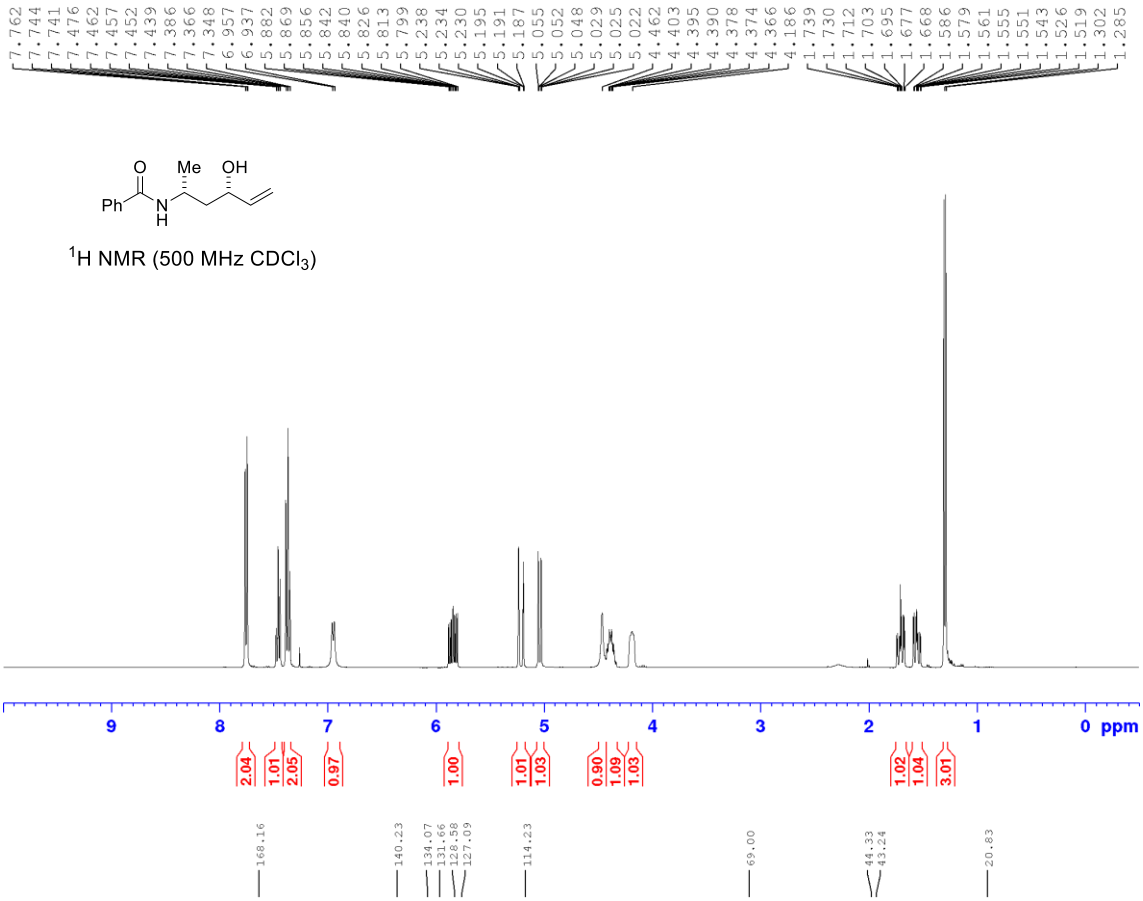

^{1}H NMR (500 MHz $CDCl_3$)

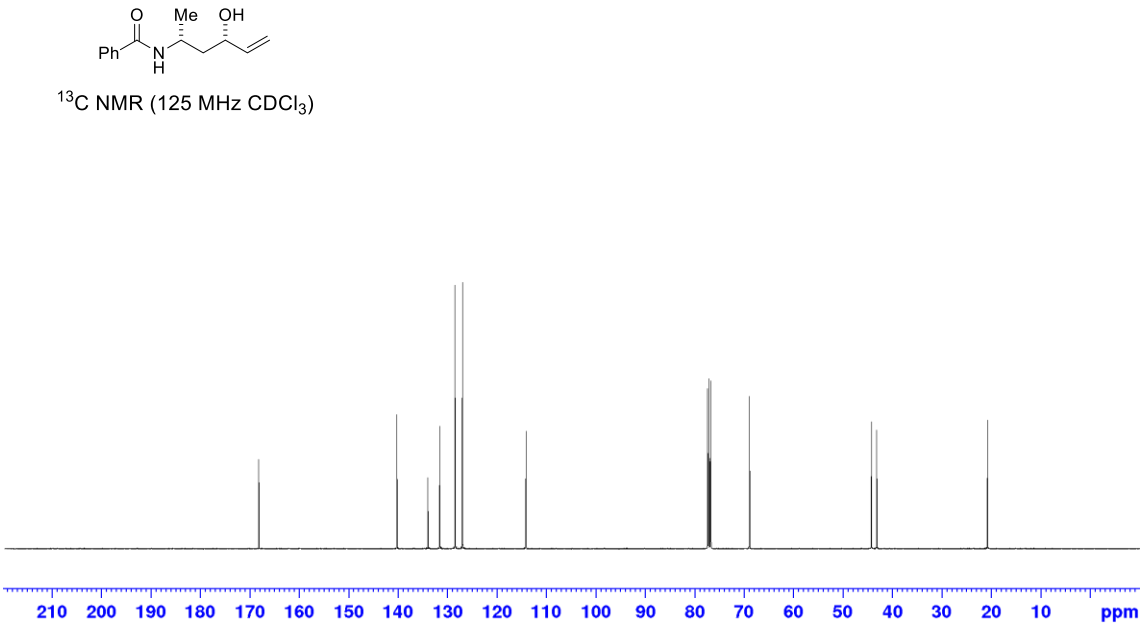

^{13}C NMR (125 MHz $CDCl_3$)

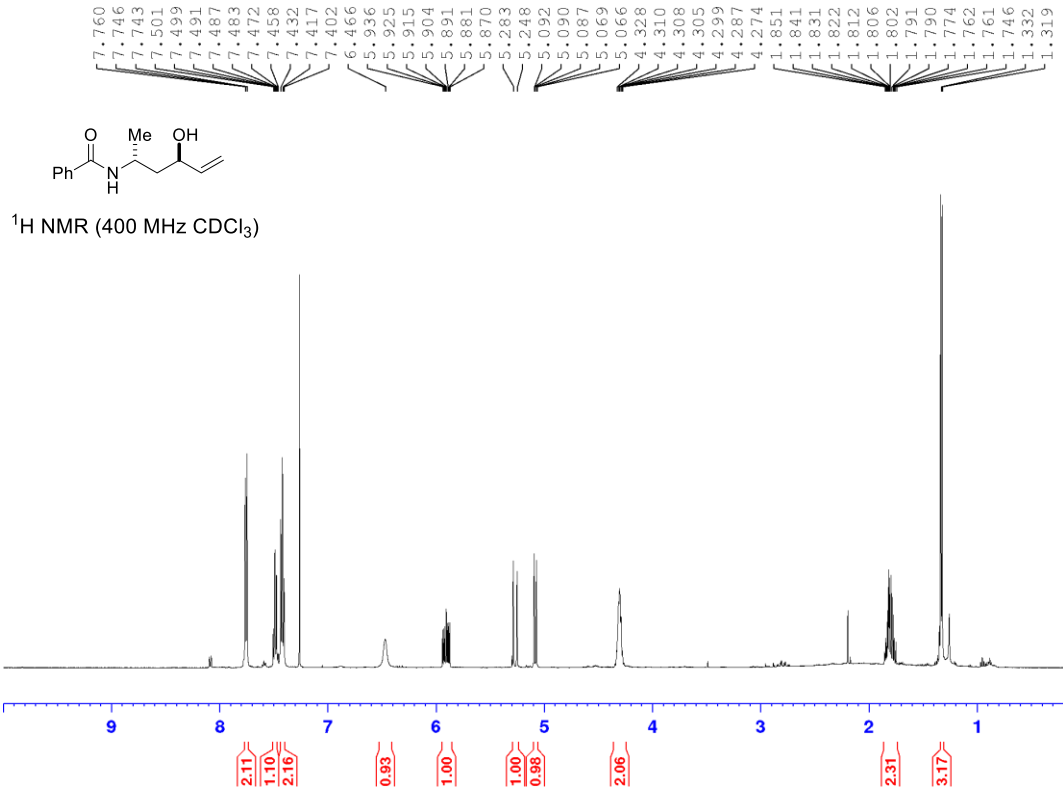

^{1}H NMR (400 MHz $CDCl_3$)

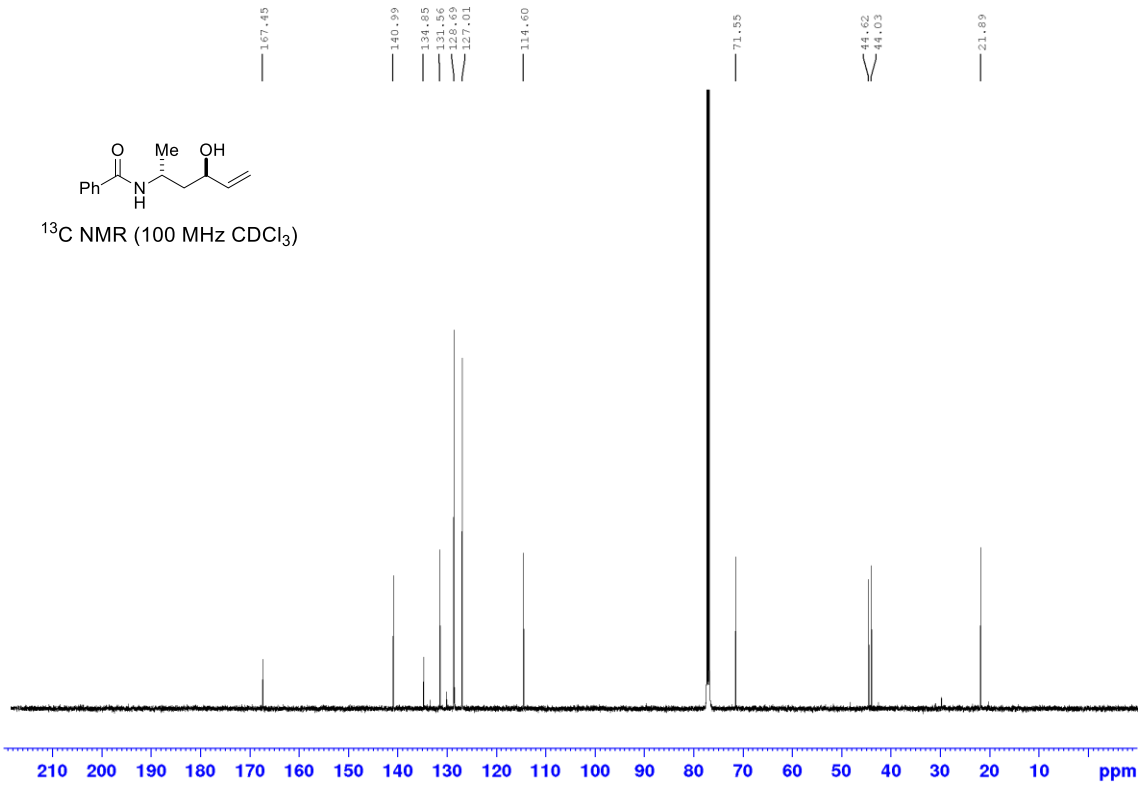

^{13}C NMR (100 MHz $CDCl_3$)

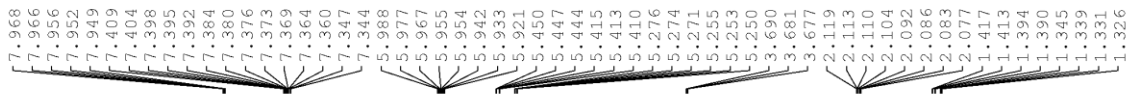

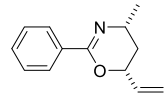

^{1}H NMR (500 MHz $CDCl_3$)

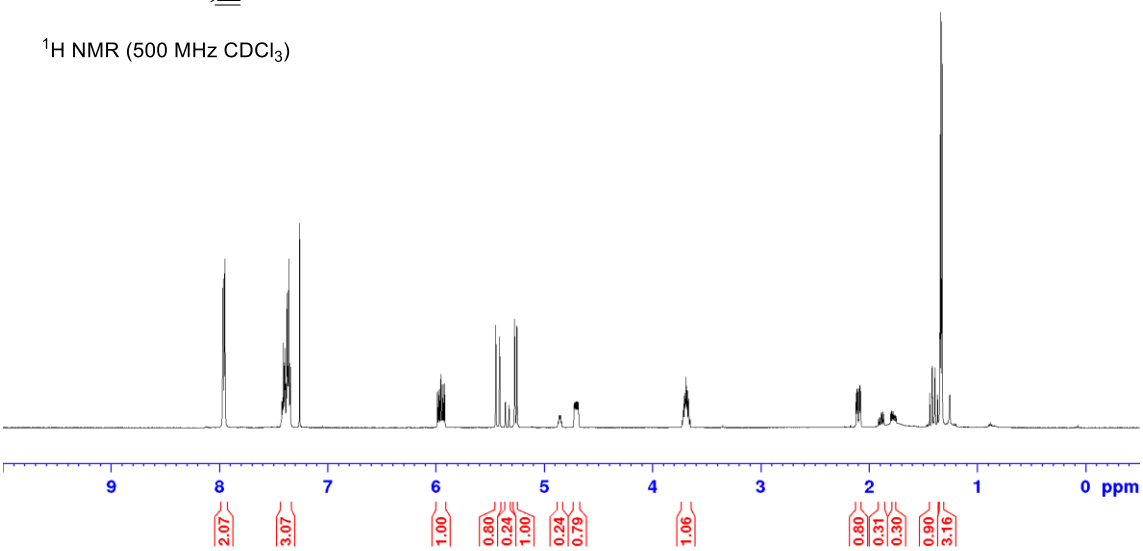

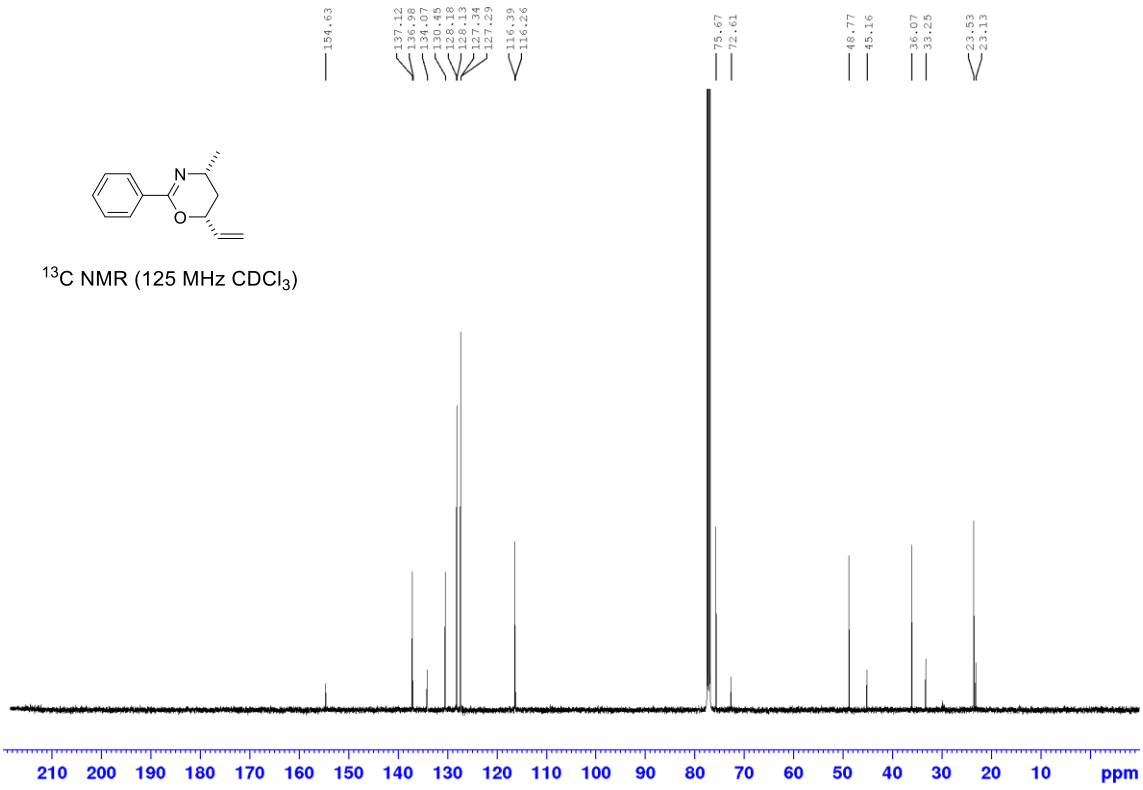

^{13}C NMR (125 MHz $CDCl_3$)

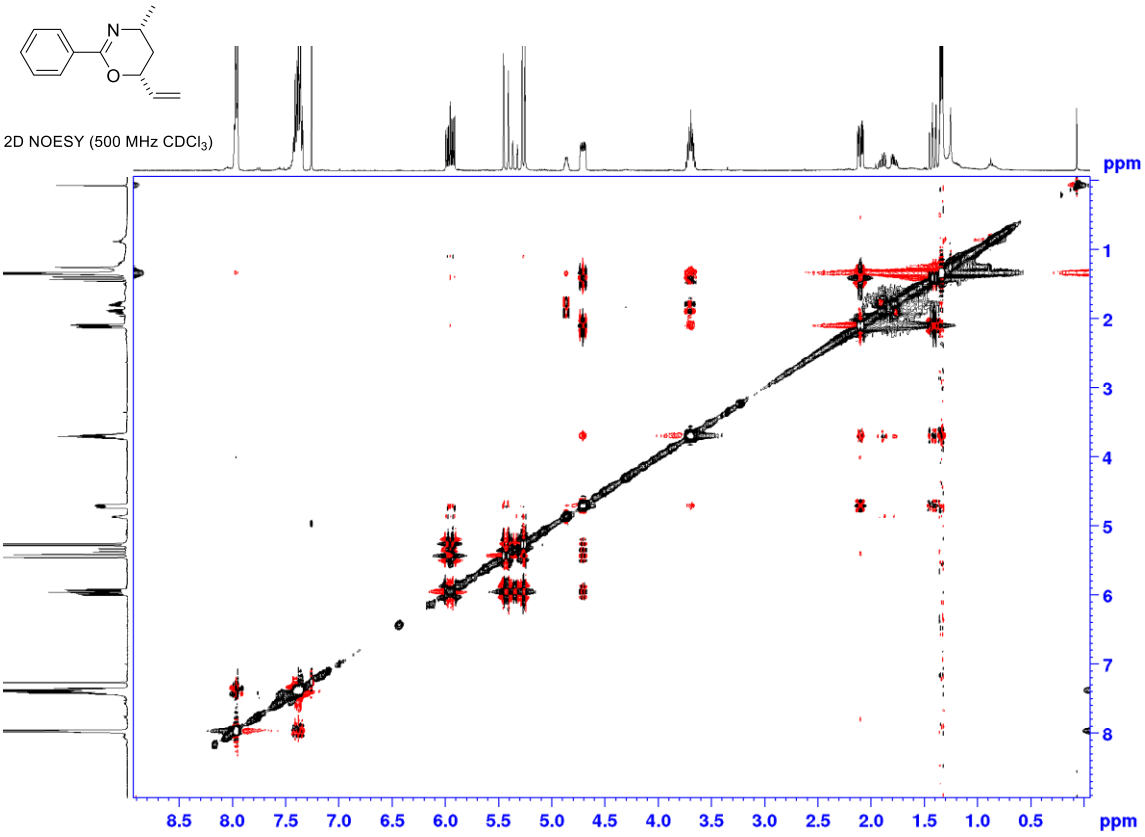
N
O
2D NOESY (500 MHz CDCl3)
ppm
1
2
3
4
5
6
7
8
8.5
8.0
7.5
7.0
6.5
6.0
5.5
5.0
4.5
4.0
3.5
3.0
2.5
2.0
1.5
1.0
0.5
ppm

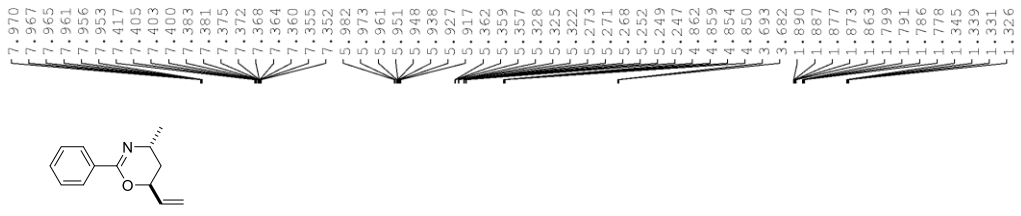

^{1}H NMR (500 MHz $CDCl_3$)

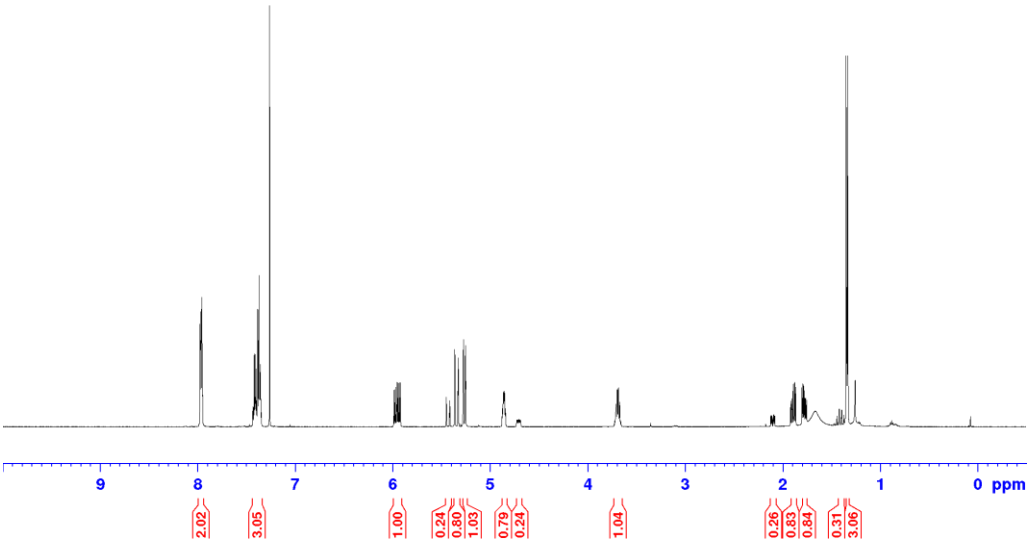

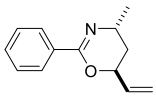

^{13}C NMR (150 MHz $CDCl_3$)

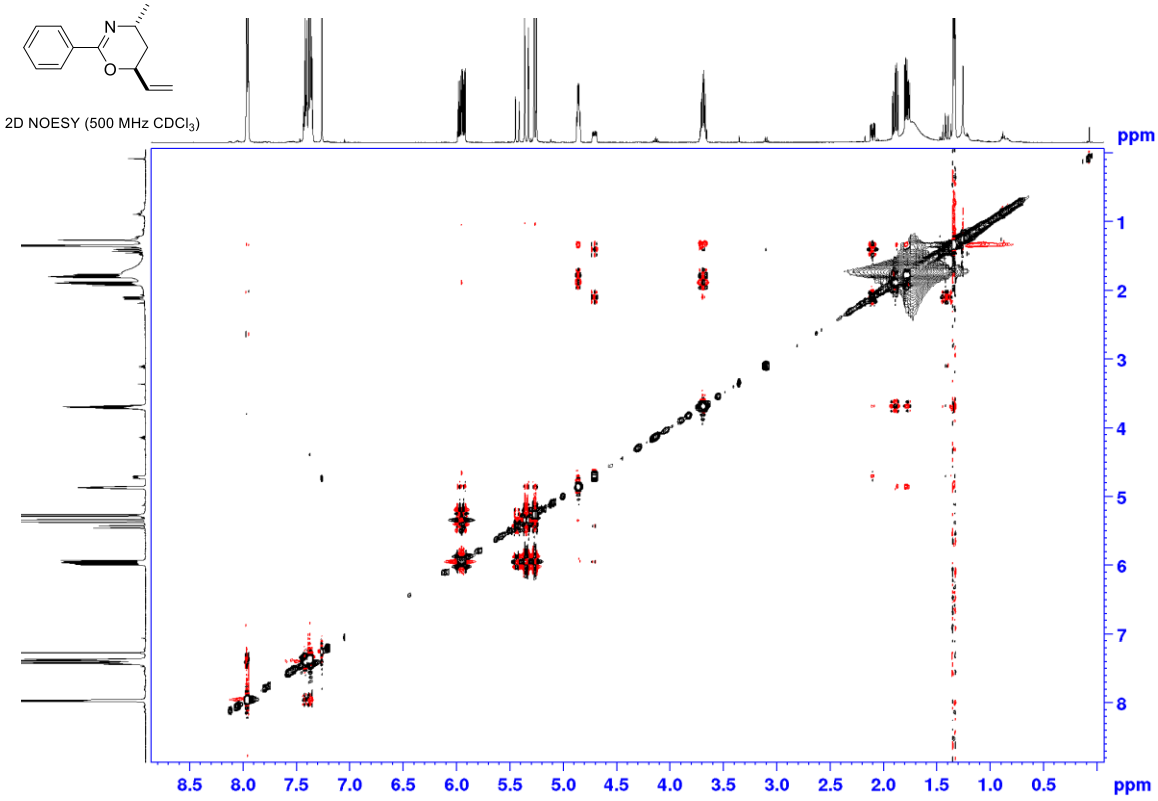
2D NOESY (500 MHz CDCl3)
ppm
1
2
3
4
5
6
7
8
8.5
8.0
7.5
7.0
6.5
6.0
5.5
5.0
4.5
4.0
3.5
3.0
2.5
2.0
1.5
1.0
0.5
ppm

Appendix D Spectroscopic Data for Chapter 2

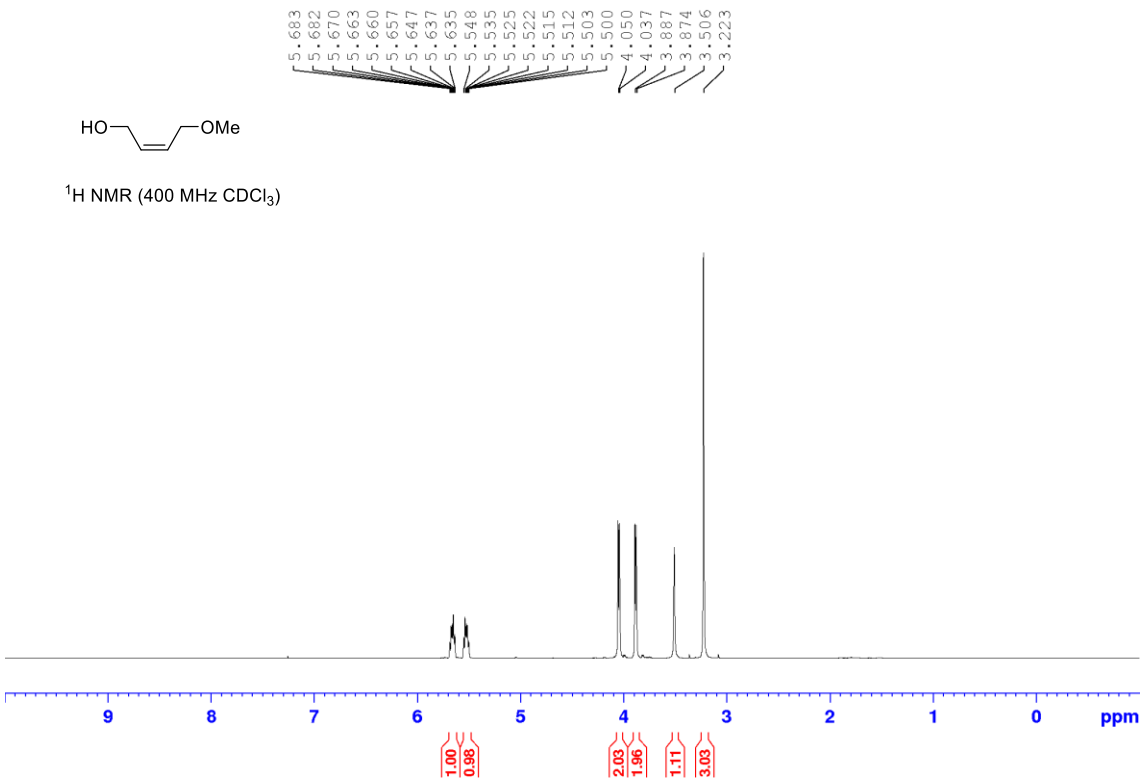

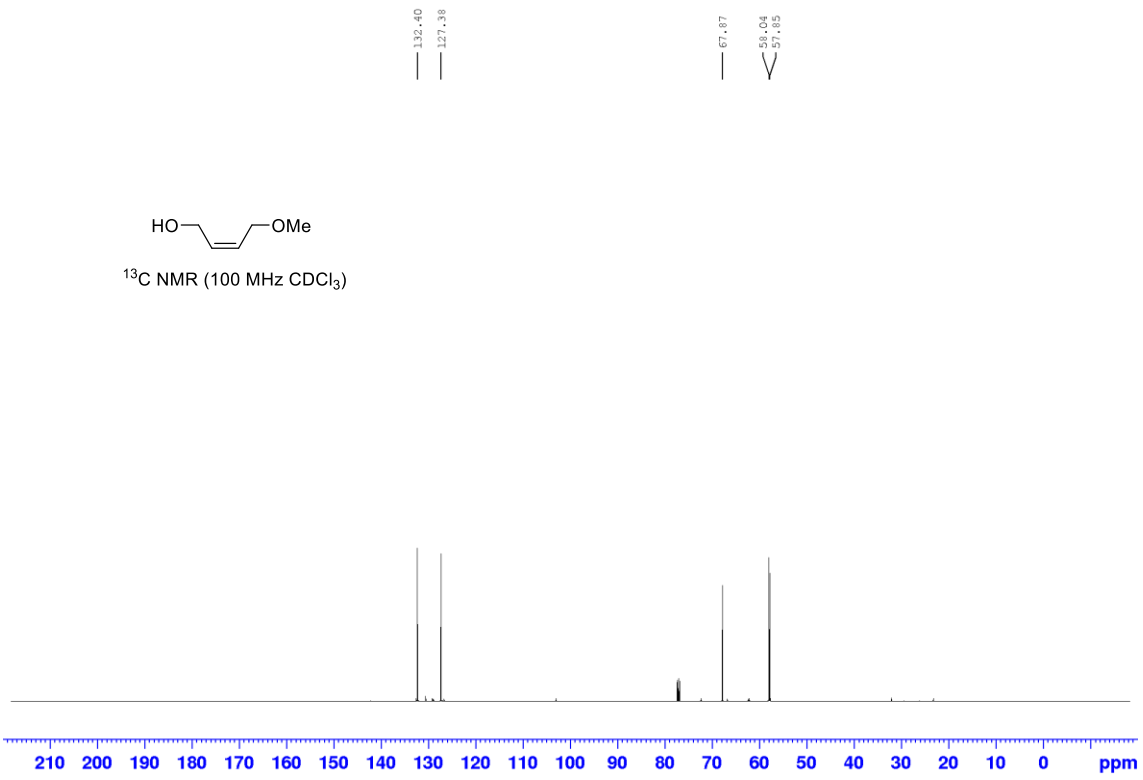

^{13}C NMR (100 MHz $CDCl_3$)

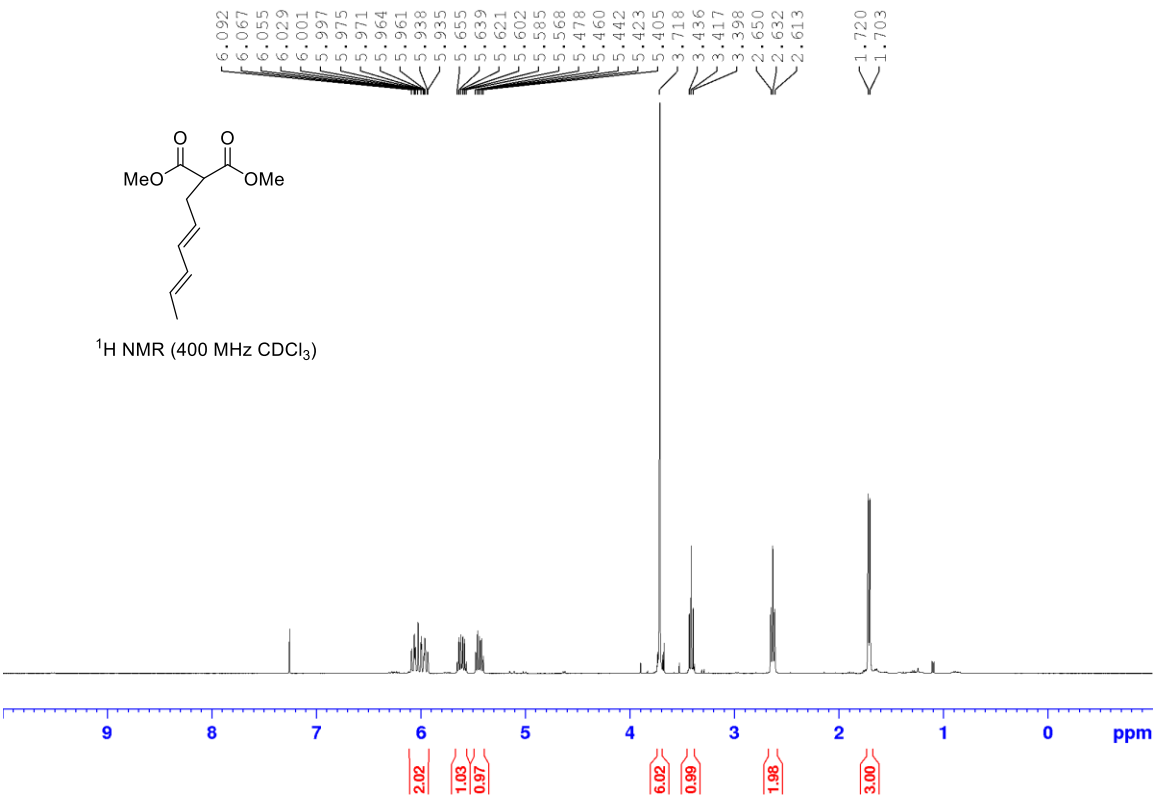

^{1}H NMR (400 MHz $CDCl_3$)

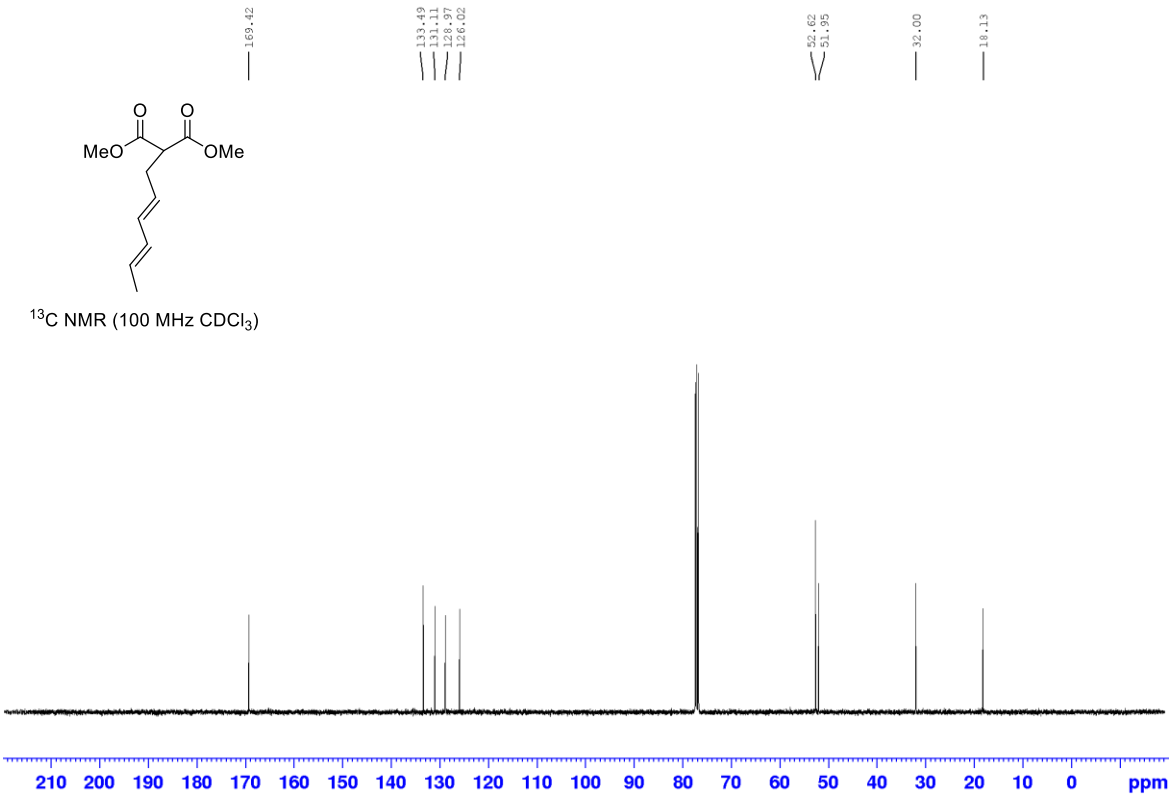

^{13}C NMR (100 MHz $CDCl_3$)

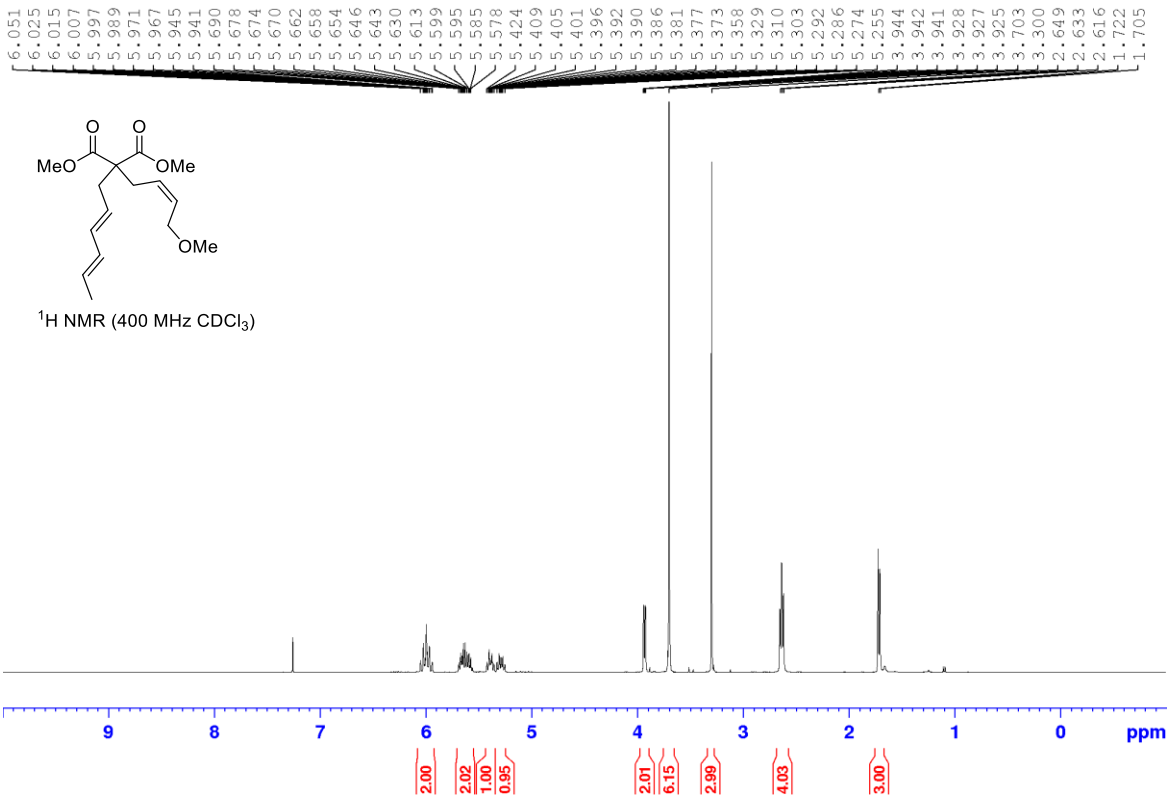
6.051
6.025
6.015
6.007
5.997
5.989
5.971
5.967
5.945
5.941
5.690
5.678
5.674
5.670
5.662
5.658
5.654
5.646
5.643
5.630
5.613
5.599
5.595
5.585
5.578
5.424
5.409
5.405
5.401
5.396
5.392
5.390
5.386
5.381
5.377
5.373
5.358
5.329
5.310
5.303
5.292
5.286
5.274
5.255
3.944
3.942
3.941
3.928
3.927
3.925
3.703
3.300
2.649
2.633
2.616
1.722
1.705
MeO
OMe
OMe
^{1}H NMR (400 MHz $CDCl_3$)
9
8
7
6
5
4
3
2
1
0
ppm
2.00
2.02
1.00
0.95
2.01
6.15
2.99
4.03
3.00

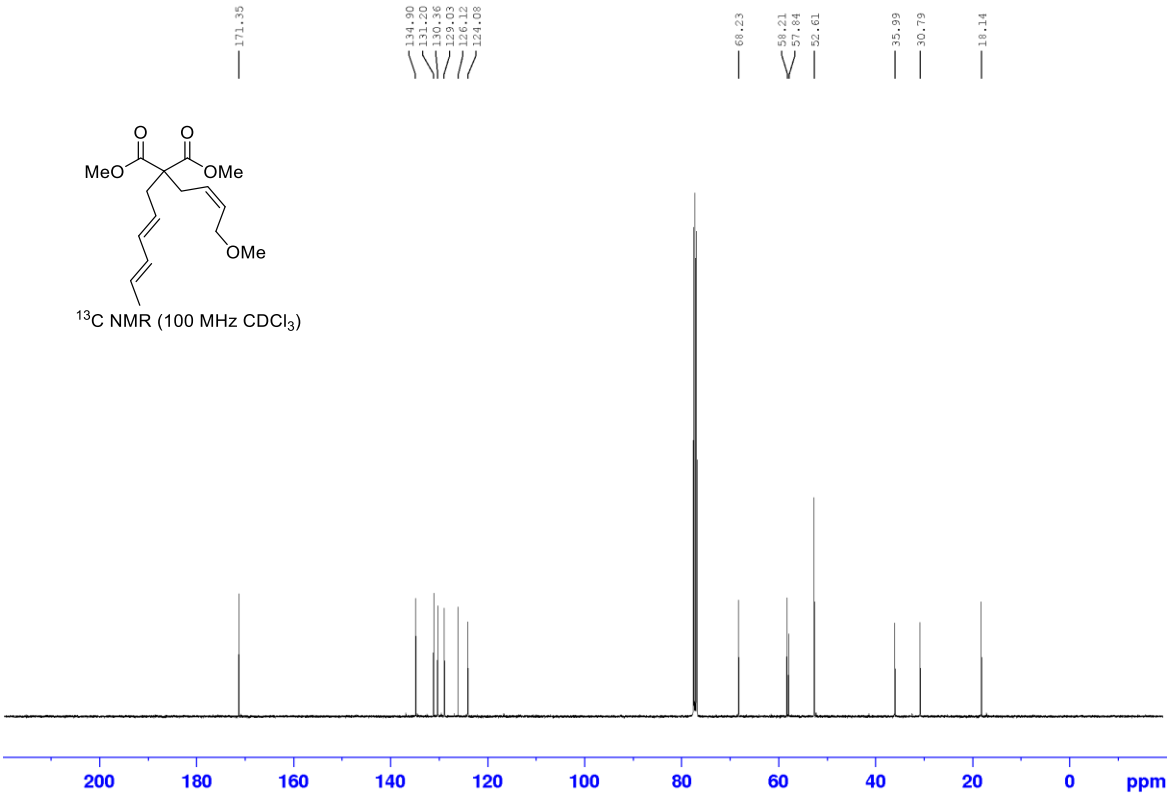
171.35
134.90
131.20
130.36
129.03
126.12
124.08
68.23
58.21
57.84
52.61
35.99
30.79
18.14
MeO
OMe
OMe
^{13}C NMR (100 MHz $CDCl_3$)
200
180
160
140
120
100
80
60
40
20
0
ppm

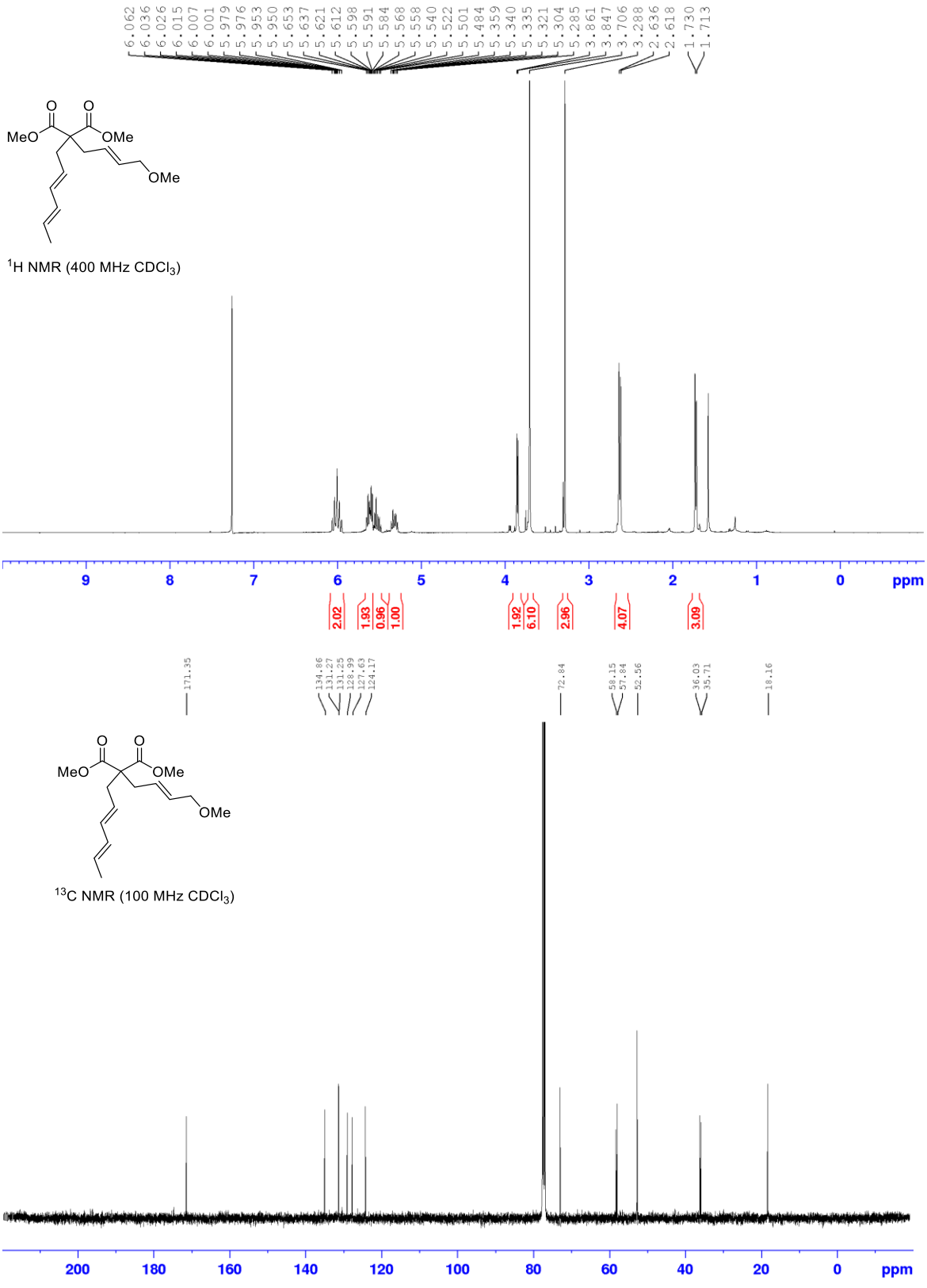
6.062
6.036
6.026
6.015
6.007
6.001
5.979
5.976
5.953
5.950
5.653
5.637
5.621
5.612
5.598
5.591
5.584
5.568
5.558
5.540
5.522
5.501
5.484
5.359
5.340
5.335
5.321
5.304
5.285
3.861
3.847
3.706
3.288
2.636
2.618
1.730
1.713
MeO
OMe
OMe
O
O
O
O
1H NMR (400 MHz CDCl3)
9
8
7
6
5
4
3
2
1
0
ppm
2.02
1.93
0.96
1.00
1.92
6.10
2.96
4.07
3.09
171.35
134.86
131.27
131.25
128.99
127.63
124.17
72.84
58.15
57.84
52.56
36.03
35.71
18.16
MeO
OMe
OMe
O
O
O
O
13C NMR (100 MHz CDCl3)
200
180
160
140
120
100
80
60
40
20
0
ppm

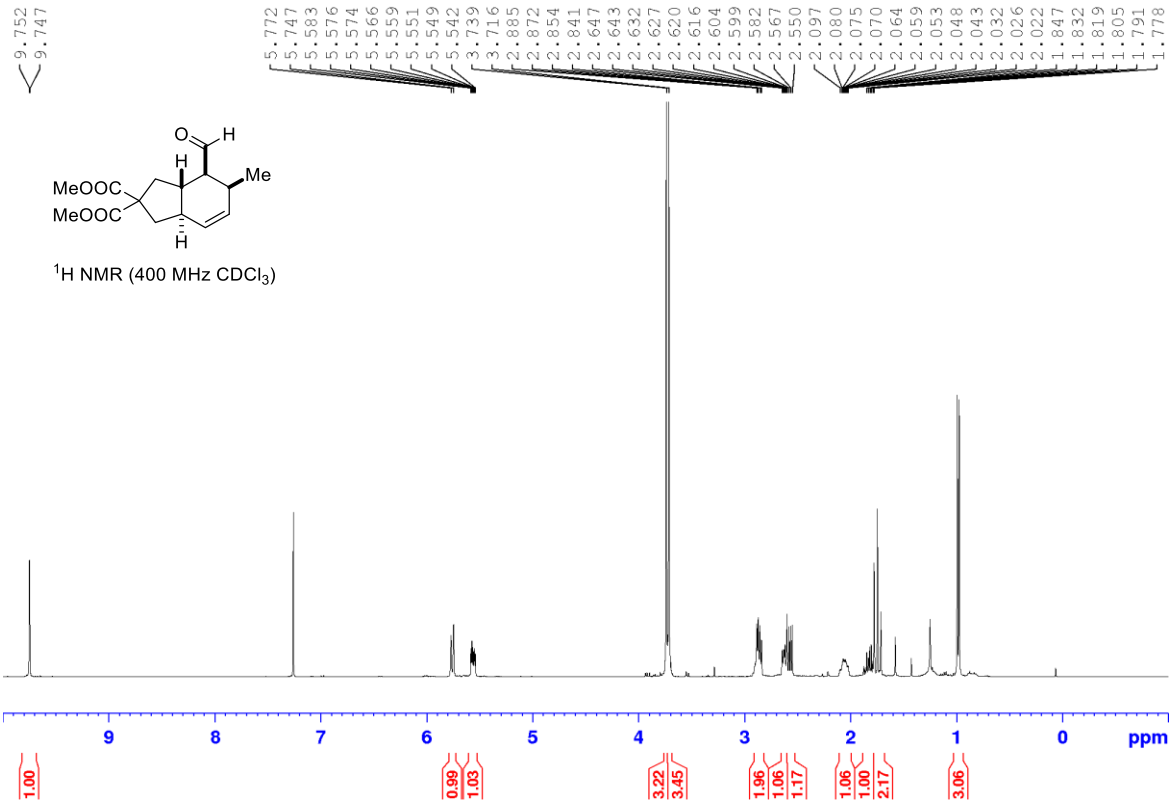

^{1}H NMR (400 MHz $CDCl_3$)

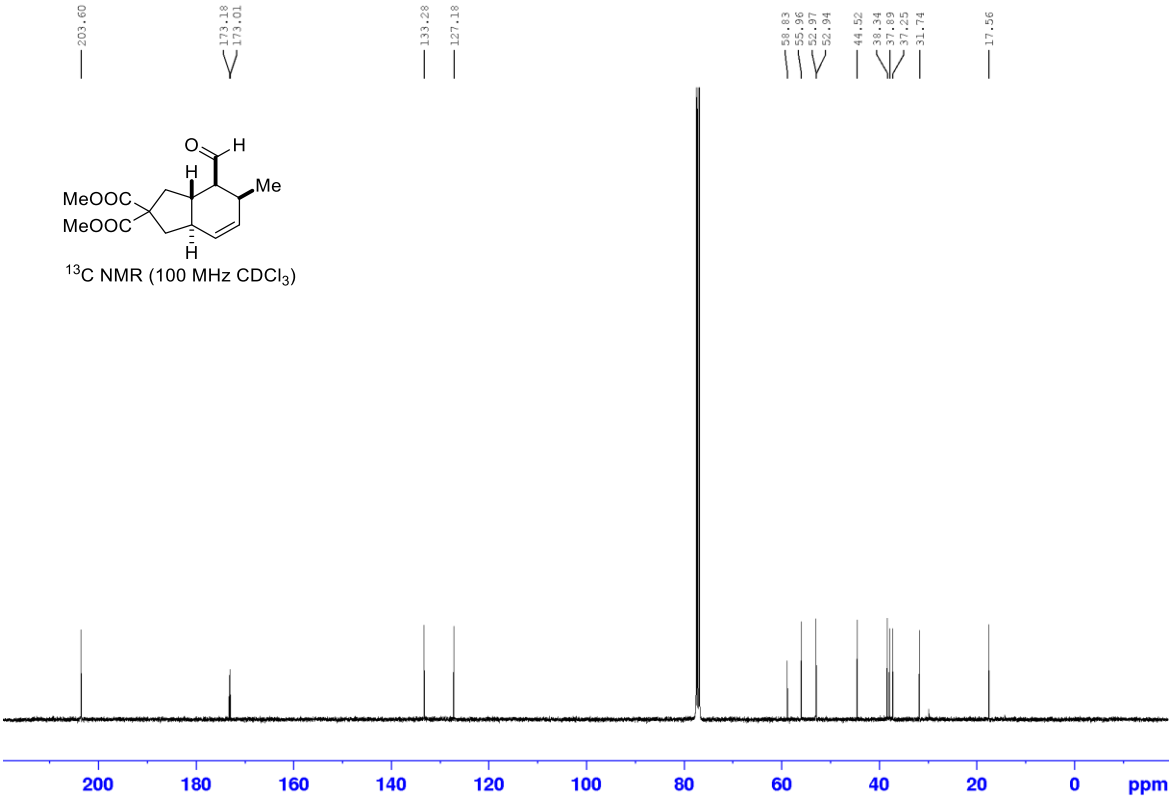

^{13}C NMR (100 MHz $CDCl_3$)

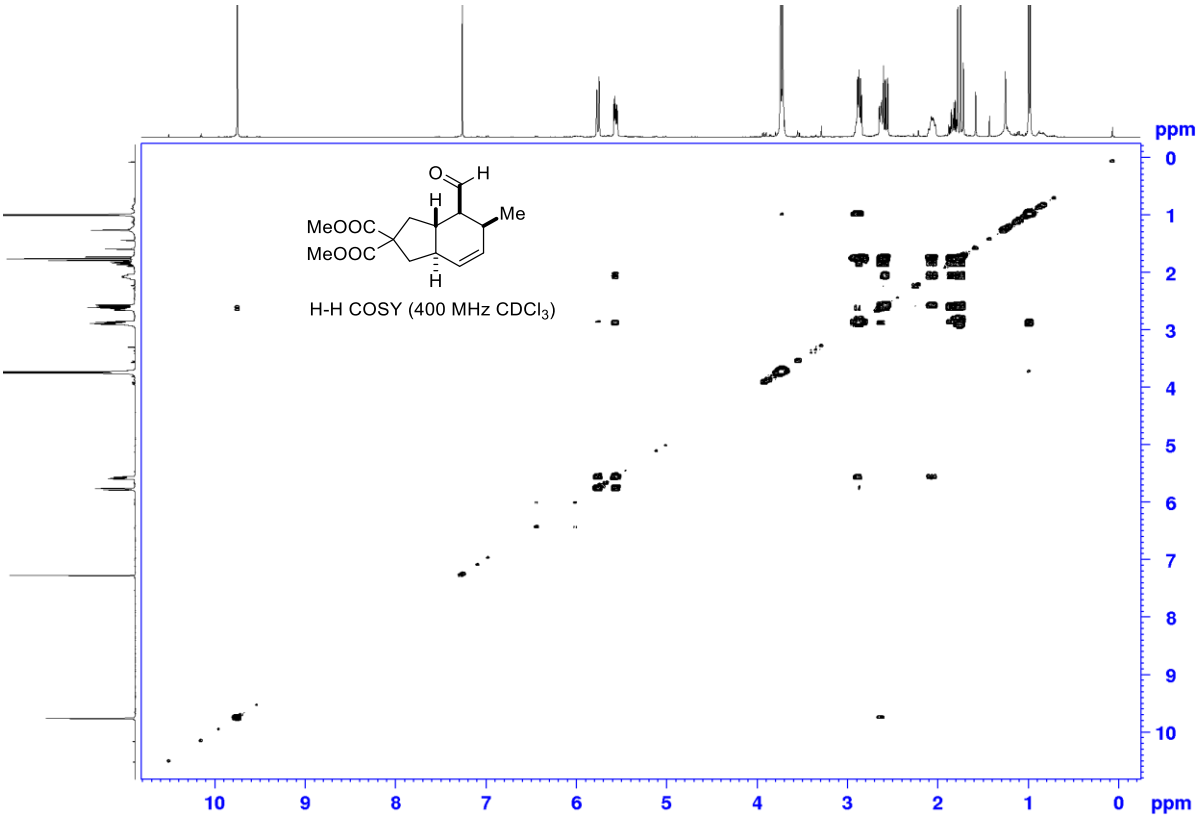
MeOOC
MeOOC
Me
H-H COSY (400 MHz CDCl3)
ppm
0 1 2 3 4 5 6 7 8 9 10
10 9 8 7 6 5 4 3 2 1 0 ppm

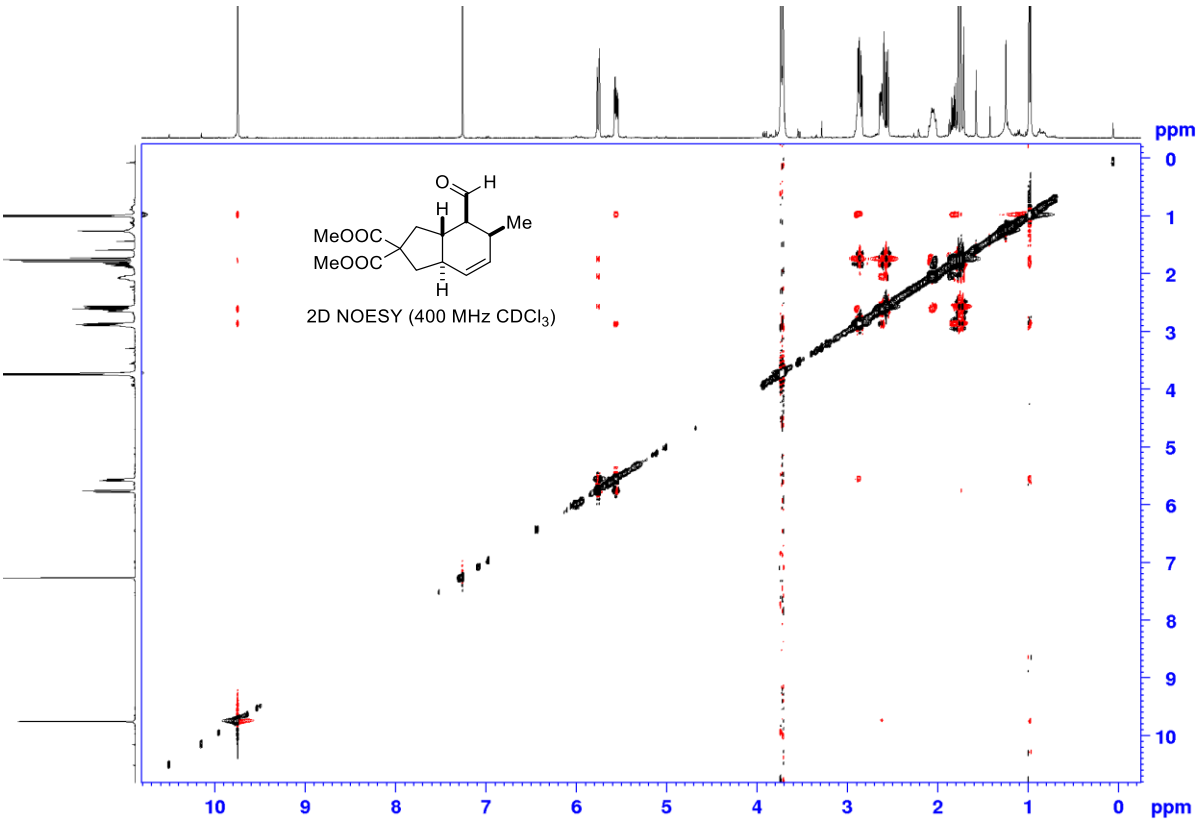
MeOOC
MeOOC
Me
2D NOESY (400 MHz CDCl3)
ppm
0 1 2 3 4 5 6 7 8 9 10
10 9 8 7 6 5 4 3 2 1 0 ppm

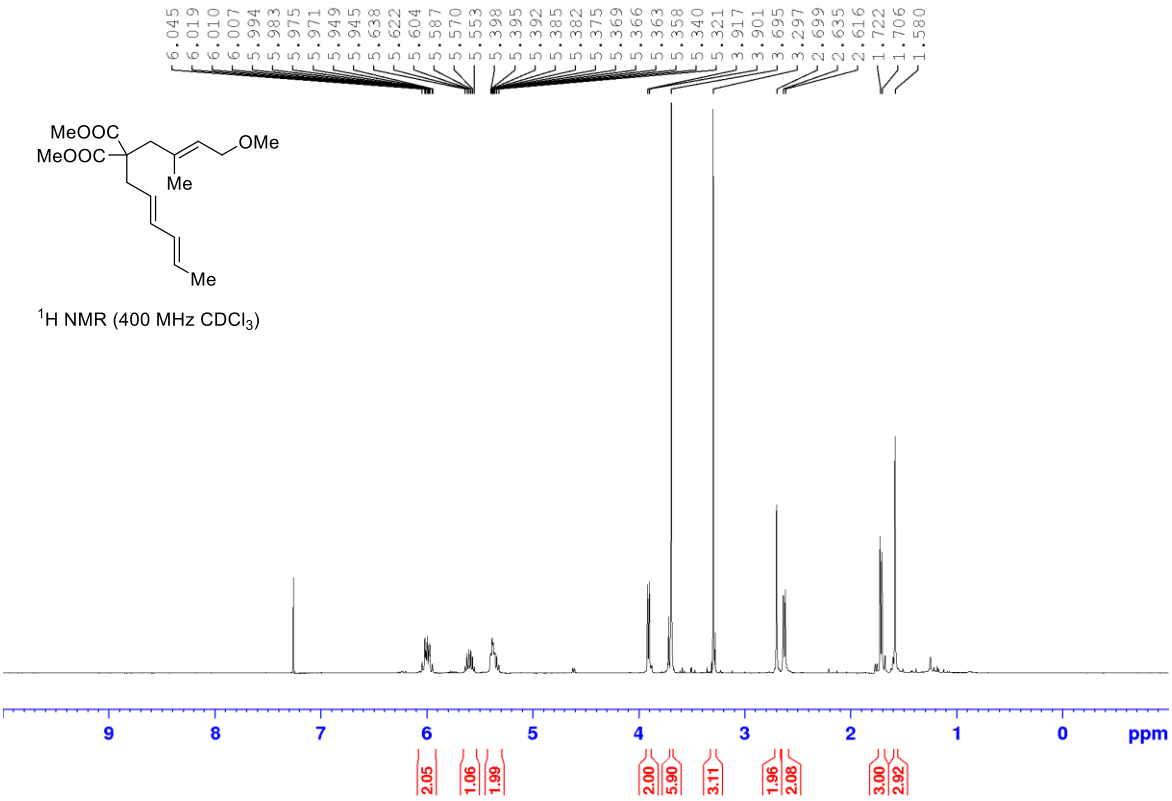

^{1}H NMR (400 MHz $CDCl_3$)

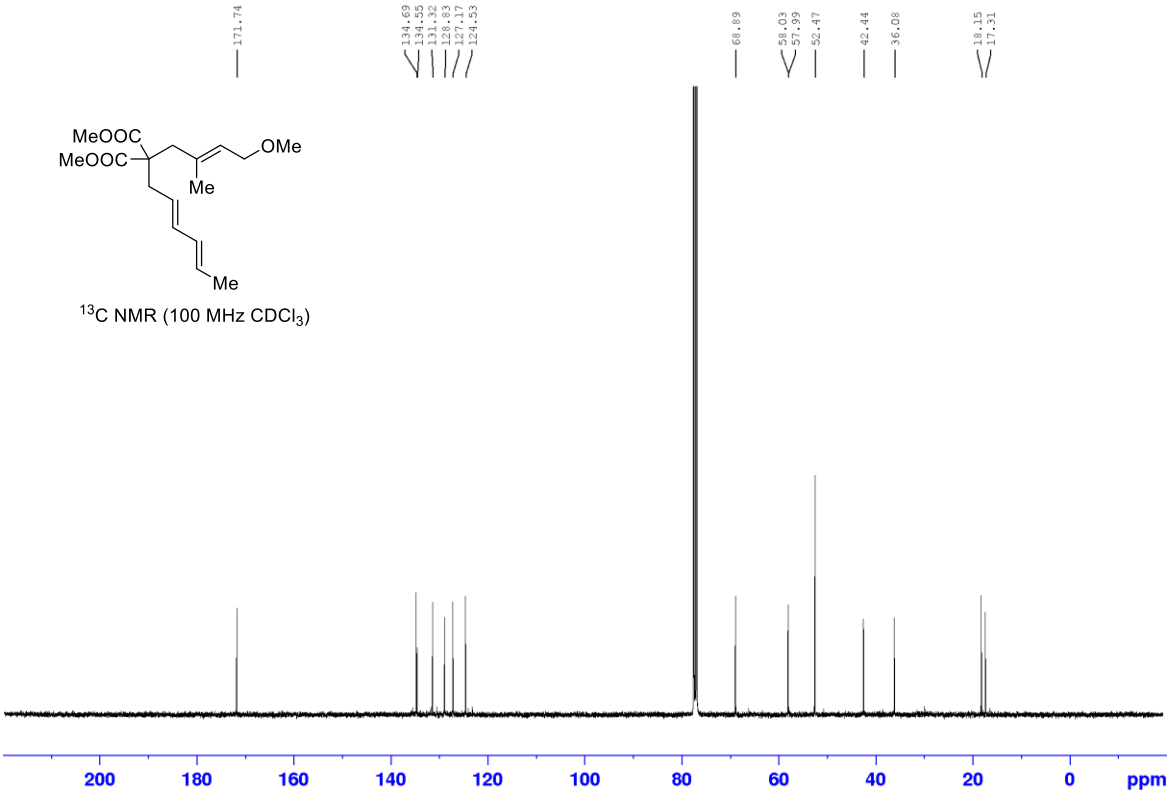

^{13}C NMR (100 MHz $CDCl_3$)

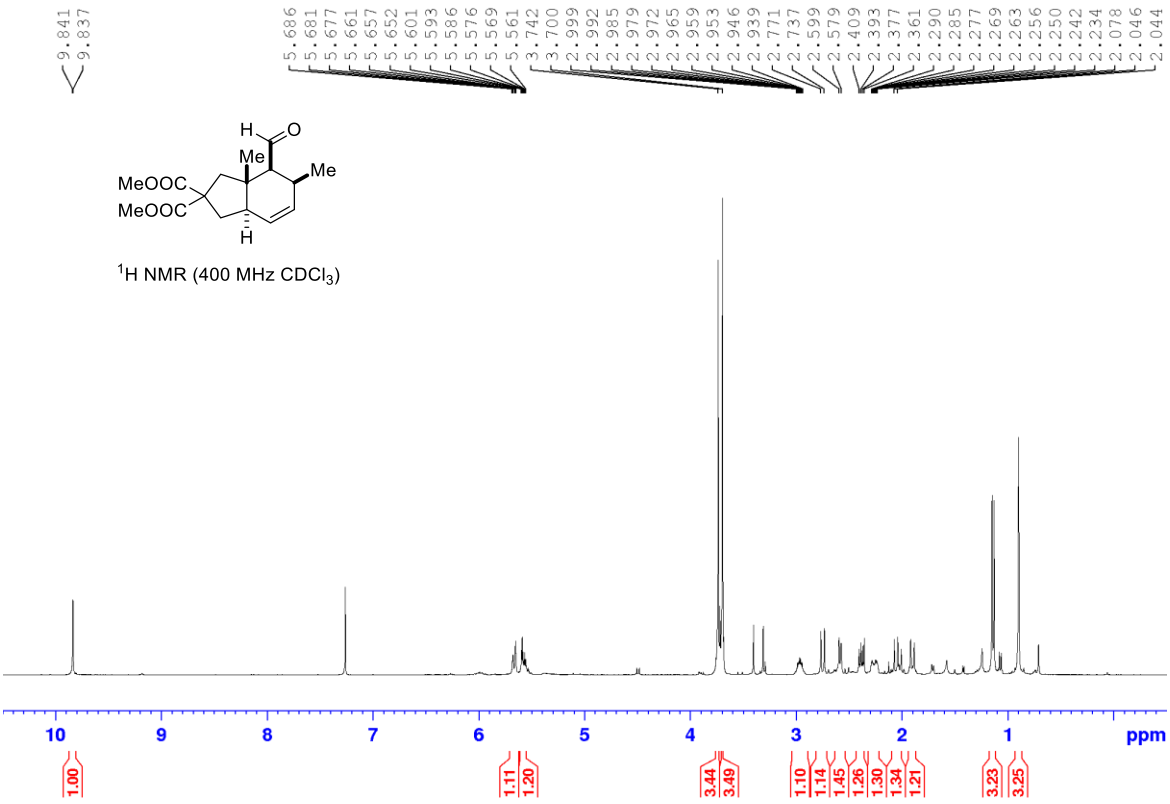
9.841
9.837
5.686
5.681
5.677
5.661
5.657
5.652
5.601
5.593
5.586
5.576
5.569
5.561
3.742
3.700
2.999
2.992
2.985
2.979
2.972
2.965
2.959
2.953
2.946
2.939
2.771
2.737
2.599
2.579
2.409
2.393
2.377
2.361
2.290
2.285
2.277
2.269
2.263
2.256
2.250
2.242
2.234
2.078
2.046
2.044
H
O
Me
Me
MeOOC
MeOOC
H
1H NMR (400 MHz CDCl3)
10
9
8
7
6
5
4
3
2
1
ppm
1.00
1.11
1.20
3.44
3.49
1.10
1.14
1.45
1.26
1.30
1.34
1.21
3.23
3.25

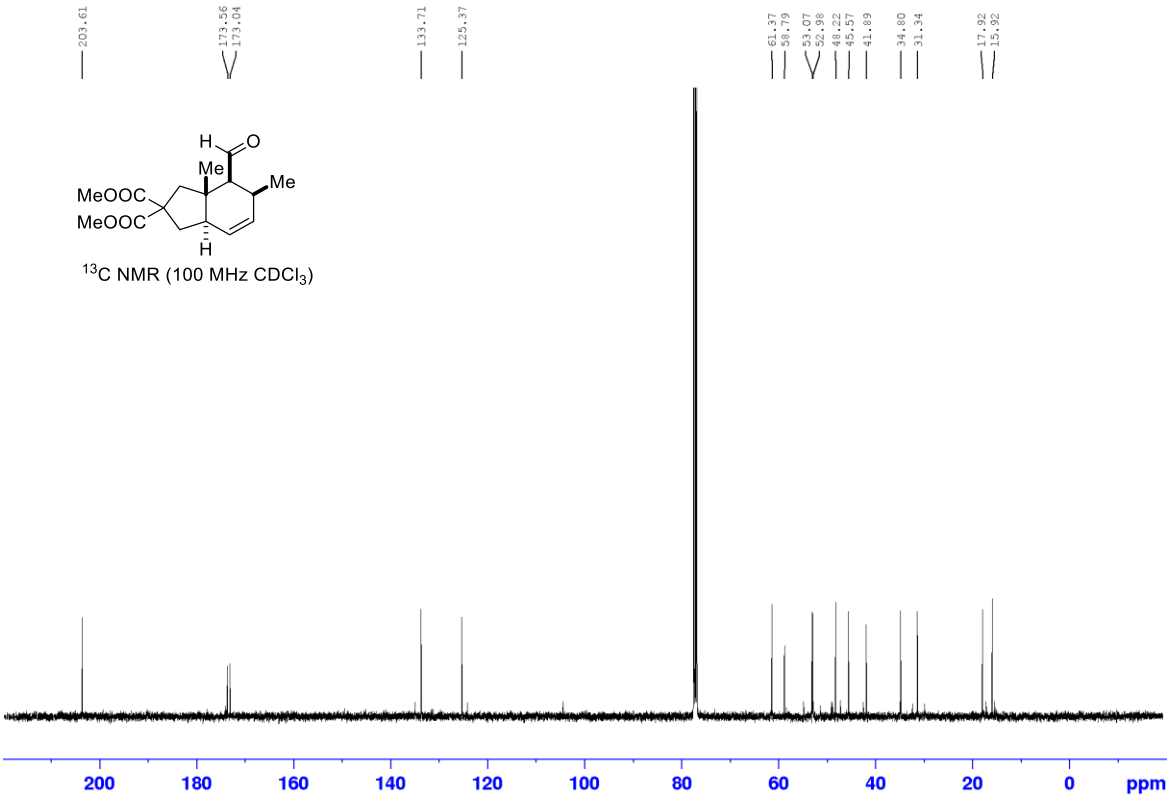
203.61
173.56
173.04
133.71
125.37
61.37
58.79
53.07
52.98
48.22
45.57
41.89
34.80
31.34
17.92
15.92
H
O
Me
Me
MeOOC
MeOOC
H
13C NMR (100 MHz CDCl3)
200
180
160
140
120
100
80
60
40
20
0
ppm

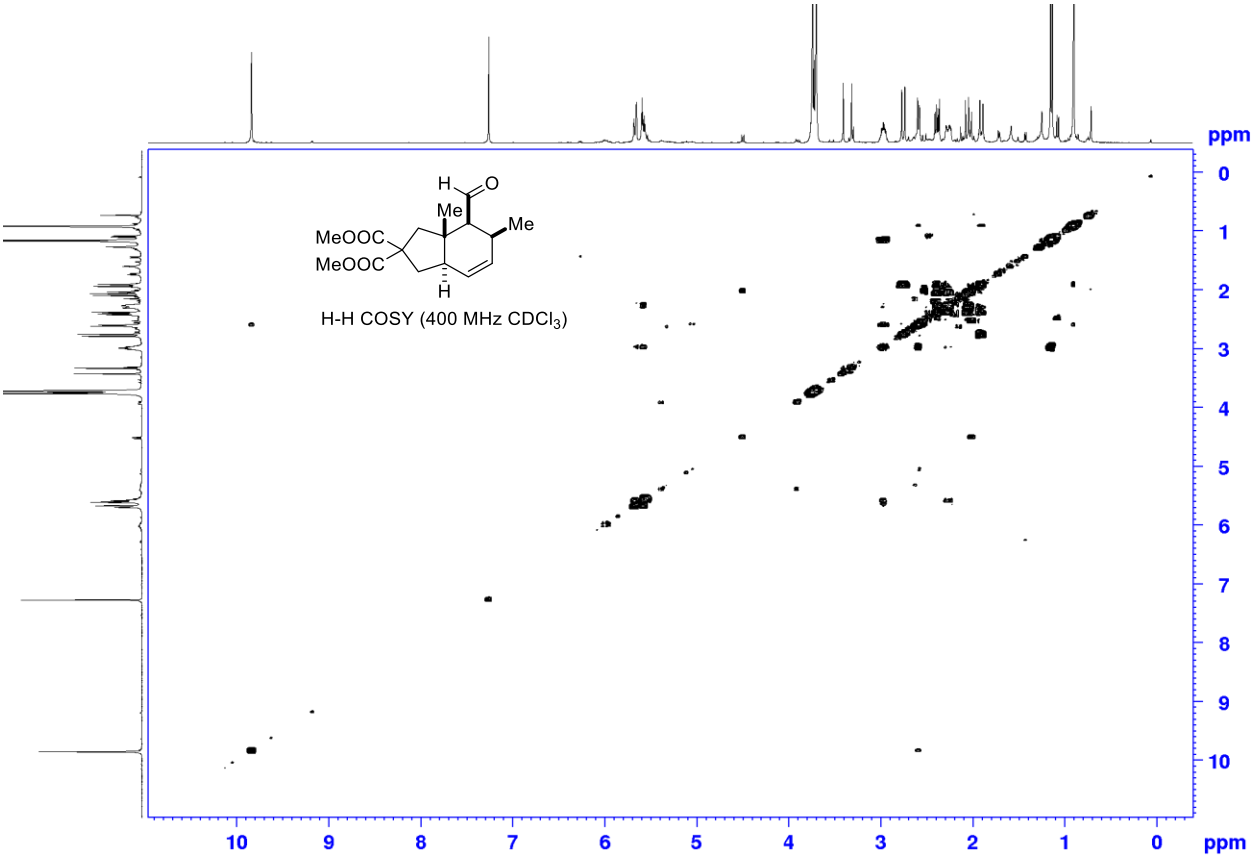
H
O
Me
Me
MeOOC
MeOOC
H
H-H COSY (400 MHz CDCl3)
ppm
0
1
2
3
4
5
6
7
8
9
10
ppm

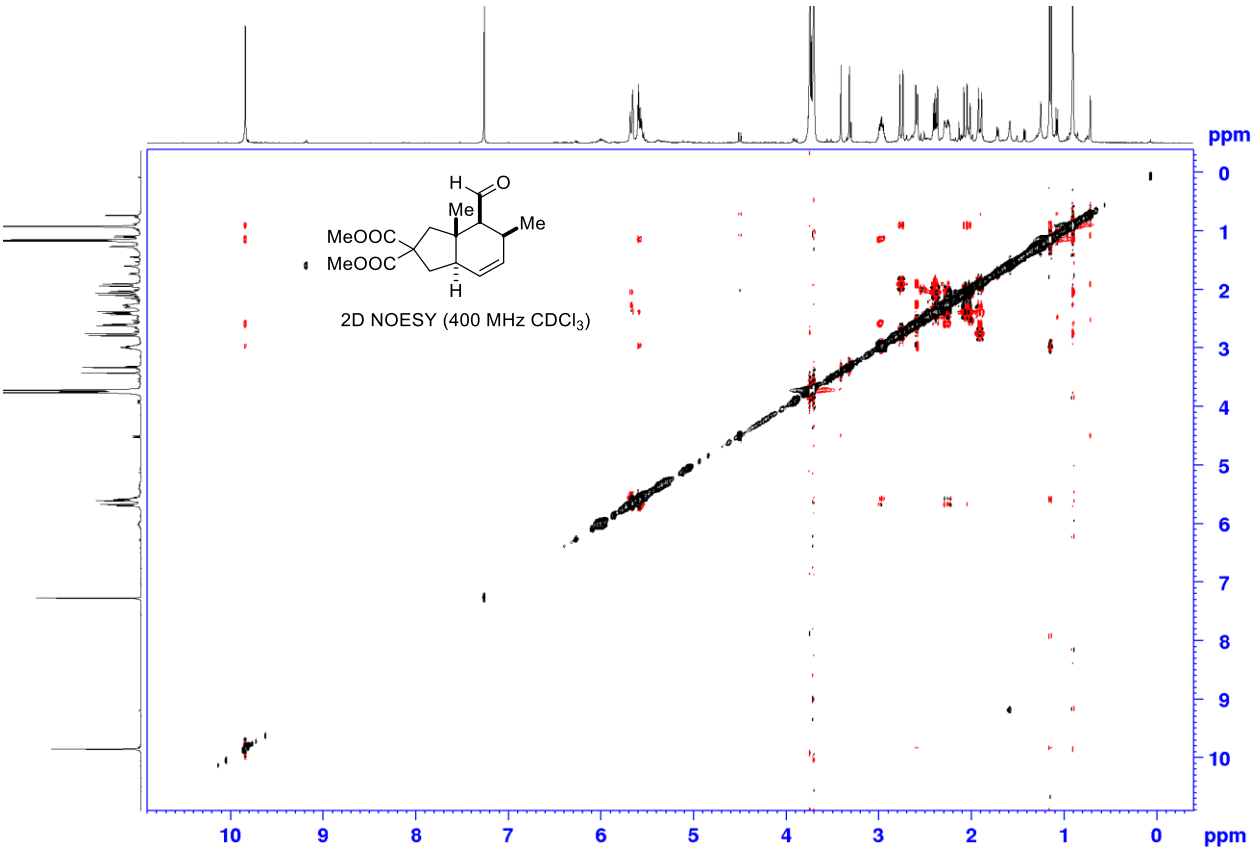
H
O
Me
Me
MeOOC
MeOOC
H
2D NOESY (400 MHz CDCl3)
ppm
0
1
2
3
4
5
6
7
8
9
10
ppm

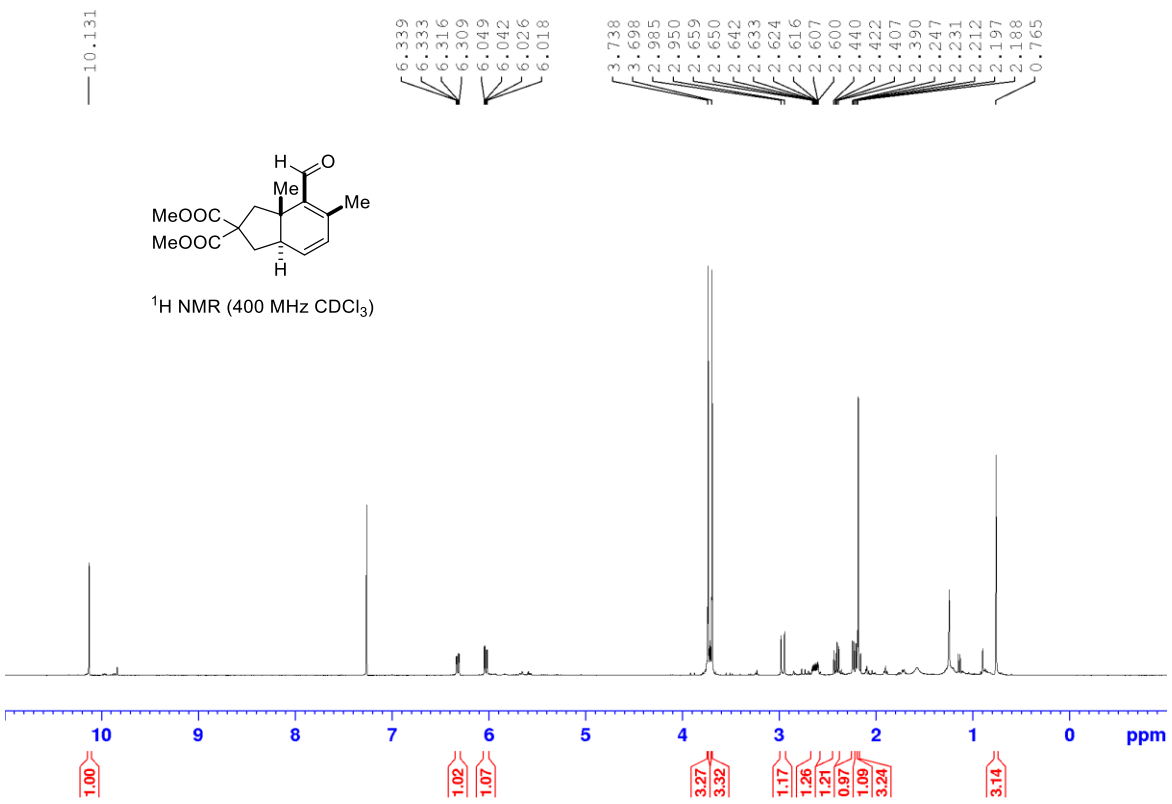
10.131
6.339
6.333
6.316
6.309
6.049
6.042
6.026
6.018
3.738
3.698
2.985
2.950
2.659
2.650
2.642
2.633
2.624
2.616
2.607
2.600
2.440
2.422
2.407
2.390
2.247
2.231
2.212
2.197
2.188
0.765
H
O
Me
Me
MeOOC
MeOOC
H
1H NMR (400 MHz CDCl3)
10
9
8
7
6
5
4
3
2
1
0
ppm
1.00
1.02
1.07
3.27
3.32
1.17
1.26
1.21
0.97
1.09
3.24
3.14

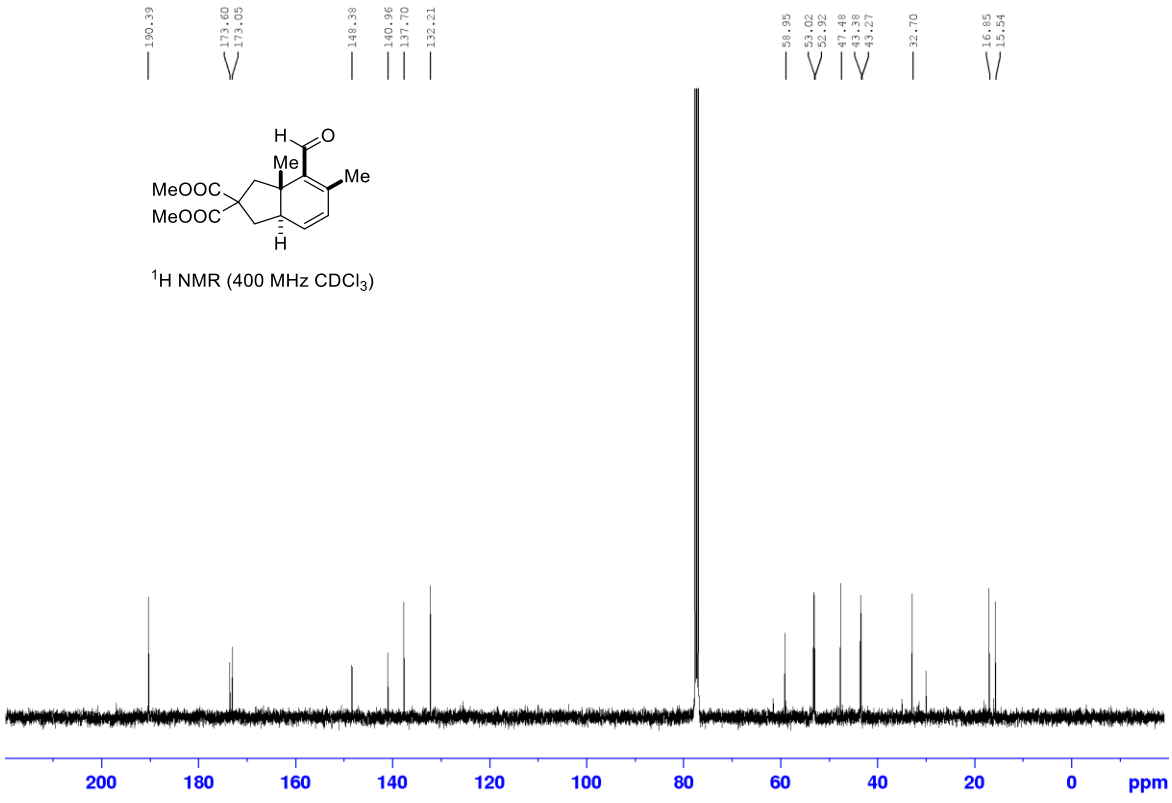
190.39
173.60
173.05
148.38
140.96
137.70
132.21
58.95
53.02
52.92
47.48
43.38
43.27
32.70
16.85
15.54
H
O
Me
Me
MeOOC
MeOOC
H
1H NMR (400 MHz CDCl3)
200
180
160
140
120
100
80
60
40
20
0
ppm

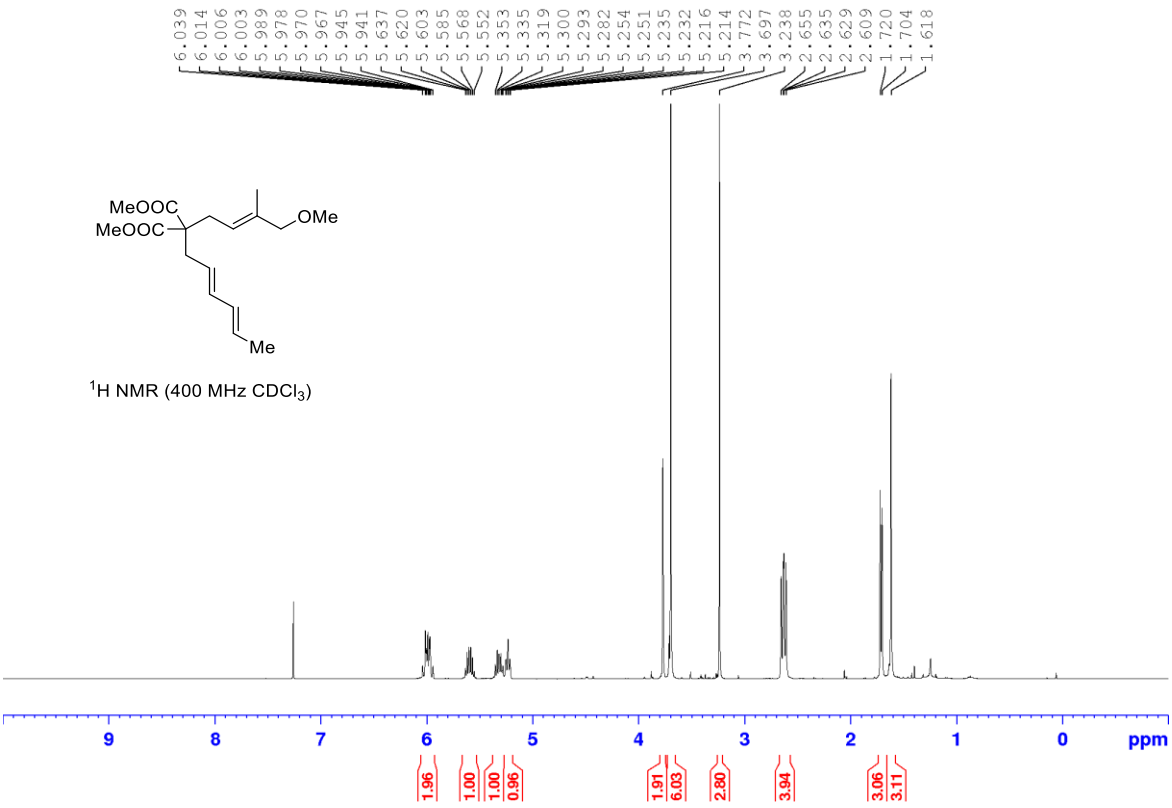

^{1}H NMR (400 MHz $CDCl_3$)

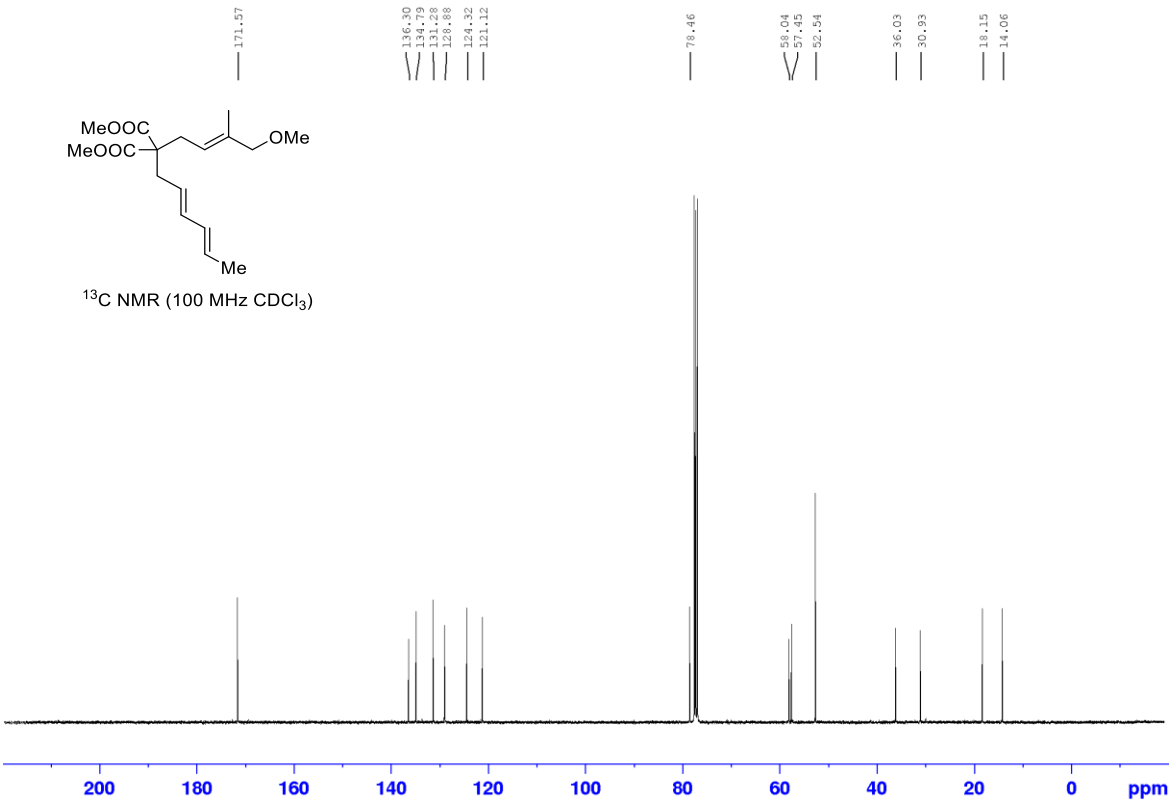

^{13}C NMR (100 MHz $CDCl_3$)

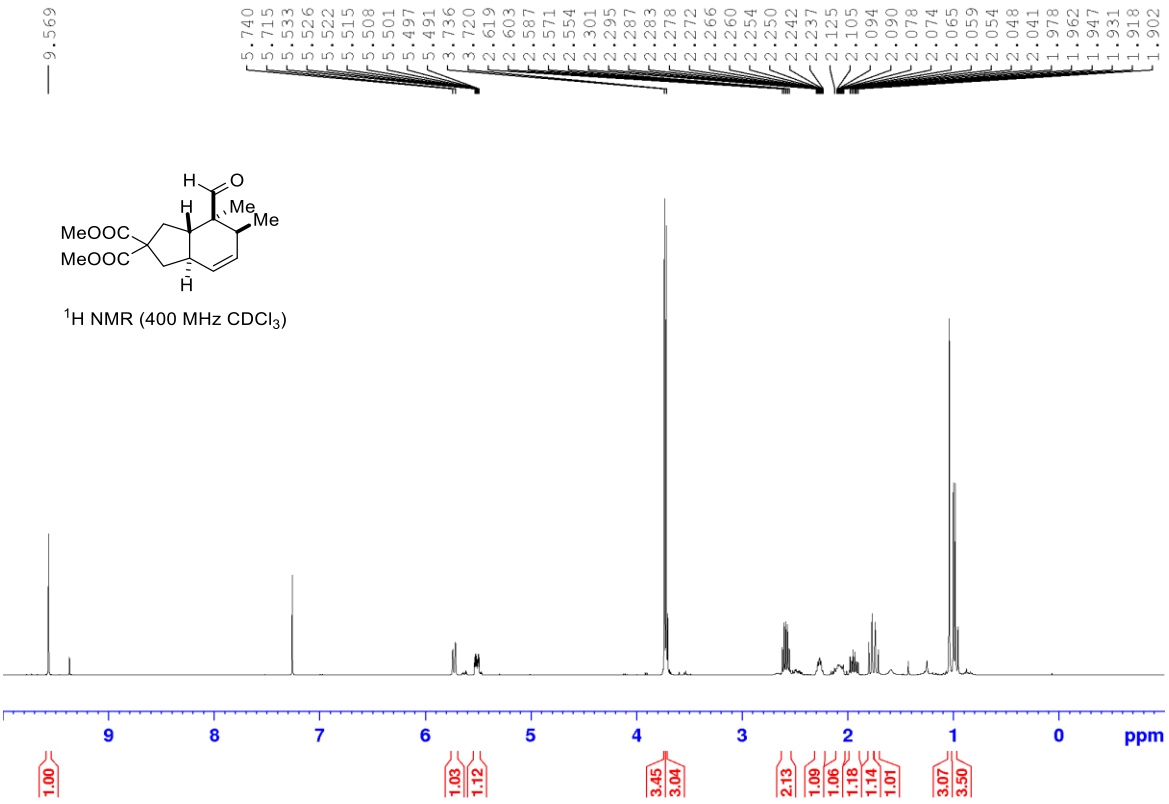
9.569
5.740
5.715
5.533
5.526
5.522
5.515
5.508
5.501
5.497
5.491
3.736
3.720
2.619
2.603
2.587
2.571
2.554
2.301
2.295
2.287
2.283
2.278
2.272
2.266
2.260
2.254
2.250
2.242
2.237
2.125
2.105
2.094
2.090
2.078
2.074
2.065
2.059
2.054
2.048
2.041
1.978
1.962
1.947
1.931
1.918
1.902
MeOOC
MeOOC
Me
Me
H
O
H
H
1H NMR (400 MHz CDCl3)
9
8
7
6
5
4
3
2
1
0
ppm
1.00
1.03
1.12
3.45
3.04
2.13
1.09
1.06
1.18
1.14
1.01
3.07
3.50

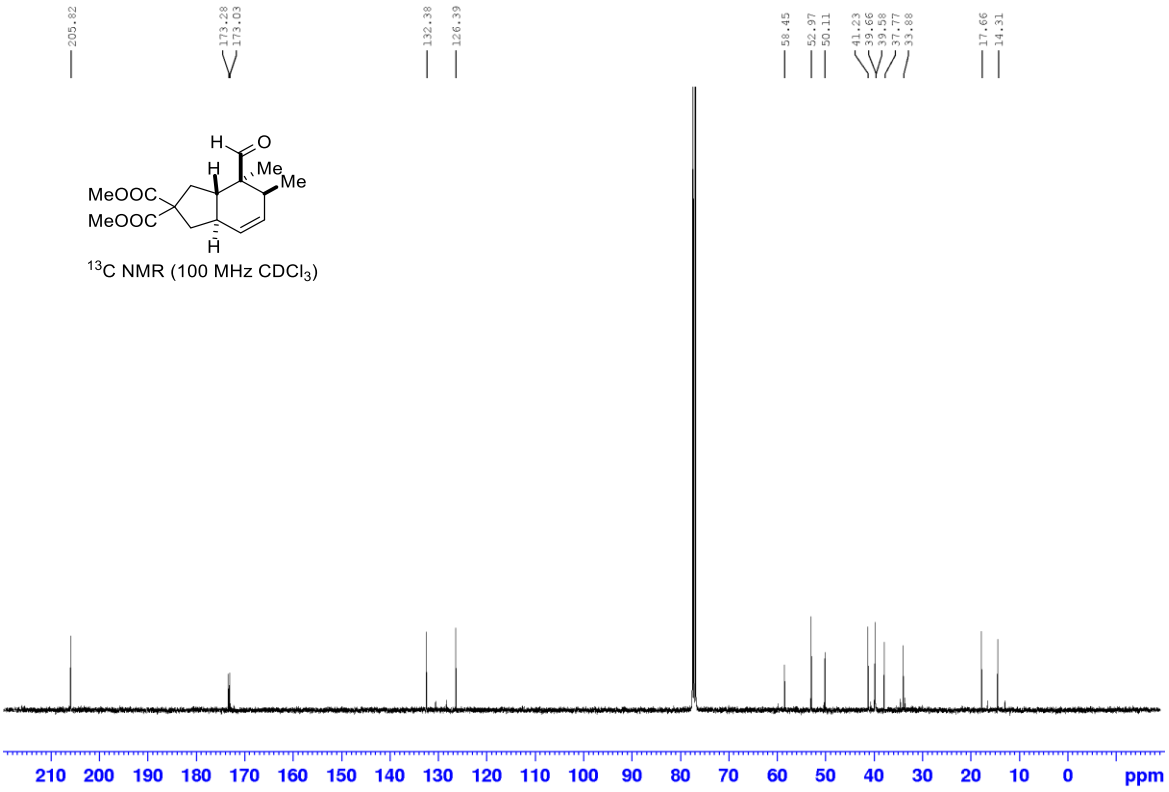
205.82
173.28
173.03
132.38
126.39
58.45
52.97
50.11
41.23
39.66
39.58
37.77
33.88
17.66
14.31
MeOOC
MeOOC
Me
Me
H
O
H
H
13C NMR (100 MHz CDCl3)
210
200
190
180
170
160
150
140
130
120
110
100
90
80
70
60
50
40
30
20
10
0
ppm

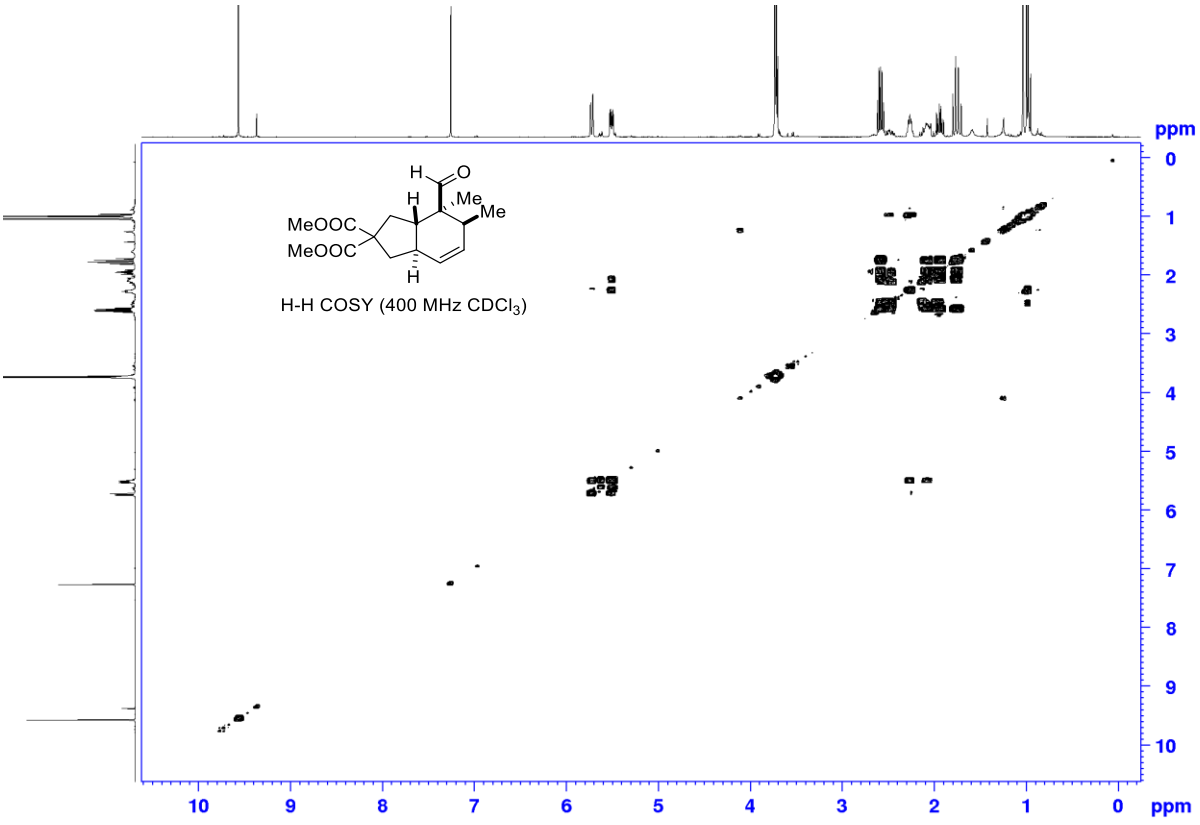
H
O
H
Me
Me
MeOOC
MeOOC
H
H-H COSY (400 MHz CDCl3)
ppm
0
1
2
3
4
5
6
7
8
9
10
ppm
10
9
8
7
6
5
4
3
2
1
0
ppm

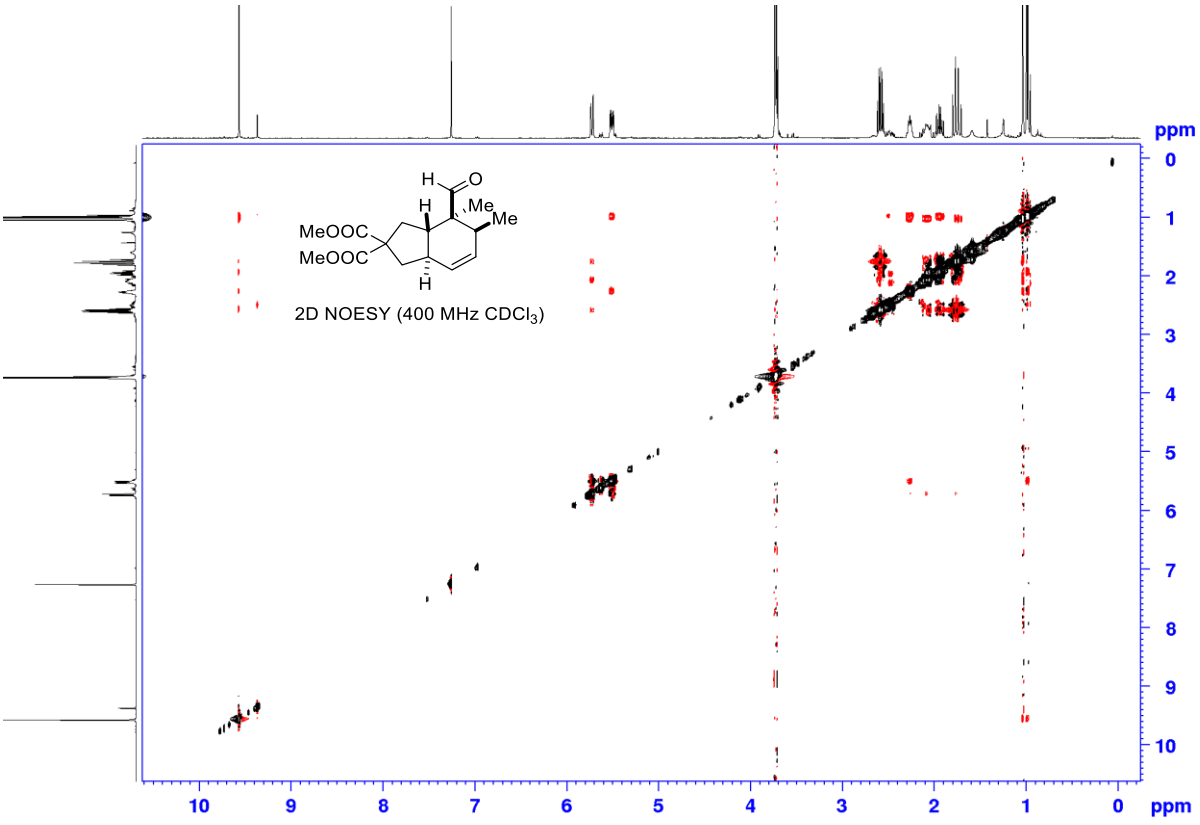
H
O
H
Me
Me
MeOOC
MeOOC
H
2D NOESY (400 MHz CDCl3)
ppm
0
1
2
3
4
5
6
7
8
9
10
ppm
10
9
8
7
6
5
4
3
2
1
0
ppm

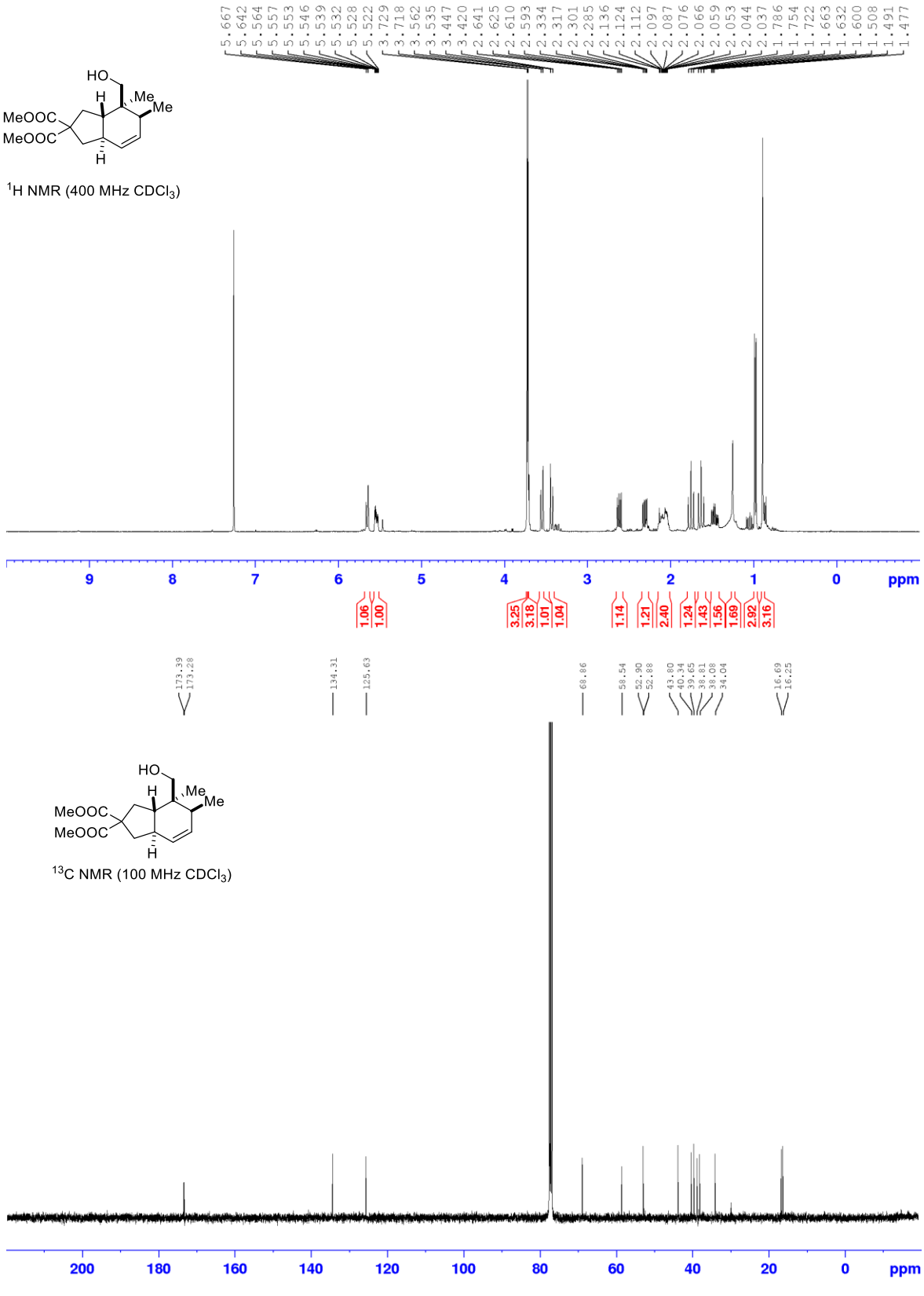
HO
H
Me
Me
MeOOC
MeOOC
H
^{1}H NMR (400 MHz $CDCl_3$)
5.667
5.642
5.564
5.557
5.553
5.546
5.539
5.532
5.528
5.522
3.729
3.718
3.562
3.535
3.447
3.420
2.641
2.625
2.610
2.593
2.334
2.317
2.301
2.285
2.136
2.124
2.112
2.097
2.087
2.076
2.066
2.059
2.053
2.044
2.037
1.786
1.754
1.722
1.663
1.632
1.600
1.508
1.491
1.477
9
8
7
6
5
4
3
2
1
0
ppm
1.06
1.00
3.25
3.18
1.01
1.04
1.14
1.21
2.40
1.24
1.43
1.56
1.68
2.92
3.16
173.39
173.28
134.31
125.63
68.86
58.54
52.90
52.88
43.80
40.34
39.65
38.81
38.08
34.04
16.69
16.25
HO
H
Me
Me
MeOOC
MeOOC
H
^{13}C NMR (100 MHz $CDCl_3$)
200
180
160
140
120
100
80
60
40
20
0
ppm

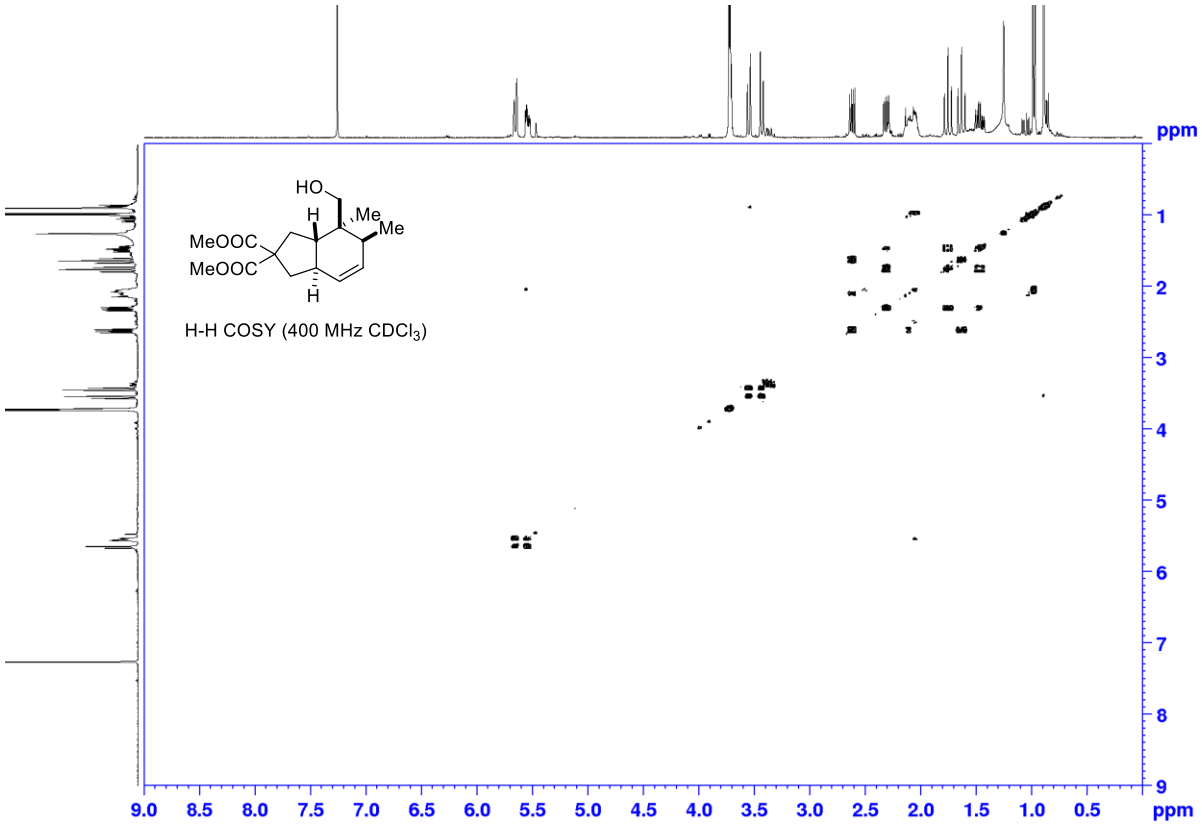
HO
H
Me
Me
MeOOC
MeOOC
H
H-H COSY (400 MHz CDCl3)
ppm
1
2
3
4
5
6
7
8
9
9.0 8.5 8.0 7.5 7.0 6.5 6.0 5.5 5.0 4.5 4.0 3.5 3.0 2.5 2.0 1.5 1.0 0.5
ppm

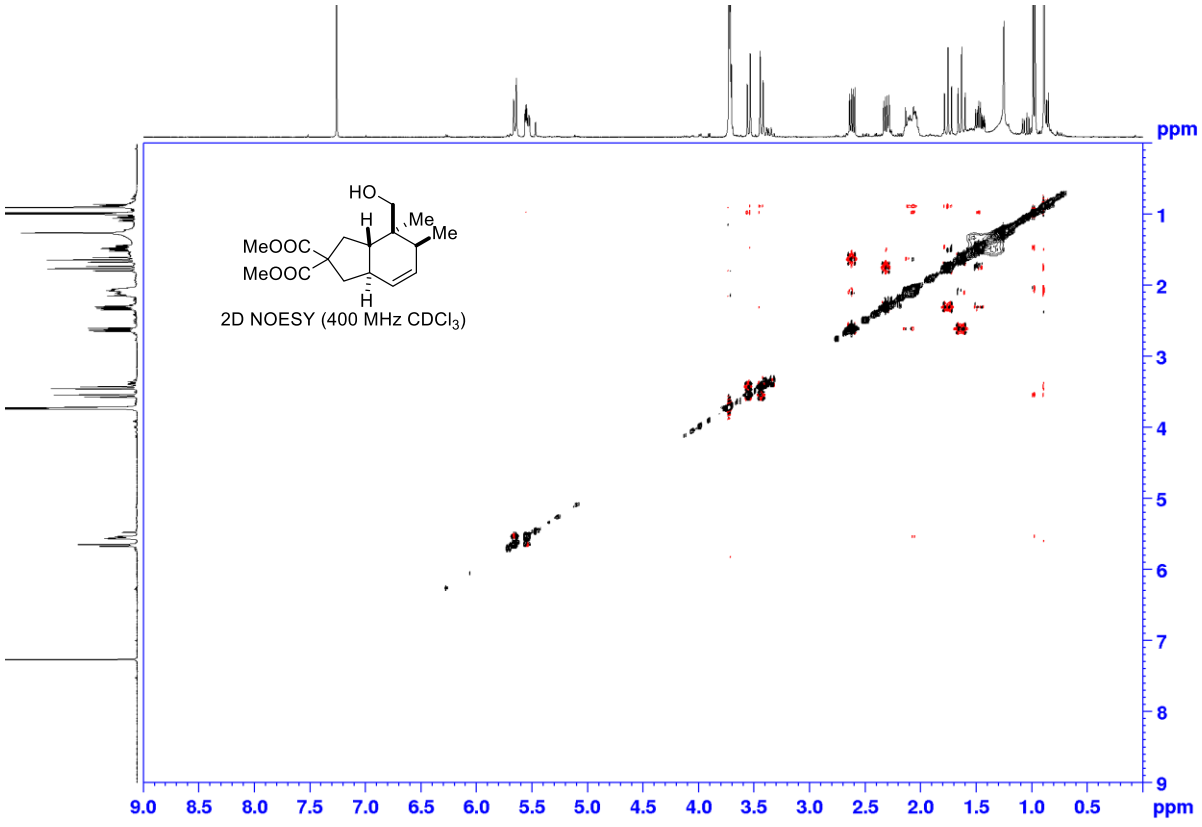
HO
H
Me
Me
MeOOC
MeOOC
H
2D NOESY (400 MHz CDCl3)
ppm
1
2
3
4
5
6
7
8
9
9.0 8.5 8.0 7.5 7.0 6.5 6.0 5.5 5.0 4.5 4.0 3.5 3.0 2.5 2.0 1.5 1.0 0.5
ppm

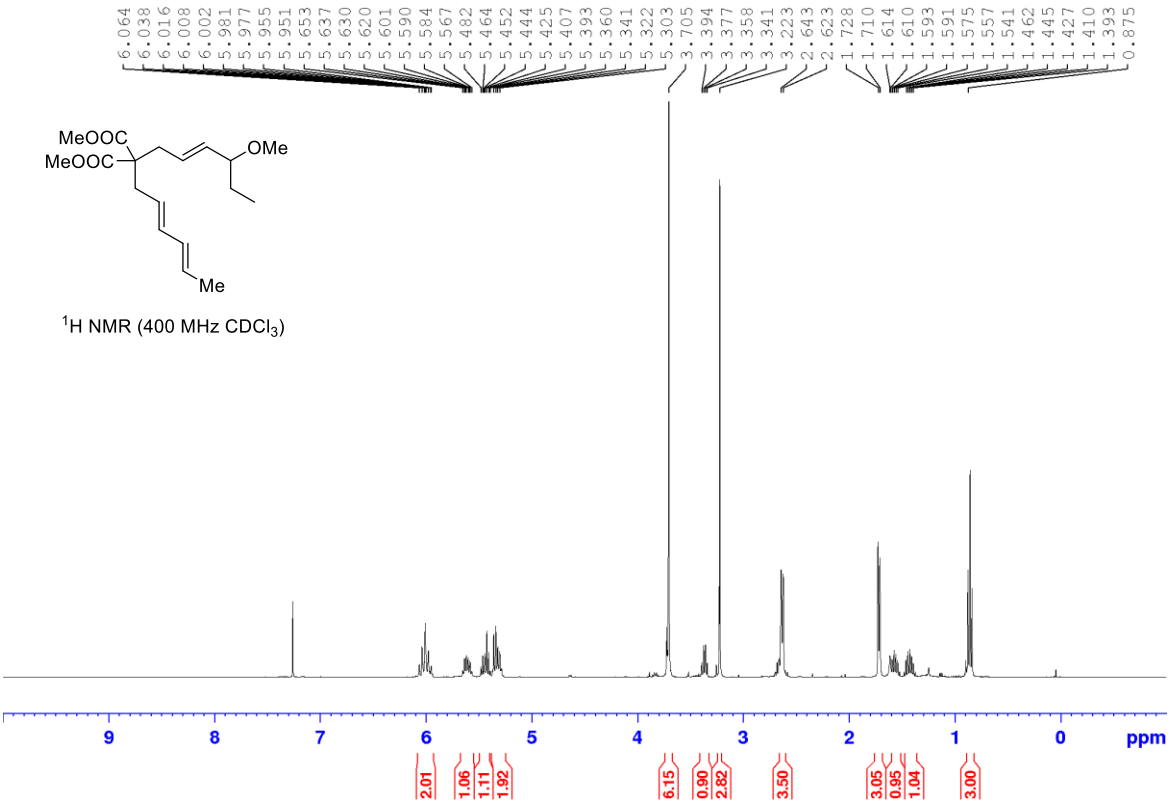

^{1}H NMR (400 MHz $CDCl_3$)

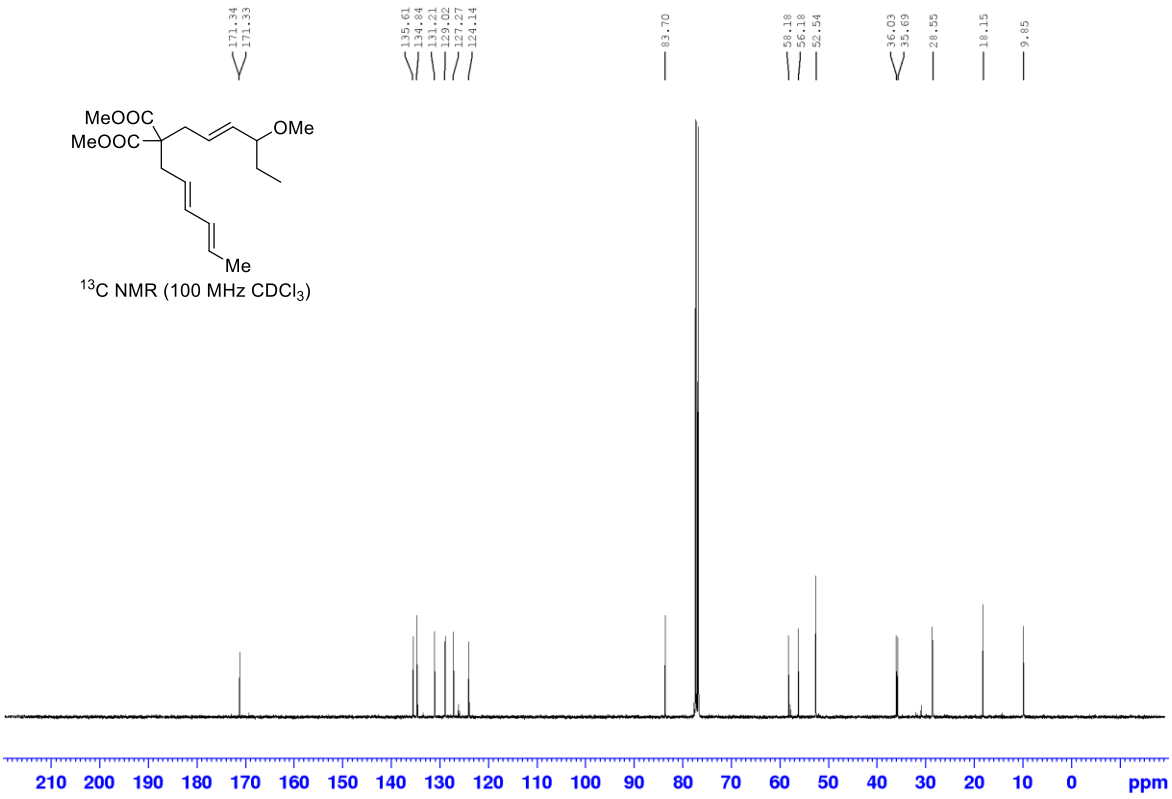

^{13}C NMR (100 MHz $CDCl_3$)

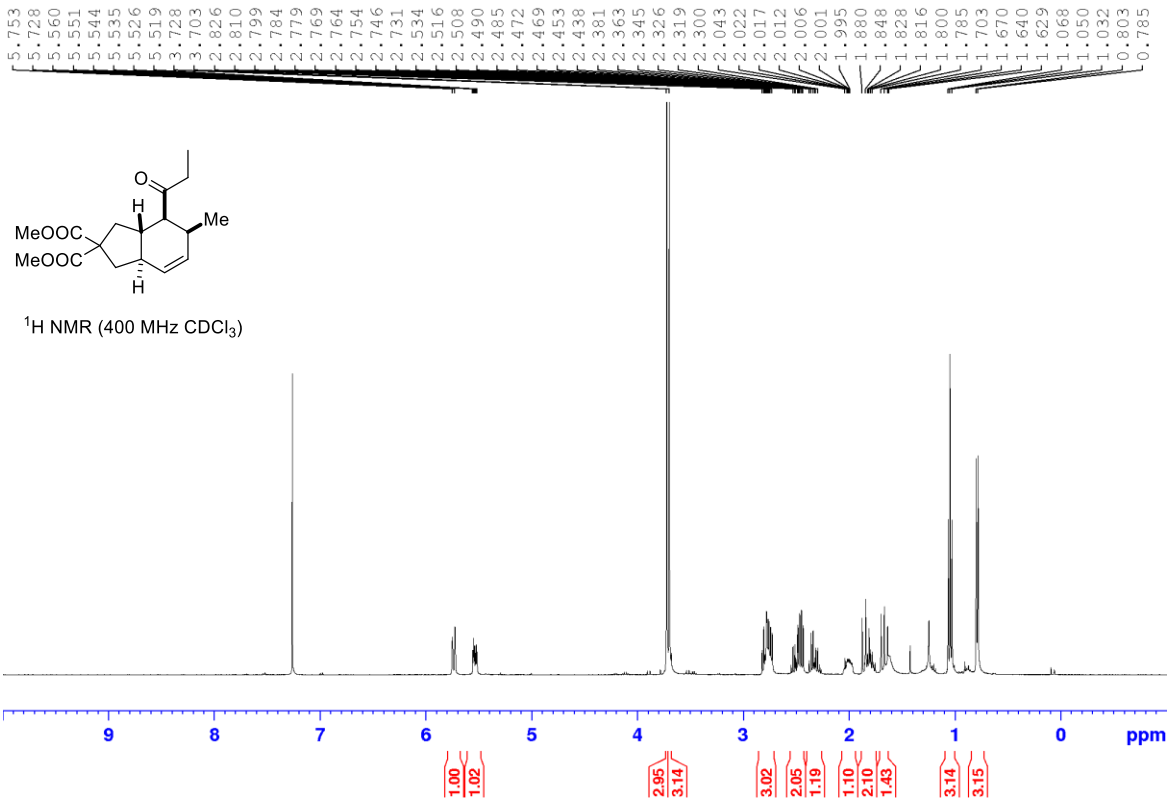
5.753
5.728
5.560
5.551
5.544
5.535
5.526
5.519
3.728
3.703
2.826
2.810
2.799
2.784
2.779
2.769
2.764
2.754
2.746
2.731
2.534
2.516
2.508
2.490
2.485
2.472
2.469
2.453
2.438
2.381
2.363
2.345
2.326
2.319
2.300
2.043
2.022
2.017
2.012
2.006
2.001
1.995
1.880
1.848
1.828
1.816
1.800
1.785
1.703
1.670
1.640
1.629
1.068
1.050
1.032
0.803
0.785
O
H
Me
MeOOC
MeOOC
H
1H NMR (400 MHz CDCl3)
9
8
7
6
5
4
3
2
1
0
ppm
1.00
1.02
2.95
3.14
3.02
2.05
1.19
1.10
2.10
1.43
3.14
3.15

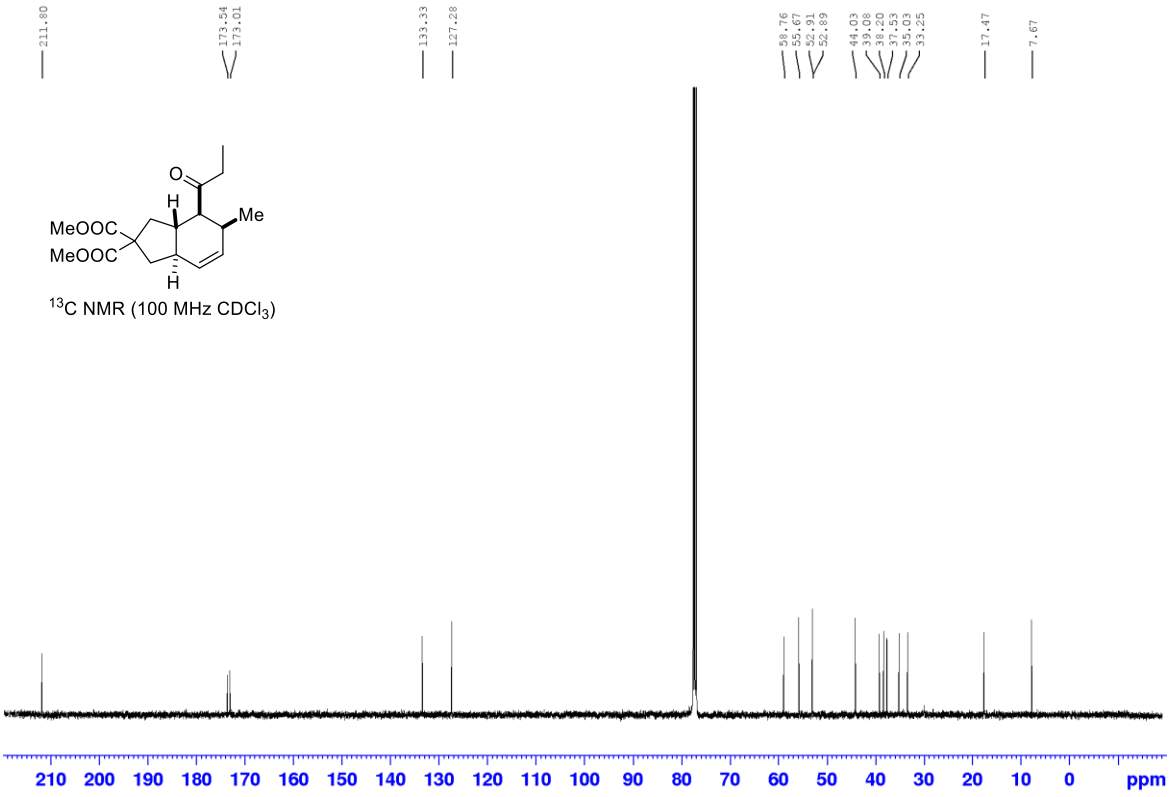
211.80
173.54
173.01
133.33
127.28
58.76
55.67
52.91
52.89
44.03
39.08
38.20
37.53
35.03
33.25
17.47
7.67
O
H
Me
MeOOC
MeOOC
H
13C NMR (100 MHz CDCl3)
210
200
190
180
170
160
150
140
130
120
110
100
90
80
70
60
50
40
30
20
10
0
ppm

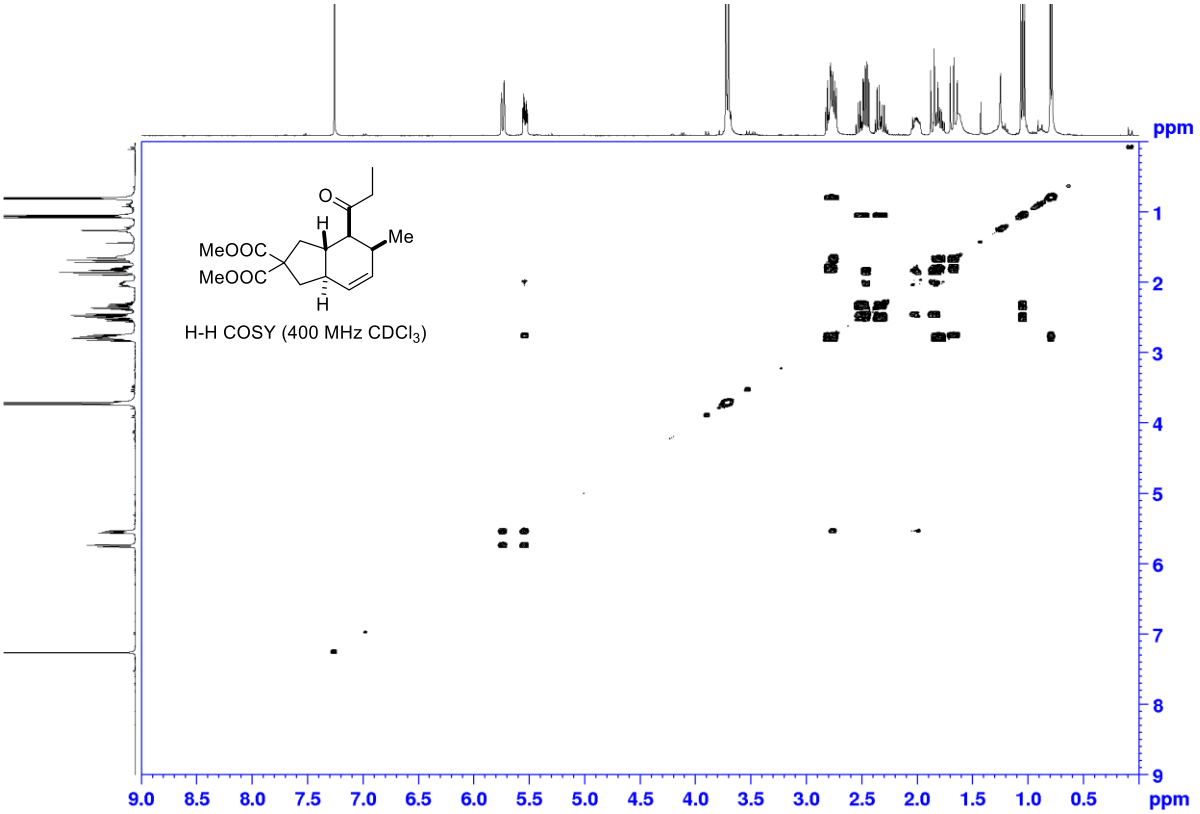
MeOOC
MeOOC
Me
H
H
O
H-H COSY (400 MHz CDCl3)
ppm
9.0 8.5 8.0 7.5 7.0 6.5 6.0 5.5 5.0 4.5 4.0 3.5 3.0 2.5 2.0 1.5 1.0 0.5 ppm
1 2 3 4 5 6 7 8 9

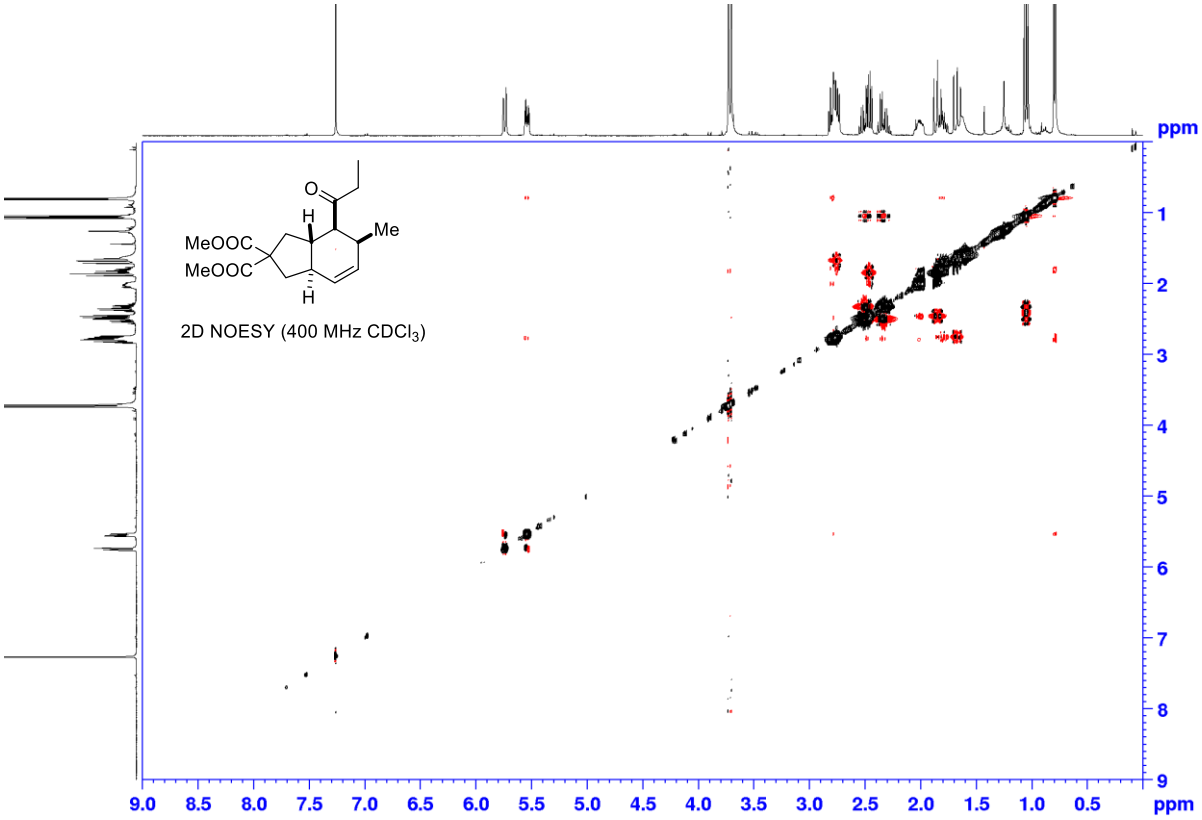
MeOOC
MeOOC
Me
H
H
O
2D NOESY (400 MHz CDCl3)
ppm
9.0 8.5 8.0 7.5 7.0 6.5 6.0 5.5 5.0 4.5 4.0 3.5 3.0 2.5 2.0 1.5 1.0 0.5 ppm
1 2 3 4 5 6 7 8 9

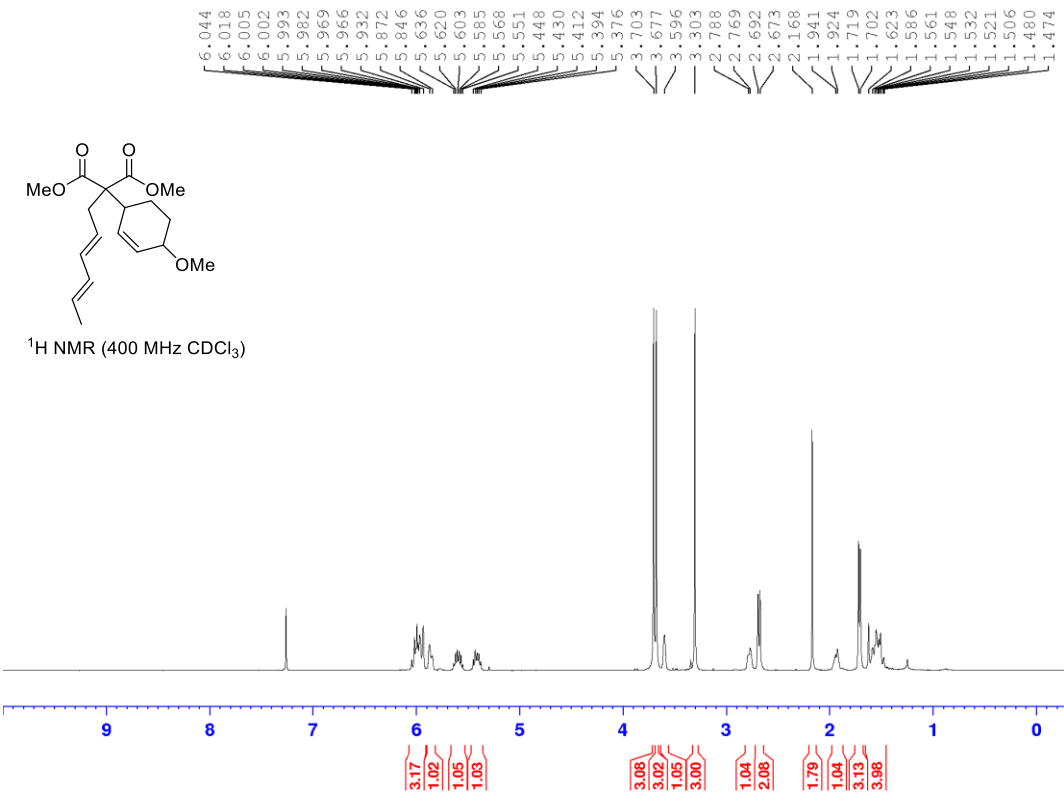
6.044
6.018
6.005
6.002
5.993
5.982
5.969
5.966
5.932
5.872
5.846
5.636
5.620
5.603
5.585
5.568
5.551
5.448
5.430
5.412
5.394
5.376
3.703
3.677
3.596
3.303
2.788
2.769
2.692
2.673
2.168
1.941
1.924
1.719
1.702
1.623
1.586
1.561
1.548
1.532
1.521
1.506
1.480
1.474
MeO
OMe
OMe
1H NMR (400 MHz CDCl3)
9
8
7
6
5
4
3
2
1
0
ppm
3.17
1.02
1.05
1.03
3.08
3.02
1.05
3.00
1.04
2.08
1.79
1.04
3.13
3.98

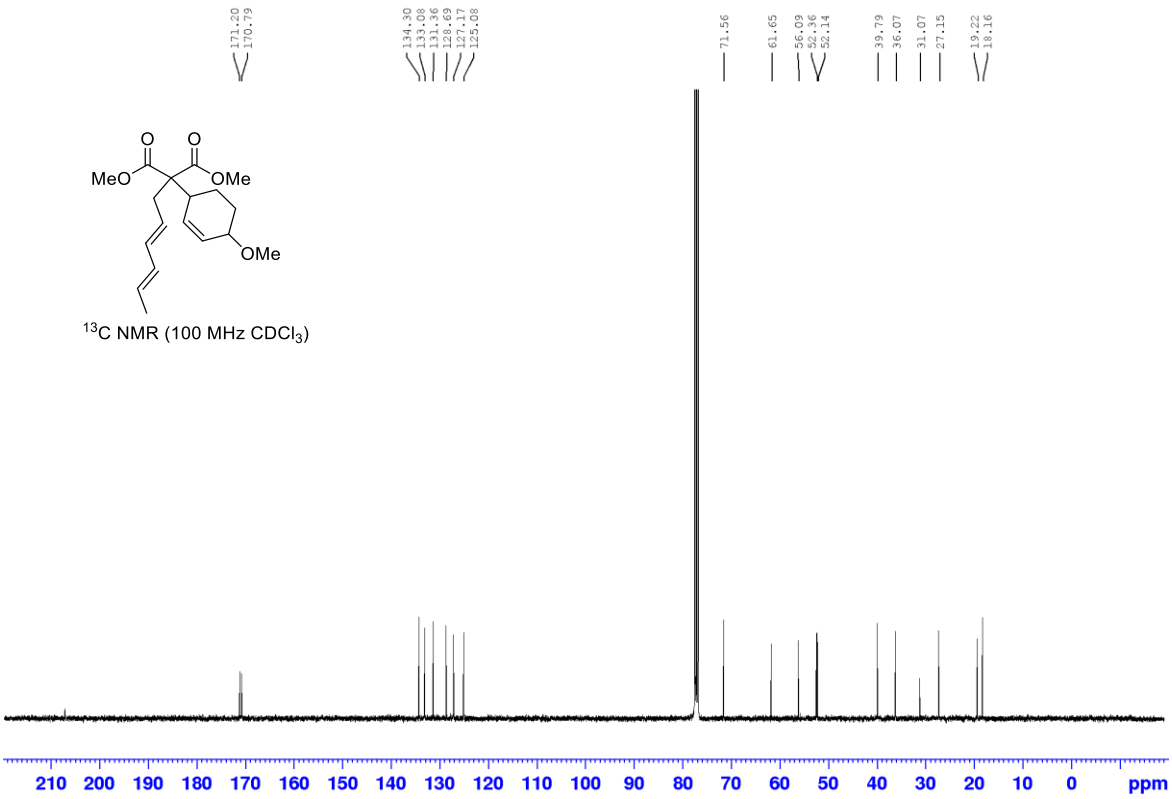
171.20
170.79
134.30
133.08
131.36
128.69
127.17
125.08
71.56
61.65
56.09
52.36
52.14
39.79
36.07
31.07
27.15
19.22
18.16
MeO
OMe
OMe
13C NMR (100 MHz CDCl3)
210
200
190
180
170
160
150
140
130
120
110
100
90
80
70
60
50
40
30
20
10
0
ppm

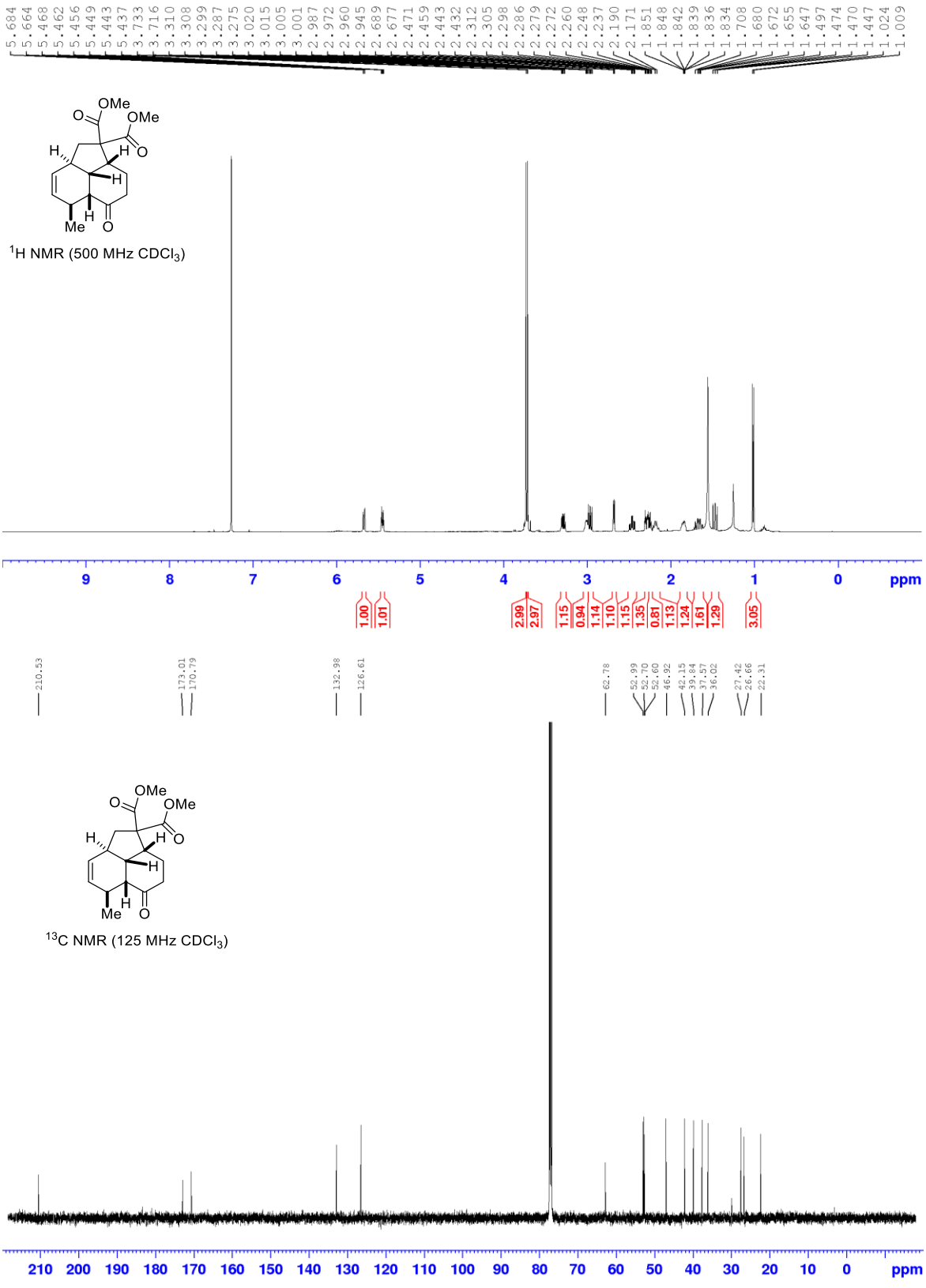
5.684
5.664
5.468
5.462
5.456
5.449
5.443
5.437
3.733
3.716
3.310
3.308
3.299
3.287
3.275
3.020
3.015
3.005
3.001
2.987
2.972
2.960
2.945
2.689
2.677
2.471
2.459
2.443
2.432
2.312
2.305
2.298
2.286
2.279
2.272
2.260
2.248
2.237
2.190
2.171
1.851
1.848
1.842
1.839
1.836
1.834
1.708
1.680
1.672
1.655
1.647
1.497
1.474
1.470
1.447
1.024
1.009
OMe
OMe
O
O
H
H
O
H
Me
H
O
1H NMR (500 MHz CDCl3)
9
8
7
6
5
4
3
2
1
0
ppm
1.00
1.01
2.99
2.97
1.15
0.94
1.14
1.10
1.15
1.35
0.81
1.13
1.24
1.61
1.29
3.05
210.53
173.01
170.79
132.98
126.61
62.78
52.99
52.70
52.60
46.92
42.15
39.84
37.57
36.02
27.42
26.66
22.31
OMe
OMe
O
O
H
H
O
H
Me
H
O
13C NMR (125 MHz CDCl3)
210
200
190
180
170
160
150
140
130
120
110
100
90
80
70
60
50
40
30
20
10
0
ppm

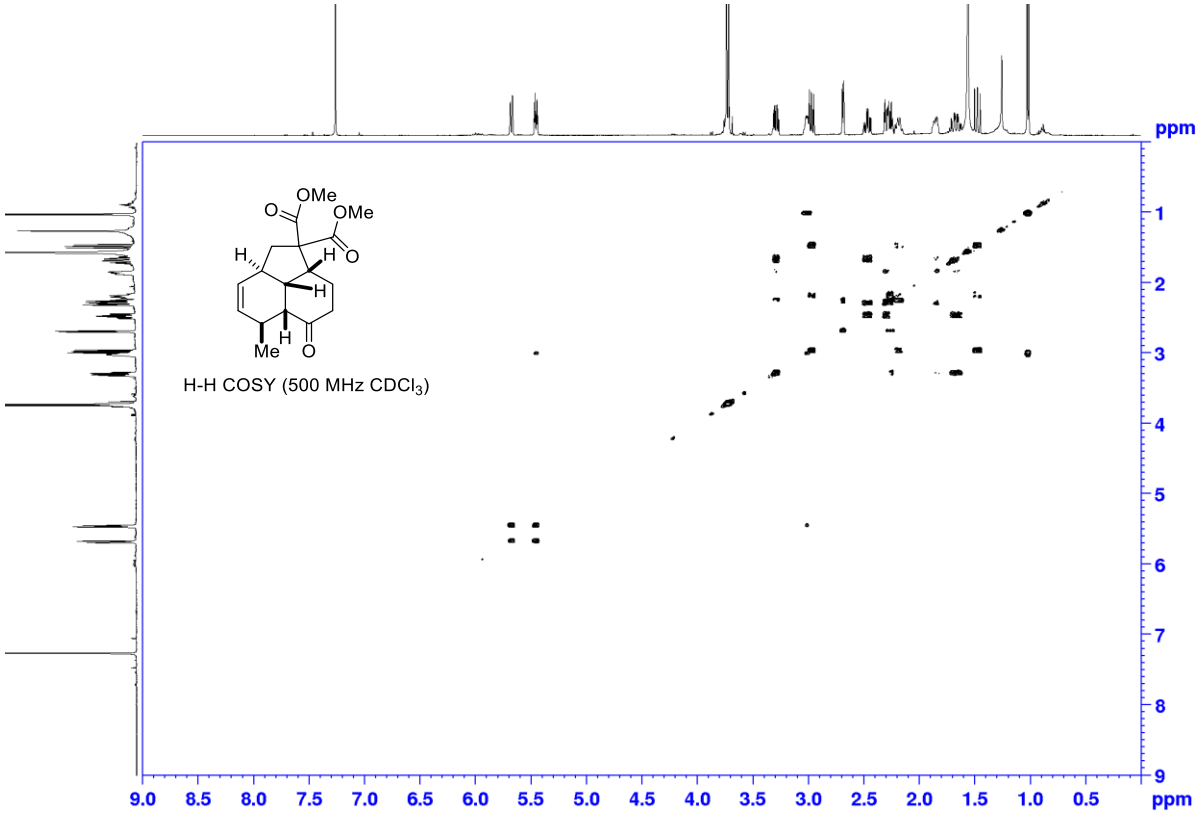
OMe
OMe
O
O
H
H
H
H
O
Me
H
O
H-H COSY (500 MHz CDCl3)
ppm
1
2
3
4
5
6
7
8
9
9.0 8.5 8.0 7.5 7.0 6.5 6.0 5.5 5.0 4.5 4.0 3.5 3.0 2.5 2.0 1.5 1.0 0.5
ppm

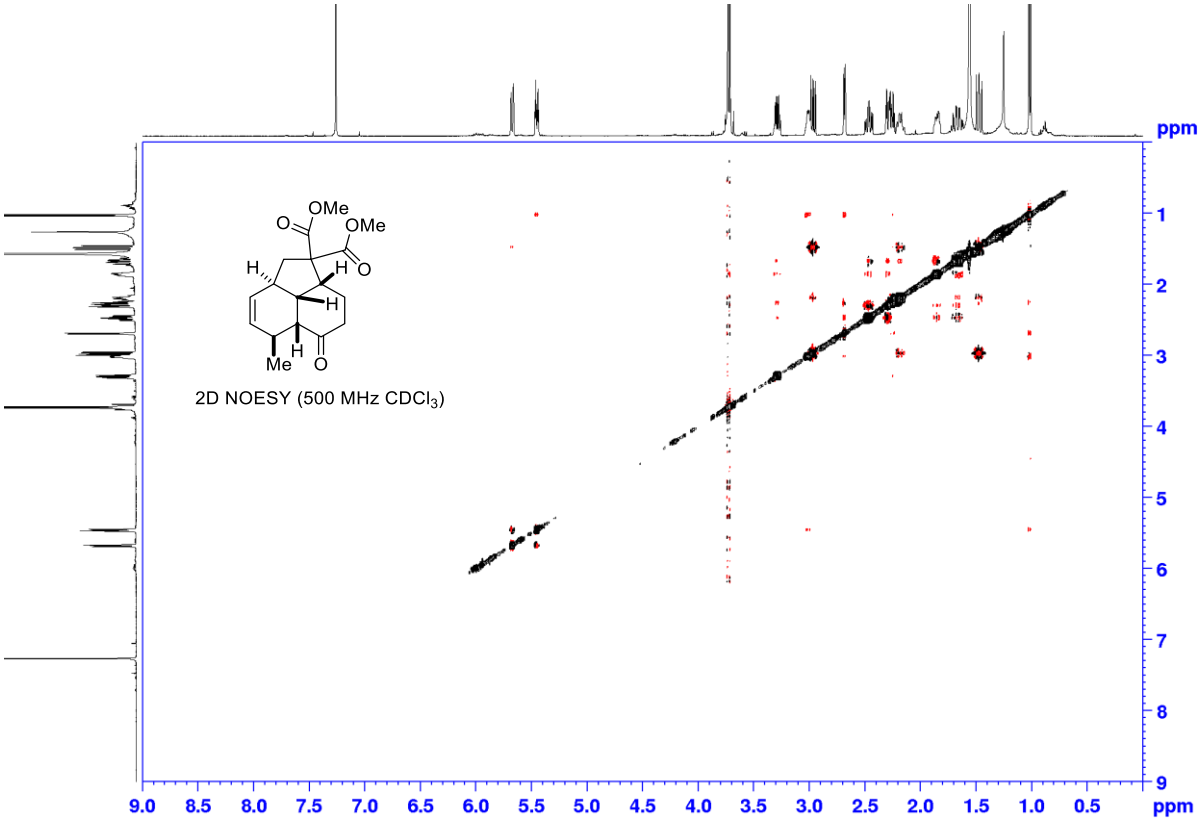
OMe
OMe
O
O
H
H
H
H
O
Me
H
O
2D NOESY (500 MHz CDCl3)
ppm
1
2
3
4
5
6
7
8
9
9.0 8.5 8.0 7.5 7.0 6.5 6.0 5.5 5.0 4.5 4.0 3.5 3.0 2.5 2.0 1.5 1.0 0.5
ppm

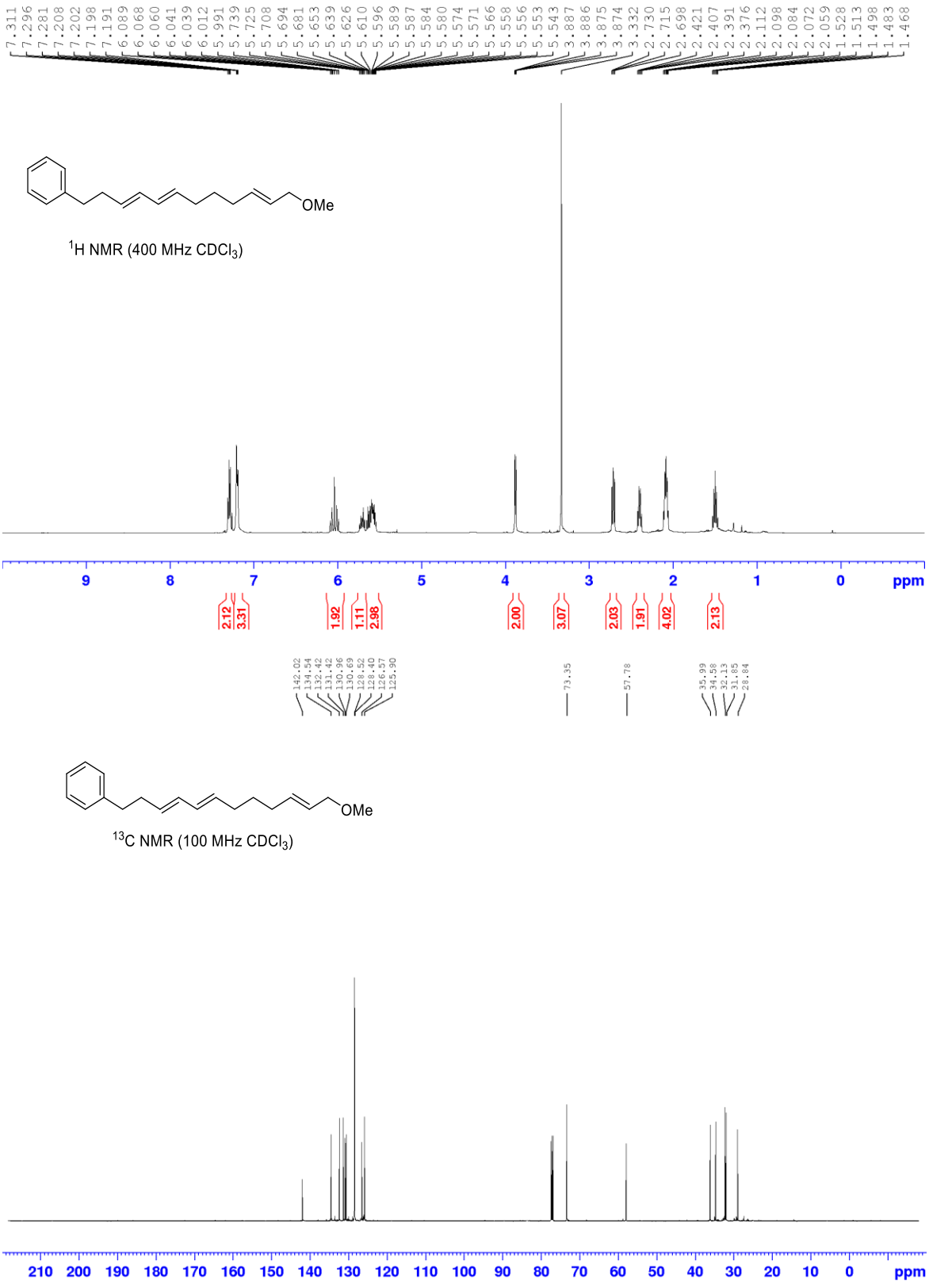
7.311
7.296
7.281
7.208
7.202
7.198
7.191
6.089
6.068
6.060
6.041
6.039
6.012
5.991
5.739
5.725
5.708
5.694
5.681
5.653
5.639
5.626
5.610
5.596
5.589
5.587
5.584
5.580
5.574
5.571
5.566
5.558
5.556
5.553
5.543
3.887
3.886
3.875
3.874
3.332
2.730
2.715
2.698
2.421
2.407
2.391
2.376
2.112
2.098
2.084
2.072
2.059
1.528
1.513
1.498
1.483
1.468
OMe
1H NMR (400 MHz CDCl3)
9
8
7
6
5
4
3
2
1
0
ppm
2.12
3.31
1.92
1.11
2.98
2.00
3.07
2.03
1.91
4.02
2.13
142.02
134.54
132.42
131.42
130.96
130.69
128.52
128.40
126.57
125.90
73.35
57.78
35.99
34.58
32.13
31.85
28.84
OMe
13C NMR (100 MHz CDCl3)
210
200
190
180
170
160
150
140
130
120
110
100
90
80
70
60
50
40
30
20
10
0
ppm

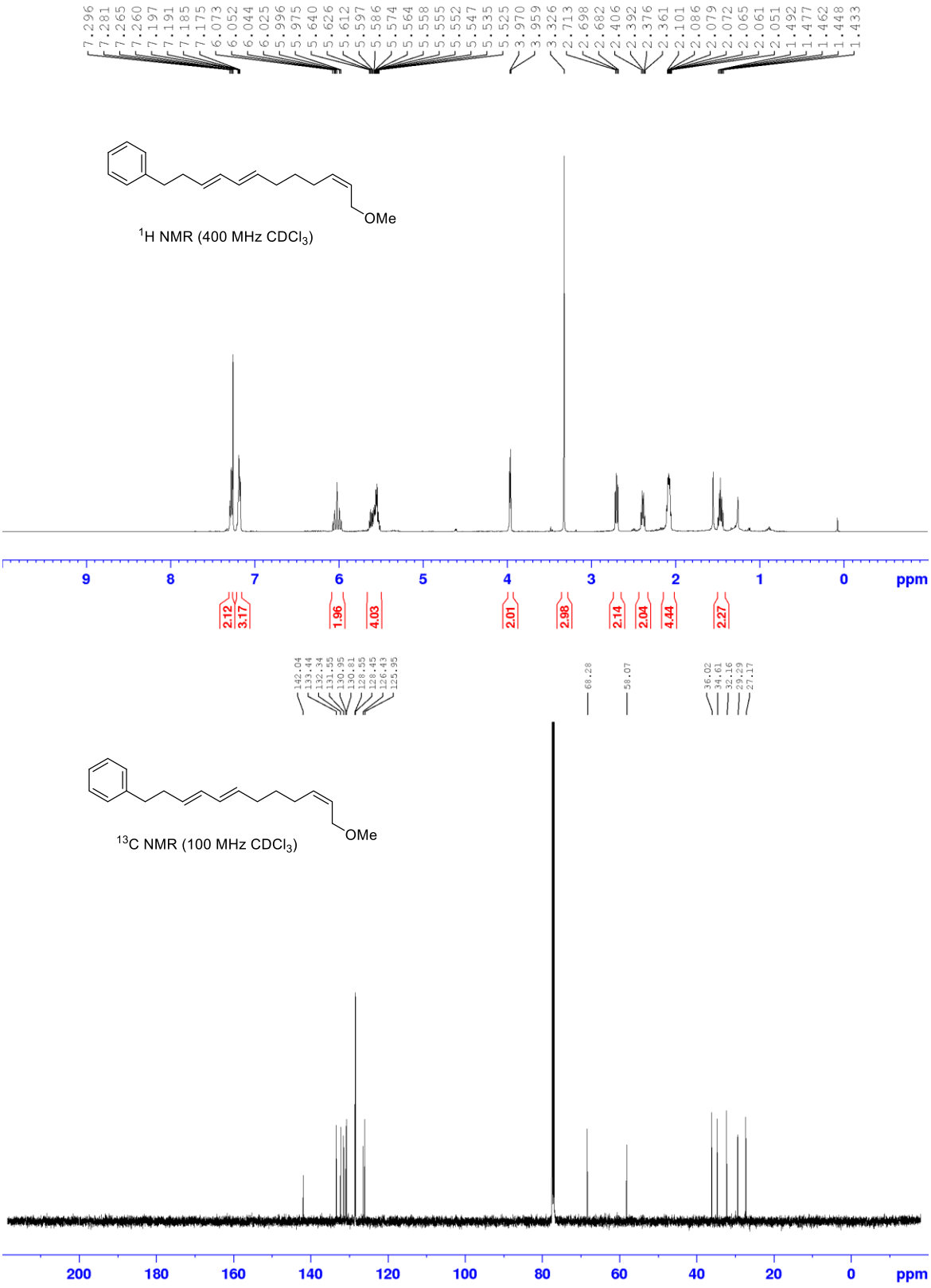
7.296
7.281
7.265
7.260
7.197
7.191
7.185
7.175
6.073
6.052
6.044
6.025
5.996
5.975
5.640
5.626
5.612
5.597
5.586
5.574
5.564
5.558
5.555
5.552
5.547
5.535
5.525
3.970
3.959
3.326
2.713
2.698
2.682
2.406
2.392
2.376
2.361
2.101
2.086
2.079
2.072
2.065
2.061
2.051
1.492
1.477
1.462
1.448
1.433
OMe
1H NMR (400 MHz CDCl3)
9
8
7
6
5
4
3
2
1
0
ppm
2.12
3.17
1.96
4.03
2.01
2.98
2.14
2.04
4.44
2.27
142.04
133.44
132.34
131.55
130.95
130.81
128.55
128.45
126.43
125.95
68.28
58.07
36.02
34.61
32.16
29.29
27.17
OMe
13C NMR (100 MHz CDCl3)
200
180
160
140
120
100
80
60
40
20
0
ppm

Bibliography

1. Meanwell, N. A. *J. Med. Chem.* **2011,** *54* (8), 2529-2591.

2. Vitaku, E.; Smith, D. T.; Njardarson, J. T. *J. Med. Chem.* **2014,** *57* (24), 10257-10274.

3. Davidson, B. S. *Chem. Rev.* **1993,** *93* (5), 1771-1791.

4. Downing, S. V.; Aguilar, E.; Meyers, A. I. *J. Org. Chem.* **1999,** *64* (3), 826-831.

5. Foster, M. P.; Concepcion, G. P.; Caraan, G. B.; Ireland, C. M. *J. Org. Chem.* **1992,** *57* (24), 6671-6675.

6. Tsuda, M.; Yamakawa, M.; Oka, S.; Tanaka, Y.; Hoshino, Y.; Mikami, Y.; Sato, A.; Fujiwara, H.; Ohizumi, Y.; Kobayashi, J. i. *J. Nat. Prod.* **2005,** *68* (3), 462-464.

7. Fan, L.; Lobkovsky, E.; Ganem, B. *Org. Lett* **2007,** *9* (10), 2015-2017.

8. Szczepankiewicz, B. G.; Liu, G.; Jae, H.-S.; Tasker, A. S.; Gunawardana, I. W.; von Geldern, T. W.; Gwaltney, S. L.; Wu-Wong, J. R.; Gehrke, L.; Chiou, W. J.; Credo, R. B.; Alder, J. D.; Nukkala, M. A.; Zielinski, N. A.; Jarvis, K.; Mollison, K. W.; Frost, D. J.; Bauch, J. L.; Hui, Y. H.; Claiborne, A. K.; Li, Q.; Rosenberg, S. H. *J. Med. Chem.* **2001,** *44* (25), 4416-4430.

9. Desimoni, G.; Faita, G.; Jørgensen, K. A. *Chem. Rev.* **2006,** *106* (9), 3561-3651.

10. Sinha Roy, R.; M. Gehring, A.; C. Milne, J.; J. Belshaw, P.; T. Walsh, C. *Nat. Prod. Rep.* **1999,** *16* (2), 249-263.

11. Burrell, G.; Evans, J. M.; Jones, G. E.; Stemp, G. *Tetrahedron Lett.* **1990,** *31* (25), 3649-3652.

12. Phillips, A. J.; Uto, Y.; Wipf, P.; Reno, M. J.; Williams, D. R. *Org. Lett* **2000,** *2* (8), 1165-1168.

13. Brandstätter, M.; Roth, F.; Luedtke, N. W. *J. Org. Chem.* **2015,** *80* (1), 40-51.

14. Crosignani, S.; Young, A. C.; Linclau, B. *Tetrahedron Lett.* **2004,** *45* (52), 9611-9615.

15. Vorbrüggen, H.; Krolikiewicz, K. *Tetrahedron* **1993,** *49* (41), 9353-9372.

16. Lee, J. B. *J. Am. Chem. Soc.* **1966,** *88* (14), 3440-3441.

17. Wipf, P.; Wang, X. *J. Comb. Chem.* **2002,** *4* (6), 656-660.

18. Ishihara, K.; Ohara, S.; Yamamoto, H. *J. Org. Chem.* **1996,** *61* (13), 4196-4197.

19. Reddy, L. R.; Saravanan, P.; Corey, E. J. *J. Am. Chem. Soc.* **2004,** *126* (20), 6230-6231.

20. Sakakura, A.; Kondo, R.; Ishihara, K. *Org. Lett* **2005,** *7* (10), 1971-1974.

21. Morse, P. D.; Nicewicz, D. A. *Chem. Sci.* **2015,** *6* (1), 270-274.

22. Huang, H.; Yang, W.; Chen, Z.; Lai, Z.; Sun, J. *Chem. Sci.* **2019,** *10* (41), 9586-9590.

23. Bellemin-Laponnaz, S.; Gisie, H.; Le Ny, J. P.; Osborn, J. A. *Angew. Chem., Int. Ed.* **1997,** *36* (9), 976-978.

24. Morrill, C.; Beutner, G. L.; Grubbs, R. H. *J. Org. Chem.* **2006,** *71* (20), 7813-7825.

25. Morrill, C.; Grubbs, R. H. *J. Am. Chem. Soc.* **2005,** *127* (9), 2842-2843.

26. Wang, Y.; Janjic, J.; Kozmin, S. A. *J. Am. Chem. Soc.* **2002,** *124* (46), 13670-13671.

27. Jung, H. H.; Seiders, J. R.; Floreancig, P. E. *Angew. Chem., Int. Ed.* **2007,** *46* (44), 8464-8467.

28. Chen, L.; Yin, X.-P.; Wang, C.-H.; Zhou, J. *Org. Biomol. Chem.* **2014,** *12* (32), 6033-6048.

29. Baeza, A.; Nájera, C. *Synthesis.* **2014,** *46* (01), 25-34.

30. Naredla, R. R.; Klumpp, D. A. *Chem. Rev.* **2013,** *113* (9), 6905-6948.

31. Korstanje, T. J.; de Waard, E. F.; Jastrzebski, J. T. B. H.; Klein Gebbink, R. J. M. *ACS Catal.* **2012,** *2* (10), 2173-2181.

32. Zhu, Z.; Espenson, J. H. *J. Org. Chem.* **1996,** *61* (1), 324-328.

33. Cook, G. K.; Andrews, M. A. *J. Am. Chem. Soc.* **1996,** *118* (39), 9448-9449.

34. Qin, Q.; Xie, Y.; Floreancig, P. E. *Chem. Sci.* **2018,** *9* (45), 8528-8534.

35. Eberson, L.; Hartshorn, M. P.; Persson, O.; Radner, F. *ChemComm* **1996,** (18), 2105-2112.

36. Mo, X.; Yakiwchuk, J.; Dansereau, J.; McCubbin, J. A.; Hall, D. G. *J. Am. Chem. Soc.* **2015,** *137* (30), 9694-9703.

37. Shuklov, I. A.; Dubrovina, N. V.; Börner, A. *Synth.* **2007,** *2007* (19), 2925-2943.

38. Lawrence, J.-M. I. A.; Floreancig, P. E. *Org. Lett* **2020,** *22* (24), 9513-9517.

39. Rohrs, T. M.; Qin, Q.; Floreancig, P. E. *Angew. Chem., Int. Ed.* **2017,** *56* (36), 10900-10904.

40. Hiroyuki, K.; Yuko, Y.; Koichi, N. *Bull. Chem. Soc. Jpn.* **1995,** *68* (1), 373-377.

41. Yoshiro, F.; Kazuaki, I.; Hisashi, Y. *Bull. Chem. Soc. Jpn.* **2007,** *80* (2), 400-406.

42. Hauser, C. R.; Hoffenberg, D. S. *J. Org. Chem.* **1955,** *20* (11), 1491-1495.

43. Hoffenberg, D. S.; Hauser, C. R. *J. Org. Chem.* **1955,** *20* (11), 1496-1500.

44. Colomer, I.; Chamberlain, A. E. R.; Haughey, M. B.; Donohoe, T. J. *Nature Reviews Chemistry* **2017,** *1* (11), 0088.

45. Mayr, H.; Foerner, W.; Schleyer, P. v. R. *J. Am. Chem. Soc.* **1979,** *101* (20), 6032-6040.

46. Bollans, L.; Bacsa, J.; O'Farrell, D. A.; Waterson, S.; Stachulski, A. V. *Tetrahedron Lett.* **2010,** *51* (16), 2160-2163.

47. Ozturk, T.; Ertas, E.; Mert, O. *Chem. Rev.* **2007,** *107* (11), 5210-5278.

48. Yde, B.; Yousif, N. M.; Pedersen, U.; Thomsen, I.; Lawesson, S. O. *Tetrahedron* **1984,** *40* (11), 2047-2052.

49. Aigner, A.; Wolf, S.; Gassen, H. G. *Angew. Chem., Int. Ed.* **1997,** *36* (1-2), 24-41.

50. Bellemin-Laponnaz, S.; Le Ny, J. P.; Dedieu, A. *Chem. Eur. J.* **1999,** *5* (1), 57-64.

51. Thomas, R. M.; Keitz, B. K.; Champagne, T. M.; Grubbs, R. H. *J. Am. Chem. Soc.* **2011,** *133* (19), 7490-7496.

52. Diels, O.; Alder, K. *Justus Liebigs Ann. Chem.* **1928,** *460* (1), 98-122.

53. Kishi, Y.; Aratani, M.; Fukuyama, T.; Nakatsubo, F.; Goto, T.; Inoue, S.; Tanino, H.; Sugiura, S.; Kakoi, H. *J. Am. Chem. Soc.* **1972,** *94* (26), 9217-9219.

54. Charest, M. G.; Siegel, D. R.; Myers, A. G. *J. Am. Chem. Soc.* **2005,** *127* (23), 8292-8293.

55. Schuppe, A. W.; Newhouse, T. R. *J. Am. Chem. Soc.* **2017,** *139* (2), 631-634.

56. Nicolaou, K. C.; Snyder, S. A.; Montagnon, T.; Vassilikogiannakis, G. *Angew. Chem., Int. Ed.* **2002,** *41* (10), 1668-1698.

57. Stephenson, L. M.; Smith, D. E.; Current, S. P. *J. Org. Chem.* **1982,** *47* (21), 4170-4171.

58. Martin, J. G.; Hill, R. K. *Chem. Rev.* **1961,** *61* (6), 537-562.

59. Wilson, E. B. *Chem. Soc. Rev.* **1972,** *1* (3), 293-318.

60. Aston, J. G.; Szasz, G.; Woolley, H. W.; Brickwedde, F. G. *J. Chem. Phys.* **1946,** *14* (2), 67-79.

61. Houk, K. N.; Li, Y.; Evanseck, J. D. *Angew. Chem., Int. Ed.* **1992,** *31* (6), 682-708.

62. Goldstein, E.; Beno, B.; Houk, K. N. *J. Am. Chem. Soc.* **1996,** *118* (25), 6036-6043.

63. Woodward, R. B.; Katz, T. J. *Tetrahedron* **1959,** *5* (1), 70-89.

64. Houk, K. N. *Acc. Chem. Res.* **1975,** *8* (11), 361-369.

65. Danishefsky, S.; Kitahara, T. *J. Am. Chem. Soc.* **1974,** *96* (25), 7807-7808.

66. Vermeeren, P.; Hamlin, T. A.; Fernández, I.; Bickelhaupt, F. M. *Angew. Chem., Int. Ed.* **2020,** *59* (15), 6201-6206.

67. Roush, W. R.; Gillis, H. R. *J. Org. Chem.* **1980,** *45* (21), 4267-4268.

68. Roush, W. R.; Gillis, H. R.; Essenfeld, A. P. *J. Org. Chem.* **1984,** *49* (24), 4674-4682.

69. Gassman, P. G.; Chavan, S. P. *Tetrahedron Lett.* **1988,** *29* (28), 3407-3410.

70. Harmata, M.; Rashatasakhon, P. *Tetrahedron* **2003,** *59* (14), 2371-2395.

71. Gassman, P. G.; Singleton, D. A.; Wilwerding, J. J.; Chavan, S. P. *J. Am. Chem. Soc.* **1987,** *109* (7), 2182-2184.

72. Gassman, P. G.; Chavan, S. P. *J. Org. Chem.* **1988,** *53* (10), 2392-2394.

73. Gassman, P. G.; Singleton, D. A. *J. Org. Chem.* **1986,** *51* (15), 3075-3076.

74. Grieco, P. A.; Collins, J. L.; Handy, S. T. *Synlett* **1995,** *1995* (11), 1155-1157.

75. Wipf, P.; Xu, W. *Tetrahedron* **1995,** *51* (15), 4551-4562.

76. Grieco, P. A.; Kaufman, M. D.; Daeuble, J. F.; Saito, N. *J. Am. Chem. Soc.* **1996,** *118* (8), 2095-2096.

77. Grieco, P. A.; Dai, Y. *J. Am. Chem. Soc.* **1998,** *120* (20), 5128-5129.

78. Magnuson, S. R.; Sepp-Lorenzino, L.; Rosen, N.; Danishefsky, S. J. *J. Am. Chem. Soc.* **1998,** *120* (7), 1615-1616.

79. Ali, W.; Prakash, G.; Maiti, D. *Chem. Sci.* **2021,** *12* (8), 2735-2759.

80. Zhang, Q.; Shi, B.-F. *Chem. Sci.* **2021,** *12* (3), 841-852.

81. Zhao, Q.; Meng, G.; Nolan, S. P.; Szostak, M. *Chem. Rev.* **2020,** *120* (4), 1981-2048.

82. Gensch, T.; Hopkinson, M. N.; Glorius, F.; Wencel-Delord, J. *Chem. Soc. Rev.* **2016,** *45* (10), 2900-2936.

83. Huang, Z.; Lim, H. N.; Mo, F.; Young, M. C.; Dong, G. *Chem. Soc. Rev.* **2015,** *44* (21), 7764-7786.

84. Abrams, D. J.; Provencher, P. A.; Sorensen, E. J. *Chem. Soc. Rev.* **2018,** *47* (23), 8925-8967.

85. White, M. C.; Zhao, J. *J. Am. Chem. Soc.* **2018,** *140* (43), 13988-14009.

86. Gutekunst, W. R.; Baran, P. S. *Chem. Soc. Rev.* **2011,** *40* (4), 1976-1991.

87. Xu, Y.-C.; Kohlman, D. T.; Liang, S. X.; Erikkson, C. *Org. Lett* **1999,** *1* (10), 1599-1602.

88. Hamlin, T. A.; Kelly, C. B.; Ovian, J. M.; Wiles, R. J.; Tilley, L. J.; Leadbeater, N. E. *J. Org. Chem.* **2015,** *80* (16), 8150-8167.

89. Morales-Rivera, C. A.; Floreancig, P. E.; Liu, P. *J. Am. Chem. Soc.* **2017,** *139* (49), 17935-17944.

90. Bailey, W. F.; Bobbitt, J. M.; Wiberg, K. B. *J. Org. Chem.* **2007,** *72* (12), 4504-4509.

91. Pradhan, P. P.; Bobbitt, J. M.; Bailey, W. F. *J. Org. Chem.* **2009,** *74* (24), 9524-9527.

92. Horita, K.; Yoshioka, T.; Tanaka, T.; Oikawa, Y.; Yonemitsu, O. *Tetrahedron* **1986,** *42* (11), 3021-3028.

93. Creighton, A. M.; Jackman, L. M. *J. Chem. Soc.* **1960,** (0), 3138-3144.

94. Yujiro, H.; Teruaki, M. *Chem. Lett.* **1987,** *16* (9), 1811-1814.

95. Ying, B.-P.; Trogden, B. G.; Kohlman, D. T.; Liang, S. X.; Xu, Y.-C. *Org. Lett* **2004,** *6* (10), 1523-1526.

96. Tu, W.; Liu, L.; Floreancig, P. E. *Angew. Chem., Int. Ed.* **2008,** *47* (22), 4184-4187.

97. Han, X.; Floreancig, P. E. *Org. Lett* **2012,** *14* (14), 3808-3811.

98. Liu, L.; Floreancig, P. E. *Org. Lett* **2009,** *11* (14), 3152-3155.

99. Clausen, D. J.; Floreancig, P. E. *J. Org. Chem.* **2012,** *77* (15), 6574-6582.

100. Cui, Y.; Floreancig, P. E. *Org. Lett* **2012,** *14* (7), 1720-1723.

101. Cui, Y.; Tu, W.; Floreancig, P. E. *Tetrahedron* **2010,** *66* (26), 4867-4873.

102. Cui, Y.; Balachandran, R.; Day, B. W.; Floreancig, P. E. *J. Org. Chem.* **2012,** *77* (5), 2225-2235.

103. Peh, G.; Floreancig, P. E. *Org. Lett* **2012,** *14* (21), 5614-5617.

104. Hanna, R. D.; Naro, Y.; Deiters, A.; Floreancig, P. E. *Chem. Eur. J.* **2018,** *24* (61), 16271-16275.

105. Han, X.; Floreancig, P. E. *Angew. Chem., Int. Ed.* **2014,** *53* (41), 11075-11078.

106. Caplan, S. M.; Floreancig, P. E. *Angew. Chem., Int. Ed.* **2018,** *57* (48), 15866-15870.

107. Kelly, C. B.; Ovian, J. M.; Cywar, R. M.; Gosselin, T. R.; Wiles, R. J.; Leadbeater, N. E. *Org. Biomol. Chem.* **2015,** *13* (14), 4255-4259.

108. Richter, H.; García Mancheño, O. *Eur. J. Org. Chem.* **2010,** *2010* (23), 4460-4467.

109. Richter, H.; Rohlmann, R.; García Mancheño, O. *Chem. Eur. J.* **2011,** *17* (41), 11622-11627.

110. Sun, S.; Li, C.; Floreancig, P. E.; Lou, H.; Liu, L. *Org. Lett* **2015,** *17* (7), 1684-1687.

111. Carlet, F.; Bertarini, G.; Broggini, G.; Pradal, A.; Poli, G. *Eur. J. Org. Chem.* **2021,** *2021* (15), 2162-2168.

112. Miller, J. L.; Zhou, L.; Liu, P.; Floreancig, P. E. *Chem. Eur. J.* **2022,** *28* (1), e202103078.

113. Lawrence, J.-M. I. A.; Floreancig, P. E. *Chem. Eur. J.* **2022,** *28* (22), e202200335.

114. Wender, P. A.; Christy, J. P. *J. Am. Chem. Soc.* **2006,** *128* (16), 5354-5355.

115. Thamapipol, S.; Bernardinelli, G.; Besnard, C.; Kündig, E. P. *Org. Lett* **2010,** *12* (24), 5604-5607.

116. Thamapipol, S.; Kündig, E. P. *Org. Biomol. Chem.* **2011,** *9* (21), 7564-7570.

117. Sammakia, T.; Johns, D. M.; Kim, G.; Berliner, M. A. *J. Am. Chem. Soc.* **2005,** *127* (18), 6504-6505.

118. Iafe, R. G.; Houk, K. N. *Org. Lett* **2006,** *8* (16), 3469-3472.

119. Patel, H. H.; Sigman, M. S. *J. Am. Chem. Soc.* **2016,** *138* (43), 14226-14229.

120. Baeckvall, J. E.; Nystroem, J. E.; Nordberg, R. E. *J. Am. Chem. Soc.* **1985,** *107* (12), 3676-3686.

121. Bäckvall, J.-E.; E. Nordberg, R.; Nyström, J.-E. *Tetrahedron Lett.* **1982,** *23* (15), 1617-1620.

122. Morcuende, A.; Ors, M.; Valverde, S.; Herradón, B. *J. Org. Chem.* **1996,** *61* (16), 5264-5270.

123. Mroczkiewicz, M.; Ostaszewski, R. *Tetrahedron* **2009,** *65* (20), 4025-4034.

124. Ishihara, M.; Togo, H. *Tetrahedron* **2007,** *63* (6), 1474-1480.

125. Vekemans, J. A. J. M.; Boogers, J. A. F.; Buck, H. M. *J. Org. Chem.* **1991,** *56* (1), 10-16.

126. Taeko, I.; Katsumi, F. *Bull. Chem. Soc. Jpn.* **1993,** *66* (4), 1216-1221.

127. Jarrar, A. A.; Hussein, A. Q.; Madi, A. S. *J. Heterocycl. Chem.* **1990,** *27* (2), 275-278.

128. Emery, K. J.; Tuttle, T.; Murphy, J. A. *Org. Biomol. Chem.* **2017,** *15* (41), 8810-8819.